PROFESSUR FÜR MOLEKULARE ERNÄHRUNGSFORSCHUNG

JUSTUS-LIEBIG-UNIVERSITÄT GIESSEN

Molecular Mechanisms Underlying the Prevention of Glucose-Induced Life Span Reduction by the Polyphenol Quercetin in the *mev-1* Mutant of *Caenorhabditis elegans*

Inaugural-Dissertation

zur

Erlangung des akademischen Grades eines

Doktors der Naturwissenschaften (Dr. rer. nat.)

der Fakultät

Biologie und Chemie

an der

Justus-Liebig-Universität Gießen

vorgelegt von

Elena Fitzenberger, M.Sc. troph.

Dezember 2012

1. Gutachter: Prof. Dr. Uwe Wenzel
   Professur für Molekulare Ernährungsforschung
   Interdisziplinäres Forschungszentrum
   Heinrich-Buff-Ring 26-32
   35392 Gießen

2. Gutachter: Prof. Dr. Adriaan Doresteijn
   Professur für allgemeine Zoologie und Entwicklungsbiologie
   Stephanstraße 24
   35390 Gießen

CONTENT

LIST OF FIGURES

LIST OF TABLES

LIST OF ABBREVIATIONS

abu	activated in blocked UPR
ADP	adenosine diphosphate
AGE	advanced glycation end products
age-1	ageing alteration family member
ALE	advanced lipoxidation end products
AMPK	adenosine monophosphate activated protein kinase
AP-1	activator protein
Apaf-1	apoptotic protease activating factor
APS	Ammonium peroxydisulphate
AR	aldose reductase
ATF	activating transcription factor
ATFS-1	activating transcription factor associated with stress
ATG	autophagy related protein
ATP	adenosine triphosphate
BAD	BCL2-associated agonist of cell death
BAK	BCL2-antagonist/killer
BAX	BCL2-associated X protein
BCL2	B-cell CLL/lymphoma 2
bec-1	beclin (human autophagy) homologue
BID	BH3-interacting domain death agonist
BIM	BCL2-interacting mediator of cell death
bp	basepairs

BSA	bovine serum albumin
bZIP	basic leucine-zipper
C. elegans	*Caenorhabditis elegans*
CAD	caspase-activated desoxyribonuclease
ced	cell death abnormality
CGC	Caenorhabditis Genetics Center
CHOP	C/EBP homologous protein
CLPP	caseinolytic peptidase
ClpXP	protease specificity-enhancing factor
CR	caloric restriction
D. melanogaster	*Drosophila melanogaster*
daf	abnormal dauer formation
DAG	diacylglycerol
DAPK	death associated protein kinase
DDL	*daf-16* dependent longevity
DED	death effector domain
Dicer	dsRNA specific endonuclease
DMSO	Dimethyl sulphoxid
dsRNA	double stranded RNA
DTT	1,4-Dithiothreitol
dve-1	DVE (defective proventriculus in *Drosophila*) homologue
E. coli	*Escherichia coli*
E1	ubiquitin activating enzyme
E2	ubiquitin conjugating enzyme

E3	ubiquitin-protein ligase
eat-2	eating: abnormal pharyngeal pumping
ECL	enhanced chemiluminescence
EDTA	ethylenediamine tetraacetic acid
egl-1	egg laying defective
ELISA	enzyme linked immunosorbent assay
eNOS	endothelial NO synthase
ER	endoplasmic reticulum
ERAD	ER associated degradation
FADD	Fas-associated death domain
$FADH_2$	flavin adenine dinucleotide
FOXO	forkhead box O
ftt-2	14-3-3 protein
FXR	farnesoid X nuclear receptor
G6PD	glucose-6-phosphate dehydrogenase
GAPDH	glyceraldehyde-3-phosphate dehydrogenase
gcs-1	γ-glutamyl cysteine synthetase
GlcNAc	N-Acetylglucosamine
GLUT	glucose transporter
GPX	glutathione peroxidase
gsk-3	glycogen synthase kinase
gst	glutathione S-transferase
HAF-1	HAIF transporter (PGP-related)
HRP	horseradish peroxidase

HSB	heat shock factor binding protein
HSF	heat shock factor
HSP	heat shock protein
IGF-1	insulin-like growth factor-1
IL-6	interleukin 6
iNOS	inducible NO synthase
IPTG	Isopropyl-β-D-thiogalactopyranoside
IRE1	inositol-requiring enzyme 1
IRS-1	insulin receptor substrate-1
JNK	c-Jun N-terminal kinase
let	lethal
lgg	LC3, GABARAP and GATE-16 family
LXR	liver X nuclear receptor
MAPK	mitogen-activated protein kinase
MEK-1	MAP kinase kinase or Erk kinase
mev-1	methyl viologen sensitivity
MG	methylglyoxal
mTOR	mammalian target of rapamycin
NADH	nicotinamide adenine dinucleotide
NADPH	nicotinamide adenine dinucleotide phosphate
NF-κB	nuclear factor κB
NGM	nematode growth medium
NHR	nuclear hormone receptor
NO	nitric oxide

NRF	nuclear respiratory factor
PA	polyacrylamide
PAI-1	plasminogen activator inhibitor
par-5	abnormal embryonic partitioning of cytoplasm
PCR	polymerase chain reaction
PDK-1	3-phosphoinositide-dependent kinase 1
PDX-1	pancreatic and duodenal homeobox 1
pek-1	PERK kinase homologue
PERK	PRKR-like ER kinase
PGC	PPARγ co-activator
PI3K	phosphatidylinositol-3-kinase
PKC	protein kinase C
pmk-1	p38 MAPK orthologue
PMSF	phenylmethanesulphonyl fluoride
PPAR	peroxisome proliferator-activated receptor
psr-1	phosphatidylserine receptor family
qRT-PCR	quantitative real time PCR
RAGE	receptor of AGEs
RISC	RNA-induced silencing complex
RNAi	RNA interference
ROS	reactive oxygen species
RT-PCR	reverse transcription PCR
S. cerevisiae	*Saccharomyces cerevisiae*
SDS	sodium dodecylsulphate

sek-1	SAPK/ERK kinase
sgk-1	serum- and glucocorticoid-inducible kinase homologue
sHSP	small heat shock protein
SIR	silent information regulators
siRNA	short interfering RNA
skn-1	skinhead family member
SREBP	sterol regulatory element binding protein
SREC	scavenger receptor
T2DM	type 2 diabetes mellitus
TAE	tris-acetate-EDTA
Taq	*Termophilus aquaticus*
TBS	tris buffered saline
TBS-T	TBS with tween
TCA	tricarboxylic acid
TEMED	N,N,N‘,N‘-Tetramethylethylenediamine
TGF	transforming growth factor
T_m	melting temperature
TNF-α	tumour necrosis factor α
TNFR	tumour necrosis factor receptor
TRAIL	TNF-related apoptosis inducing ligand
TRI reagent	total RNA isolation reagent
TRIS	tris(hydroxmethyl)-aminomethane
TSC	tuberous sclerosis
Ub	ubiquitin

uba-1	ubiquitin-activating enzyme
ubl-5	ubiquitin-like protein
ubq-1	ubiquitin locus
UDP	uridine diphosphate
ULK	*unc-51* like kinases
unc	uncoordinated
UPR	unfolded protein response
UPR^{ER}	ER specific unfolded protein response
UPR^{mt}	mitochondria specific unfolded protein response
UPS	ubiquitin-proteasome system
XBP1	X-box binding protein 1

1 INTRODUCTION

Over the past centuries life expectancy continuously increased from about 40 years in 1875 to over 80 years in 2003 [1]. Associated with this, a rise of age-related diseases, such as type 2 diabetes mellitus (T2DM), cardiovascular diseases, and Alzheimer's disease is observed. Thus the preservation of health and physical ability is of fundamental interest in the field of ageing research.

1.1 Ageing

Ageing is a multifactorial process of progressive decline in performance and health that is a common feature of multicellular organisms [2, 3]. Numerous ageing theories, both evolutionary and mechanistic, have been proposed. Evolutionary ageing theories, like the mutation accumulation, antagonistic pleiotropy, and disposable soma theories, are based on the assumption that selective pressure decreases with age. In order to slow the ageing process, interventions such as increasing stress resistance mechanisms, which can be achieved best by dietary restriction, are the most successful so far [3].

1.2 Glucose Metabolism during Ageing and Pathology

Ageing is often accompanied by impaired glucose tolerance and reduced insulin sensitivity of insulin-responsive tissues, such as muscle, liver, and adipose tissue [4-6]. In accordance with this the incidences of insulin resistance and T2DM are increased in the elderly.

Relevant factors that contribute to age-related insulin resistance are changes in the circulating concentrations of adipokines, like adiponectin, tumour necrosis factor (TNF)-α or interleukin (IL)-6, oxidative stress, mitochondrial dysfunction, and endoplasmic reticulum stress [7]. Moreover, detrimental effects such as accumulation of triglycerides and fatty acyl intermediates, and activation of serine-threonine kinases may contribute to impaired glucose tolerance (Figure 1-1) [8].

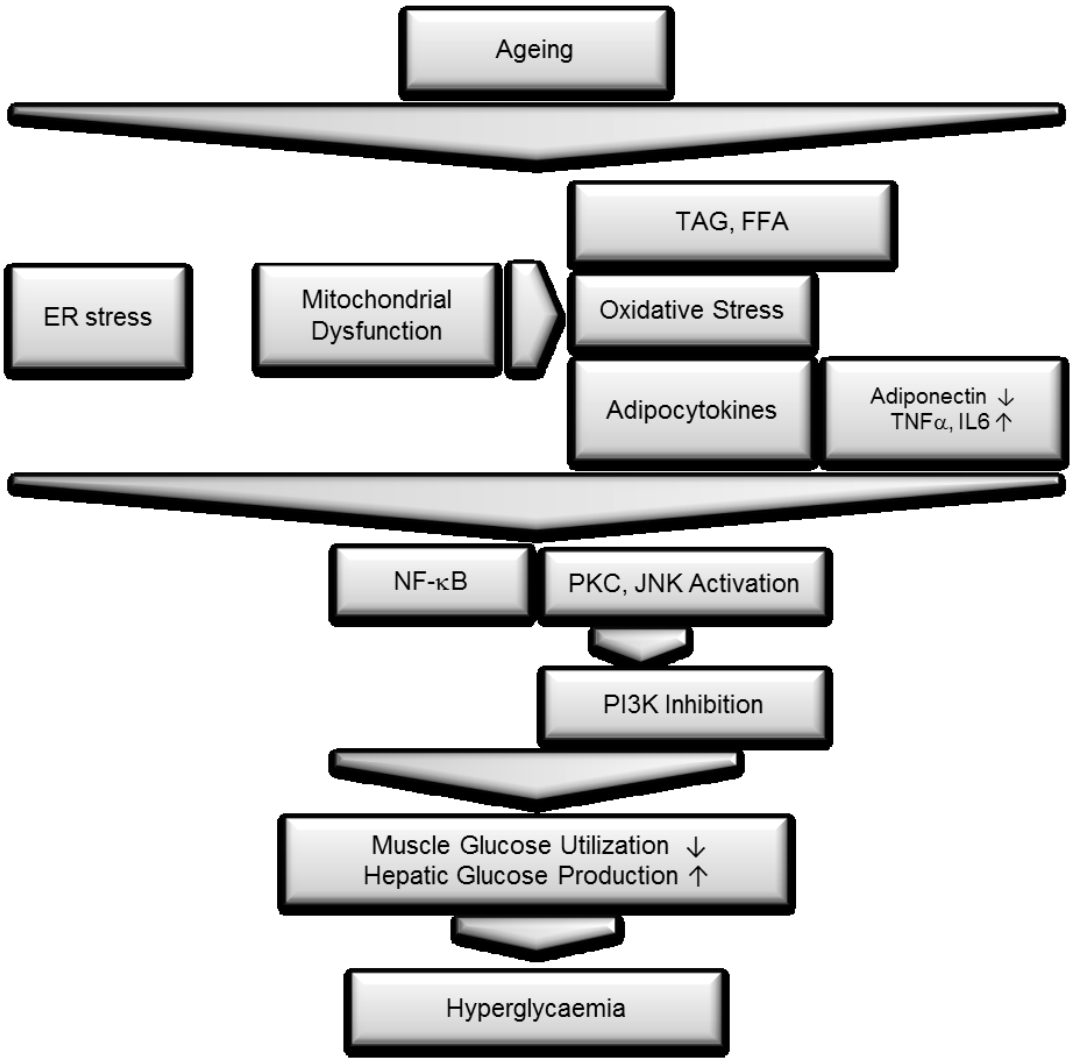

Figure 1-1. Development of ageing-associated hyperglycaemia.

TAG: triacylglycerides, FFA: free fatty acids, ER: endoplasmic reticulum, TNFα: tumour necrosis factor α, IL6: interleukin 6, NF-κB: nuclear factor κB, PKC: protein kinase C, JNK: c-Jun N-terminal kinase, PI3K: phosphatidylinositol-3-kinase

As a result of ageing-associated changes in β-cell function and gene expression of β-cell specific genes, such as insulin, glucose transporter 2 (GLUT2), and pancreatic and duodenal homeobox 1 (PDX1) [9], the glucose-stimulated insulin release declines [10]. The mechanisms of alteration in β-cell function are not fully understood. It has been proposed that oxidative stress promotes β-cell apoptosis and that inhibition of β-cell proliferation plays an important role as well [10].

It is well known that diabetes mellitus is associated with a variety of late onset complications, such as retinopathy, nephropathy, neuropathy and angiopathy, which are mainly caused by damage of small vessels. Currently it is assumed that transiently elevated blood glucose plays a major role in the development of long-term diabetic consequences.

High rates of glucose breakdown in tissues with unrestricted glucose uptake lead to increased generation of superoxide by the oxidation of nicotinamide adenine dinucleotide (NADH) and flavin adenine dinucleotide ($FADH_2$) in the mitochondrial electron transport chain. Enhanced superoxide formation has been associated with the inhibition of GAPDH by adenosine diphosphate (ADP)-ribosylation [11]. As a consequence upstream metabolites of glyceraldehyde-3-phosphate derived from glycolysis accumulate and increase the flux into pathways known to be relevant for diabetic complications, such as the aldose reductase (AR)/polyol pathway, the diacylglycerol (DAG) pathway leading to protein kinase C (PKC) activation, or pathways that lead to the formation of advanced glycation end products (AGEs) or N-Acetylglucosamine (GlcNAc, Figure 1-2).

In the polyol pathway, glucose is converted to sorbitol by AR and then further to fructose and other metabolites. Besides the development of cataract due to intracellular accumulation of sorbitol and fructose and subsequent failure of the cellular osmoregulation, increased AR expression is associated with the development of vascular disease. AR-expressing macrophages show greater expression of the inducible nitric oxide synthase (iNOS) and the inflammatory cytokine IL-6. The iNOS produces much more nitric oxide (NO) than the constitutively expressed endothelial NO synthase (eNOS) and has been related to cellular damage, inflammation, and apoptosis [12]. Moreover, AR-expressing macrophages have greater potential to acquire lipoproteins that allow for

conversion into foam cells, which is a major event in the development of atherosclerosis. Glutathione depletion as a consequence of AR-induced reduction in the expression of glucose-6-phosphate dehydrogenase (G6PD) and glutathione peroxidase (GPX) has also been proposed to contribute to the formation of atherosclerotic lesions [13].

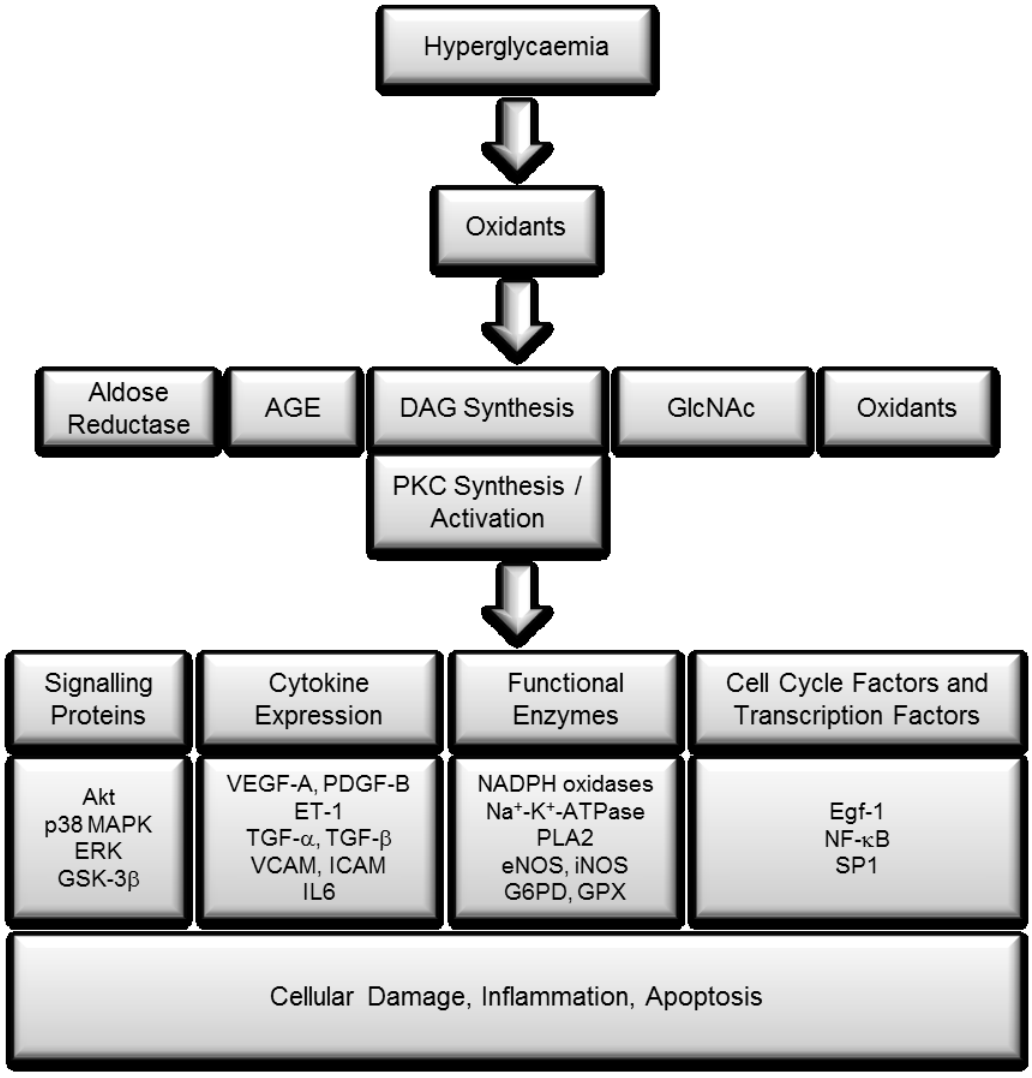

Figure 1-2. Consequences of ageing-dependent hyperglycaemia.

AGE: advanced glycation end products, DAG: diacylglycerol, GlcNAc: N-Acetylglucosamine, PKC: protein kinase C, MAPK: mitogen activated protein kinase, ERK: extracellular signal-regulated kinase, GSK: glycogen-synthase kinase, VEGF: vascular endothelial growth factor, PDGF: platelet derived growth factor, ET: endothelin, TGF: transforming growth factor, VCAM: vascular cell adhesion molecule, ICAM: intracellular adhesion molecule, IL: interleukin, PLA: phospholipase A, eNOS: endothelial NO: synthase, iNOS: inducible NO synthase, G6PD: glucose-6-phosphate dehydrogenase, GPX: glutathione peroxidase, Egf: epidermal growth factor, NF-κB: nuclear factor κB, SP: specificity protein

DAG is an activator of various PKC isoforms. Raised DAG levels are the result of increased dihydroxyacetone phosphate production from glycolysis and mitochondrial superoxide generation. Altered PKC expression has been associated with numerous abnormal cellular processes and deregulations, such as cell growth and apoptosis, endothelial dysfunction, enzyme activity changes, and alterations in transcription factors [14]. For example, activation of PKC in endothelial cells leads to decreased expression of eNOS and increases superoxide production from nicotinamide adenine dinucleotide phosphate (NADPH) oxidase, which results in a reduction of the vasodilating NO. Simultaneously, vasoconstrictors like endothelin 1 and thromboxane are increased. Furthermore, PKC action causes accumulation of extracellular matrix by increased transforming growth factor (TGF)-β expression [14].

Accumulation of fructose-6-phosphate due to inhibition of GAPDH or increased flux of glucose through the hexosamine pathway is another mechanism by which hyperglycaemia contributes to the pathogenesis of diabetic complications. Fructose-6-phosphate from glycolysis is converted by glutamine:fructose 6-phosphate amidotransferase to glucosamine 6-phosphate and further to uridine diphosphate (UDP)-N-Acetylglucosamine (GlcNAc). The latter is used by specific O-GlcNAc transferases for posttranslational modification of specific serine and threonine residues and mediates for example the increased transcription of key genes such as TGF-α [15], TGF-β [16], and plasminogen activator inhibitor (PAI)-1 [17]. Additionally, eNOS is inhibited by O-GlcNAcylation in endothelial cells [18].

Moreover, elevated blood glucose boosts the accumulation of oxidation and glycation products, which are involved in miscellaneous age-related diseases [4]. The non-enzymatic reaction of reducing sugars or reactive carbonyls derived from glucose and fatty acid oxidation, like 3-deoxyglucosone, methylglyoxal (MG), and glyoxal, with proteins or lipids results in the formation of AGEs or advanced lipoxidation end products (ALEs) [2]. These are heterogeneous groups of compounds that are generated as part of normal glucose metabolism and accumulate during ageing. The accumulation of AGEs has been shown to inversely correlate with overall longevity of several mammal species [19] and is enhanced during hyperglycaemia and increased oxidative stress [2]. AGEs can

damage cells by structural and functional changes of AGE-modified proteins, abnormal interaction of glycated extracellular matrix components with other extracellular matrix components and receptors as well as by binding of AGE-modified plasma proteins to AGE receptors (RAGEs). RAGE mediates AGE signalling through ROS production, activation of NF-κB, and p21 ras [20, 21]. This alters gene expression patterns, induces procoagulatory changes [22], increases the adhesion of inflammatory cells to the endothelium [23], and contributes to enhanced vascular permeability [24]. However, RAGE signalling may also be activated by endogenously produced proinflammatory protein ligands, which are found to be elevated under hyperglycaemic conditions [25]. Moreover, the glucose-derived dicarbonyl MG has been shown to interfere with the cellular proteostasis network by covalent modification of the 20S proteasome and inhibition of the polyubiquitin receptor [26] (see below).

1.3 The Cellular Protein Quality Control System

To counteract AGE formation, the maintenance of protein homoeostasis is essential for health. As cells age efficiency of proteostasis declines, which leads to the accumulation of damaged and misfolded proteins and thus to reduced cellular viability and the development of diseases. A complex network of biological processes is required to ensure correct protein folding, transport, and degradation. This includes molecular chaperones, heat shock and unfolded protein responses (UPR), as well as the ubiquitin-proteasome system (UPS) (Figure 1-3).

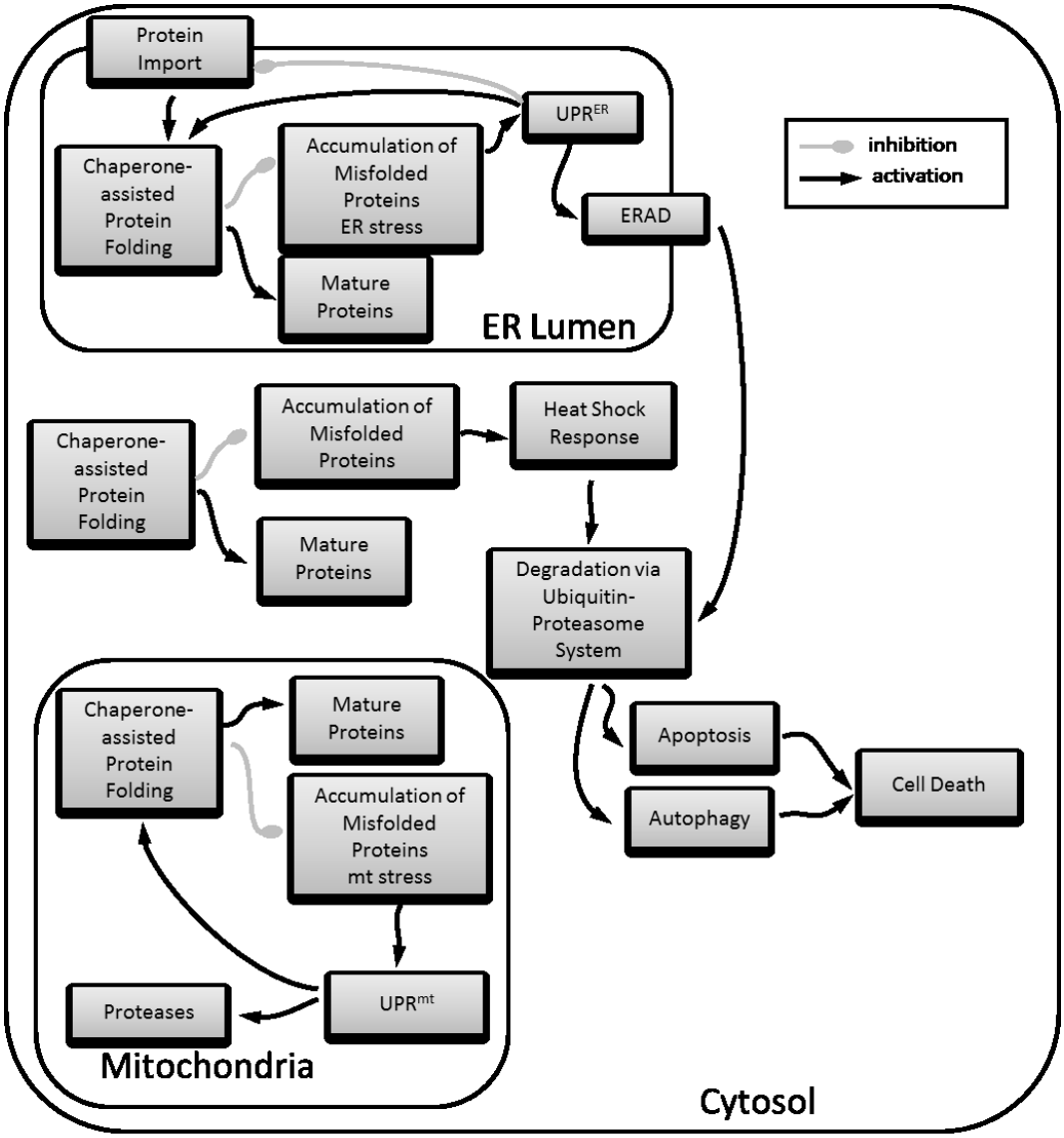

Figure 1-3. Cellular proteostasis network.

UPR: unfolded protein response, ER: endoplasmic reticulum, ERAD: ER-associated degradation, mt: mitochondria

1.3.1 Assistance of Protein Folding by Chaperones

Correct and efficient protein folding strongly depends on the assistance from molecular chaperones [27]. They are present in all folding compartments of the eukaryotic cell, i. e. the cytoplasm, the ER, and mitochondria (Figure 1-3). Moreover, they are found in the nucleus and peroxisomes [28]. Chaperones are a diverse group of proteins that play several roles in protein biogenesis, like the prevention of irreversible intermolecular interaction, assistance of protein folding, assembly of protein complexes, protein translocation, integration into membranes, and degradation [27, 29]. Although many chaperones are constitutively expressed, their synthesis is greatly enhanced under stress conditions, such as heat stress [30]. Thus, a major chaperone family is referred to as heat shock proteins (HSPs) [31]. In general, chaperones recognize hydrophobic or unstructured backbone regions in their client proteins. These are typically structural features of non-native proteins, and usually not exposed upon completion of folding [30].

HSP 70s are very likely the best-studied class of chaperones. They have a molecular mass of approximately 70 kD and are highly conserved among all three domains of life. Chaperone activity of HSP 70s includes cycles of protein binding and adenosine triphosphate (ATP) hydrolysis, regulated by co-chaperones and nucleotide exchange factors. Among others, HSP 40s act as co-chaperones for HSP 70s and induce their ATPase activity [28].

Chaperonins are a class of large double-ring complexes enclosing a central cavity. In this cavity non-native, aggregation-prone proteins are protected from the environment, which facilitates correct protein folding. For instance, HSP 60 is a member of the approximately 60 kD chaperonin family. Together with cofactors of the HSP 10 family it forms large cage-like structures. Similarly to HSP 70s, HSP 60s facilitate folding through cycles of substrate binding and release regulated by their ATPase activity and cofactors [31].

Other classes of chaperones include HSP 90s, which are specialized ATP-dependent chaperones [30], HSP 100s, which have the ability to unfold proteins and disrupt small protein aggregates [30], and small heat shock proteins (sHSPs) that bind substrates rather non-specifically and prevent proteins from irreversible aggregation [28].

1.3.2 Unfolded Protein Responses in the Endoplasmic Reticulum and Mitochondria

The cytosol, ER, and mitochondria all have dedicated protein folding machineries that constitute each organelle's protein folding capacity (Figure 1-3). If the quantity of unfolded or misfolded proteins exceeds a compartment's protein folding capacity this leads to stress, which is counteracted by organelle-specific signalling pathways known as unfolded protein responses (UPR) [32].

The cytosolic protein folding environment is protected by the heat shock response, which is regulated by the transcription factor heat shock factor 1 (HSF1). If unfolded proteins accumulate in the cytosol, HSF1 interacts with the promoters of genes that are involved in heat shock response. As a result the expression of cytosolic chaperones, like HSP70 and HSP90, is upregulated to increase the cytosolic folding capacity. Additionally, HSF1 induces the expression of the ubiquitin-proteasome system, which degrades terminally misfolded proteins and thereby reduces the load on the folding machinery [32].

The protein folding environment of the ER is protected by a distinct unfolded protein response (UPR^{ER}), which consists of three branches that act in parallel [32, 33]. The most conserved branch of the UPR^{ER} is composed of the ER membrane spanning kinase inositol-requiring enzyme 1 (IRE1) and the basic leucine-zipper (bZIP) transcription factor X-box binding protein 1 (XBP1). Upon ER stress the cytosolic kinase domain of IRE1 is activated and a functional bZIP protein translated, which induces the expression of UPR^{ER} genes [32]. The transcriptional response increases the levels of luminal chaperones, ER associated degradation (ERAD) components, and protein transport to other compartments [34]. Moreover, the ER membrane spanning protein kinase PRKR-like ER kinase (PERK) and the activating transcription factor (ATF) 6 transiently attenuate protein translation to reduce the burden on ER folding capacity and further increase the levels of components that ameliorate stress. These signal transducers can also initiate apoptosis if ER stress cannot be compensated [32, 34]. Additionally, the UPR^{ER} activates expression of ERAD components. The ERAD pathway recognizes proteins that are unable to pass the ER quality control. These

are retranslocated to the cytosol where they are ubiquitinated and degraded by the proteasome [32, 34].

Accumulating evidence supports the existence of another, mitochondria specific unfolded protein response (UPR^{mt}). A mitochondria-to-nucleus signal transduction pathway, known as mitochondrial retrograde signalling, senses accumulation of unfolded proteins in the mitochondrial lumen and transmits a signal from mitochondria to the nucleus where the expression of mitochondrial chaperones and proteases is selectively upregulated to re-establish mitochondrial protein homoeostasis [31, 32]. In mammalian cells the transcription factor C/EBP homologous protein (CHOP) plays a central role in UPR^{mt} as it regulates a number of mitochondrial chaperones and proteases including mtHSP60, mtHSP10, and caseinolytic peptidase (CLPP). A current model proposes that unfolded proteins in mitochondria initiate CHOP expression, which subsequently induces UPR^{mt}-responsive genes that contain CHOP elements in their promoter regions [31]. Moreover, it has been suggested that c-Jun and JNK play a role upstream of CHOP in UPR^{mt} signalling, since activated c-Jun binds to an activator protein (AP)-1 consensus sequence that is present within the CHOP promoter [32].

1.3.3 Protein Degradation by the Ubiquitin-Proteasome System

The majority of intracellular proteins, including AGEs [35], is degraded via the ubiquitin-proteasome system (UPS) in eukaryotic cells [36]. This involves two discrete steps: first of all, the substrate protein is tagged by covalent attachment of multiple ubiquitin molecules; secondly, the polyubiquitinated protein is degraded by the 26S proteasome complex [37] (Figure 1-4).

Generally, a first ubiquitin moiety is transferred to an ε-NH_2 group of an internal lysine residue in the substrate. Further ubiquitin moieties are added to internal lysine-48 residues on the previously conjugated ubiquitin molecule by the formation of isopeptide bonds. In this way, a polyubiquitin chain is synthesized, which serves as degradation signal that is recognized by the 26S proteasome complex [38].

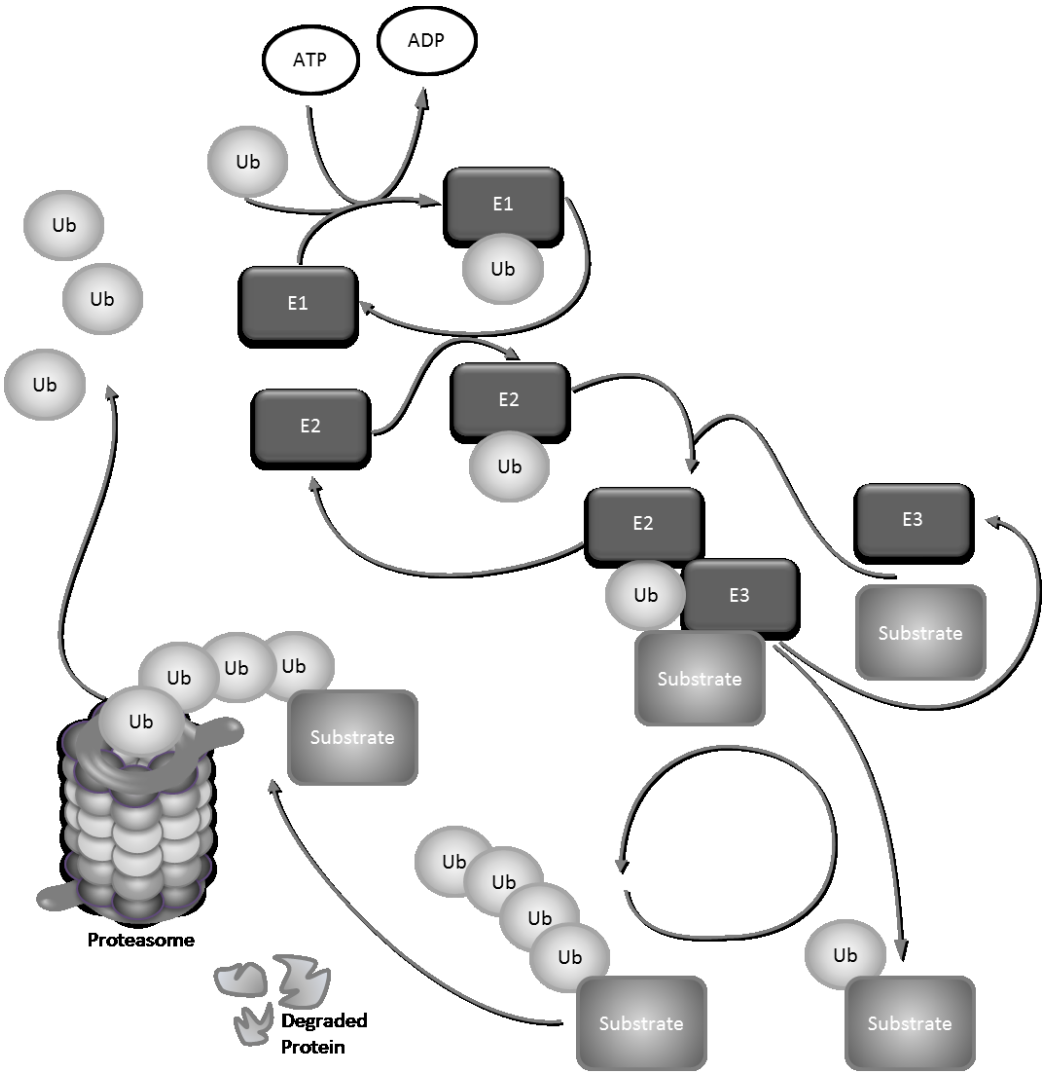

Figure 1-4. Ubiquitin-proteasome mediated protein degradation.

Ub: ubiquitin, E1: ubiquitin-activating enzyme, E2: ubiquitin-conjugating enzyme, E3: ubiquitin-protein ligase

The covalent attachment of ubiquitin to a target protein proceeds via a three-step mechanism. Initially, a high-energy thioester intermediate E1-S~ubiquitin is formed by the ubiquitin activating enzyme (E1) in an ATP-dependent reaction. In a next step, one of several ubiquitin conjugating enzymes (E2) forms another high-energy thioester intermediate E2-S~ubiquitin. Finally, the activated ubiquitin is transferred to the substrate that is specifically bound to an ubiquitin-protein ligase (E3). E3 ligases serve as the specific substrate recognition factors of the ubiquitin-proteasome system. So far several hundred different E3s have been identified in the human genome [37-39].

Degradation of polyubiquitinated proteins is carried out by the 26S proteasome, which is a large, multicatalytic protease complex. The 26S proteasome is composed of a 20S catalytic core particle and two 19S regulatory particles. The 20S core particle has a barrel-shaped structure that is made of two outer α rings and two inner β rings. The eukaryotic α and β rings consist each of seven distinct subunits. Three of the seven β subunits contain catalytic activity [37, 40, 41].

Most of the 20S complexes are capped by two 19S complexes that are not necessarily identical. This can secure unidirectional flow of substrates. Two ubiquitin-binding subunits of the 19S regulatory complex have been identified. They are supposed to recognize ubiquitinated proteins, which are subsequently unfolded and translocated into the proteolytic chamber. After degradation of the substrate, short peptide fragments that are further degraded by cytosolic peptidases and free, reusable ubiquitin are released [37, 40, 41].

During ageing a decline in proteasome function is observed. This is attributed to downregulation of genes coding for proteasome components, proteasome inhibition, and post-translational modification of proteasome subunits [42]. Hyperglycaemia has been shown to reduce the chymotrypsin-like proteasomal activity by methylglyoxal-modifications of the β subunits 2, 3, and 5. Also, reduced levels of the 19S regulatory complex were found under hyperglycaemic conditions, resulting in the accumulation of polyubiquitinated proteins [26]. Moreover, AGE-modification of ubiquitin and E2s contributes to impaired UPS activity [35]. In contrast, caloric restriction has been shown to be an efficient intervention to delay these age-related declines in proteasome function. It seems to alter proteasome biogenesis, composition, and activity in a tissue specific way [43], thereby preventing the accumulation of damaged proteins.

1.4 Apoptosis as Response to Impaired Proteostasis

In metazoan organisms the cell number of different tissues is tightly regulated [44]. The elimination of redundant, damaged, or infected cells is vital for development, tissue homoeostasis, and for an effective immune system [45]. To this end, each cell possesses a suicide mechanism termed programmed cell death

or apoptosis. The apoptotic programme is also initiated, if proteostasis is severely impaired and cannot be restored by the activation of the different quality control mechanisms [46].

Apoptosis is characterized by the contraction of the nucleus due to chromatin condensation, followed by fragmentation and decay of the cell into apoptotic particles, which are eliminated by macrophages to prevent inflammatory reactions [44]. Two principal pathways to apoptosis are known. The extrinsic way is triggered by the engagement of "death receptors" on the cell surface. The intrinsic way is based on the release of cytochrome c from mitochondria (Figure 1-5) [44].

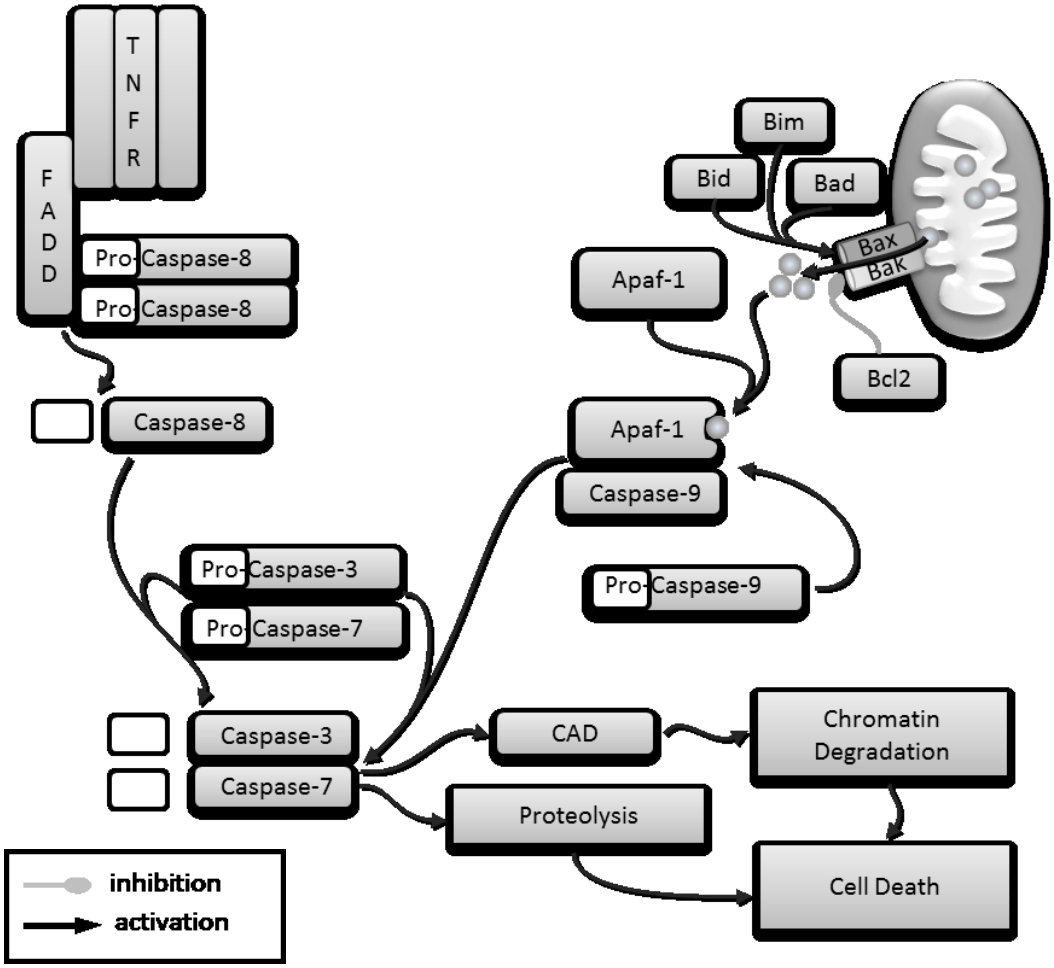

Figure 1-5. Principles of apoptosis.

TNFR: tumour necrosis factor receptor, FADD: Fas-associated via death domain, CAD: caspase activated desoxyribonuclease, Bim: BCL2-interacting mediator of cell death, Bid: BH3-interacting domain death agonist, Bad: BCL2-associated agonist of cell death, Bax: BCL2-associated X protein, Bak: BCL2-antagonist/killer, Bcl2: B-cell CLL/lymphoma 2, Apaf-1: apoptotic protease activating factor

Common to both pathways is the intracellular signalling through caspases. These are cysteine proteases that cleave after certain aspartate residues and are classified into initiator and executioner caspases. Caspases are maintained as zymogens, which are activated by adaptor proteins and proteolytic cleavage, respectively. The activation of initiator caspases, like caspase-8 and caspase-9, is triggered by the dimerization of the zymogen on an adaptor protein. The active initiator caspases then cleave the zymogens of executioner caspases (caspase-3, -6, and -7), which subsequently can attack their cellular substrates [45].

The extrinsic pathway activates caspase-8 and caspase-10 via the adaptor protein Fas-associated death domain (FADD), which is attracted by ligand-induced aggregation of TNF-receptor family members (e. g. CD95 or TRAIL) and recruits procaspase-8 or procaspase-10 molecules through death effector domains (DED). This is followed by the dimerization and autocatalysis of the zymogens [45].

The intrinsic way is provoked by various forms of stress, including ER stress, and typically activates caspase-9. Cytochrome c that is released from mitochondria due to permeabilization of the outer membrane leads to a conformational change of the scaffold protein apoptotic protease activating factor (Apaf-1), which allows it to recruit procaspase-9 and form the apoptosome together with ATP or 2'-deoxy ATP. In the apoptosome caspase-9 is activated and processes the executioner caspases-3 and -7, which results in proteolysis and degradation of chromatin by the caspase-activated desoxyribonuclease (CAD) [45].

The release of cytochrome c from damaged mitochondria can be triggered by a variety of factors and is closely regulated. A major role in this regulation play members of the B-cell CLL/lymphoma 2 (BCL2) family, which can be divided into pro-apoptotic an anti-apoptotic factors. Pro-apoptotic factors are BCL2-associated X protein (BAX) and BCL2-antagonist/killer (BAK). They are present as a heterodimer and likely form pores in the outer mitochondrial membrane through which cytochrome c can effuse. The activity of BAX and BAK is positively regulated by BCL2-interacting mediator of cell death (BIM), BH3-interacting domain death agonist (BID) and BCL2-associated agonist of cell death (BAD), which are in turn controlled by distinct mechanisms. Anti-apoptotic

factors are BCL2 itself as well as some closely related proteins. Decisive for the fate of a cell is the balance of these pro- and anti-apoptotic factors [44].

As described above, the UPR^{ER} is activated under ER stress conditions to reduce the load of unfolded proteins through several survival mechanisms. However, if proteostasis is not re-established, the UPR triggers apoptosis (Figure 1-3). Apoptosis under ER stress depends on the intrinsic, mitochondrial pathway that is regulated by the BCL2 family. Chronic ER stress leads to apoptosis through BAX- and/or BAK-dependent caspase activation. Additionally, the key UPR pro-apoptotic player CHOP promotes apoptosis by induction of BIM and downregulation of BCL2 expression. Together with ATF4 and p53, CHOP is also involved in the transcriptional upregulation of BH-3 only proteins under ER stress. Moreover, the activation of BID, calcium release from the ER, and JNK activation by IREα possibly link ER stress to apoptosis [46].

1.5 Autophagy Regulates Cell Homoeostasis

Autophagy is a catabolic process that regulates lysosomal degradation of cellular components. On the one hand, autophagy plays an important homoeostatic role balancing synthesis, degradation, and recycling of cellular components. In starving cells autophagy ensures the supply of metabolites by degrading intracellular macromolecules [47]. Under physiological conditions autophagy seems to promote cell survival acting as antagonist of apoptosis. On the other hand, autophagy can also be self-destructive and contribute to cell death, for example, under persisting extreme conditions. Hence, autophagy is often associated with cell death; and the inhibition of some autophagic proteins decreases the cell death rate [48]. Moreover, autophagy plays a role in disease. Especially in neurodegenerative diseases that involve aggregation of certain proteins, autophagy seems to be activated as a beneficial physiological response [49]. But also myodegenerative, liver, and cardiac diseases as well as cancer are related to defective autophagy [47].

At least three mechanisms of autophagy are known: macroautophagy, microautophagy, and chaperone-mediated autophagy. Most studied and hitherto

referred to as autophagy is macroautophagy. This involves the formation of the autophagosome that engulfs a targeted cellular region containing proteins, carbohydrates, lipids, RNA, or whole organelles. Autophagosomes fuse with lysosomes to form auto(phago)lysosomes in which lysosomal hydrolases degrade the content [47, 48].

Initially it was hypothesized that inhibition of apoptosis results in increased autophagic cell death. However, it has become clear that the relationship between autophagy and apoptosis is more complex in that both can also act cooperatively to induce cell death [48]. For example, the anti-apoptotic Bcl-2 family members inhibit autophagy by binding Beclin1 [50]. Moreover, JNK and death associated protein kinase (DAPK) are key regulators of apoptosis that are also able to trigger autophagy [51, 52]. On the contrary, Beclin1 has been shown to be cleaved by caspases, resulting in the inhibition of autophagy during active apoptosis [53]. As described before, prolonged ER stress may eventually lead to cell death by apoptosis and it may induce autophagy, too. Thereby autophagy may act either upstream or in parallel to apoptosis (Figure 1-6) [54].

Autophagosome assembly is based on the activation of a Beclin1-Class III PI3K complex [55], which leads to the production of omegasomes, i. e. phosphoinositide-3,4,5-P_3-rich membrane domains [56], and the recruitment of further proteins, such as autophagy related proteins (ATG) 5, 12, and 16 [57]. Autophagy is mainly controlled by class I and III PI3K that have opposite roles. Class I PI3K/Akt signalling suppresses autophagy mainly by stimulating TOR signalling via phosphorylation and inactivation of tuberous sclerosis (TSC)1/TSC2 dimers, which act as negative regulators of mammalian target of rapamycin (mTOR) activity [58, 59]. Since insulin/IGF-1 signals via PI3K [60] it would be argued that glucose inhibits autophagy as well. The mTOR is a conserved serine/threonine kinase that is involved in the activation of multiple anabolic processes, such as protein synthesis, transcription, and ribosome biogenesis. Simultaneously, mTOR inhibits catabolic processes including autophagy. Conversely, lack of nutrients inhibits mTOR signalling via AMPK-dependent activation of TSC1/TSC2 dimers and induces autophagy [58, 59]. The mTOR inhibits the initiation step of autophagy by phosphorylation of *unc-51* like

kinases (ULK) that are required for the formation of the Beclin1-Class III PI3K complex [61, 62].

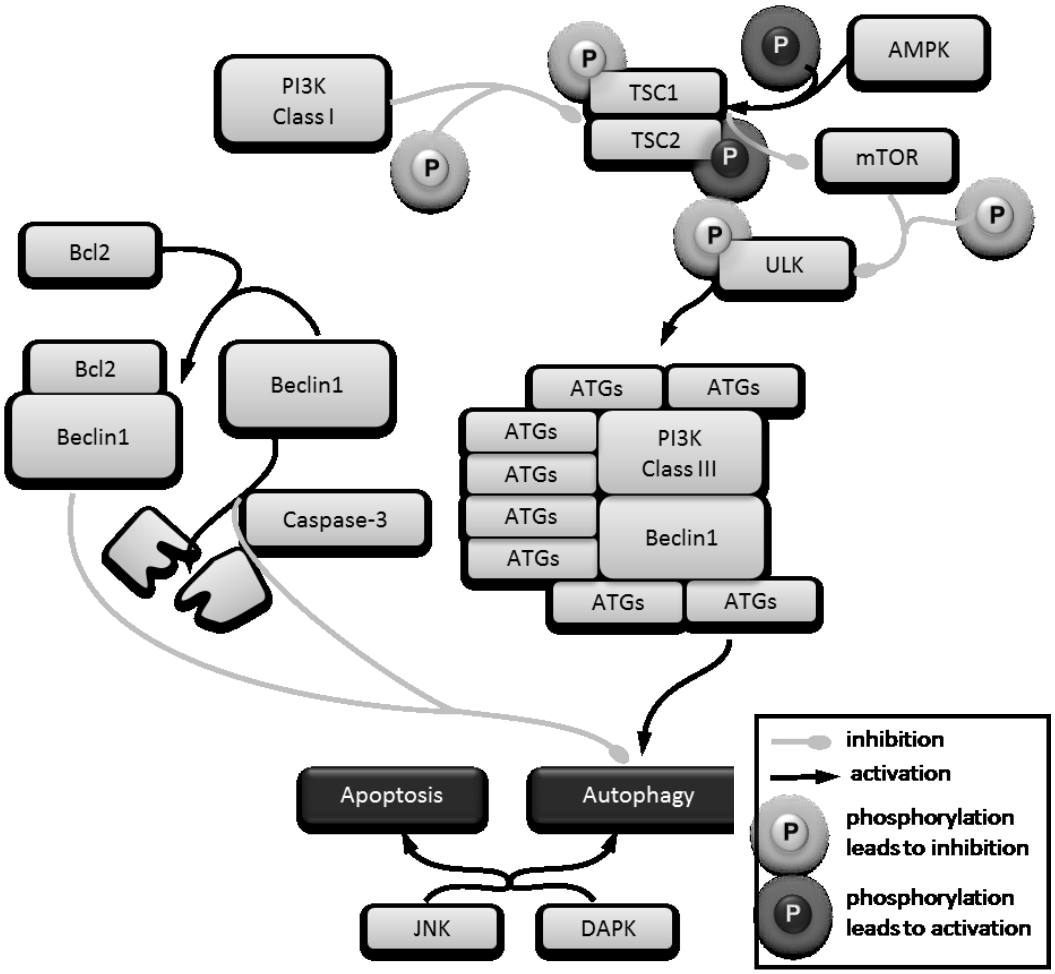

Figure 1-6. Regulation of autophagy.

Bcl2: B-cell CLL/lymphoma 2, JNK: c-Jun N-terminal kinase, DAPK: death associated protein kinase, PI3K: phosphatidylinositol-3-kinase, ATG: autophagy related protein, TSC: tuberous sclerosis, AMPK: AMP-activated kinase, mTOR: mammalian target of rapamycin, ULK: *unc-51* like kinase

1.6 Sirtuins as Mediators of Caloric Restriction to Antagonize Ageing and Hyperglycaemic Damage

For many species, ranging from yeast to rodents, caloric restriction (CR) has been shown to be the most effective dietary intervention to slow the ageing process and extend life span [63-67]. The effects of caloric restriction include the delay of age-dependent declines in insulin sensitivity [68, 69], the conservation of DNA repair mechanisms [70, 71], immune function [72, 73], and proteostasis [43, 74, 75] as well as the retard of age-associated increases in protein cross-linking [76] and oxidative stress [77]. Many studies provide evidence that sirtuins are involved in caloric restriction-mediated longevity and salutary effects [78].

Sirtuins are a family of enzymes that are highly conserved from bacteria to mammals [78]. These silent information regulators (SIR) were first identified in the yeast *Saccharomyces cerevisiae* as NAD^+-dependent histone deacetylases [79] and ADP-ribosyltransferases [80]. The functional role of sirtuins in ageing was initially established in yeast, too, and later shown in more complex model organisms such as *Drosophila melanogaster* and *Caenorhabditis elegans*.

Mammals possess seven sirtuins (SIRT1-7). These share the conserved core domain, which consists of the NAD^+-binding site and the catalytic domain [81]. However, they differ in enzymatic activity, subcellular localization, and substrate specificity [82]. Mammalian sirtuins are rather substrate specific protein deacetylases that remove acetyl of modified lysine residues consuming NAD^+ to produce O-Acetyl-ADP-ribose and free nicotinamide [78]. SIRT1, 6, and 7 are predominantly localized in the nucleus, SIRT2 in the cytoplasm, and SIRT3-5 in mitochondria. Yet, translocation between these compartments is possible for at least some sirtuins [83, 84]. SIRT1 is the closest homologue to yeast Sir2 [81] and has been studied most extensively.

In the past decade it was found that sirtuins are involved in multiple pathways affecting life span and health [78]. For example, SIRT1 protects from ageing-associated pathologies like diabetes mellitus, cardiovascular disease, neurodegenerative disorders, and cancer [63]. Moreover, sirtuins play a role in mediating the beneficial effects of caloric restriction. First, rodent studies showed that SIRT1 is upregulated in a variety of tissues in CR rats and in human cells

treated with serum from these animals [85]. Additionally, overexpression of SIRT1 driven by the β-actin promoter [86] or SIRT1 promoter in mice leads to improved glucose tolerance and attenuates, obesity-induced glucose intolerance, respectively. Moreover it reduces blood cholesterol, adipokines, and insulin [87]. Yet, in contrast to Sir2 overexpression in yeast, flies, and nematodes, overexpression of SIRT1 in mice is not sufficient to extend mean or maximum life span [88].

The effects of SIRT1 in metabolism are manifold and well characterized. Sirtuins can be summarized as pleiotropic energy sensors that regulate energy intake, storage, and expenditure, i. e. energy homoeostasis. In mice SIRT1 improves glucose tolerance and protects from diet-induced obesity [87, 89]. By binding and deacetylating, e.g. peroxisome proliferator-activated receptor (PPAR)γ, PPARα, PPARγ co-activator (PGC)-1α, and forkhead box O (FOXO) transcription factors, SIRT1 regulates insulin secretion [90], gluconeogenesis [91], and fatty acid oxidation [92]. Moreover, interactions with liver X nuclear receptor (LXR) [93] and farnesoid X nuclear receptor (FXR) [94] as well as inhibition of sterol regulatory element binding protein (SREBP) [89, 95] and repression of the PPARγ promoter [92] have been described. Deregulation of this energy sensor results in an imbalance of energy homoeostasis and can lead to obesity, insulin resistance, and T2DM.

Deacetylation and activation of PGC-1α by sirtuins increases mitochondrial biogenesis as well as uptake and utilization of substrates for energy production [96, 97]. The shift in mitochondrial substrate usage leads to the induction of gluconeogenic genes [98] and repression of glycolytic genes. As a result, glucose is preserved and more fatty acids are oxidized. Moreover, fatty acid catabolic genes are induced by PPARα, which is itself activated by PGC-1α [91].

Additionally, it has been shown that adenosine monophosphate activated protein kinase (AMPK), which can be activated by physical exercise, is also activated by SIRT1. Together with PGC-1α, FOXO1, and FOXO3 this ameliorates insulin secretion, glucose uptake and utilization, leading to improved glucose tolerance [99]. White adipose tissue is the place of fat storage, on the one hand, and on the other hand an important endocrine tissue secreting adipokines. In cell culture models SIRT1 binds PPARγ and inhibits transcription of its target

genes that are involved in fat storage. Therefore, activation of SIRT1 in fat cells enhances lipolysis and reduces fat mass [92].

Besides diseases that are linked to imbalanced energy homoeostasis, such as obesity, insulin resistance, and T2DM, sirtuins also play a role in cancer, cardiovascular disease, cholesterol metabolism, neurodegenerative diseases as well as inflammation and infection. The reduced inflammatory response seen under SIRT1 activation is due to lower levels of NF-κB [63].

1.7 Polyphenols and Ageing

The activation of sirtuins by polyphenols, such as quercetin, is of particular interest, since it appears to offer an opportunity to take advantage of the salutary effects of CR without the life-long constraint on calorie intake [100]. Polyphenols are a class of secondary plant compounds with more than 10000 substances [101]. In plant physiology they play roles as attractive colours, defence against insects, catalysts, and stress protectants, for example [102]. Moreover, they are components of the human diet and can positively influence human health. Sources of polyphenols are for instance tea, coffee, fruits and vegetables, nuts, herbs and spices, red and white wines as well as chocolate. Depending on the diet, the daily intake of polyphenols ranges between 50 and 800 mg/day [103].

A large subclass of polyphenols are flavonoids, which are characterized by at least two aromatic rings that are connected with a third oxygen-containing ring and have each one or more hydroxyls groups at the aromatic rings. Flavonoids are further subdivided into (1) flavanols, like catechins and catechingallates, which are present in teas, red grapes and wines, (2) flavanones, like hesperetin and naringenin in citrus fruits, (3) flavones, like apigenin and luteolin that are found in green leafy spices, (4) isoflavones, e. g. daidzein and genistein, found in soy foods and legumes, (5) flavonols, like quercetin (Figure 1-7) and myricetin that are ubiquitously found in plant foods, e. g. in onions or apples, and (6) anthocyanidins, such as delphinidin and cyanidin, present in berries [103].

Further polyphenol classes are lignans, tannins (proanthocyanidins, derived tannins, hydrolysable tannins), phenolic acids (e. g. caffeic acid, p-coumaric acid), and stilbens (e. g. resveratrol) [103].

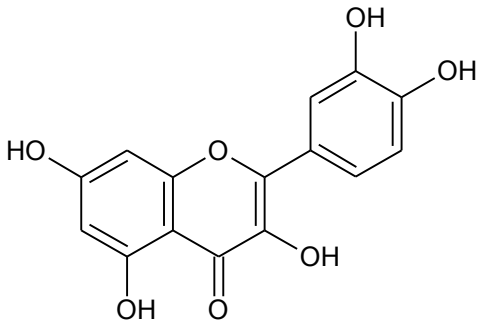

Figure 1-7. Chemical structure of quercetin.

Besides their functions in plant physiology, polyphenols also have influence on human health. Experimental studies show beneficial effects in the prevention of cardiovascular diseases, cancer, osteoporosis, diabetes mellitus, and neurodegenerative diseases [104]. A substantial attribute is the antioxidant capacity of polyphenols. Moreover, activation of sirtuins, induction of apoptosis, blocking of cell proliferation, inhibition of enzymes as well as interaction with signal transduction pathways and cell receptors have been described [105].

Additionally, polyphenols can have modulating effects on mitochondrial function, interfere with intermediary metabolism and decrease the expression of adhesion molecules. For example, polyphenols can selectively interact with kinases, such as PI3K, AKT, PKC, and mitogen-activated protein kinase (MAPK). Inhibitory effects as well as stimulatory effects are possible by influencing the phosphorylation status of target molecules and by modulation of gene expression. On the one hand, such effects could be advantageous in cancer, proliferative diseases, inflammation, and neurodegeneration; on the other hand, adverse effects are conceivable, especially during the development of the nervous system [106].

1.8 *Caenorhabditis elegans* as Model Organism to Study Ageing-Related Processes

Caenorhabditis elegans is a eukaryote organism of the phylum nematoda, which is the metazoan group that is richest in species and individuals [107]. Nematodes live in terrestrial and aquatic environments. The majority is free-living, however about 25% live as parasites that infect plants, animals, or humans [108]. *C. elegans* is a free-living soil nematode of the class secernentea and the order rhabditida [109]. It feeds mainly on bacteria and was first established as model organism for biological research by Sydney Brenner [110].

Among the many advantages of *C. elegans* as model organism are its simple body plan, short life cycle, large number of progeny, compact and completely sequenced genome, stereotypical development, ease of propagation and small size [111, 112]. The genome sequence of *C. elegans* is available since 1998 and was the first complete genome sequence of a multicellular organism [113]. *C. elegans* exists as self-fertilizing hermaphrodite (XX) and as male (XO). Self-fertilization of the hermaphrodite allows easy generation and maintenance of homozygous populations [112]. Moreover, the animals are transparent throughout their life cycle and can thus be examined *in vivo* by microscopy. For long-term storage, stocks of different strains can be frozen and kept for long periods of time [111, 112]. In the laboratory *C. elegans* can be easily maintained on agar plates or in liquid cultures with *Escherichia coli* as food source [114].

1.8.1 Anatomy and Physiology

C. elegans possesses the typical nematode body plan (Figure 1-8). The unsegmented, cylindrical body consists of an outer tube and an inner tube. The outer one, which is the body wall, is made of the cuticle, hypodermis, excretory system, neurons, and muscles. The inner tube comprises the alimentary system (pharynx, intestine) and the reproductive system (gonad). The tubes are separated by the pseudocoelomic cavity, which harbours a primitive immune system. Furthermore, *C. elegans* possesses an osmoregulatory system that is made of excretory cells and regulates the internal hydrostatic pressure in all tissues [112].

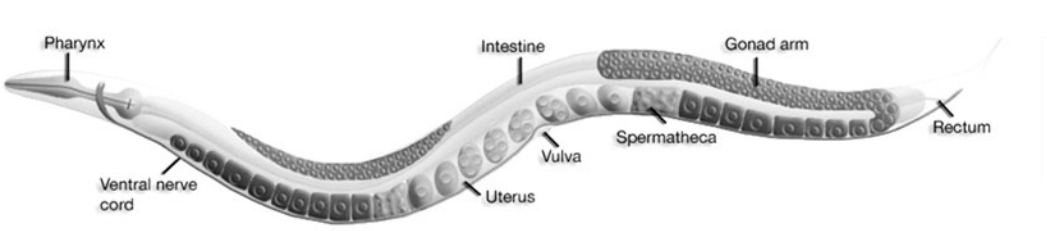

Figure 1-8. ***Caenorhabditis elegans*** **anatomy.**
Adapted and modified from WormAtlas [(112)]

C. elegans feeds on bacteria in liquid suspension. The particles are concentrated in the pharynx by expelling the liquid, transported through the bilobed pharynx, and ground in the terminal bulb. Ground particles enter the intestinal lumen. The pharynx is nearly an autonomous organ with an own neuronal system. The lumen of the pharynx merges into the lumen of the intestine. Posterior, the gut is connected to rectum and anus by a rectal valve.

The intestine is composed of 20 cells that are arranged in nine rings to form a tube with a central lumen. The large, cuboidal cells have distinct apical, lateral and basal regions, carrying plentiful microvilli at the apical surface. This apical pole forms part of the intestinal lumen. From the basal pole the components of the basal lamina are secreted. The intestinal cells contain large nuclei, numerous mitochondria, a large rough ER with many ribosomes, and a wide range of membrane-bound vesicles. The main function of the intestine is digestion. Intestinal cells secrete digestive enzymes and resorb nutrients. The fact that intestinal cells contain many granules implies also a role as storage organ. Autofluorescent gut granules can be examined by light microscopy and are supposed to be secondary lysosomes. Similar to muscles, the intestine is a major organ of fatty acid metabolism. Beyond fat storage, the intestine plays a role in various functions that are carried out by specialized tissues in higher organisms [(112)].

The pseudocoelom is a fluid-filled body cavity that is surrounded by the basal laminae of the hypodermis, the nervous tissues, the gonad and the intestine. Among other things, the pseudocoelom provides a medium for nutrient transport and intercellular signalling. Hence, it fulfils functions that are performed by the bloodstream in higher organisms. From larger nematode species it is known that

the pseudocoelomic fluid has a neutral pH, which is buffered by bicarbonate and phosphate, contains proteins, fat, glucose, mineral nutrients, and micronutrients. Fluid homoeostasis is regulated by the excretory system, the hypodermis and canal-associated neurons. Moreover, the pseudocoelomic cavity harbours the coelomocytes that act as a primitive immune system in *C. elegans* [112].

The life cycle of *C. elegans* is similar to other nematodes: a nematode develops from the embryonic stage through four larval stages (L1-L4) to adulthood (Figure 1-9). The larvae moult at the end of each stage and synthesize a new, stage-specific cuticle.

Embryogenesis consists of proliferation and organogenesis/morphogenesis. During proliferation, cell divisions from a single cell to approximately 550 undifferentiated cells take place. When the embryo reaches the 30-cell stage (at gastrulation) the egg is deposited. Organogenesis/morphogenesis is marked by terminal differentiation and elongation of the embryo [112].

Post-embryonic development begins 3 hours post-hatching in the presence of food [115]. That is, cell divisions resume in fixed temporal and spatial patterns through the four larval stages. By this means, a constant number of cells with determined fates develops [116, 117].

In the absence of food L1 larvae arrest development and can survive up to ten days. They resume normal development after food becomes available [118]. Under non-favourable environmental conditions, such as too dense population, shortage of food, and high temperature, L2 larvae enter an arrested state called the dauer larvae. These show reduced locomotion and arrest feeding. The duration of the dauer stage does not affect postdauer life span and is thus called a non-ageing state. After conditions get better, dauer larvae continue their development and moult to the L4 stage within 14 hours [112].

Approximately 45-50 hours post-hatch at 22 °C – 25 °C the nematode completes its 3-day reproductive life cycle [112]. The newly matured hermaphrodite consists of 959 somatic nuclei, since 131 from 1090 somatic cells undergo apoptosis [119]. The adult male consists of 1031 somatic nuclei [119]. Yet, it is shorter and more slender than the hermaphrodite [112].

The young adult hermaphrodite lays eggs for around 4 days. By self-fertilization a hermaphrodite can produce circa 300 progeny, whereupon the number of sperm is the limiting factor. Thus, by mating with a male the number of progeny can increase to 1200 - 1400. The adult hermaphrodite lives for additional 10 - 15 days [112].

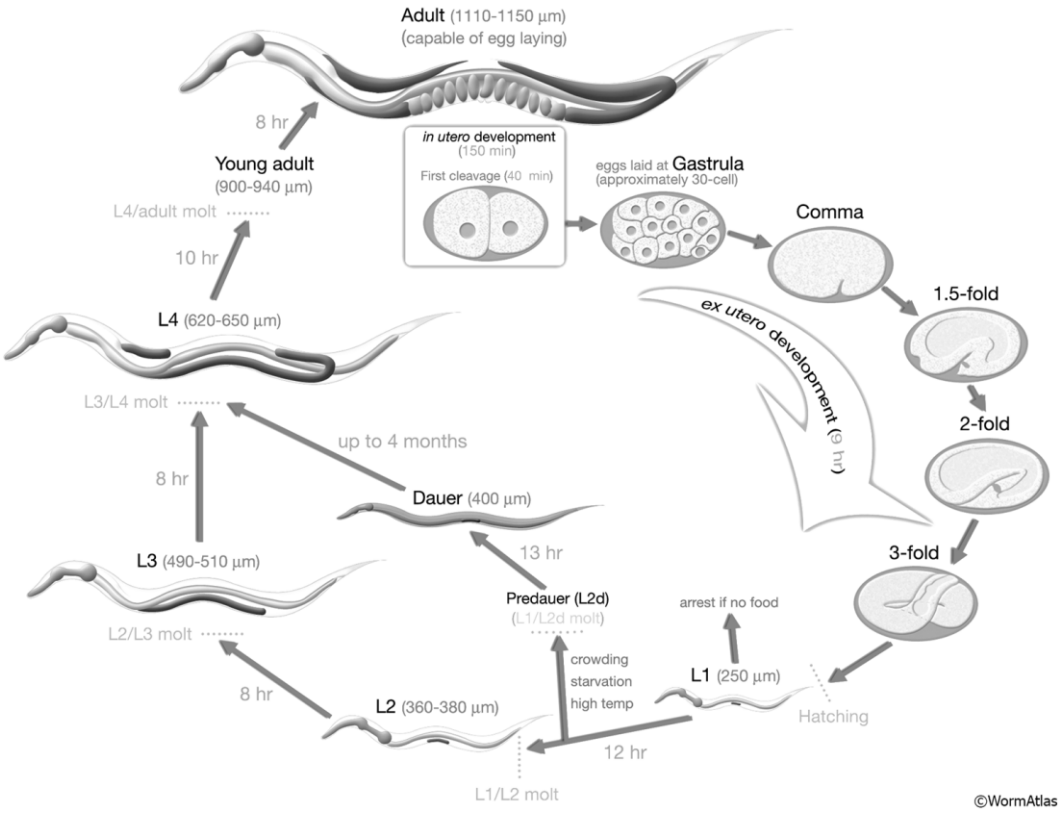

Figure 1-9. *C. elegans* life cycle at 22 °C.

Fertilization at 0 min. Numbers next to the arrows indicate the duration of the stage. Next to the stage name the length of the animal at this stage is given in micrometre (µm). Adapted from WormAtlas [112]

1.8.2 *C. elegans* as Model for Glucose-Induced Reduction of Stress Response and for Ageing

Oxidative stress causes damage of cellular components like lipids and proteins and can account for lifestyle-related diseases such as insulin resistance and diabetes mellitus [120]. As described earlier, increased superoxide production by the mitochondrial electron transport chain is supposed to be the hallmark of hyperglycaemia-induced disorders. In *C. elegans*, many mutations that increase life span also provide resistance to oxidative stress and heat stress. Moreover, mutants with reduced insulin signalling display an increased resistance to oxidative damage and reduced protein carbonylation [121].

Mev-1 (methyl viologen sensitive) mutants carry a mutation in the cytochrome b subunit of succinate dehydrogenase that results in excessive mitochondrial superoxide production and premature death [122]. Similar to insulin resistant subjects [123], superoxide in *mev-1* mutants is probably generated at complex II of the electron transport chain [120, 124], while under normal conditions it mainly derives from complexes I and III [123]. Moreover, *mev-1* mutants show *ced-3* (abnormal cell death)-dependent, abnormal apoptosis that accounts for the observed life span reduction [120]. Likewise, a high glucose diet causes *ced-3*-dependent, ectopic apoptosis and decreased survival, which can both be prevented by a loss-of-function mutation of *ced-3* [125]. *C. elegans* also possesses a protein quality control system that shares substantial similarities with the mammalian proteostasis network (chapter 1.8.4).

1.8.3 Stress Response Signalling Pathways

In order to adjust metabolism to internal or external stressors, *C. elegans* possesses an elaborate stress response system with the insulin/IGF signalling cascade as central determinant. The regulation of stress response further includes the heat shock response and its transcription factor HSF-1, xenobiotic metabolism that is regulated by SKN-1 (skinhead family member, homologous to mammalian nuclear respiratory factor (NRF)1 and NRF2) [126] as well as MAPK signalling through JNK-1, and nuclear hormone receptors like DAF-12 (abnormal dauer

formation) that mediate steroid signalling. The target of rapamycin pathway is an important regulator of stress resistance, too (Figure 1-10).

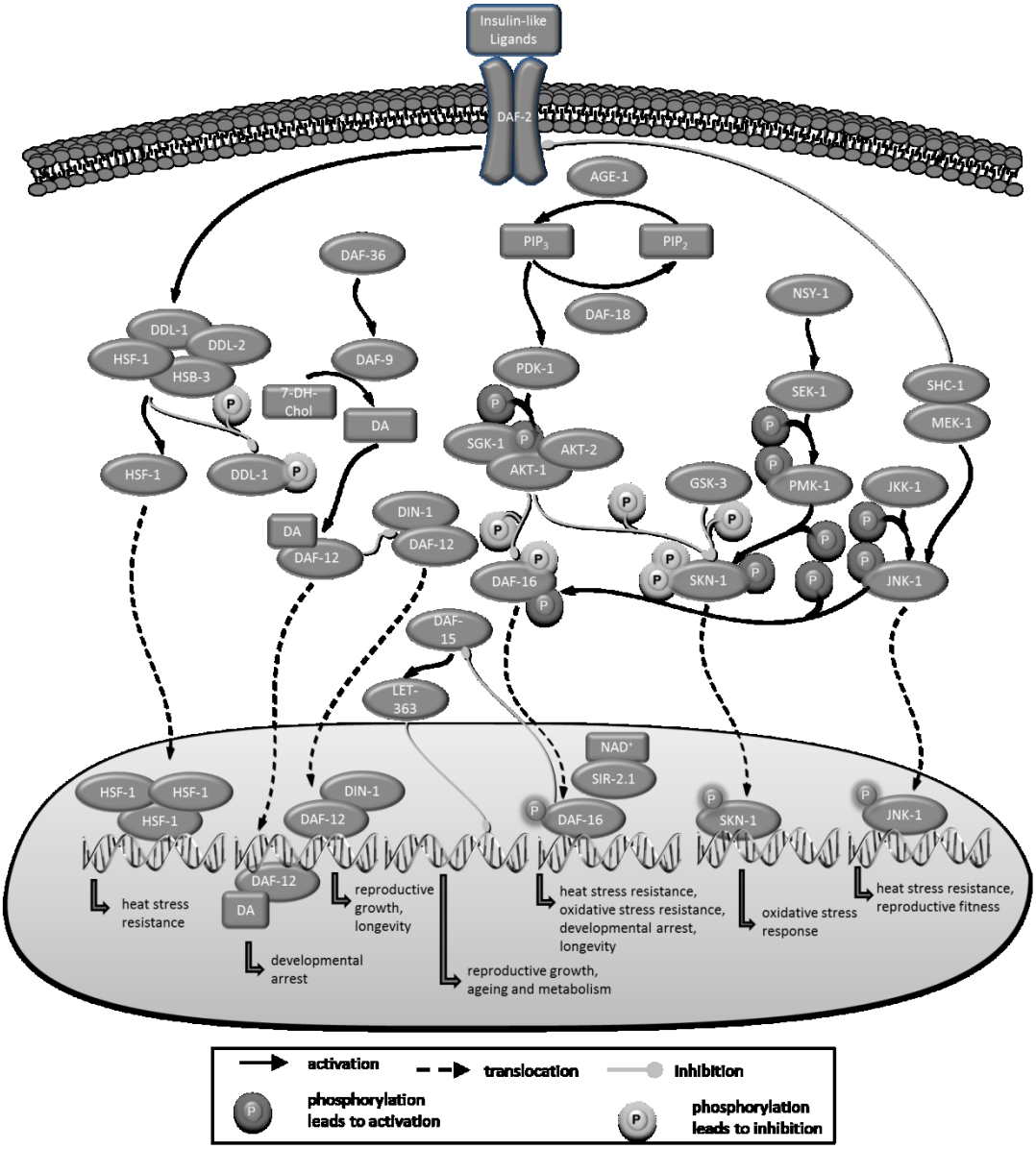

Figure 1-10. *C. elegans* stress response pathways.

Regulation and interaction of different stress response pathways that regulate resistance to oxidative stress or heat stress as well as development and reproduction in *C. elegans* are shown. 7-DH-Chol: 7-dehydrocholesterol, DA: dafachronic acids, PIP_3: phosphoinositide-3,4,5-P_3, PIP_2: phosphoinositide-4,5-P_2

1.8.3.1 Insulin/IGF-1 Signalling

The nematode expresses a single receptor, DAF-2, that is homologous to insulin and IGF-1 receptors of higher organisms [121]. Upon ligand binding to DAF-2 a phosphorylation cascade is activated. First of all, the PI3K homologue, AGE-1 (ageing alteration family member), is activated and produces phosphoinositide-3,4,5-P3 [127]. This mainly affects 3-phosphoinositide-dependent kinase 1 (PDK-1) that in turn activates several kinases, such as AKT kinase family members AKT-1 and -2 as well as serum- and glucocorticoid- inducible kinase homologue (SGK)-1 by phosphorylation [128, 129]. Finally, these kinases phosphorylate and thereby inactivate the transcription factor DAF-16, which is retained in the cytoplasm and thus cannot induce transcription of its target genes [130] (Figure 1-10). DAF-16 is a main regulator of heat stress, oxidative stress resistance, developmental arrest, fat storage, fertility, and metabolism [131, 132]. For example, the activation of DAF-16 by loss-of-function mutations in the insulin/IGF-1 receptor DAF-2 leads to increased heat stress resistance and longevity [133].

Many stress response pathways exist that act in parallel to insulin signalling and are integrated in this pathway by interaction with DAF-16. For instance, phosphorylation of DAF-16 by JNK-1 leads to increased nuclear translocation of the former [134]. Similarly, HSF-1 [135], SKN-1 [136] and the TGF-β ligand DAF-7 [130] have been shown to interfere with insulin signalling.

1.8.3.2 Heat Shock Response

The heat shock transcription factor HSF-1 is induced upon heat stress and required for maintenance of proteostasis. Downstream target genes of HSF-1 are, among others, chaperones and small heat shock proteins that are also controlled by DAF-16. Moreover, HSF-1 is required for longevity and increased stress resistance of *daf-2* mutants [135, 137]. The activation of HSF-1 is a multistep process that is negatively controlled by insulin/IGF-1 signalling. Currently it is assumed that insulin/IGF-1 signalling regulates the formation of an HSF-1 inhibitory

complex consisting of HSF-1, DDL-1 (*daf-16*-dependent longevity), DDL-2 and HSB-1 (heat shock factor binding protein, Figure 1-10), which reduces the nuclear localization and DNA binding activity of HSF-1 as well as the induction of HSF-1 target genes upon heat stress [138].

1.8.3.3 MAPK Signalling: JNK-1 and SKN-1

The MAPK signalling cascade and its transcription factor JNK-1 are activated by environmental stress conditions. Overexpression of JNK-1 increases resistance to oxidative and heat stress and leads to a *daf-16*-dependent life span extension. JNK-1 was shown to phosphorylate DAF-16 differently to AKT-1, AKT-2, and SGK-1, which results in enhanced nuclear localization of DAF-16 (Figure 1-10) [134].

Accordingly, activation and nuclear localization of SKN-1 are negatively controlled by the insulin/IGF-1 signalling kinases AKT-1, -2, and SGK-1 [139] but also by the glycogen synthase kinase (GSK) -3 [136]. Upon oxidative stress SKN-1 is phosphorylated in a different manner by PMK-1, which is a p38 MAPK orthologue, and translocates to the nucleus (Figure 1-10). There SKN-1 induces the transcription of target genes, like γ-glutamyl cysteine synthetase (*gcs-1*), a phase II detoxification enzyme, and glutathione S-transferase (*gst*) genes [139, 140].

1.8.3.4 The Nuclear Hormone Receptor DAF-12

Another pathway that regulates longevity and interferes with insulin/IGF-1 signalling is the DAF-9/DAF-12 pathway [141]. DAF-12 is one of 248 nuclear hormone receptors and has structural similarity to vitamin D, pregnane-X, liver-X, and androstane receptors [121]. DAF-9 is a CYP2 cytochrome P450 enzyme that generates cholesterol-derived, steroid-like ligands, termed dafachronic acids, for DAF-12. The DAF-9/DAF-12 pathway regulates reproductive growth, dauer formation, and longevity due to germ line ablation by integration of signals from the insulin/IGF-1 pathway and TGF-β signalling [141].

Comparative cell culture and *C. elegans* studies have revealed a functional similarity of DAF-12 to PPARs, although they do not have structural *C. elegans* homologues [142]. It was shown that *daf-12* and *daf-16* interact in insulin/IGF-1 signalling in *C. elegans* as do PPARγ and FOXO1 in mammalian cells [142]. PPARs interact with a family of transcriptional co-activators (PGC-1s, such as PGC-1α) that are critical for the control of glucose, lipid, and energy metabolism [143]. Similar to PPARs, the *C. elegans* genome seems to lack a structural PGC-1 orthologue [144]. However, MDT-15, a subunit of the *C. elegans* mediator complex, has been described to have partially overlapping functions with PGC-1α. MDT-15 physically interacts with NHR-49, which is functionally similar to PPARα, and is a transcriptional co-activator of NHR-49 target genes [145]. Moreover, MDT-15 is involved in the regulation of fat storage, numerous metabolic genes, and in caloric restriction [145, 146].

1.8.4 Protein Quality Control in *C. elegans*

C. elegans possesses a protein quality control system that is comparable to that of humans. The maintenance of proteostasis requires chaperones that ensure correct and efficient protein folding, heat shock and unfolded protein responses in the cytosol, mitochondria and the endoplasmic reticulum as well as the ubiquitin-proteasome system for protein degradation.

1.8.4.1 Chaperones and Protein Folding

The *C. elegans* proteins HSP-6 and HSP-60 are mitochondrial matrix chaperones, homologous to mammalian HSP70 and HSP60. Upon perturbations that are likely to impair the mitochondrial protein folding environment *hsp-6* and *hsp-60* gene expression is strongly induced [29].

RNAi-induced knockdown of *hsp-6* causes a reduction of *hsp-60* expression and leads to lower motility, defects in oogenesis, early accumulation of autofluorescent material and reduced survival, i. e. the major phenotypes of ageing worms. Consistently, *hsp-6* expression decreases during ageing [147].

1.8.4.2 Unfolded Protein Response

Accumulation of misfolded or aggregated proteins in the cytosol is prevented by the heat shock response that is controlled by HSF-1 and DAF-16. HSF-1 is the transcriptional regulator of heat shock genes, which mainly encode molecular chaperones and components of degradative machineries [148].

Downstream targets of HSF-1 are, for example, *hsp-70*, *hsp-90*, and small heat shock proteins, such as *hsp-16.1*, *hsp-16.49* and *hsp-12* [149]. Especially the induction of sHSPs, which bind to unfolded proteins and prevent them from aggregation, depends on both HSF-1 and DAF-16. Moreover, HSF-1 overexpression increases life span in a *daf-16*-dependent manner, and *vice versa*. Therefore, substantial cross-talk between heat shock response and insulin-like signalling exists in *C. elegans* [135]. Additionally, *hsf-1*-dependent, improved proteostasis seems to be involved in CR-mediated longevity [150].

As for mammalian cells (chapter 1.3.2), it is assumed that a specific unfolded protein response in mitochondria (UPR^{mt}) exists in *C. elegans* that is activated upon mitochondrial stress and, for example, by knockdown of mitochondrial chaperones or proteases. A model for UPR^{mt} in *C. elegans* suggests that the ABC-transporter HAF-1 pumps unfolded or unassembled mitochondrial proteins into the cytosol where they are degraded to peptides by the AAA+ protease ClpXP. Subsequently, the bZip transcription factor ATFS-1 (activating transcription factor associated with stress) activates the transcription of mitochondrial chaperones like *hsp-60* assisted by the homeobox protein DVE-1 (defective proventriculus in *Drosophila* homologue) and the ubiquitin-like protein UBL-5. As a result, the availability of mitochondrial chaperones is increased and proteostasis can be re-established [151].

Similar to humans, ER stress in *C. elegans* leads to the activation of an ER-specific UPR (UPR^{ER}) that is mediated by IRE-1, the PERK kinase homologue PEK-1, and ATF-6 [152, 153]. IRE-1 and PEK-1 play partially redundant roles, in which IRE-1 signals to activate UPR transcription targets and PEK-1 signals to attenuate protein synthesis. The induction of UPR target genes requires furthermore *xbp-1*, the mRNA of which is spliced by IRE-1 to produce a functional bZip transcription factor [152].

If the IRE-1/XBP-1 signalling pathway is blocked, a family of genes termed *abu* (activated in blocked UPR) is induced to protect from ER stress [154]. The *abu* family consists of nine highly related transmembrane proteins that are located within the endomembrane system. Inactivation of *abu-1*, a representative *abu* family member, leads to ER stress and enhances the phenotype of defective ER-associated protein degradation. In summary, it is assumed that ABU proteins play a role in ER function also under basal conditions but become particularly important in nematodes with impaired UPR [154].

1.8.4.3 The Ubiquitin-Proteasome System in *C. elegans*

C. elegans has two ubiquitin (Ub) loci, *ubq-1* and *ubq-2* [155]. As in other eukaryotes, *ubq-1* encodes an 838 amino acid peptide that includes 11 tandem Ub sequences and is post-translationally cleaved into single Ub peptides [156, 157]. *Ubq-2* includes a broadly conserved fusion gene of Ub and the L40 ribosomal subunit [158]. RNAi of *ubq-1* or *ubq-2* during larval stages produces larval arrest and lethality while RNAi depletion in adult hermaphrodites produces a one-cell stage arrest during meiotic divisions [159, 160].

The nematode possesses one ubiquitin-activating enzyme (*uba-1*), 20 putative ubiquitin-conjugating enzymes, and possibly several hundred of ubiquitin-protein ligases [161]. The sequential actions of these enzymes lead to the covalent attachment of multiple Ub that marks the proteins for degradation by the 26S proteasome. Disruption of *uba-1* activity would be expected to completely inactivate the Ub proteolytic pathway. However, RNAi of *uba-1* is not as penetrant as RNAi for *ubq-1* or particular proteasome components [161].

The *C. elegans* 26S proteasome consists of 14 conserved subunits that form the 20S core and 18 subunits that make up the 19S components [162]. Similar to *ubq-1* RNAi, RNAi depletion of proteasome components in larvae is lethal and leads to progeny that arrest at the one-cell stage in adult hermaphrodites [159, 163].

1.8.5 Apoptosis in *C. elegans*

Apoptosis occurs during development of the soma [116, 164], on the one hand, and in the gonad of adult hermaphrodites [117, 119, 165], on the other hand.

Egl-1 (egg laying defective), *ced-3* (cell death abnormality), and *ced-4* are death-promoting genes and required for most developmental cell death in *C. elegans* [166]. *Ced-9*, on the other hand, protects cells from developmental apoptosis [167]. *Egl-1* induces cell death by inhibition of *ced-9*, which results in the activation of *ced-4* and *ced-3* to kill cells [166]. CED-9 has similarity to the human anti-apoptotic BCL2 [168]. EGL-1 has a BH3 motif that is common to pro-apoptotic members of the BCL2 family [169, 170]. CED-3 is the major *C. elegans* caspase [171, 172] with homology to caspase-3 and its protease activity seems to be essential for programmed cell death in *C. elegans* [173]. CED-4 shows similarity to human Apaf-1: both contain a caspase-recruitment domain and nucleotide-binding motifs [174, 175].

The recognition and elimination of apoptotic cells is mediated by two signalling pathways that involve CED-1, CED-6 and CED-7, on the one hand, and CED-2, CED-5, CED-10, CED-12 and PSR-1 (phosphatidylserine receptor family), on the other hand [166]. CED-1 shares similarity with the human scavenger receptor SREC and clusters around cell corpses. Thus, it is assumed that CED-1 functions as cell corpse-recognizing receptor [176]. A loss-of-function of CED-1 leads to a partial block of cell corpse removal and results in the accumulation of dead cells [177].

The *C. elegans* germ line is the only adult tissue that is maintained by stem cells and is more similar to self-renewing mammalian tissues than the post-mitotic somatic tissues of adult nematodes. Moreover, germ cells are the only cells in which apoptosis is not regulated by an invariant cell lineage and that can undergo stress-induced apoptosis [178]. Similarly to somatic apoptosis, germ line apoptosis relies on the core apoptotic machinery, including CED-3 and CED-4 [179]. Physiological germ line apoptosis reduces the number of cells that complete oogenesis and can be distinguished from stress-induced germ line apoptosis that is triggered by DNA-damage or environmental insults [178]. The former is independent of the pro-apoptotic BH3-only protein EGL-1. On the contrary,

DNA-damage induced apoptosis relies on the p53-like CEP-1 and EGL-1, whereas environmental insults activate apoptosis via MAPK signalling and require, e.g. the MAP kinases SEK-1 (SAPK/ERK kinase) and MEK-1 (MAP kinase kinase or Erk kinase) as well as the downstream kinase PMK-1 and JNK-1 [178]. This indicates that stress-induced and physiological germ line apoptosis are regulated through differing pathways. The removal of cell corpses relies on the same mechanisms for both somatic and germ line apoptosis [178].

1.8.6 Autophagy in *C. elegans*

Autophagy in *C. elegans* plays various roles in the adaption to stress, ageing, and cell death but also in reproductive growth and cell growth control. Many genes that are required for autophagy in *S. cerevisiae* have orthologues in *C. elegans* and mammals. Hence, it is assumed that autophagy is similar in *C. elegans*, yeast and mammalian cells [180].

Bec-1 is the *C. elegans* orthologue of Beclin1 and is required for vesicle nucleation together with the PI3K LET-512 [181]. Vesicle expansion and completion involve two enzymatic complexes, i. e. the atg12 conjugation system and the atg8 lipidation system in yeast. The corresponding *C. elegans* homologues are LGG (LC3, GABARAP and GATE-16 family)-3 and LGG-1 [182].

It is presumed that autophagy in *C. elegans* occurs at basal levels but is strongly induced in response to stress, such as nutrient starvation, high temperature or hypoxia, to produce energy and remove damaged cellular components [180].

Although direct evidence for a regulatory role of TOR signalling in *C. elegans* autophagy is lacking, several studies indicate that this may be the case. For example, *let-363* RNAi in L4 hermaphrodites extends life span of adult nematodes and depends on autophagy genes, like *bec-1*. Moreover, increased autophagy was found in *daf-15* mutants that have low TOR signalling activity [183]. Additionally, *C. elegans* TOR pathway has nutrient-sensing function and can serve as a link between increased autophagy and life span extension in dietary restricted *eat-2* mutants [183, 184].

Similar to mammals, cross-talk between autophagy and apoptosis is likely to exist in *C. elegans*. As in mammals, *C. elegans* BEC-1 interacts with the anti-apoptotic Bcl-2 orthologue CED-9 [181]. An anti-autophagic role for CED-9 has not yet been reported. However, gain-of-function of the pro-apoptotic EGL-1, which acts upstream of CED-9, has been demonstrated to induce autophagy, while loss of *egl-1* reduces the induction of autophagy by starvation [50]. The p53-like CEP-1 is a further protein that functions in both autophagy and apoptosis. Knockdown of *cep-1* was shown to induce life span extension and autophagy in a *bec-1*-dependent manner [185]. Interestingly, expression of *sir-2.1* induces autophagy in *C. elegans in vivo*, which is suppressed by *bec-1* depletion. Moreover the sirtuin activation induces autophagy and mimics caloric restriction, while its inhibition prevents the induction of autophagy [186, 187].

1.8.7 Sirtuins as Mediators of Caloric Restriction and Their Role for Longevity in *C. elegans*

In *C. elegans* a variety of diet manipulating methods exists that all extend life span albeit this may involve several independent or overlapping mechanisms [188]. It is proposed, however, that life span extension by caloric restriction is dependent on the activation of the *C. elegans* sirtuin *sir-2.1* [189, 190] and subsequent inhibition of TOR signalling [191].

C. elegans possesses the four sirtuins *sir-2.1* to *sir-2.4*, whereof *sir-2.1* is the closest homologue to yeast Sir2 and human SIRT1. It is known that duplication of the *sir-2.1* gene in *C. elegans* extends life span up to 50% and that the transcription factor DAF-16 is required therefore [192]. In addition, the 14-3-3 (FTT) proteins FTT-2 and PAR-5 (abnormal embryonic partitioning of cytoplasm), which have been shown to interact with mammalian FOXO, physically interact with SIR-2.1 and are required for life span extension by *sir-2.1* overexpression. A current model proposes that SIR-2.1, DAF-16, and FTT proteins form a complex that leads to increased stress resistance mediated by active DAF-16.

In genetic models for CR in *C. elegans*, e. g., *unc-13* (uncoordinated) or *eat-2* (eating: abnormal pharyngeal pumping) mutants, *sir-2.1* is required for life span extension. These experiments as well as expression analyses also showed that *sir-2.1* and *daf-16* have both overlapping and distinct roles [(190)].

2 AIMS OF THE WORK

Ageing is an inevitable process that is associated with the development of age-related pathologies such as hyperglycaemia. In the present work the model organism *Caenorhabditis elegans* was used to study first of all, the molecular mechanisms by which glucose leads to reduced stress resistance, and secondly interventions that increase stress resistance and prevent glucose-induced toxicity.

Since mitochondrial biogenesis and respiration, oxygen consumption, reactive oxygen species (ROS) and ATP production are in the focus of discussions about relevant parameters for ageing, their response to feeding a high glucose diet were looked at in the first instance.

Moreover, the formation of methylglyoxal and protein oxidation were examined, because both are crucially involved in the generation of advanced glycation end products (AGEs). To identify which of the above mentioned pathways that regulate stress response, protein folding, unfolded protein response (UPR), proteasomal protein degradation, apoptosis and autophagy are relevant with regard to glucose-induced lifespan reduction, essential members of those pathways were knocked down by RNA interference (RNAi). Subsequently it was assessed, whether the response to glucose is altered or not, to verify the contribution of distinct genes in the mediation of glucose toxicity.

Secondary plant compounds are part of the daily human nutrition and can have a variety of beneficial effects on health. Hence, in the second part of this work it was analysed how the polyphenol quercetin, present in apples and onions, prevents glucose toxicity. Here, it was finally assessed, whether crucial regulators of cell fate can be rescued in their activities by the polyphenol after inhibition by glucose.

3 MATERIAL AND METHODS

Nematode and bacteria strains that were used in the present work, as well as instruments, chemicals and reagents are listed in the Appendix (section A) including information about suppliers and order numbers. Additionally, the composition and relevant components of buffers and solutions are indicated there.

3.1 Cultivation of *C. elegans*

According to Stiernagle *et al.* [114], all *C. elegans* strains were cultured on nematode growth medium (NGM) agar plates (Table A-36) seeded with concentrated *E. coli* OP50 liquid culture. Worms were transferred regularly to fresh plates before starving. With a sterilized scalpel a chunk of agar was moved from an old plate to a fresh one. Depending on the strain, worms were maintained at 15 °C and 20 °C, respectively.

For long term storage C. elegans strains were frozen and stored at –80 °C. *Therefore, plates containing f*reshly starved young larvae (L1 and L2 stage) were washed with freezing buffer A (Table A-17). To the liquid an equal volume of freezing buffer B (Table A-18) containing 30 % glycerol was added. Aliquots were placed into an isopropanol-filled freezing container to ensure a 1 °C decrease in temperature per minute during freezing [114].

3.1.1 Preparation of NGM Agar Plates

NGM agar was prepared according to Table A-36. After autoclaving the agar was chilled to 60 °C in a water bath and subsequently the sterile filtered solutions were added. Under sterile conditions about 20 ml of NGM solution were dispensed into petri dishes (9.2 cm). After the plates had dried they were seeded with 600 µl of a concentrated *E. coli* OP50 liquid culture. These plates could be stored for several days at room temperature and were used for cultivation of *C. elegans* [110].

3.1.2 Cultivation of *E. coli* OP50

E. coli OP50 is a uracil auxotroph *E. coli* strain whose growth is limited on NGM agar [110]. A starter culture was obtained from the Caenorhabditis Genetics Center (CGC). From this culture single colonies were isolated on 2xYT agar (Table A-34) using the quadrant streak technique. The streak plate was incubated overnight at 37 °C. The following day 3 ml 2xYT medium (Table A-35) were inoculated with a single colony from the streak plate and incubated overnight at 37 °C in a shaking incubator at 300 rpm. 500 µl of this overnight culture were used the next morning to inoculate 200 ml 2xYT medium. This culture was grown for 6 h at 37 °C in a shaking incubator at 300 rpm. Subsequently, the culture was pelleted by centrifugation at 5000x g for 5 min. The supernatant was removed and the bacteria were resuspended in 4.5 ml 2xYT medium. Such a concentrated liquid culture had an $OD_{600} = 2.6$ and was stored at 4 °C [114].

For long-term storage of bacteria 800 µl of an overnight culture were mixed with 200 µl glycerol and frozen at *–80* °C.

3.1.3 Synchronisation of *C. elegans* by Bleaching

For all experiments synchronous *C. elegans* populations were used. To obtain homogeneous nematode populations worms were synchronised by bleaching. Therefore, *C. elegans* stock plates containing many gravid hermaphrodites were washed with M9 buffer (Table A-13). Liquid and worms were collected in a 15 ml conical centrifuge tube and washed twice with M9 buffer. To a volume of 2.5 ml M9 buffer an equal volume of bleaching solution was added. The tube was shaken intensely for 2 minutes and subsequently centrifuged for 2 minutes at 1200x g to pellet the released eggs. The pellet was washed several times in M9 buffer. Overnight, the tube was shaken in an overhead rotator at 25 rpm and eggs hatched. The next morning larvae were centrifuged for 2 minutes at 1200x g and the pellet was resuspended in M9 buffer after the supernatant had been removed [193].

3.1.4 Cultivation of *C. elegans* in Liquid NGM

For all experiments synchronised L1 larvae were grown in liquid NGM (Table A-37) with bacteria in 96 well microtiter plates. In a volume of 10 µl M9 buffer about 10 larvae were transferred to each well. By centrifugation for 2 min at 2500 x g 300 µl concentrated *E. coli* were pelleted and resuspended in about 10 ml liquid NGM. The OD_{600} of the NGM solution was adjusted to 1.0, which corresponds to 8 x 10^8 bacteria/ml. To each well 46 µl of this suspension were added. Nematodes were grown protected from evaporation at 20 °C and shaking at 150 rpm.

For protein extraction and RNA isolation large amount of worms were needed. Thus, experiments were scaled up by factor 10 and set up in 24 well plates. For each treatment 2 – 4 plates were used.

3.1.5 RNA Interference

RNA interference (RNAi) is a well-established method to knockdown the expression of specific genes. The ingestion of double stranded RNA (dsRNA) leads to a rapid and strong degradation of the corresponding mRNA in *C. elegans*. First of all, dsRNA is cleaved into fragments of 21 to 25 basepairs (bp) called short interfering RNA (siRNA) by a dsRNA specific endonuclease (Dicer). The antisense strand of a siRNA molecule is bound by a protein complex called RNA induced silencing complex (RISC) and targets this complex to the corresponding mRNA, which is subsequently cleaved and degraded by an endonuclease that is part of the RISC (Figure 3-1).

E. coli HT115 carrying L4440 plasmids (Table A-8, Figure A-2) that encode the specific dsRNAs were fed to *C. elegans*. HT115 is RNaseIII deficient, which prevents the degradation of dsRNA. Bacteria from glycerol stocks of RNAi clones were replicated on 2xYT agar containing 100 µg/ml ampicillin and 25 µg/ml tetracycline (Table A-31) and grown overnight at 37 °C. An isolated colony was inoculated into 2 ml 2xYT medium containing 100 µg/ml ampicillin and grown overnight in a shaking incubator at 37 °C and 300 rpm. 50 µl of this overnight culture were then inoculated into 2 ml 2xYT medium containing 100 µg/ml

ampicillin and the transcription of dsRNA was induced by the addition of IPTG at a final concentration of 1 mM. The cultures were incubated for 4 hours at 37 °C, shaking at 300 rpm. Then, 1 ml bacteria suspension was pelleted and resuspended in about 1 ml NGM containing 25 µg/ml kanamycin (Table A-37). The OD_{600} was adjusted to 1.0. Kanamycin was used to inactivate bacteria and thereby prevent metabolism of glucose and plant compounds. For all RNAi experiments *E. coli* HT115 carrying the empty L4440 vector were used as negative control [(194)]. *Zmp-2* RNAi leads to delayed development and reduced progeny and was used as positive control in RNAi experiments [(195)]. Moreover, efficient knock-down of genes was verified by quantitative real-time PCR.

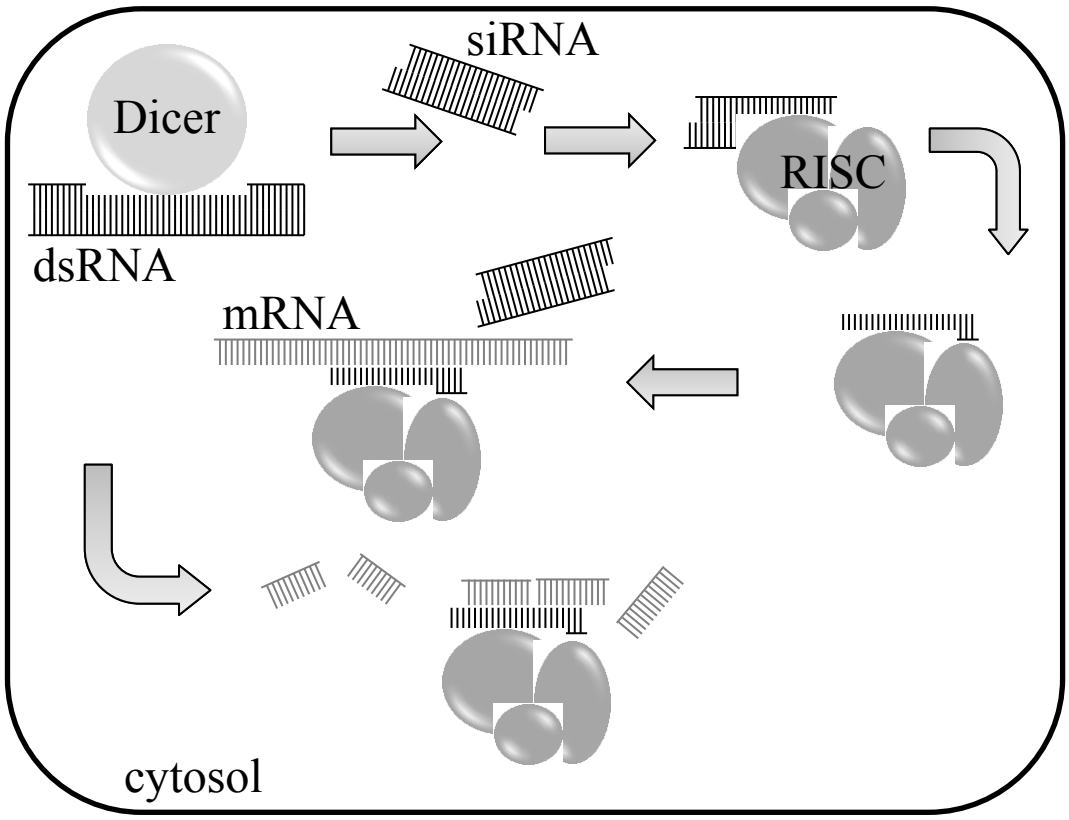

Figure 3-1. The principle of RNA interference.

Double stranded RNA (dsRNA) is cleaved by a protein complex called DICER to short interfering RNA (siRNA). The antisense strand of a siRNA molecule is bound by the RNA induced silencing complex (RISC). The bound siRNA hybridizes with a complementary mRNA strand, which is subsequently cleaved by the RISC. Hence, translation into a protein is prevented.

3.1.6 Incubation of *C. elegans*

At the young adult stage, which was usually reached 4 days after synchronisation, worms were treated with different substances for 48 hours. For each treatment a control group was set up, which received the solvent only.

Stock solutions (Table A-31) of the substances were warmed up to room temperature or prepared freshly. Working solutions with a 10fold higher concentration than the final concentration and an ethanol-content of maximal 10 % were prepared from the stock solutions by dilution with M9 buffer. Controls were always treated with the same amount of solvent.

At the end of the incubation period worms were transferred to 15 ml centrifuge tubes and washed several times in M9:TWEEN®20 (Table A-14) to remove bacteria and treatment substances.

3.1.7 Life Span Determination under Heat Stress Conditions

The measurement of life span under heat stress conditions according to Gill *et al.* [196] enables a high-throughput measurement of survival in *C. elegans*. This assay is based on the usage of the nucleic acid stain SYTOX green, which enters only dead cells, where it intercalates with DNA and gives a green fluorescence signal that is measured in a fluorescence microplate reader (Fluoroskan Ascent FL).

Therefore, 6.5 µl M9:TWEEN®20 were dispensed to each well of a black 384 well microtiter plate. Worms were separated one per well in a volume of 1 µl using a stereomicroscope. Finally, 7.5 µl of a 2 µM SYTOX Green solution (diluted in M9:TWEEN®20) were added. The plate was coated with sealing film and covered with a lid to prevent evaporation. At 37 °C the SYTOX green signal was measured every 30 min for 12 hours with an excitation wavelength of 485 nm and an emission wavelength of 538 nm.

To determine the life span for each nematode an individual fluorescence curve was generated (Figure 3-2). Time of death was defined as one hour after an increase in fluorescence over the baseline level was observed and was verified by

touch provocation first. From the individual times of death Kaplan-Meier survival curves were drawn.

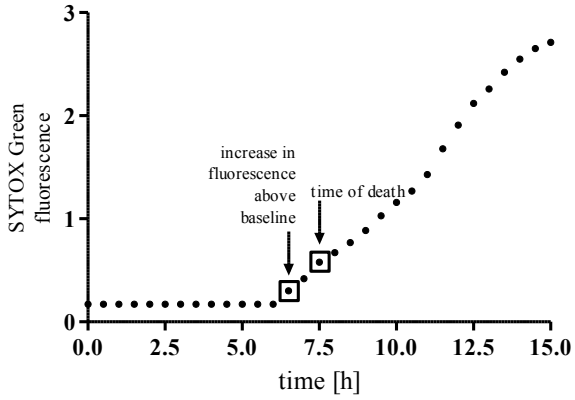

Figure 3-2. Typical fluorescence curve in a life span experiment under heat stress.

Each fluorescence curve was analysed to determine the time of death. The latter was defined as one hour after an increase in fluorescence above the baseline level was observed. Based on the individual times of death Kaplan-Meier survival curves were generated for each treatment group.

3.1.8 Epifluorescence Microscopy

For epifluorescence microscopy with an Axioskop 2 microscope (Zeiss, Jena, Germany) worms were washed in M9:TWEEN®20 until the supernatant had cleared. Thereafter, the supernatant was removed and nematodes were anaesthetized by addition of 500 µl 2 mM levamisol (Table A-31). In a volume of 40 µl worms were transferred onto a glass slide and covered with a cover slip. Images were taken at 50fold magnification and saved as jpeg-files.

Fluorescent intensities of whole nematodes were quantified using ImageJ, version 1.43. RGB images were split into three 8-bit grayscale images containing the red, green and blue components of the original. In the relevant colour channel a lower threshold was set so that only the nematode but not the background was selected. The integrated density, which is the sum of the values of the pixels, in the selected area was then measured.

3.1.8.1 Quantification of Reactive Oxygen Species in Mitochondria with MitoTracker® CM-H_2XRos

To determine reactive oxygen species (ROS) production in mitochondria the dye MitoTracker® CM-H_2XRos was used. The reduced, non-fluorescent form of the dye accumulates in mitochondria of active, respiring cells and is oxidized by ROS. Upon oxidation the dye forms a fluorescent conjugate with thiol groups of mitochondrial proteins and peptides, which can be detected by epifluorescence microscopy.

For detection a filter with an excitation wavelength of 530 - 585 nm and emission wavelength of 615 nm was used. The excitation maximum of CM-H_2XRos is 579 nm, the emission maximum is 599 nm.

The stock solution of the dye was prepared as 300 µM in DMSO (Table A-33) and further diluted to 5 µM in M9 buffer. The dye was used in a final concentration of 0.5 µM and added to the nematodes at the young adult stage together with treatment substances. After a 48−hour incubation period, worms were washed and images were taken as described above.

3.1.8.2 Quantification of Mitochondrial Biogenesis by MitoTracker® Green FM

MitoTracker® Green FM accumulates in the lipid environment of mitochondria irrespective of mitochondrial membrane potential. Therefore, it is a useful tool to determine mitochondrial mass. Fluorescence excitation and emission maxima are 490 nm and 516 nm, respectively. For detection of MitoTracker® Green FM a filter set with an excitation wavelength of 450 - 490 nm and emission wavelength of 515 - 565 nm was used.

The stock solution was prepared as 1 mM in DMSO (Table A-33). The dye was used in a final concentration of 200 nM and added to liquid NGM. After the incubation period nematodes were washed in M9 : TWEEN® 20 and transferred to fresh NGM plus *E. coli* OP50 for 2 hours. This step allowed elimination of excess

dye from the intestinal lumen. Then, worms were washed again in M9 : TWEEN® 20 and analysed microscopically.

3.1.8.3 Quantification of Mitochondrial Membrane Potential by MitoTracker® CM-XRos

MitoTracker® CM-XRos was utilized to measure active, respiring mitochondria. CM-XRos is a derivate of X-rosamine that diffuses passively across cell membranes and accumulates in active, respiring mitochondria where it forms fluorescent conjugates with thiol groups of proteins and peptides.

For detection a filter set with an excitation wavelength of 530 - 585 nm and emission wavelength of 615 nm (low-pass) was used. The excitation maximum of CM-XRos is 579 nm, the emission maximum is 599 nm.

The stock solution was prepared at a concentration of 100 µM in DMSO (Table A-33) and further diluted to 5 µM in M9 buffer. The dye was applied in a final concentration of 0.5 µM and added to the nematodes at the young adult stage together with treatment substances. After a 48−hour incubation period, worms were washed in M9 : TWEEN® 20 and images were taken as described above.

3.1.8.4 DAF-16::GFP Localization

DAF-16 is a transcription factor that translocates between the cytosol and the nucleus depending on its phosphorylation state (chapter1.8.3.1). The localization of DAF-16 was determined in a transgenic strain that expresses the transgene zIS356[*Pdaf-16::daf-16::gfp; rol-6*] in TK22 (*mev-1*). The transgenic strain was generated by microinjection and kindly provided by Dr. Kai Lüersen (University of Kiel, Germany). The transgene zIS356 consists of GFP coupled to DAF-16 under control of the DAF-16 promoter. For microscopy, a filter set with excitation at 450 - 490 nm and emission at 515 - 565 nm was used.

DAF-16::GFP localization was classified into three categories: predominantly cytosolic, predominantly nuclear, and intermediate. Figure 3-3 shows representative examples of these categories. Each nematode was assigned to one of these groups.

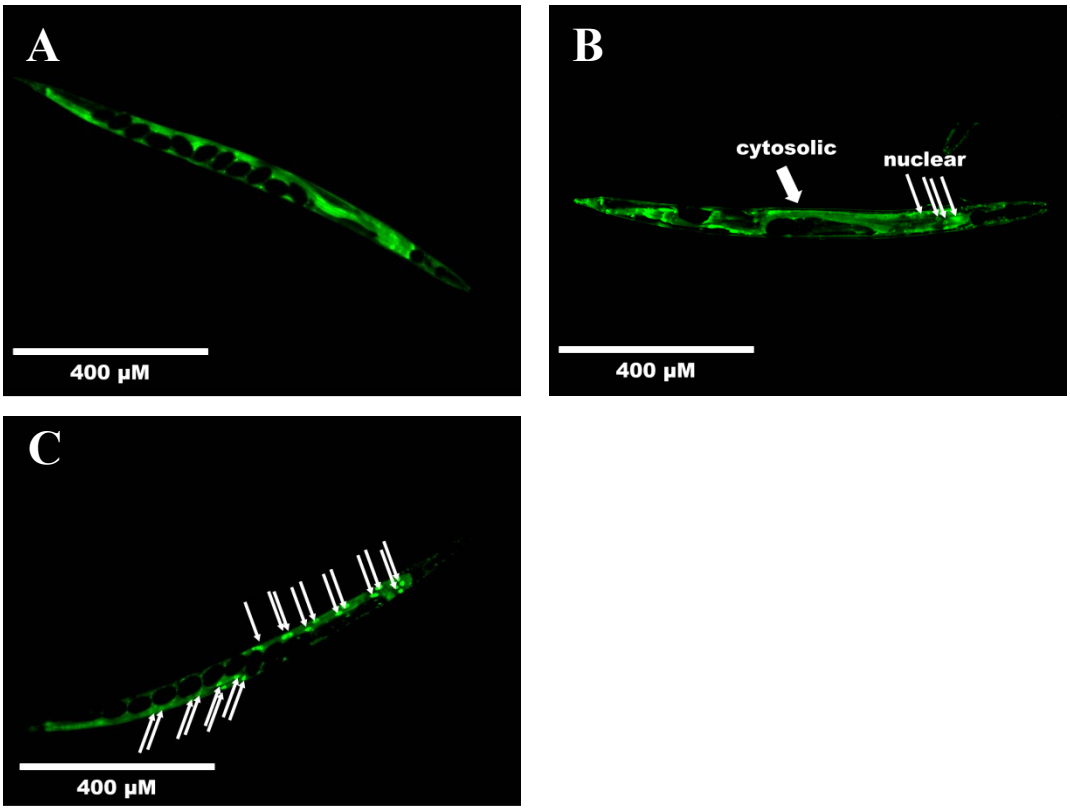

Figure 3-3. Subcellular DAF-16::GFP localization in transgenic *C. elegans mev-1.*

(A) Predominantly cytosolic DAF-16 localization, (B) Intermediate DAF-16 localization, (C) Predominantly nuclear DAF-16 localization. Arrows indicate exemplary nuclear localized DAF-16::GFP. Images were taken at 100fold magnification focusing on intestinal cells.

3.1.8.5 Quantification of Germ Cell Apoptosis Using SYTO12

Apoptosis in *C. elegans* was visualized using the DNA binding dye SYTO12. After the 48-hour incubation with treatment substances, worms were transferred to a 15 ml centrifuge tube, washed in M9:TWEEN®20 and the supernatant was removed. To the remaining worm suspension 100 µl of the SYTO12 working solution (66 µM, diluted in M9) were added. After a 4-hour incubation period at 20 °C in the dark, worms were washed twice in M9:TWEEN®20. Then the tube was filled up to 10 ml with M9 and worms were incubated for another hour in the dark at 20 °C. This step allowed the elimination of bacteria from the intestinal

lumen, which otherwise would also be stained by SYTO12. Then, worms were washed again in M9:TWEEN®20 and anaesthetized with 2 mM levamisol.

For detection of SYTO12 a filter with an excitation wavelength of 440 - 520 nm and emission wavelength of 497-557 nm was used. The excitation maximum of SYTO12 in presence of DNA is 499 nm, the emission maximum is 522 nm. Apoptotic cells of one gonad arm were counted at 400x magnification (Figure 3-4).

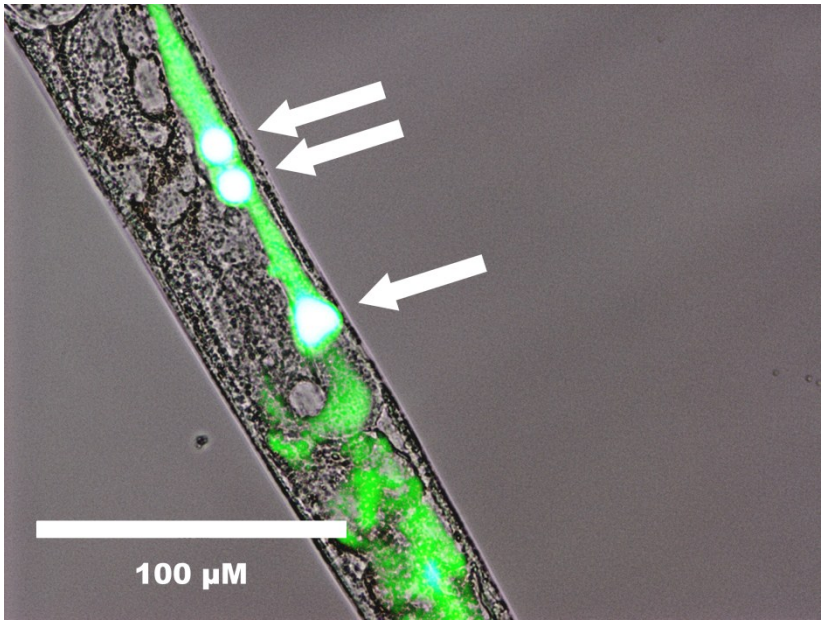

Figure 3-4. Apoptotic germ line cells in the anterior gonad arm of *C. elegans* TK22 (*mev-1*).

Apoptotic germ line cells were stained with the fluorescent dye SYTO12 and quantified microscopically. Arrows indicate apoptotic cells in the anterior gonad arm of C. elegans TK22 (*mev-1*).

3.1.9 Quantification of Oxygen Consumption

Oxygen consumption of nematodes was determined using PreSens OxoPlates® (Table A-1). The 96 well microplates have integrated sensors that contain an O_2 indicator and a reference dye, which can be read in a fluorescence reader. Prior to use a two-point calibration was performed with O_2-free water and air-saturated water. O_2-free water was prepared by adding 1 g Na_2SO_3 to 100 ml ddH_2O. Air-saturated water was prepared by rigorously shaking a water-filled tube for 2 minutes. Four replicates of each standard were measured. Therefore 200 µl

solution were filled in the wells and fluorescence was measured in the dual kinetic mode using the filter pairs 540/650 nm for the indicator dye and 540/590 nm for the reference dye. Measurements were performed in 1 minute intervals for 30 min. The referenced signal I_R (3-1), which corresponds to the oxygen concentration, was used to calculate the reader-constants k_0 (3-2) and k_{100} (3-3).

$$I_R = \frac{I_{indicator}}{I_{reference}} \quad \textbf{(3-1)}$$

$$k_0 = \overline{I_{R,0}} \quad \textbf{(3-2)}$$

$$k_{100} = \overline{I_{R,100}} \quad \textbf{(3-3)}$$

For the measurement of nematodes' O_2 consumption, approximately 100 young adult nematodes were transferred to a well in a volume of 180 µl. To the wells 20 µl treatment (or control) solution were added and the measurement was started immediately. For each treatment four replicates were prepared. The O_2 concentration pO_2 (% air saturation) was calculated for each measurement point (3-4).

$$pO_2 = 100\left(\frac{k_0}{I_R} - 1\right) / \left(\frac{k_0}{k_{100}} - 1\right) \quad \textbf{(3-4)}$$

3.2 Biochemical Methods

3.2.1 Protein Extraction

For protein extraction about 10000 nematodes per group were washed several times in M9:TWEEN®20. Then, 300 µl lysis buffer (Table A-29) were added and the tubes were frozen at –80 °C over night. After thawing on ice, the nematode suspension was sonicated 5 times for 1 min (amplitude 35, cycle 0.5). During sonication probes were kept on ice to prevent heating. The resulting suspension was then centrifuged for 20 min at 380 x g and 4 °C. The supernatant, which contained the proteins, was transferred to 2 ml reaction tubes and kept on ice or stored at –20 °C.

3.2.2 Determination of Protein Concentration

For determination of protein concentration the Bio-Rad Protein Assay was used. This assay is based on the method of Bradford [197]. The binding of proteins to Coomassie® Brilliant Blue G-250 results in a shift of the absorbance maximum from 465 nm to 595 nm, which can be measured spectrophotometrically.

A standard curve was prepared using BSA (0 µg/ml, 100 µg/ml, 250 µg/ml, 500 µg/ml, 1000 µg/ml) dissolved in lysis buffer (Table A-29). To 25 µl standard solution 975 µl H_2O and 250 µl Dye Reagent Concentrate were added and mixed well. For each concentration two replicates were prepared. After exactly 10 min incubation at room temperature absorbance was measured at 595 nm in an Eppendorf Biophotomer plus. The standard curve was calculated by the Biophotometer using a 3rd degree polynomial regression.

For protein determination of the samples 25 µl probe were mixed with 975 µl H_2O and 250 µl Dye Reagent Concentrate. Two replicates were prepared for each probe. The concentration was calculated by the Biophotometer using the calibration curve prepared before.

3.2.3 SDS Polyacrylamide Gel Electrophoresis

For gel casting and electrophoresis the Mini-PROTEAN 3 system (Bio-Rad, Munich, Germany) was used according to the instruction manual.

An 8.5% resolving gel (Table 3-1) was cast between to glass plates with 0.75 mm spacers to resolve proteins of 43 – 200 kD. The gel was layered with 1-methyl-2-propanol to exclude oxygen and facilitate polymerization.

Table 3-1. Composition of an 8.5 % SDS-PA resolving gel.

3.0 ml	1.5 M Tris (pH 8.8)
0.12 ml	10 % SDS (w/v)
3.4 ml	30 % acrylamide solution
5.44 ml	H_2O
0.16 ml	10 % APS
7 µl	TEMED

After the resolving gel had polymerized, 1-methyl-2-propanol was removed and a 5 % stacking gel (Table 3-2) was cast on top. A 10-well comb was inserted and the gel was allowed to polymerize completely for 1 hour.

Table 3-2. Composition of a 5 % SDS-PA stacking gel.

1.0 ml	0.5 M Tris-HCl (pH 6.8)
0.04 ml	10 % SDS (w/v)
0.68 ml	30 % acrylamide solution
2.24 ml	H_2O
0.04 ml	10 % APS
2 µl	TEMED

For protein denaturation 30 µg protein sample were mixed with the 2fold volume of 3x Laemmli loading dye (Table A-22) and incubated for 15 min at 55 °C in a water bath. One third or the denaturation reaction (equals 10 µg protein) was loaded onto the gel. Electrophoresis was run at 200 V (constant voltage) for 45 minutes using 1x running buffer (Table A-21).

3.2.4 Western Blot

After proteins had been separated by electrophoresis, they were blotted onto a PVDF membrane and detected by specific antibodies. Therefore, a 7 x 10 cm piece of PVDF membrane was activated in methanol and incubated in Towbin buffer (Table A-23) for 15 minutes. Six pieces of Whatman 3MM paper were also equilibrated in Towbin buffer. A semi-dry blotter was used for blotting. Three pieces of equilibrated Whatman paper were put onto the cathode, followed by the gel, the PVDF membrane, and another three pieces of Whatman paper. Blotting of proteins was accomplished by electrotransfer at 1 mA/cm^2 for 45 minutes.

3.2.4.1 Immunodetection

After blotting, the membrane was incubated for 1 hour in blocking buffer (Table A-26) to cover unspecific binding sites on the membrane. The DAF-12 antibody stock (Table A-6) was diluted 1:500 in 15 ml blocking buffer. The membrane was treated with the primary antibody for 1 hour under gentle shaking. Afterwards, the membrane was washed thrice for 5 minutes with 1x TBS-T (Table A-25). Then the membrane was incubated for 1 hour with the horseradish peroxidase (HRP)-conjugated secondary antibody (Table A-6), which had been diluted 1:1000 in blocking buffer. The membrane was washed twice for 5 min in 1x TBS-T and twice in 1x TBS (Table A-24).

After DAF-12 had been detected (chapter 3.2.4.2), primary and secondary DAF-12 antibodies were removed from the membrane by stripping. Therefore, the membrane was incubated for 45 min in strip buffer (Table A-28) at 50 °C in a water bath and afterwards washed twice in TBS-T buffer for 5 min. Subsequently, the omnipresent reference protein β-actin was detected on the same membrane.

This was done analogously to DAF-12 detection. All steps beginning with the incubation in blocking buffer were repeated using a β-actin specific antibody (Table A-6), which was diluted 1:500 in blocking buffer. After washing, the membrane was incubated for 1 hour with the secondary, HRP-conjugated antibody, which was used diluted 1:1000 in blocking buffer.

3.2.4.2 Chemiluminescence Detection

Chemiluminescence detection is based on the use of luminol combined with HRP-conjugated antibodies. Luminol exhibits chemiluminescence upon oxidation in the presence of peroxides like H_2O_2. Initially a luminol dianion is formed, which reacts with oxygen to a very unstable organic peroxide. When electrons go from the excited state to the ground state, energy is emitted as a photon. HRP is used as catalyst to accelerate the reaction that proceeds very slowly in the absence of a catalyst. Because the HRP is immobilized on the membrane the peroxide formation is localized. The light emission from the epoxide decay is captured with an X-ray film.

For chemiluminescence detection the membrane was incubated for 1 min with freshly prepared enhanced chemiluminescent solution (ECL, Table A-27), placed inside a plastic page protector and put into a film cassette. In a darkroom an autoradiography film was placed on top of the membrane, exposed for 2 to 5 min, and then developed in an X-ray film processor. X-ray films were scanned and the band intensity was analysed by ImageJ that was used to translate the optical density into peaks and measure the area under curve.

3.2.5 Detection of Oxidatively Modified Proteins

The Millipore OxyBlot™ Protein Oxidation Detection Kit (Table A-4) was used for immunoblot detection of oxidatively modified proteins. This kit is based on the derivatization of carbonyl groups that were introduced into proteins by oxidative reactions with 2,4-dinitrophenylhydrazine to 2,4-dinitrophenyl-hydrazone.

Two aliquots of each sample were needed. One was used for derivatization, the other one as negative control. 5 µl protein sample was denatured by adding 5 µl of 12% SDS. For derivatization 10 µl of 1x DNPH solution were added, while the negative control was incubated with 10 µl of 1x derivatization-control solution. After 15 min incubation at room temperature the reaction was stopped by adding 7.5 µl neutralization solution to both aliquots.

The derivatized protein samples were separated by polyacrylamide gel electrophoresis (chapter 3.2.3) followed by Western blotting (chapter 3.2.4). Therefore, the primary antibody, rabbit-anti-DNP, was diluted 1:150 in blocking buffer (Table A-26). The secondary antibody was a HRP-conjugated goat-anti-rabbit-IgG. It was diluted 1:300 in blocking buffer. Chemiluminescent detection and evaluation of band intensities was performed analogously to Western blotting (chapter 3.2.4.2).

3.2.6 Determination of Methylglyoxal

Methylglyoxal was determined from protein extracts by use of the OxiSelect Methylglyoxal ELISA Kit (Cell Biolabs, Table A-4). Proteins were prepared as described in chapter 3.2.1 and diluted to 100 µg/ml in 1x TBS buffer. Standards (1000 ng/ml, 125 ng/ml, 0 ng/ml MG) were prepared by dilution of 100 µg/ml MG-BSA with 100 µg/ml reduced BSA. Samples and standards were assayed in duplicate. 100 µl protein sample or standard were added to the 96well protein binding plate and incubated overnight at 4 °C. Subsequently, wells were washed twice with 250 µl 1 x TBS buffer. After incubation with 200 µl assay diluent per well for 1 hour at room temperature on an orbital shaker, wells were washed thrice with 250 µl 1x wash buffer. Afterwards, 100 µl primary antibody were added, which had been diluted 1:1000 in assay diluent before. After an incubation period of 1 hour on an orbital shaker, wells were washed again thrice with 250 µl 1x wash buffer. Next, 100 µl of the secondary antibody-HRP conjugate (diluted 1:1000 in assay diluent) were added and the plate was incubated for another hour on an orbital shaker. Finally, wells were washed 5 times with 1x wash buffer, and incubated for 10 min with 100 µl substrate solution. The enzyme reaction was stopped by the addition of 100 µl stop solution. Absorbance at 450 nm was read immediately on a microplate reader (Multiskan EX).

3.2.7 Measurement of the ATP Content from Nematode Homogenate

The ATP Content of TK22 (*mev-1*) homogenate was determined by use of the ATP Bioluminescence Assay Kit CLS II (Roche, Table A-4). The determination relies on the ATP dependency of the light emitting luciferase-catalysed oxidation of luciferin for the measurement of ATP (Figure 3-5).

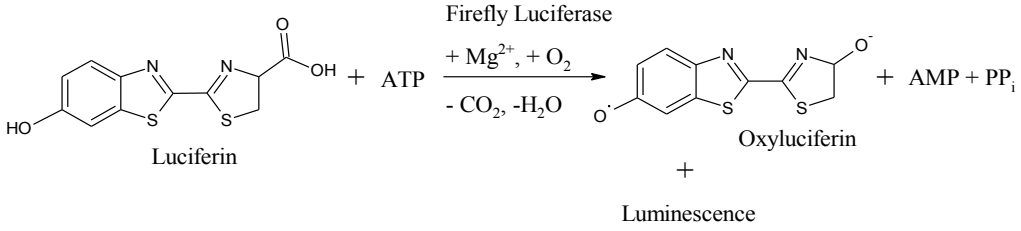

Figure 3-5. ATP-dependent luminescence generation catalysed by firefly luciferase.

Firefly luciferase catalyses the generation of adenyl-luciferin from D-luciferin and ATP. Adenyl-luciferin reacts with oxygen to oxyluciferin, water and carbondioxide. During this reaction luminescence is emitted. The emitted light is proportional to the available ATP.

To obtain a sufficient quantity of homogenate, about 600 worms per group were washed in M9 : TWEEN® 20 and centrifuged at 1200 x g. After the supernatant had been removed 500 µl lysis buffer (Table A-30) were added. The worms were frozen at –80 °C and subsequently homogenized in boiling water for 15 min. After centrifugation for 2 min at 2500 x g the supernatant was transferred to a fresh reaction tube and kept on ice until measurement.

The luciferase reagent was prepared by the addition of 10 ml ddH_2O to a bottle of lyophilized luciferase reagent. The bottle was incubated for 5 min on ice and afterwards gently mixed. For the preparation of ATP standards 10 ml ddH_2O were added to a bottle of 10 mg lyophilized ATP to get a final concentration of 10 mg/ml or 16.5 mM, respectively. The ATP standard curve was prepared by serial dilution with ddH_2O in the range of 1 nM to 1 µM.

The assay was set up in a white 96 well microplate with four replicates for each ATP standard concentration and probe. Per well 50 µl ATP standard or probe were mixed with 50 µl luciferase reagent. Luminescence was measured in a Fluoroskan Ascent FL using the default voltage of 890 V and an integration time of 1 s. The remaining probe was used to determine the protein concentration (chapter 3.2.2), which was used as reference value.

3.3 Molecular Biology Methods

3.3.1 Construction of RNAi Clones

The *sir-2.4* and *abu-11* RNAi clones were constructed as part of the present work, since they were not available from the Ahringer library [198]. Total RNA from *C. elegans* wildtype was used (chapter 3.3.2) as starting material for the *sir-2.4* clone. The cDNA was synthesized by reverse transcription polymerase chain reaction (RT-PCR, chapter 3.3.3) using *sir-2.4* specific primers (Table A-7) as well as oligo(dT)$_{18}$ primers. Since RT-PCR from total *C. elegans* wildtype RNA did not lead to valid *abu-11* cDNA, genomic DNA from *C. elegans* wildtype, isolated as described in chapter 3.3.3 was used for the construction of the *abu-11* clone.

The cDNA and genomic DNA were amplified by polymerase chain reaction (PCR, chapter 3.3.5) and cloned into pCR®2.1-TOPO® vector (Table A-8) for storage and further amplification (chapter 3.3.7). Vectors were transformed into *E. coli* NovaBlue Giga Singles (Table A-11, 3.3.8). After purification by plasmid midi-preparation (chapter 3.3.9) the pCR®2.1-TOPO® vector with the *sir-2.4* or *abu-11* inserts and the target L4440 vector (Table A-8) were digested by *HindIII* and *XhoI* (Table A-5, chapter 3.3.10). The digest was separated by agarose gel electrophoresis and subsequently purified using the peqGold Gel Extraction Kit (Table A-4). The purified insert DNA and L4440 vector DNA were ligated and transformed into chemically competent *E. coli* HT115 (chapter 3.3.11).

3.3.2 RNA Extraction

For RNA extraction 10000 to 15000 worms are needed. Adult worms were transferred into a 15 ml centrifuge tube, washed thoroughly in M9 buffer and centrifuged at 20000 x g for 2 min. The worm pellet was lysed in 1 ml total RNA isolation (TRI) reagent. Then, worms were frozen for 2 hours at –80 °C. After thawing and vortexing the worm pellet was centrifuged at 14000 x g for 10 min. The supernatant was transferred into a reaction tube and 400 µl chloroform were added to dissolve RNA. After incubation the mixture was centrifuged for 15 min at 20000 x g and 4 °C and the resulting clear, aqueous phase was collected. To precipitate the RNA 500 µl isopropanol were added. The RNA was pelleted by centrifugation for 15 min at 20000 x g and 4 °C. The supernatant was removed and the RNA was washed in 75% ethanol. Under sterile conditions ethanol was evaporated completely and the dry pellet was resuspended in 20 µl sterilised water containing 0.1% RNAsin.

Concentration and purity of RNA samples were determined spectrophotometrically: Samples were diluted 10fold in sterile ddH_2O to a final volume of 70 µl. The diluted sample was transferred to an Ultra-micro UV cuvette and the absorbance was measured at wavelengths 260 nm, 280 nm, and 230 nm. From the absorbance at 260 nm the RNA concentration (µg/ml) was calculated by multiplication with factor 30. The ratios 260/280 and 260/230 were used as indicators for protein and ethanol contamination of the nucleic acid samples. The dissolved RNA was stored at –80 °C.

3.3.3 cDNA Synthesis for Cloning

For cDNA synthesis the RevertAid^{TM} First Strand cDNA Synthesis Kit (Fermentas, Table A-4) was used. According to the manual 1 µg mRNA (0.5 µl), 20 pmol gene-specific primer (2 µl, 10 µM) or 100 pmol oligo$(dT)_{18}$ primer (1 µl, 100 µM), and to a final volume of 13.5 µl nuclease-free water were mixed. After denaturation at 65 °C for 5 min, the mixture was chilled on ice and the following components were added:

4 µl	5x reaction buffer
0.5 µl	RiboLock™ RNase inhibitor (20 u/µl)
1 µl	10 mM dNTP Mix
2 µl	RevertAid™ M-MULV reverse transcriptase (200 u/µl)

For reverse transcription the mix was incubated for 60 min at 42 °C and then terminated by heating up to 70 °C for 5 min. The cDNA was stored at –20 °C. For reverse transcription both oligo(dT)$_{18}$ and gene-specific primers were tried. The resulting cDNA was amplified by PCR using different combinations of gene specific primers. As can be seen from Figure 3-6, only PCR of cDNA generated with the oligo(dT)$_{18}$ primer and amplified with the gene specific primers sir-2.4-fw-282 and sir-2.4-rev-878 resulted in a detectable PCR product (lane 8). This was used for cloning in the following.

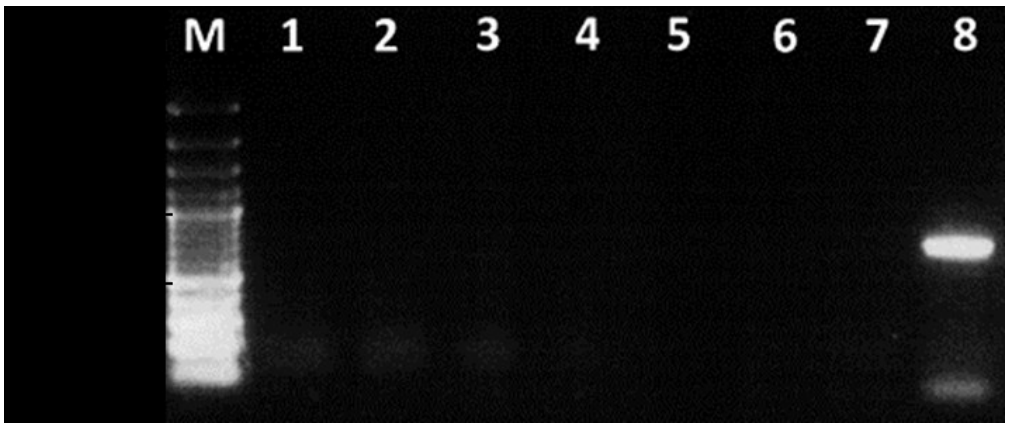

Figure 3-6. DNA gel electrophoresis of amplified *sir-2.4* cDNA.

M: marker, Gene Ruler™ 100 bp Plus DNA Ladder;
RT-PCR with gene specific primers sir-2.4-rev-878 (lane 1-4) or oligo(dT)$_{18}$ primer (lane 5-8) and PCR amplification of cDNA with sir-2.4-fw-282, sir-2.4 rev-857 (lanes 1 and 5); sir-2.4-fw-328, sir-2.4-rev-857 (lanes 2 and 6); sir-2.4-fw-328, sir-2.4-rev-878 (lanes 3 and 7), sir-2.4-fw-282, sir-2.4-rev-878 (lanes 4 and 8)

3.3.4 Genomic DNA Extraction

Genomic DNA from *C. elegans* wildtype was isolated using the GenElute Mammalian Genomic DNA Miniprep Kit (Sigma-Aldrich). Nematodes were transferred from NGM agar plates with M9 into a 15 ml centrifuge tube, washed several times and finally concentrated in a 1.5 ml reaction tube. To digest the worms 180 µl lysis solution T and 20 µl proteinase K solution were added. After vortexing the mixture was incubated for 2 hours at 55 °C in a water bath. To the completely digested sample 200 µl of lysis solution C were added, mixed well, and incubated for 10 min at 70 °C in a water bath. 200 µl ethanol were added to the lysate before it was transferred to a GenElute Miniprep Binding Colum, which had been set up with 500 µl column preparation solution, and subsequently centrifuged at 12000x g. After loading the lysate, the column was centrifuged at 10000x g for 1 min before it was washed twice with 500 µl wash solution and centrifuged for 1 min at 10000x g and 3 min at 12000x g, respectively. Finally, DNA was eluted by the addition of 200 µl elution solution and centrifugation for 1 min at 10000x g.

Concentration and purity of DNA samples were determined spectrophotometrically as described in chapter 3.3.2.

From the absorbance at 260 nm the dsDNA concentration (µg/ml) was calculated by multiplication with factor 50. Genomic DNA was stored at –20 °C until further use. Figure 3-7 shows the result of agarose gel electrophoresis of genomic DNA, which had been amplified with *abu-11* specific primers.

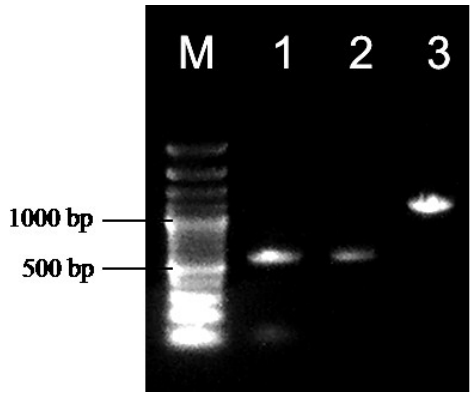

Figure 3-7. DNA gel electrophoresis of amplified *abu-11* from genomic DNA.

M: marker, Gene Ruler™ 100 bp Plus DNA Ladder;
PCR amplification of genomic DNA with abu-11-fw-699-1, abu-11-r-1198-1 (lane 1), abu-11-fw-184-2, abu-11-r-683-2 (lane 2), abu-11-fw-184-2, abu-11-r-1198-1 (lane 3)

3.3.5 Polymerase Chain Reaction

PCR was used to amplify cDNA or genomic DNA as well as control reaction to check for successful ligation and transformation reactions. A PCR master mix was prepared by mixing water, buffer, dNTPs, primers (Table A-7) and *Taq* DNA polymerase. The master mix was aliquoted into individual PCR tubes and finally the template DNA was added. For each 50 µl reaction the following components were needed:

5 µl	10x *Taq* buffer
5 µl	dNTP mix (2 mM each)
0.5 µM	forward primer
0.5 µM	reverse primer
2 µl	template DNA (10 pg – 1 µg)
1.25 u	*Taq* DNA polymerase
to 50 µl	nuclease-free water

The PCR was performed using thermal cycling conditions as listed below (Table 3-3), in which the annealing temperature was varied depending on the melting temperature of primers.

Table 3-3. Thermal cycling conditions for PCR.

Step	Temperature, °C	Time	No. of cycles
Initial denaturation	95	2 min	1
Denaturation	95	30 s	
Annealing	55	30 s	30
Extension	72	1 min	
Final extension	72	10 min	1

Different primer combinations were tried for the amplification of *sir-2.4* cDNA. The PCR was performed as touch-down PCR with annealing temperatures of 60 °C, 58 °C, and 56 °C for 15 cycles each.

To enhance the specificity of *abu-11* amplification, nested PCR was done using abu-11-fw-184-2 and abu-11-r-1198-1 primers for the first PCR and abu-11-fw-190-4 and abu-11-r-689-4 primers for the second. The annealing temperature was set to 57 °C.

3.3.6 DNA Electrophoresis

For DNA electrophoresis gels of 1% agarose in 1x TAE buffer (Table A-19) were prepared. 1x SYBR® Safe was added to the gel to visualize DNA. Sample DNA was mixed with 6x DNA loading dye (1:6 dilution). Equal volumes of marker DNA (Gene Ruler™ 100 bp Plus DNA Ladder) and sample DNA were loaded. Electrophoresis was run for 1 hour at 80 V. For detection a VisiBlue transilluminator was used, equipped with a 12x lens and MotiCam 2500.

3.3.7 TOPO TA Cloning®

TOPO TA Cloning® is an efficient one-step cloning method for PCR products that were amplified with *Taq* polymerase. Due to its terminal transferase activity, *Taq* polymerase adds a single deoxyadenosine (A) to the 3' ends of PCR products. This allows PCR inserts to ligate efficiently with the pCR®2.1-TOPO® vector that is supplied with single 3'-thymidine (T) overhangs and covalently bound Topoisomerase I. Topoisomerase I is bound to the overhanging 3' T of the vector by a phospho-tyrosyl bond that can be attacked by the 5' hydroxyl of the PCR product. As a result the PCR product is ligated with the vector and Topoisomerase I is released.

For long-term storage and amplification, *Taq* polymerase-amplified PCR products were cloned into the pCR®2.1-TOPO® vector (Figure 3-8) using the TOPO® TA Cloning Kit (Table A-4). The following components were mixed and incubated for 5 min at room temperature:

1 µl fresh PCR product
1 µl salt solution
3 µl water
1 µl pCR®2.1-TOPO® vector (10 ng/µl)

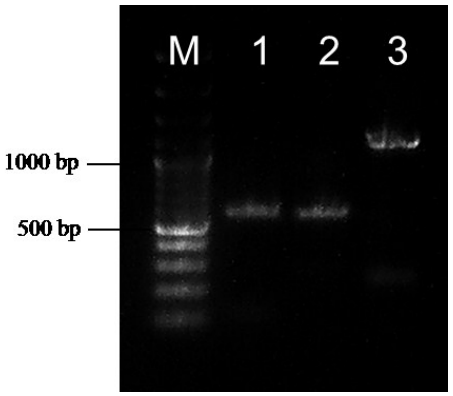

Figure 3-8. DNA gel electrophoresis after ligation of the *abu-11* insert into pCR®2.1-TOPO® vector and amplification by PCR.

M: marker, Gene Ruler™ 100 bp Plus DNA Ladder;
lane 1: abu-11-fw-699-1, abu-11-r-1198-1; lane 2: abu-11-fw-184-2, abu-11-r-683-2; lane 3: abu-11-fw-184-2, abu-11-r-1198-1

3.3.8 Transformation into *E. coli* NovaBlue Giga Singles

For transformation of the TOPO® cloning reaction into chemically competent *E. coli* NovaBlue Giga Singles, selection plates were prepared as follows: 40 µl of 40 mg/ml X-gal and 100 mM IPTG (Table A-31) each, were spread on 2xYT plate containing 50 µg/ml ampicillin (Table A-34) and incubated at 37 °C until usage. X-gal and IPTG were needed for blue/white screening: The successful cloning of the PCR product into the pCR®2.1-TOPO® vector leads to the disruption of the LacZα fragment of the plasmid vector, which is required for α-complementation of the β-galactosidase, because NovaBlue *E. coli* carry a lacZ deletion (lacZΔM15). IPTG is needed to induce the expression of the *lac* promoter, since NovaBlue overexpress the Lac repressor $lacI^q$. As a result, transformants that have taken up the correctly ligated plasmid cannot cleave X-gal into 5-bromo-4-chloro-indoxyl. The latter forms a bright blue pigment by dimerization and oxidation. Thus, transformants that carry the insert appear white, while others appear blue.

2 µl of the TOPO® cloning reaction were added to a vial of NovaBlue Giga Singles *E. coli* and mixed gently. After incubation cells were heat-shocked for exactly 30 s at 42 °C and subsequently put on ice for 5 min. Then 250 µl SOC medium were added and the tube was shaken for 1 hour at 37 °C. 50 µl of the transformation reaction were spread on a pre-warmed selection plate and incubated at 37 °C overnight. The following day, blue/white screening was performed and white or light blue colonies were picked for analysis. Successful transformation was checked by PCR using gene-specific primers and subsequent DNA gel electrophoresis (Figure 3-9).

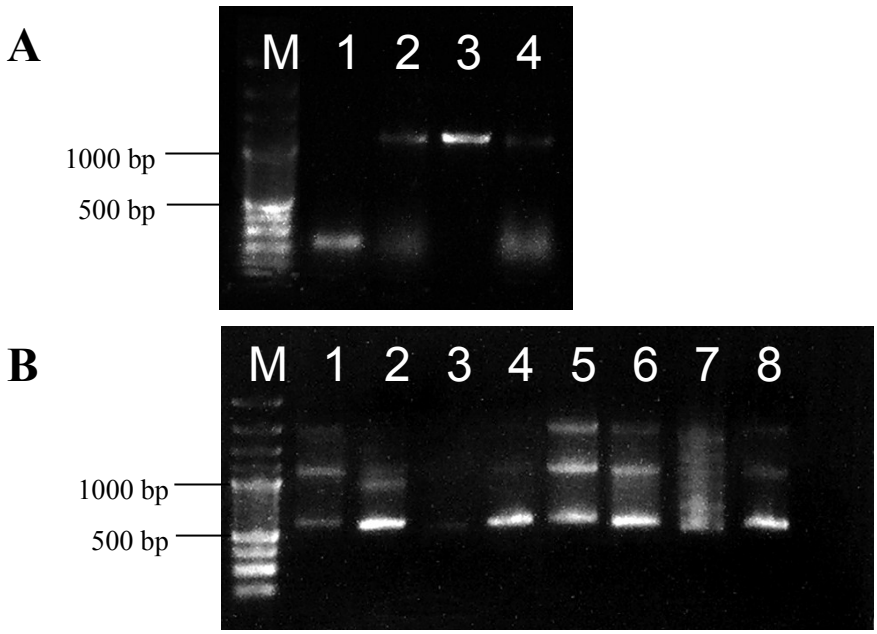

Figure 3-9. DNA gel electrophoresis of PCR-amplified *abu-11* (nested PCR) from white NovaBlue Giga Singles transformants carrying the pCR®2.1 vector with *abu-11* insert.

M: marker, Gene Ruler™ 100 bp Plus DNA Ladder; (A) 1st PCR amplification of *abu-11* with gene specific primers abu-11-fw-184-2 and abu-11-r-1198-1 from four different transformants. Templates 2 and 3 were used for nested PCR. (B) 2nd PCR amplification of *abu-11*, template 2 (lanes 1 – 4) and template 3 (lanes 4 – 8) with gene specific primers: lanes 1 & 5 abu-11-fw-699-1, abu-11-r-1198-1; 2 & 6: abu-11-fw-184-2, abu-11-r-683-2; 3 & 7: abu-11-fw-343-3, abu-11-r-842-3; 4 & 8: abu-11-fw-190-4, abu-11-r-689-4.

3.3.9 Plasmid Purification

For plasmid purification the FastPlasmid™ Mini Kit (Table A-4) was used according to the manual (5'Prime). In brief, 2 ml bacteria culture were centrifuged to pellet the cells. After decanting the supernatant, 400 µl ice-cold complete lysis solution were added and thoroughly vortexed. The lysate was transferred to a spin column assembly and centrifuged. The DNA was washed with 400 µl diluted wash buffer. Then, the spin column was transferred to a collection tube and eluted by addition of 50 µl elution buffer and centrifugation. The concentration of the purified plasmid was determined photometrically at 260 nm (chapter 3.3.4).

An aliquot of the purified plasmid sample was checked for the presence of the desired insert by sequencing. This was performed at the sequencer lab of the interdisciplinary research centre (University of Gießen). The remaining sample was stored at –20 °C until further use.

The preparation of larger amounts of plasmid DNA was done with the QIAfilter Plasmid Purification Kit (Qiagen, Table A-4) according to the supplier's manual.

3.3.10 Subcloning of *sir-2.4* and *abu-11* Inserts

For subcloning of the *sir-2.4* or *abu-11* inserts from pCR®2.1-TOPO® vector into L4440 a restriction digests of the pCR®2.1-TOPO® vector carrying the insert of interest and the empty L4440 vector were performed using *XhoI* and *HindIII* (Fermentas). A 50 µl reaction was set up according to the suppliers recommendations for use:

2.5 µl	plasmid DNA (0.5–1 µg/µl)
5 µl	10x buffer R
5 µl	*XhoI* (10 u/µl)
5 µl	*HindIII* (10 u/µl)
32.5 µl	nuclease-free water

The reaction components were gently mixed and incubated at 37 °C for 4h. Subsequently, the restriction digest reactions were separated by DNA gel electrophoresis (Figure 3-10) and the DNA fragments of interest were excised

from the gel and extracted with the PeqGOLD Gel Extraction Kit (Table A-4). Therefore, the gel slice was dissolved in an equivalent volume of binding buffer by incubation at 55–65 °C in a water bath for about 10 min. According to the suppliers manual (Peqlab), the pH of the solution was adjusted with sodium acetate to pH < 7.5. Next, the DNA/agarose solution was applied onto a PerfectBind DNA column and centrifuged for 1 min at 10000x g. The column was washed with 600 µl CG wash buffer and dried by centrifugation (1 min, 10000x g). DNA was eluted with 30 µl elution buffer and 1 min centrifugation at 5000x g.

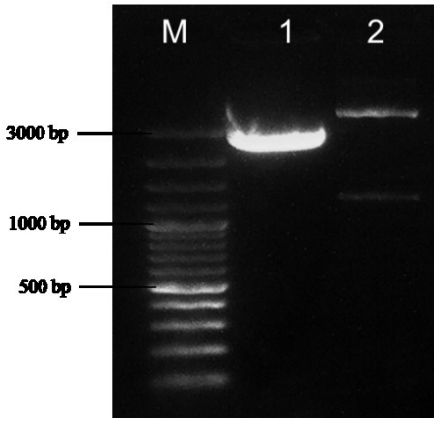

Figure 3-10. Restriction digest of the L4440 plasmid and pCR-2.1®TOPO® with *abu-11* insert for gel extraction.

M: marker, Perfect DNA™ 1 kbp Ladder;
lane 1: *XhoI* and *HindIII* digested L4440 plasmid;
lane 2: *XhoI* and *HindIII* digested pCR-2.1®TOPO® with *abu-11* insert

For ligation of digested and purified L4440 vector and *sir-2.4* or *abu-11* insert DNA the following components were mixed and incubated at 4 °C for 16 h:

0.5 µl	vector DNA (0.5 µg/µl)
1.5 µl	insert DNA (0.1 µg/µl)
3 µl	10x ligation buffer
2 µl	T4 DNA ligase (2 u/µl)
to 30 µl	sterile ddH_2O

The clone charts of the constructed RNAi clones are displayed in Figure 3-11.

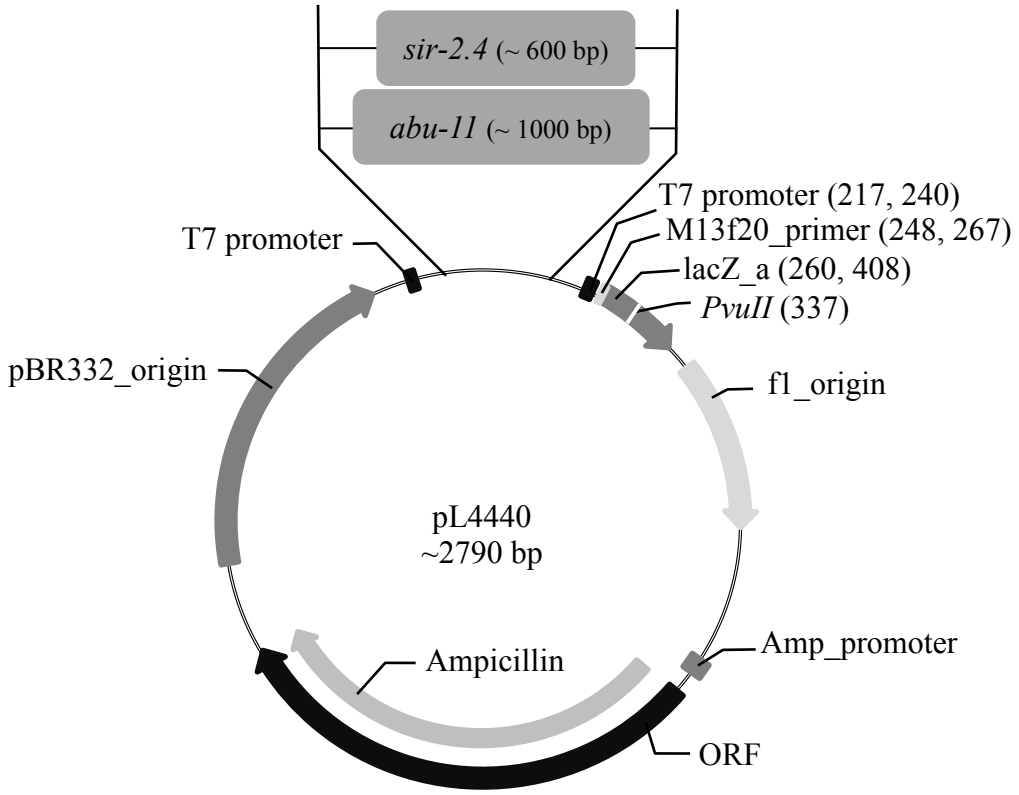

Figure 3-11. Schematic diagram of the constructed *abu-11* and *sir-2.4* RNAi plasmids.

Segments were cloned between flanking copies of the bacteriophage T7 promoter into a bacterial plasmid vector (pPD129.36 (L4440)). The bacterial strain *E. coli* HT115 expressing the T7 polymerase gene from an inducible (Lac) promoter was used as host.

The success of ligation was checked by PCR and subsequent gel electrophoresis (Figure 3-12).

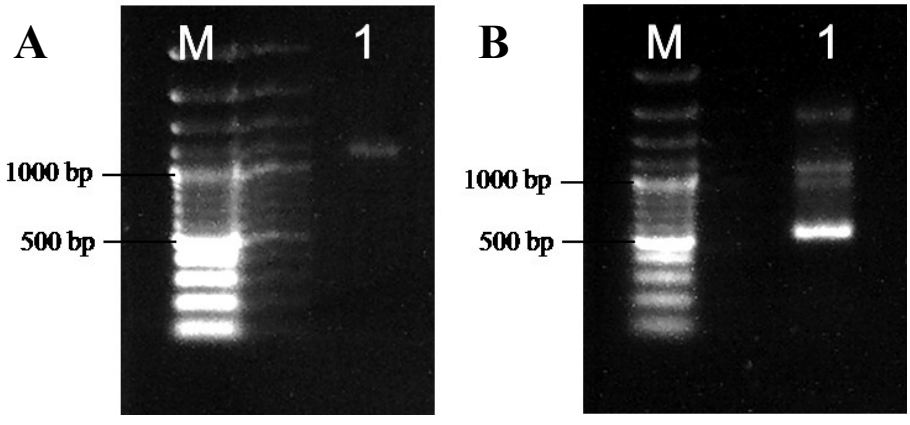

Figure 3-12. Nested PCR after ligation of *abu-11* insert into L4440 vector.

M: marker, Gene Ruler^{TM} 100 bp Plus DNA Ladder;
(A) 1st PCR with abu-11-fw-184-2 and abu-11-r-1198-1 primers
(B) 2nd PCR with abu-11-fw-190-4 and abu-11-r-689-4 primers

3.3.11 Transformation into Chemically Competent *E. coli* HT115

For the preparation of chemically competent *E. coli* HT115, a 50 ml culture of *E. coli* HT115 was grown for 3h at 37 °C. Bacteria were chilled on ice and centrifuged. The supernatant was discarded and the pellet was resuspended in 30 ml ice cold $MgCl_2/CaCl_2$ solution (Table A-20). The bacteria were again pelleted and this time resuspended in 4 ml ice cold $CaCl_2$ solution (1 M, Table A-31). After addition of 15% glycerol bacteria were stored at –80 °C.

Selection plates for transformation into *E. coli* HT115 contained 100 µg/ml ampicillin and 25 µg/ml tetracycline (Table A-34). Transformation was carried out as described in chapter 3.3.8. However, blue/white screening could not be performed after transformation into HT115. Thus, the success of transformation was checked by PCR (Figure 3-13) and sequencing.

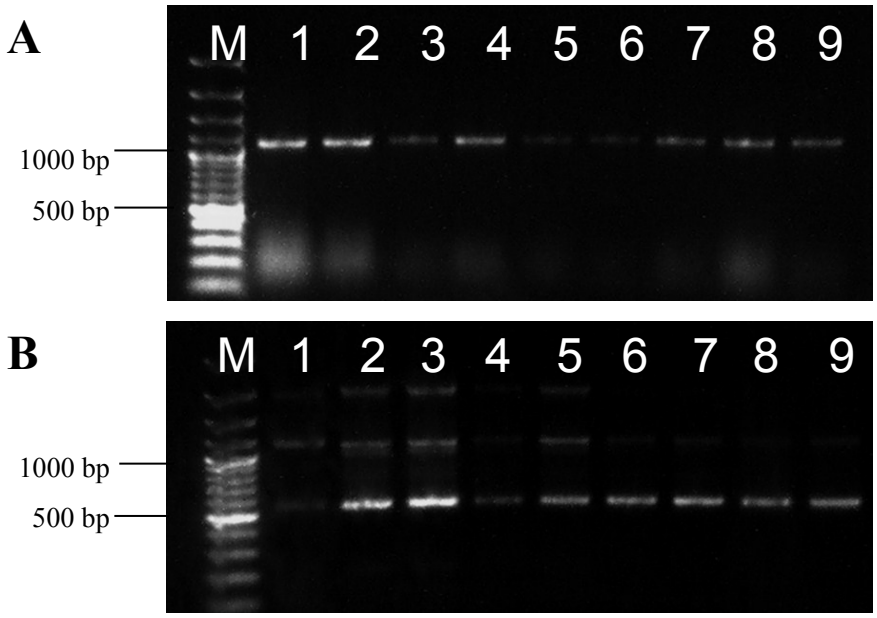

Figure 3-13. DNA gel electrophoresis of PCR-amplified *abu-11* (nested PCR) from different *E. coli* HT115 transformants carrying the L4440 vector with *abu-11* insert.

M: marker, Gene Ruler™ 100 bp Plus DNA Ladder; (A) 1st PCR amplification of *abu-11* from nine different transformants with abu-11-fw-184-2, abu-11-r-1198-1; (B) 2nd PCR amplification of *abu-11* using abu-11-fw-190-4, abu-11-r-689-4 primers.

3.3.12 Quantitative Real-Time PCR

Quantitative real-time PCR (qRT-PCR) has become the standard method for quantification of RNA targets. First of all, RNA is transcribed into cDNA by RT-PCR. Secondly, cDNA is amplified by PCR and detected in real-time. For quantification, here the binding of SYBR Green I to dsDNA was monitored. During amplification increasing amounts of dye bind to the amplified dsDNA and result in rising fluorescence signals. Quantification was performed relative to the reference gene 18S. C_t values from target RNAs are expressed as ratios to the reference gene [199].

For qRT-PCR, mRNA of treated nematodes was extracted as described in chapter 3.3.2 and adjusted to concentrations of 0.01 ng/µl and 10 ng/µl. Each reaction contained the following constituents (Table 3-4):

Table 3-4. Constituents of qRT-PCR reactions.

SYBR Green I Mastermix	5 µl
reverse transcriptase	0.4 µl
forward primer (1 µM)	0.75 µl
reverse primer (1 µM)	1.25 µl
template RNA	1 µl
H_2O (RNase free)	1.6 µl

From SYBR Green I Mastermix, reverse transcriptase and H_2O a mastermix was prepared. Primers and template were added individually to each reaction. For each treatment the extracted RNA was amplified with 18S primers and gene-specific primers for the gene of interest. In combination with 18S primers the template RNA was used in a concentration of 0.01 ng/µl and with gene-specific primers it was used in a concentration of 10 ng/µl. For each primer combination four replicates were prepared. The PCR strips were sealed and the qRT-PCR was run in a Bio-Rad CFX96™Real-Time-PCR Detection System. The following programme was used (Table 3-5):

Table 3-5. Thermal cycling conditions for qRT-PCR.

Step	Temperature, °C	Time	No. of cycles
Reverse transcription	50	15 min	1
Initial denaturation	95	10 min	1
Denaturation	95	30 s	40
Annealing	52	15 s	
Plate read			
Extension	60	30 s	
Final extension	95	1 min	1
Melt curve	52 to 95	30 s	increment 0.5
Plate read			

The Bio-Rad CFX Manager Software was used to generate fluorescence curves and determine C_T-values for each reaction. Mean and standard deviation of C_T-values were calculated from the replicates for each treatment. For evaluation the $\Delta\Delta C_T$ method was used [200]. That is, the mean C_T-value for a treatment analysed with gene-specific primers is subtracted from the mean C_T-value for the same treatment analysed with primers for the reference gene 18S (3-5). $\Delta\sigma_{CT}$ was calculated as square route of the sum of squared standard deviation (3-6).

$$\boldsymbol{\Delta C_T = \overline{C_{T_{gs}}} - \overline{C_{T_{18S}}}} \quad \textbf{(3-5)}$$

$$\Delta\sigma_{C_T} = \sqrt{\sigma^2_{C_{T,gs}} - \sigma^2_{C_{T,18S}}} \quad \textbf{(3-6)}$$

$\Delta\Delta C_T$ is defined as difference of ΔC_T for control and ΔC_T for treatment (3-7). $\Delta\Delta\sigma_{CT}$ was calculated as described for $\Delta\sigma_{CT}$ (3-8).

$$\Delta\Delta C_T = \Delta C_{T_{control}} - \Delta C_{T_{treatment}} \quad \textbf{(3-7)}$$

$$\Delta\Delta\sigma_{C_T} = \sqrt{\Delta\sigma^2_{C_{T,control}} - \Delta\sigma^2_{C_{T,treatment}}} \quad \textbf{(3-8)}$$

The fold change was calculated as 2 to the power of $-\Delta\Delta C_T$ (3-9).

$$fold\ change = 2^{-\Delta\Delta C_T} \quad \textbf{(3-9)}$$

3.4 Statistics

For each variable at least three independent experiments were carried out. Statistical analyses were performed using the software GraphPad Prism 5.0 (Table A-38). For the analyses the following significance levels were assumed: $p < 0.05$ (*), $p < 0.01$ (**), $p < 0.001$ (***).

Results of life span experiments were displayed as Kaplan-Meier survival curves and analysed with the Mantel-Haenszel Logrank test.

Unpaired t-test or one-way analysis of variance (ANOVA) and Bonferroni's multiple comparison test were performed to analyse epifluorescence microscopy experiments, methylglyoxal and ATP formation, Western and Oxy blot experiments as well as qRT-PCR. Results were illustrated as bar graphs showing mean and standard deviation. For Methylglyoxal and ATP formation calibration curves were calculated by linear regression. With respect to Western blots, the ratio of DAF-12 and β-actin expression was calculated for each lane. The ratios were normalized, i. e. the DAF-12 expression of the control group was set to 1. The same procedure was applied to Oxy blots.

Oxygen consumption was analysed by two-way ANOVA and Bonferroni's multiple comparison test. The time-dependent decrease in O_2 concentration was displayed as mean ± standard error from four replicates with 100 nematodes each.

4 RESULTS

Increased blood glucose concentrations in diabetic patients have pleiotropic effects on metabolism that terminally influence life span. The effects of feeding a high-glucose diet on life span and metabolic parameters of the nematode *C. elegans* were studied in the present work. Moreover the effect of glucose on different protein quality control systems was examined. Finally, polyphenols were used to activate stress response pathways and to counteract glucose toxicity.

4.1 Effects of Glucose on Life Span and Metabolic Parameters of *C. elegans mev-1* Mutants

4.1.1 Glucose Feeding Shortens the Life Span of *C. elegans*

First of all, the effect of glucose feeding on life span was studied in *C. elegans* TK22 (*mev-1*) under heat stress. Therefore, a synchronous population of young adult nematodes was treated with 10 mM glucose for 48 h. Previously, it was demonstrated that the glucose concentration in the culture medium correlates with the glucose concentration in the nematode [201].

Figure 4-1 shows a significant life span reduction by glucose in the *mev-1* mutant. The treatment with 10 mM glucose led to a 34% reduction in mean life span. Similar results were obtained in the *C. elegans* wildtype N2 (Table B-1).

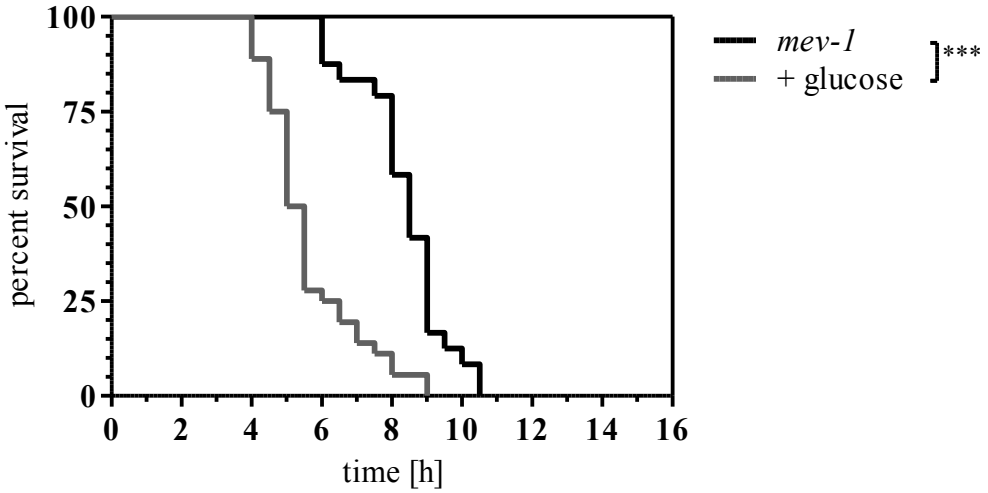

Figure 4-1. Glucose treatment shortens the life span of *C. elegans* TK22 (*mev-1*).
Young adult *mev-1* nematodes were treated for 48 h with M9 buffer (control) or 10 mM glucose. Subsequently, the life span under heat stress (37 °C) was measured. *** $p < 0.001$

4.1.2 Glucose Effects on Mitochondria

4.1.2.1 Glucose Increases Mitochondrial ROS Levels

Reduction equivalents from glucose oxidation are used for ATP production by the electron transport chain in mitochondria. As a major site of endogenous ROS production and oxidative stress, the respiratory chain is an important factor for ageing and degenerative diseases. For studying the effect of glucose treatment on ROS generation, the fluorescent dye MitoTracker Red® CM-H_2XRos (chapter 3.1.8.1) was used. Figure 4-2 shows that treatment with 10 mM glucose significantly increased ROS production. Compared to control animals glucose treated nematodes generated 45% more ROS.

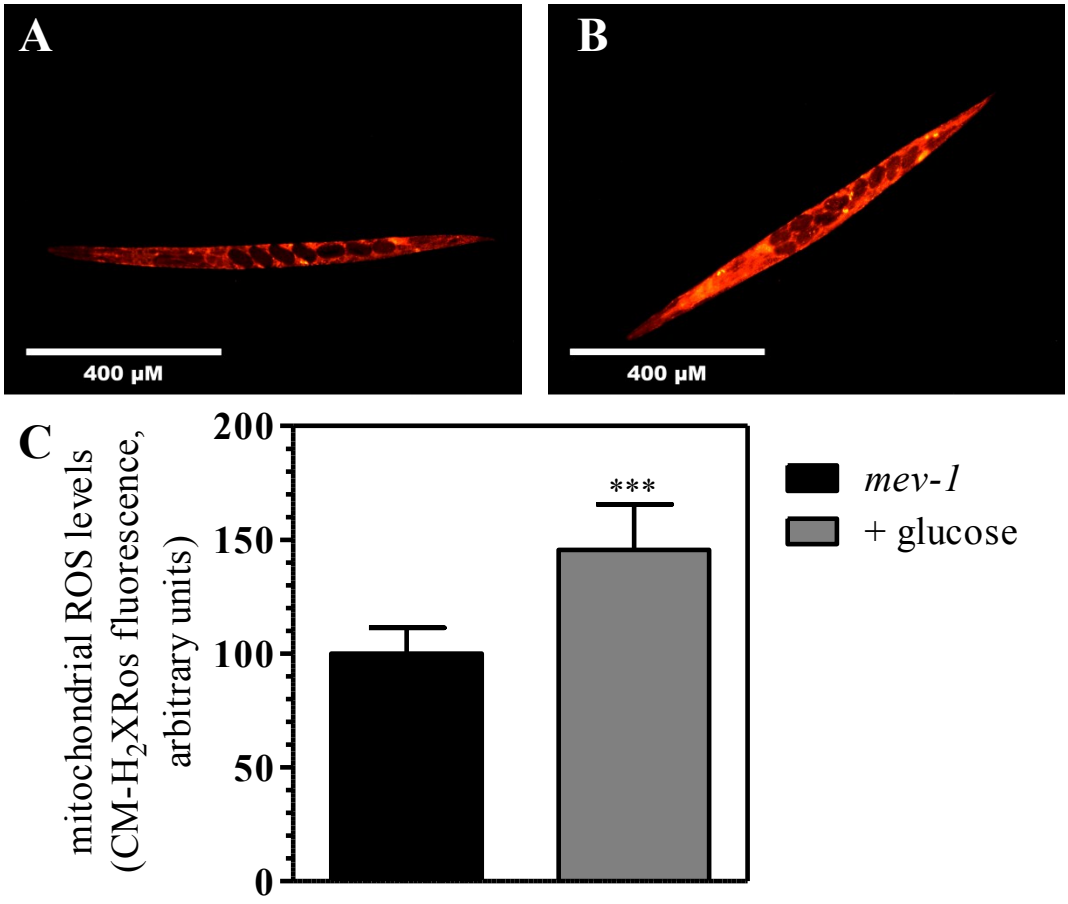

Figure 4-2. Glucose treatment increases mitochondrial ROS levels in *C. elegans* TK22 (*mev-1*).

Young adult *mev-1* nematodes were treated for 48 h with (A) M9 buffer (control) or (B) 10 mM glucose. Mitochondrial ROS were stained with the fluorescent dye CM-H_2XRos and detected microscopically. (C) Quantification of mitochondrial ROS levels. *** $p < 0.001$compared to the control

To examine whether the increased ROS production causes the life span reduction in glucose treated *mev-1* nematodes, the antioxidant ascorbic acid was applied simultaneously with 10 mM glucose to scavenge ROS. From Figure 4-3 arises that ascorbic acid dose-dependently suppressed ROS production, with 250 µM yielding ROS concentrations that were not different from the untreated control. The treatment with ascorbic acid only reduced ROS generation by 21% (100 µM) and 45% (250 µM) compared to control animals (data not shown).

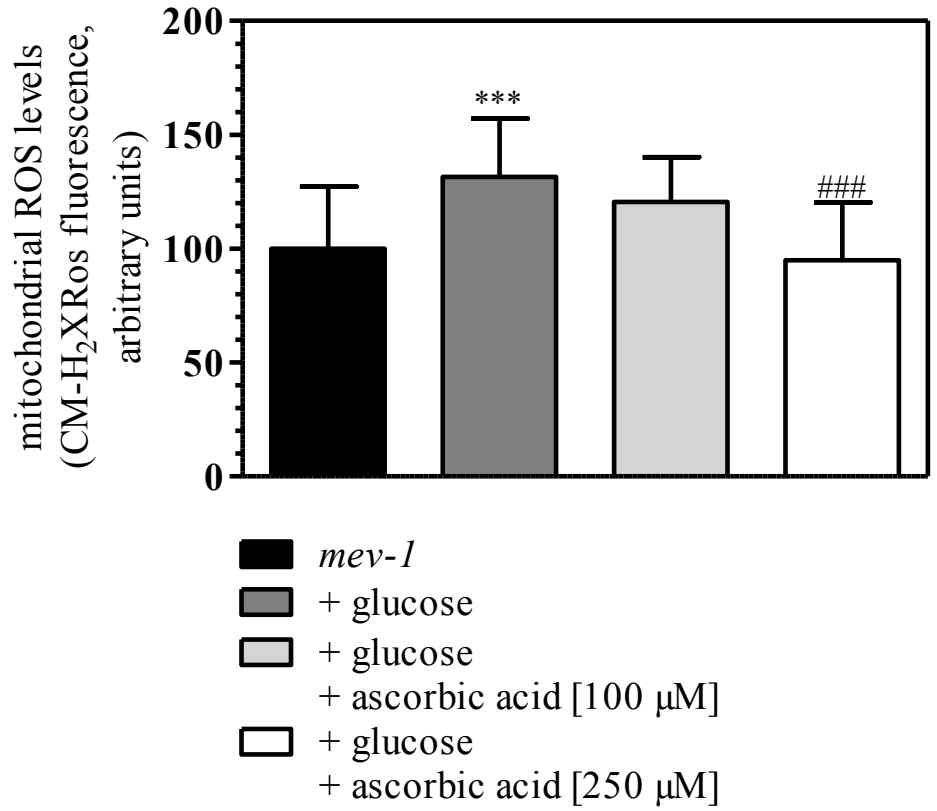

Figure 4-3. Ascorbic acid reduces mitochondrial ROS levels in the presence of glucose.

Young adult *mev-1* nematodes were treated for 48 h with M9 buffer (control), 10 mM glucose, or 10 mM glucose plus ascorbic acid at 100 µM or 250 µM. Mitochondrial ROS were stained with the fluorescent dye MitoTracker Red® CM-H_2XRos and detected microscopically. *** $p < 0.001$ compared to control; ### compared to treatment with 10 mM glucose

However, in spite of completely reverting ROS levels to control values, ascorbic acid did not influence the life span of glucose treated worms ($p = 0.837$ vs. glucose, Figure 4-4).

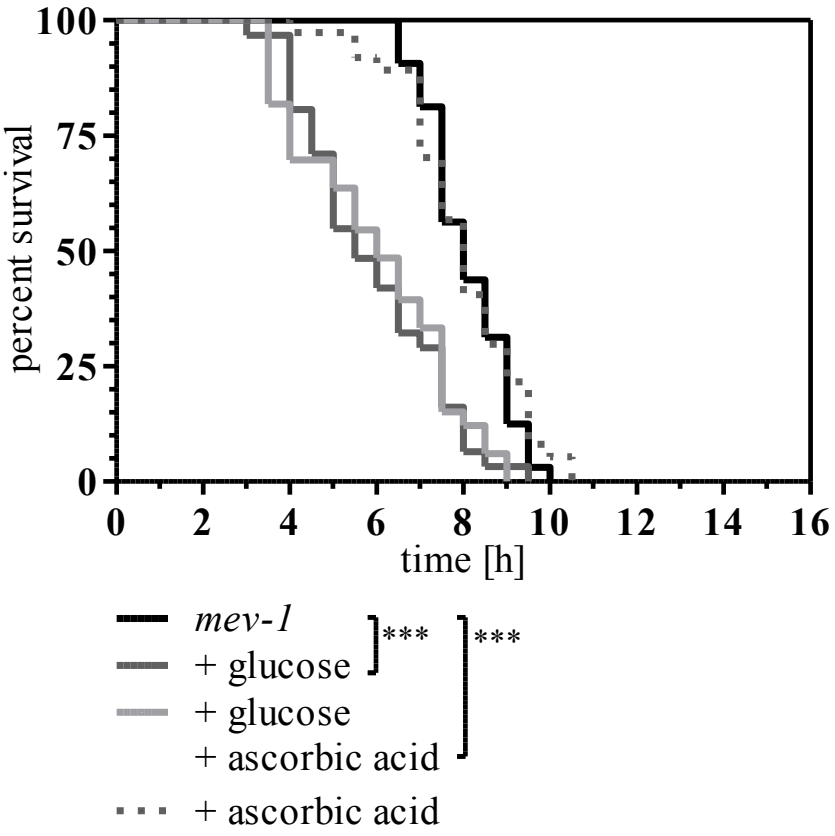

Figure 4-4. Life span of *C. elegans* TK22 (*mev-1*) in the absence (control) or presence of ascorbic acid, glucose, or a combination of both.

Young adult nematodes were treated with M9 buffer (control), 10 mM glucose, 250 µM ascorbic acid or a combination of 10 mM glucose and 250 µM ascorbic acid for 48 h. Subsequently life span under heat stress (37 °C) was measured. *** $p < 0.001$ compared to control

These results imply that glucose-induced life span reduction is independent of enhanced ROS production.

4.1.2.2 Glucose Effects on Mitochondrial Activity and Mass

Sustained exposure to excess nutrients serves as a potential link between ageing and insulin resistance and is supposed to exert deleterious cellular effects among others by mitochondrial dysfunction. Thus, the effects of glucose feeding on mitochondrial mass and activity were examined. Mitochondrial activity was determined using the fluorescent dye MitoTracker Red® CM-XRos that was added to young adult nematodes together with 10 mM glucose. Figure 4-5 shows that a 48-hour treatment with 10 mM glucose led to a significantly increased mitochondrial activity.

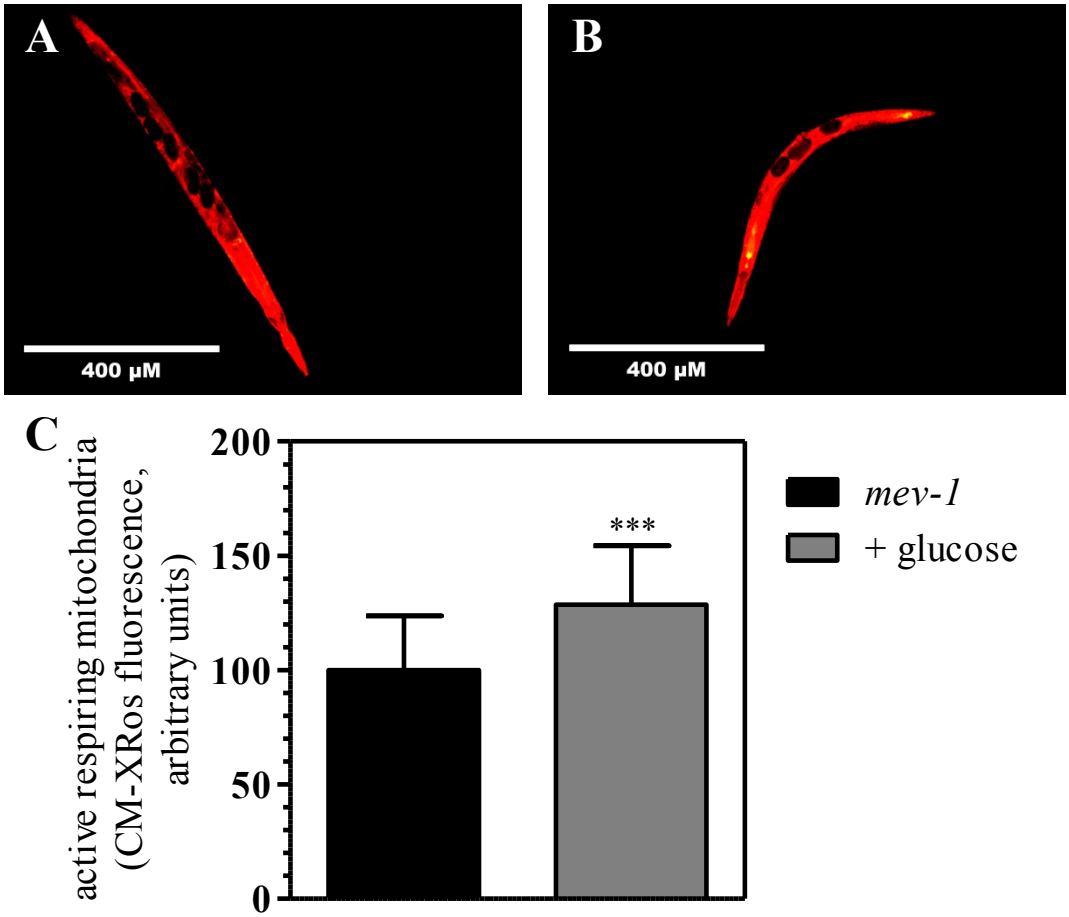

Figure 4-5. Active respiring mitochondria after glucose treatment in *C. elegans* TK22 (*mev-1*).

Young adult nematodes were treated with (A) M9 buffer (control) or (B) 10 mM glucose for 48 h. Active respiring mitochondria were stained using MitoTracker® Red CM-XRos and detected microscopically. (C) Quantification of active respiring mitochondria. *** $p < 0.001$ compared to control

Mitochondrial mass was determined using MitoTracker® Green FM, which was added to synchronous L1 larvae and accumulates in the lipid environment of mitochondria. When the nematodes had reached the young adult stage they were treated with 10 mM glucose for 48 hours and subsequently examined microscopically. Similarly to mitochondrial activity, the treatment with 10 mM glucose led to a highly significant increase of mitochondrial mass (Figure 4-6).

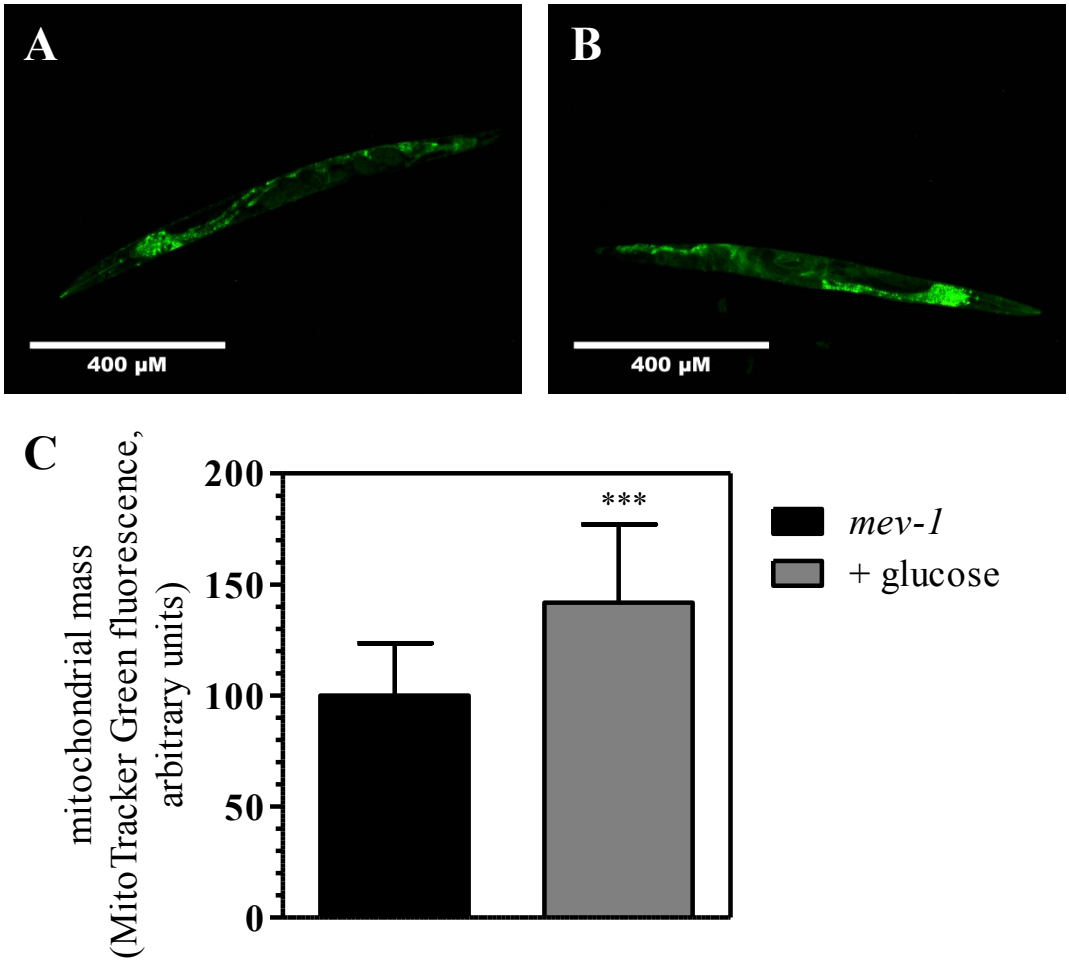

Figure 4-6. Mitochondrial mass is increased by glucose treatment in *C. elegans* TK22 (*mev-1*).

Young adult nematodes were treated with (A) M9 buffer (control) or (B) 10 mM glucose for 48 h. Mitochondrial mass was quantified microscopically using the fluorescent dye MitoTracker® Green FM. (C) Quantification of mitochondrial mass. *** $p < 0.001$ compared to control

As a measure for mitochondrial efficiency the ratio of mitochondrial activity and mitochondrial mass was calculated. This revealed a 10% reduction by glucose treatment (Figure 4-7).

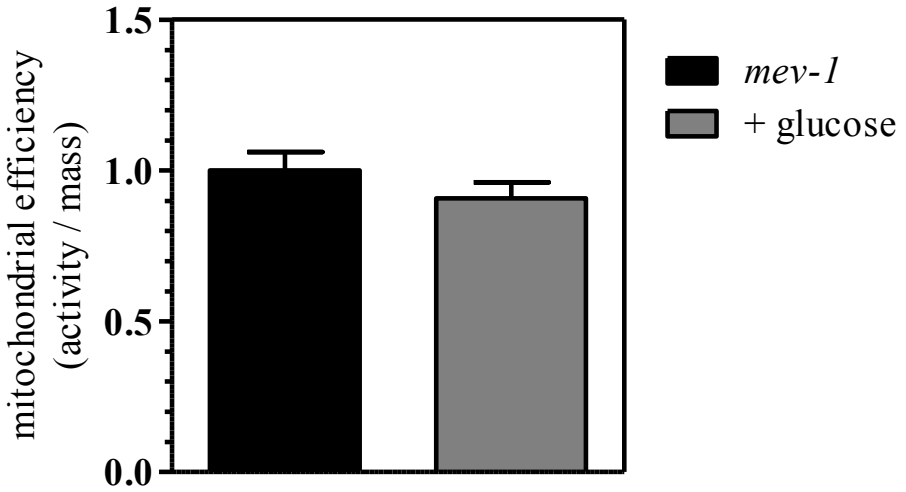

Figure 4-7. Mitochondrial efficiency after treatment with glucose of *C. elegans* TK22 (*mev-1*).

Young adult nematodes were treated with M9 buffer (control) or 10 mM glucose for 48 h. Mitochondrial efficiency was calculated as ratio of active respiring mitochondria and mitochondrial mass.

As a result, neither changes in mitochondrial activity nor in mitochondrial mass can account for glucose-toxicity. However, a reduced mitochondrial efficiency was shown for both glucose concentrations and point to a contribution of mitochondrial physiology on life span.

4.1.2.3 Glucose Increases Oxygen Consumption but Not ATP Production

As further parameters of metabolic activity, oxygen consumption and ATP production were determined in *mev-1* mutants treated with 10 mM glucose. For oxygen consumption measurement synchronous young adult nematodes were transferred to an oxygen sensor plate. The application of glucose led to a highly significant increase of oxygen consumption in the first 15 min of incubation (Figure 4-8).

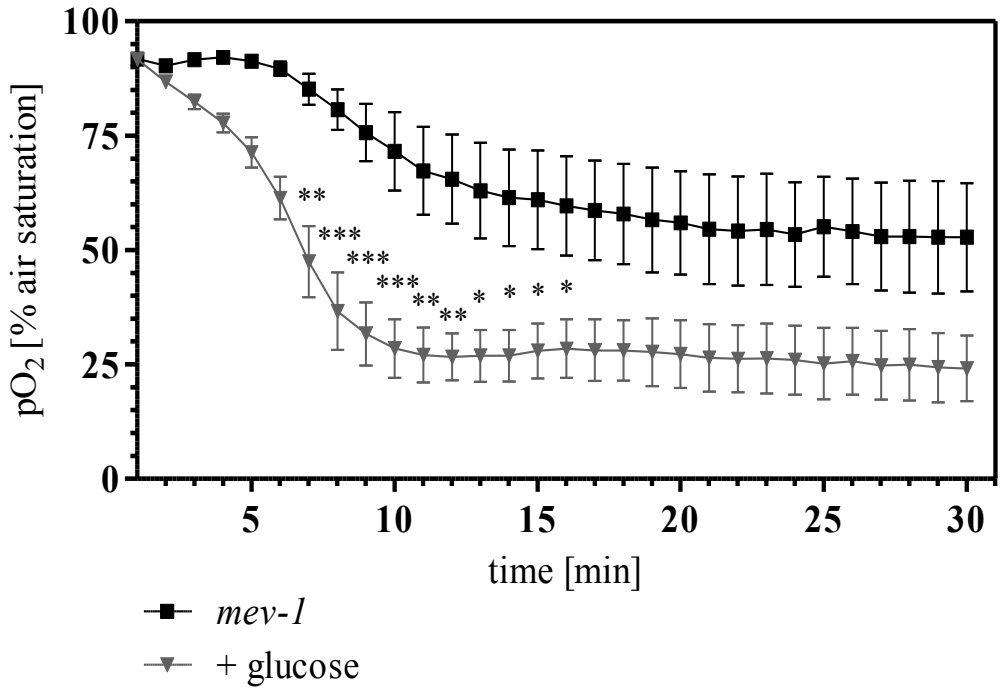

Figure 4-8. Glucose treatment increases oxygen consumption of *C. elegans* TK22 (*mev-1*).

Oxygen consumption of young adult nematodes was measured in the absence (control) or presence of 10 mM glucose. * $p < 0.05$, ** $p < 0.01$, *** $p < 0.001$ compared to control

To measure the ATP content of glucose treated *mev-1* nematodes, worm lysates were prepared after a 48 hour incubation with 10 mM or 100 mM glucose. The lysates were used in the ATP Bioluminescence Assay Kit, which is based on the ATP-dependent light emission in the luciferase-catalysed oxidation of luciferin (chapter 3.2.7).

From Figure 4-9 it can be seen that treatment with 10 mM glucose did not affect the ATP content of *mev-1* nematodes.

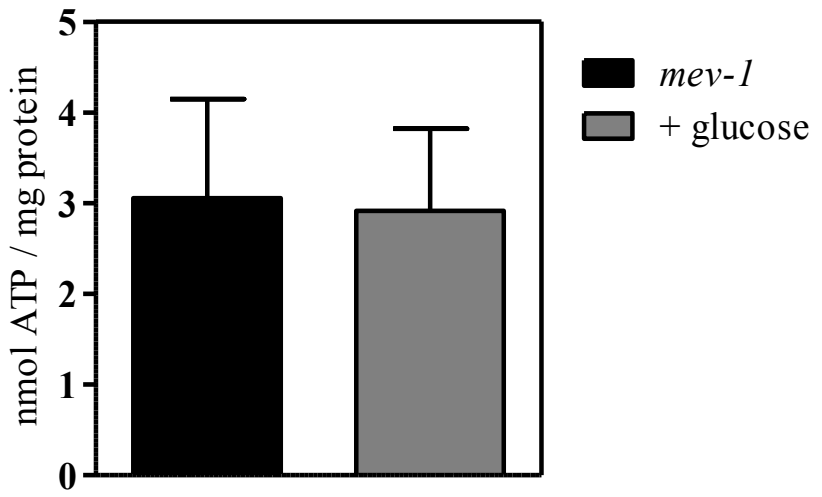

Figure 4-9. Glucose treatment does not alter ATP levels of *C. elegans* TK22 (*mev-1*).

Young adult nematodes were treated with M9 buffer (control) or 10 mM glucose for 48 h. ATP content was determined from worm homogenate using the ATP Bioluminescence Assay Kit CLS II (Roche).

These results substantiate a reduced mitochondrial efficiency upon glucose treatment leading to increased ROS production without affecting ATP levels. However, they do not approve that these impairments are the reason for glucose-induced life span reduction.

4.1.3 Glucose Effects on Protein Modification

Advanced glycation end products are the result of the non-enzymatic reaction of reducing carbohydrates with proteins. Formation of AGEs leads to changes of protein structure, function, and half-life and contributes to the pathophysiology of ageing and diabetic complications.

Methylglyoxal (MG) results from triose phosphates by non-oxidative mechanisms during glycolysis and can form AGEs. First of all, the MG production upon glucose feeding was examined by use of ELISA. Moreover, the effect of pyridoxamine, which is a known AGE-breaker, on glucose-induced life span reduction under heat stress was examined.

4.1.3.1 Glucose at 10 mM Does Not Increase Protein Oxidation

The introduction of carbonyl groups into proteins by oxidative reactions can for example alter enzymatic activity, DNA binding activities of transcription factors, the rate of proteolytic degradation, and AGE formation and has been related to ageing. The OxyBlot^{TM} Kit was used to study the effects of glucose treatment on oxidative modifications of proteins. Therefore, proteins from adult nematodes that had been treated with 10 mM glucose (or control) for 48 h were extracted, derivatized with 2,4-dinitrophenylhydrazine and detected by Western blotting. Figure 4-10 shows that the application of 10 mM glucose had no effect on the amount of carbonylated proteins.

4.1.3.2 Treatment with 10 mM Glucose Does Not Increase Methylglyoxal Production

MG was determined by ELISA. Therefore, proteins were extracted from adult nematodes that had been treated with 10 mM glucose or left untreated (control) for 48 h. As Figure 4-11 shows, the treatment with 10 mM glucose did not alter the content of MG-modified proteins compared to control treatment.

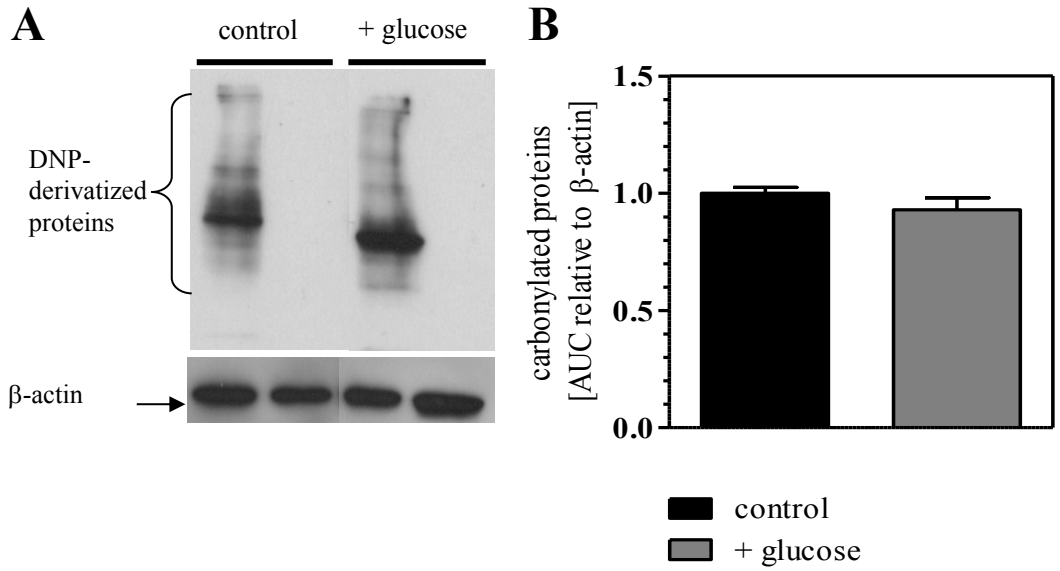

Figure 4-10. Glucose treatment does not enhance protein carbonylation.

Proteins were extracted from young adult nematodes that had been treated with M9 buffer (control) or 10 mM glucose for 48 h and were analysed by Oxy blotting. (A) A representative Oxy blot of DNP-derivatized proteins with β-actin as reference protein is shown. Lanes 1 & 2: control, lanes 3 & 4: 10 mM glucose; to lanes 1, and 3 DNP-derivatized proteins were loaded, to lanes 2 and 4 the corresponding, non-derivatized proteins were loaded as negative control. (B) DNP-derivatized proteins were quantified densitometrically. DNP: 2,4-dinitrophenol, AUC: area under curve

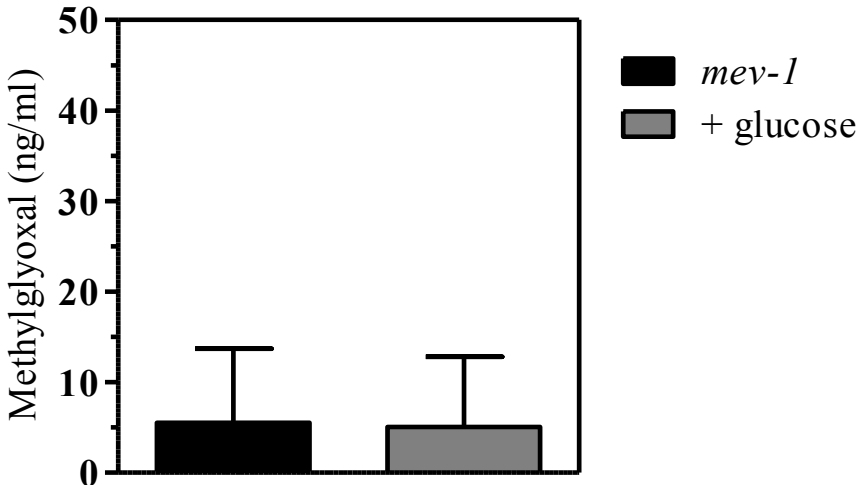

Figure 4-11. Glucose treatment does not increase the formation of methylglyoxal-modified proteins in *C. elegans* TK22 (*mev-1*).

Young adult nematodes were treated with M9 buffer (control) or 10 mM glucose for 48 h. Subsequently, methylglyoxal-modified proteins were quantified by ELISA from protein extracts.

Accordingly, protein carbonylation and MG formation do not appear to underlie the life span-reducing effects of glucose.

4.1.3.3 Pyridoxamine Prevents Glucose Toxicity

Besides MG-derivatives, other AGE structures, such as N^{ε}-(carboxymethyl) lysine, N^{ε}-(carboxyethyl) lysine and pentosidine derivatives, have been described. Because pyridoxamine is known to block the formation of AGEs the effects of simultaneous treatment with 10 mM glucose and pyridoxamine on life span under heat stress were examined in the following.

From Figure 4-12 can be seen that the additional treatment with 50 mM pyridoxamine significantly alleviated the life span reduction caused by glucose. On the contrary, lower concentrations tested (10 mM) were without effect (Table B-3). The treatment with solely pyridoxamine did not prolong life span under heat stress, indicating that 50 mM pyridoxamine prolongs the lifespan in *mev-1* mutants of *C. elegans* selectively by counteracting glucose toxicity.

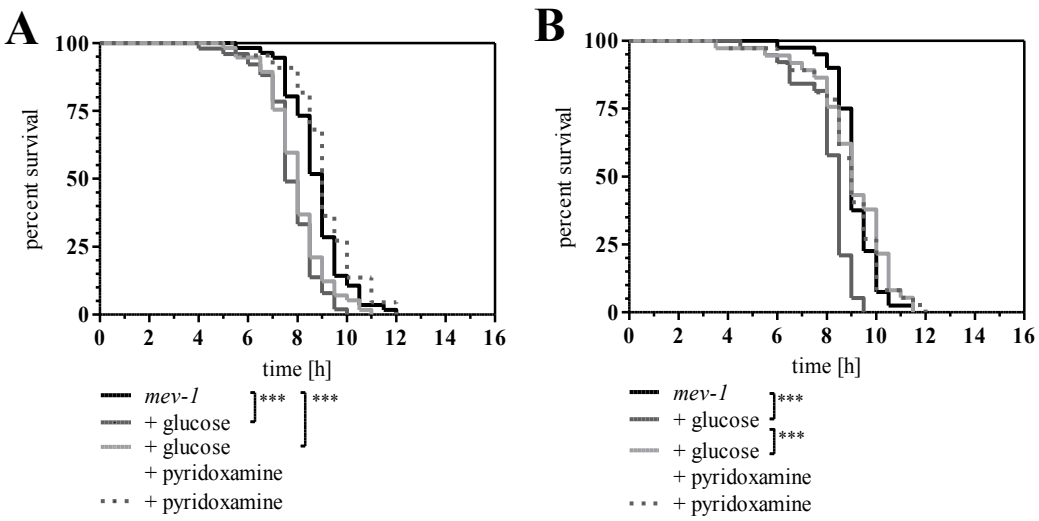

Figure 4-12. Life span of *C. elegans* TK22 (*mev-1*) in the absence (control) or presence of pyridoxamine, glucose, or a combination of both.

Young adult nematodes were treated with (A) 10 mM glucose, 10 mM pyridoxamine, or 10 mM pyridoxamine plus 10 mM glucose, and (B) 10 mM glucose, 50 mM pyridoxamine, or 50 mM pyridoxamine plus 10 mM glucose. Subsequently life span under heat stress (37 °C) was measured. *** $p < 0.001$

Moreover, these results imply that AGEs, though not MG-derived, may account for glucose-induced life span reduction.

4.1.4 A Higher Glucose Concentration Affects Classical Ageing Markers

To finally demonstrate that classical markers related to ageing and diabetic complications are associated with high glucose levels, concentrations of 100 mM glucose were applied to *mev-1* nematodes. The treatment with 100 mM glucose reduced the mean life span by 25% (Figure 4-13 A), which was not different from 10 mM glucose ($p = 0.08$, Table B-1). Moreover, 100 mM glucose increased ROS production to a similar extent as 10 mM glucose (Figure 4-13 B). In contrast to treatment with 10 mM glucose, 100 mM glucose led to significantly raised protein oxidation and MG formation (Figure 4-13 C - E).

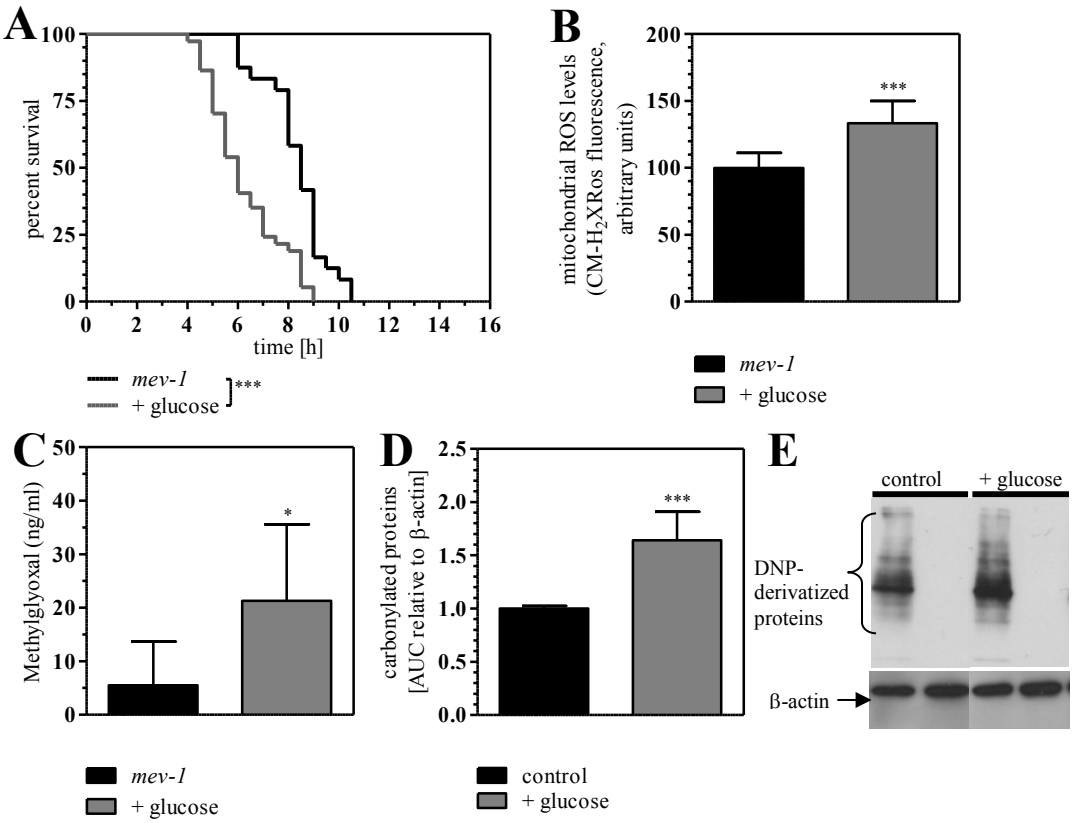

Figure 4-13. Treatment with 100 mM glucose affects classical ageing markers.

Young adult *C. elegans* nematodes were treated with M9 buffer (control) or 100 mM glucose. (A) Life span under heat stress was measured at 37 °C. (B) Mitochondrial ROS were stained with the fluorescent dye MitoTracker Red® CM-H_2XRos and detected microscopically. (C) Methylglyoxal-modified proteins were quantified by ELISA. (D) DNP-derivatized proteins were quantified densitometrically relative to β -actin. (E) A representative Oxy blot of DNP-derivatized proteins with β-actin as reference protein is shown. Lanes 1 & 2: control, lanes 3 & 4: 100 mM glucose; to lanes 1, and 3 DNP-derivatized proteins were loaded, to lanes 2 and 4 the corresponding, non-derivatized proteins were loaded as negative control. * $p < 0.05$, *** $p < 0.001$ versus control. DNP: 2,4-dinitrophenol, AUC: area under curve

4.2 Influence of Glucose on the Protein Quality Control System

The maintenance of proteostasis is essential for normal cellular functions and viability. The quality control of proteostasis includes molecular chaperones, the ubiquitin-proteasome system, heat shock response, and unfolded protein response to assure correct protein folding and degradation of misfolded or damaged proteins. These pathways are present in the cytosol as well as in mitochondria and the endoplasmic reticulum to encounter unfolded proteins and promote efficient folding by compartment-specific chaperones. For example, acute endoplasmic reticulum stress leads to unfolded protein response, which has been implicated in several diseases such as diabetes and neurodegenerative disorders.

To assess whether glucose-induced life span reduction is linked to impaired proteostasis, various factors of the protein quality control system were knocked down by RNAi and life span under heat stress was measured after glucose treatment.

4.2.1 Glucose Does Not Further Reduce Life Span in UPR^{mt}-Deficient Nematodes

Chaperones bind unfolded or misfolded proteins, prevent aggregation, and accelerate correct folding. *hsp-6* and *hsp-60* encode mitochondrial-specific chaperones that are members of the HSP70 and HSP40 superfamilies of molecular chaperones. UBL-5 and DVE-1 are regulators of the mitochondrial unfolded protein response that bind to *hsp-6* and *hsp-60* promoters upon mitochondrial stress.

The knockdown of *hsp-6*, *hsp-60*, *ubl-5* or *dve-1* highly significantly reduced the life span of TK22 (*mev-1*) under heat stress. However, the treatment with 10 mM glucose for 48 h did not lead to a further decrease of survival under these conditions (Figure 4-14, Table B-4).

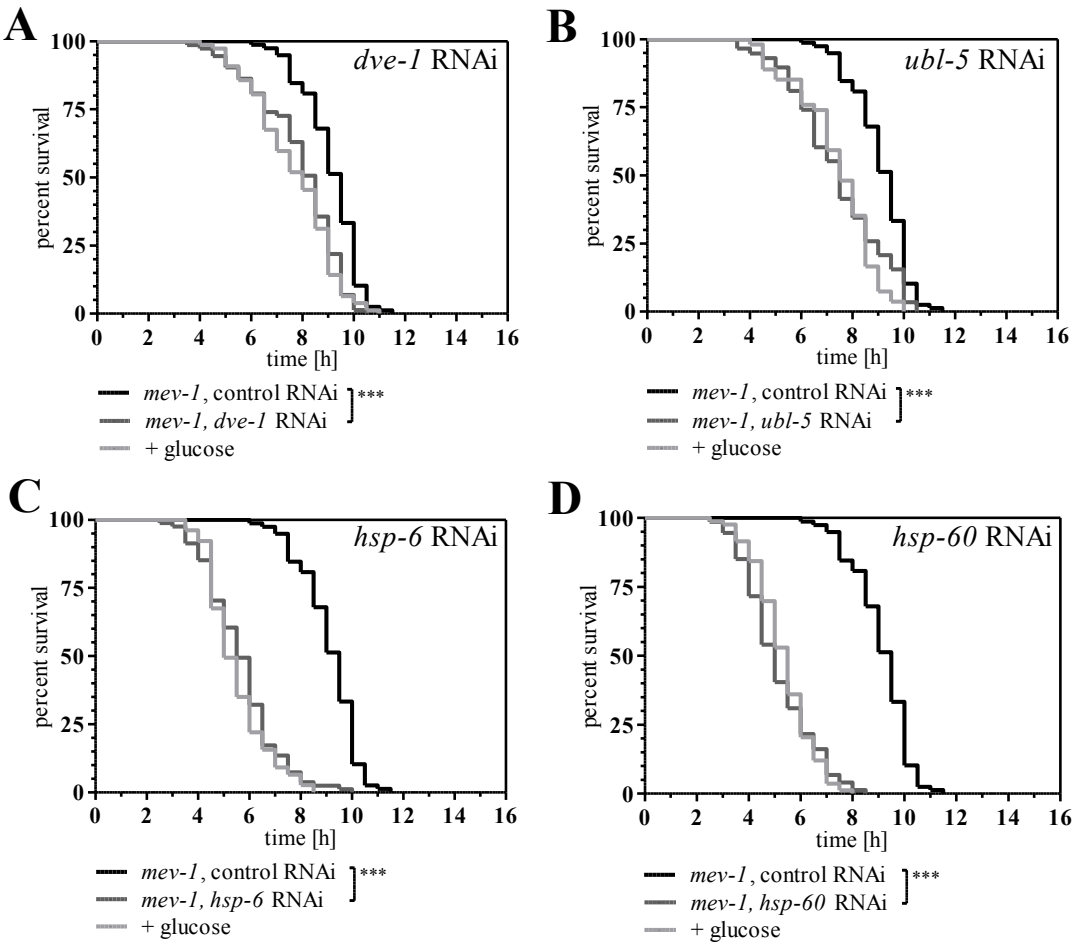

Figure 4-14. Glucose treatment does not further reduce the life span of nematodes with impaired mitochondrial stress response.

Nematodes were subjected to (A) *dve-1* RNAi, (B) *ubl-5* RNAi, (C) *hsp*-6 RNAi, or (D) *hsp*-60 RNAi and treated with M9 buffer (control) or 10 mM glucose for 48 h at the young adult stage. Subsequently, the life span under heat stress (37 °C) was measured. *** $p < 0.001$ compared to control RNAi

Thus it may be assumed that the life span reduction under glucose treatment can be ascribed to a reduced efficiency of the mitochondrial UPR system.

4.2.2 Glucose Does Not Further Reduce Life Span in UPR^{ER}-Deficient Nematodes

Overproduction of non-folded proteins or defects of ER-associated protein degradation lead to ER stress. As a result UPR is activated and chaperone expression increased. ER chaperones and the ER-associated degradation machinery are mainly regulated by the transcription factor XBP-1. If the unfolded protein response of the ER is blocked, for example due to *xbp-1* knockdown, a protein family called activated in blocked UPR (*abu*) is induced. Similar to the knockdown of mitochondrial chaperones, *xbp-1*, *abu-1*, or *abu-11* RNAi resulted in reduced survival of the *mev-1* mutant (Table B-5), which was not further reduced by glucose (Figure 4-15). These results suggest that besides UPR^{mt} also different pathways of the UPR^{ER} are impaired upon glucose treatment.

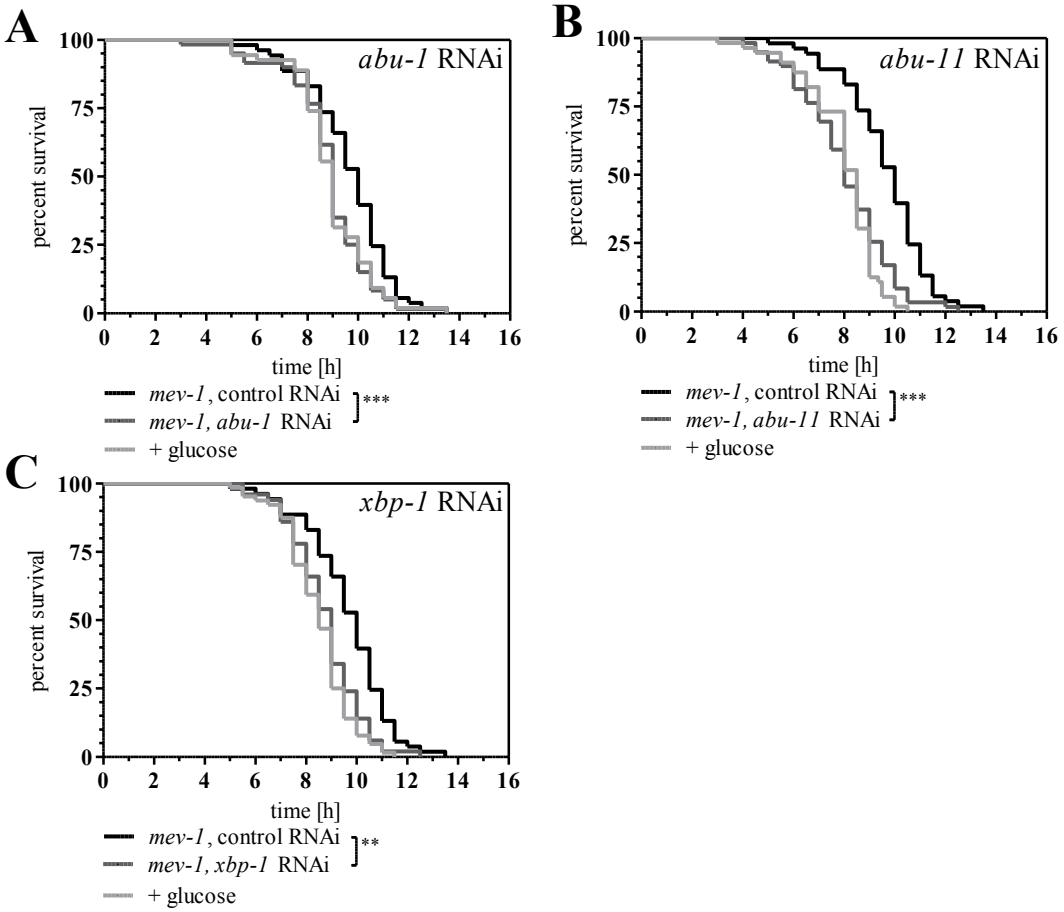

Figure 4-15. Glucose treatment does not further reduce the life span of nematodes with impaired UPR^{ER}.

Nematodes were subjected to (A) *abu-1* RNAi, (B) *abu-11* RNAi, or (C) *xbp*-1 RNAi and treated with M9 buffer (control) or 10 mM glucose for 48 h at the young adult stage. Subsequently, the life span under heat stress (37 °C) was measured. UPR^{ER}: endoplasmic reticulum unfolded protein response. ** $p < 0.01$, *** $p < 0.001$ compared to control RNAi

4.2.3 Glucose Overburdens the Ubiquitin-Proteasome System

Ubiquitin is a ubiquitously expressed, highly conserved polypeptide. By polyubiquitination target proteins are marked for proteasome-dependent degradation. This requires the concerted actions of a ubiquitin-activating enzyme, a ubiquitin-conjugating enzyme, and a ubiquitin-protein ligase (chapter 1.3.3).

4.2.3.1 Glucose Does Not Further Reduce the Life Span of *ubq-1*- or *uba-1*-Deficient Nematodes

Because RNAi of *ubq-1*/*2* or *uba-1* is expected to completely inactivate the Ub proteolytic pathway and leads to embryonic arrest, RNAi was performed in young adult nematodes, which had been grown on RNAi negative control during the larval stages. Due to sequence homology *ubq-1* RNAi is likely to knockdown *ubq-2* as well. As indicated in Table B-6, *ubq-1* and *uba-1* RNAi led to a highly significant life span reduction under heat stress although nematodes were treated with the corresponding RNAi bacteria for only three days. The survival of RNAi treated nematodes was not further decreased by the application of 10 mM glucose (Figure 4-16).

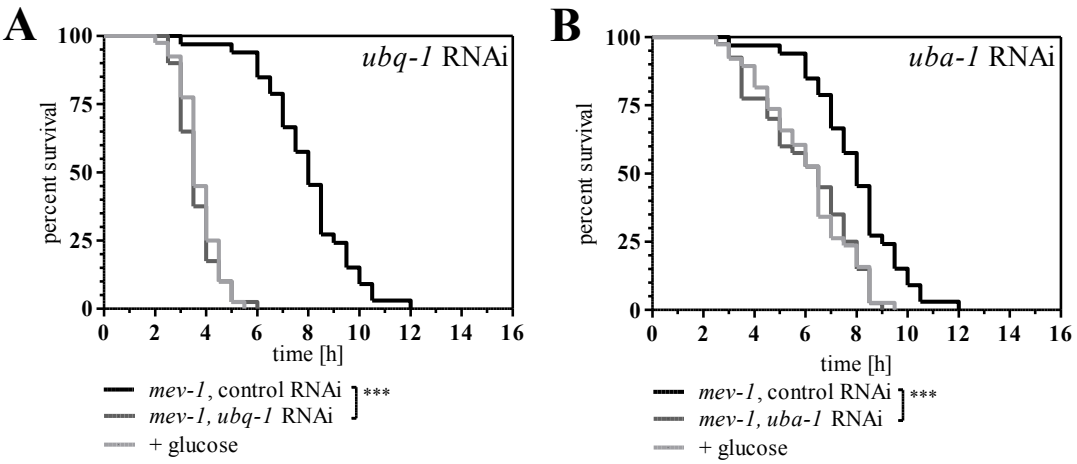

Figure 4-16. Knockdown of *ubq-1* or *uba-1* reduces the life span of *C. elegans* TK22 (*mev-1*), which is not further decreased by glucose treatment.

Nematodes were raised on control RNAi. At the young adult stage they were transferred to (A) *ubq-1* or (B) *uba-1* RNAi and treated with M9 buffer (control) or 10 mM glucose. Subsequently, the life span under heat stress (37 °C) was measured. *** $p < 0.001$ compared to control RNAi

4.2.3.2 Glucose Inhibits the Proteasome Similar to MG132

In a final step, the importance of the 26S proteasome on glucose-induced life span reduction was examined. Since knocking down components of the 26S proteasome by RNAi during larval stages is described to be lethal, the proteolytic activity was inhibited by treatment with MG132. Figure 4-17 shows that the treatment of young adult nematodes with 200 µM MG132 led to a significant life span reduction although not as strong as the treatment with 10 mM glucose. Moreover, the simultaneous treatment with 10 mM glucose and 200 µM MG132 did not result in an additional decrease of survival compared to 10 mM glucose treatment alone, indicating that glucose and MG132 both affect life span by inhibition of the proteasome (Table B-7).

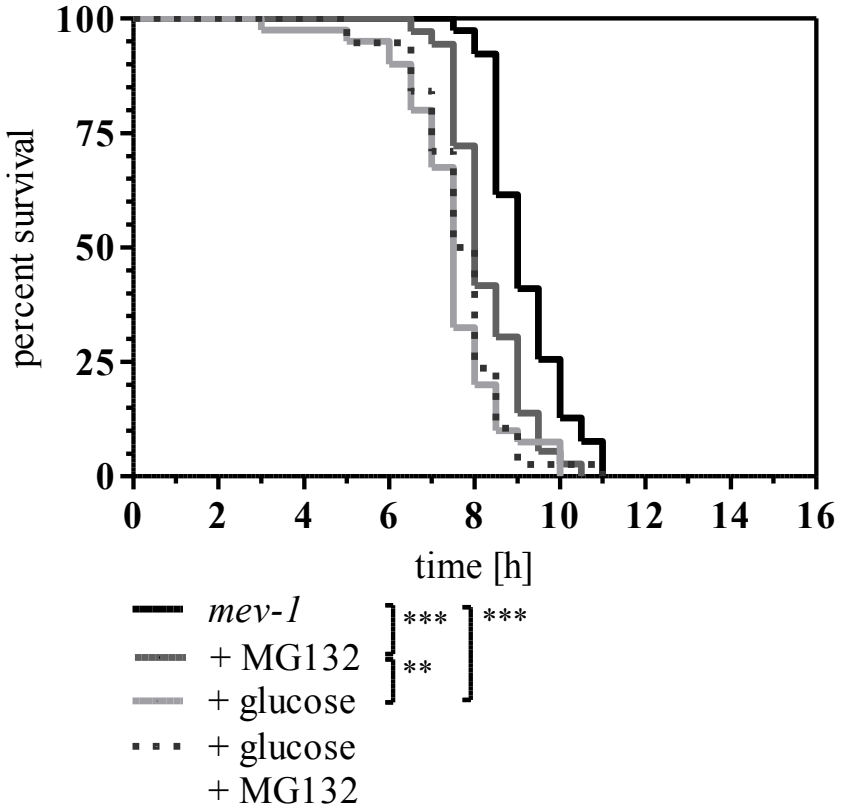

Figure 4-17. Life span of *C. elegans* TK22 (*mev-1*) in the absence (control) or presence of MG132, glucose, or a combination of both.

Young adult nematodes were treated with M9 buffer (control), 200 µM MG132, 10 mM glucose, or 200 µM MG132 plus 10 mM glucose. Subsequently, life span under heat stress was measured at 37 °C. ** $p < 0.01$, *** $p < 0.001$

In summary, the experiments on the protein quality control system suggest that the treatment of *C. elegans* with glucose severely impairs proteostasis. The mitochondrial and endoplasmic reticulum UPR pathways as well as the ubiquitin-proteasome system are disrupted by glucose treatment, since no additive effects of any single RNAi to knock down members of these systems and glucose application were found.

4.3 Glucose Induces Apoptosis

If proteostasis is seriously disturbed and cannot be re-established, mediators of the unfolded protein response, e.g. PERK or ATF6, trigger the apoptotic programme. On this account, germ line apoptosis was measured using the fluorescent dye SYTO12 that specifically accumulates in nuclei of apoptotic cells.

Figure 4-18 shows that the treatment with 10 mM glucose significantly induced germ line apoptosis in the *mev-1* mutant. To validate these results, germ line apoptosis was also determined in the *C. elegans* strain CB3203 (*ced-1*). These nematodes carry a loss-of-function mutation in the *ced-1* gene and thus are defective in the removal of apoptotic cell corpses.

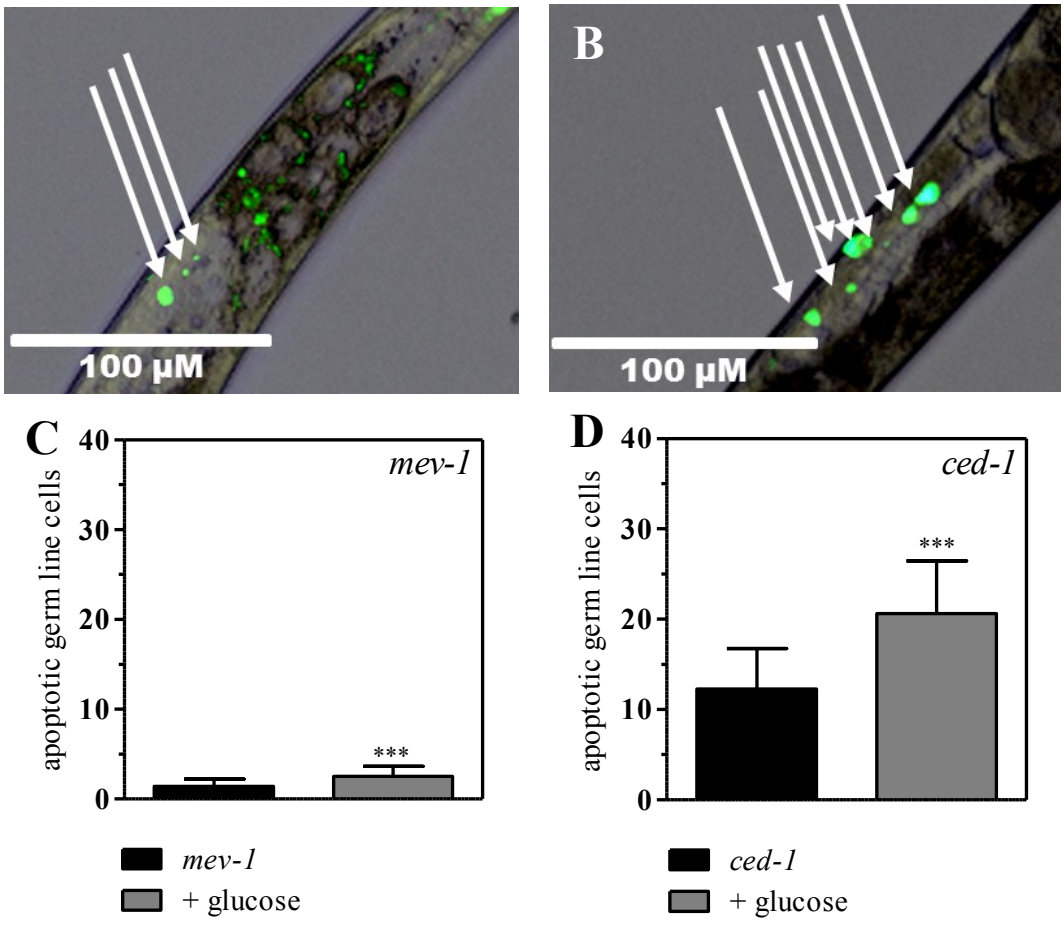

Figure 4-18. Glucose treatment increases germ line apoptosis in *C. elegans*.
Young adult nematodes were treated with M9 buffer (control) or 10 mM glucose for 48 h. Apoptotic cell corpses were stained with the fluorescent dye SYTO12 and quantified microscopically. (A, B) Arrows indicate apoptotic cells in the anterior gonad arm of *mev-1* nematodes treated with (A) M9 buffer (control) or (B) 10 mM glucose. (C, D) Quantification of germ line apoptosis in *C. elegans* (C) TK22 (*mev-1)* or (D) CB3203 (*ced-1*). *** $p < 0.001$ compared to control

After a glucose-induced increase of germ line apoptosis had been shown, it was asked how life span is affected by glucose treatment if the apoptotic machinery is inhibited by RNAi knockdown of different components. Therefore, first of all RNAi of the executioner caspase *ced-3* was studied. *Ced-3* RNAi significantly decreased the life span of *mev-1* nematodes (Figure 4-19 A). Moreover, glucose treatment did not further reduce the life span when *ced-3* was knocked down. Additionally, germ line apoptosis was measured upon glucose treatment in *ced-3*-deficient nematodes. Figure 4-19 B shows that germ line apoptosis was virtually absent in *ced-3* RNAi treated animals. Moreover, glucose did not enhance apoptosis under these conditions. While, on the one hand, these results suggest that glucose needs CED-3 in order to promote apoptosis and life span reduction, it indicates that CED-3 has also survival enhancing activities, on the other hand.

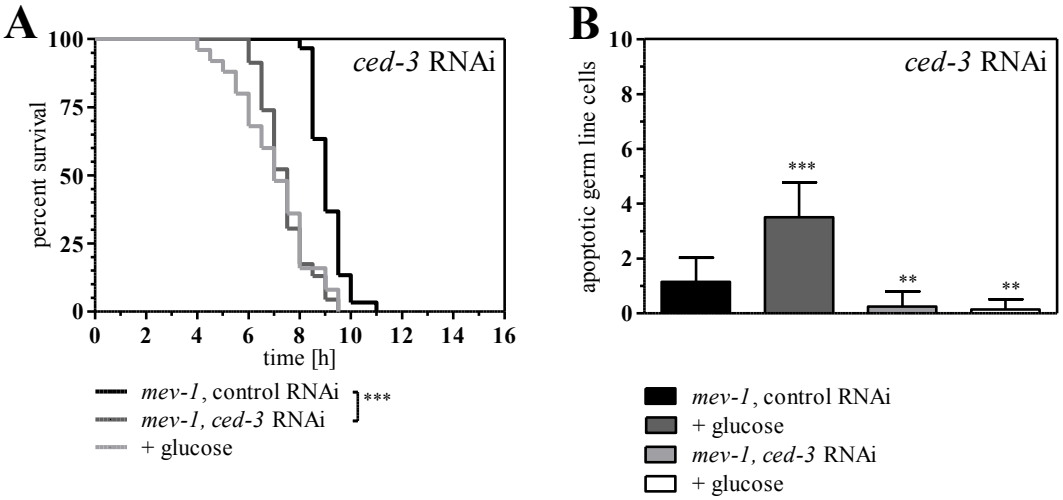

Figure 4-19. *Ced-3* RNAi prevents glucose-induced life span reduction and apoptosis in *C. elegans* TK22 (*mev-1*).

Young adult nematodes were treated with M9 buffer (control) or 10 mM glucose for 48 h. (A) Life span under heat stress was measured at 37 °C. (B) Apoptotic cell corpses were stained with the fluorescent dye SYTO12 and quantified microscopically. *** $p < 0.001$ compared to control RNAi, control treatment

In contrast to *ced-3* RNAi, *ced-4* RNAi had no effect on life span (Table B-9). Similarly, glucose treatment did not affect the survival after knockdown of *ced-4* (Figure 4-20 A), substantiating the requirement of active pro-apoptotic proteins in order to enable glucose to reduce life span. Analogously, germ line apoptosis was suppressed by *ced-4* RNAi. When *ced-4* was knocked down the application of glucose did not increase apoptosis anymore (Figure 4-20 B).

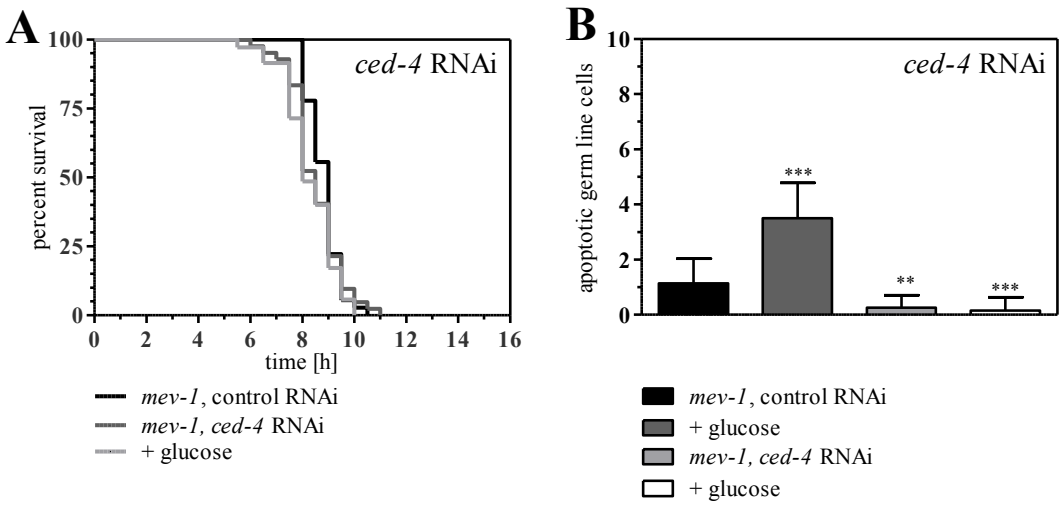

Figure 4-20. Effect of *ced-4* RNAi on glucose-induced life span reduction and apoptosis in *C. elegans* TK22 (*mev-1*).

Young adult nematodes were treated with M9 buffer (control) or 10 mM glucose for 48 h. (A) Life span under heat stress was measured at 37 °C. (B) Apoptotic cell corpses were stained with the fluorescent dye SYTO12 and quantified microscopically. *** $p < 0.001$ compared to control RNAi, control treatment

While DNA damage induced apoptosis relies on *cep-1* and *egl-1*, environmental insults, such as oxidative stress, heat stress, and starvation, do not require *cep-1* or *egl-1* for the induction of germ line apoptosis. To explore, whether glucose affects apoptosis and life span by DNA-damage, the impact of *egl-1* and *cep-1* RNAi on these parameters were examined. Neither knockdown of *egl-1* nor *cep-1* affected the survival of *mev-1*. With respect to glucose treatment, *egl-1* RNAi and *cep-1* RNAi led to differing results: In *egl-1*-deficient nematodes glucose treatment had no effect on life span (Figure 4-21 A). In contrast, a significant life span reduction by glucose treatment was observed after *cep*-1 RNAi (Figure 4-21 C). Referring to germ line apoptosis, neither *cep-1* nor *egl-1* RNAi had any effects. The *cep-1* and *egl-1* RNAi controls showed a similar number of apoptotic germ line cells as

the control RNAi group (Figure 4-21 B and D). Glucose treatment led to a significant increase of germ line apoptosis both after *cep-1* and *egl-1* RNAi.

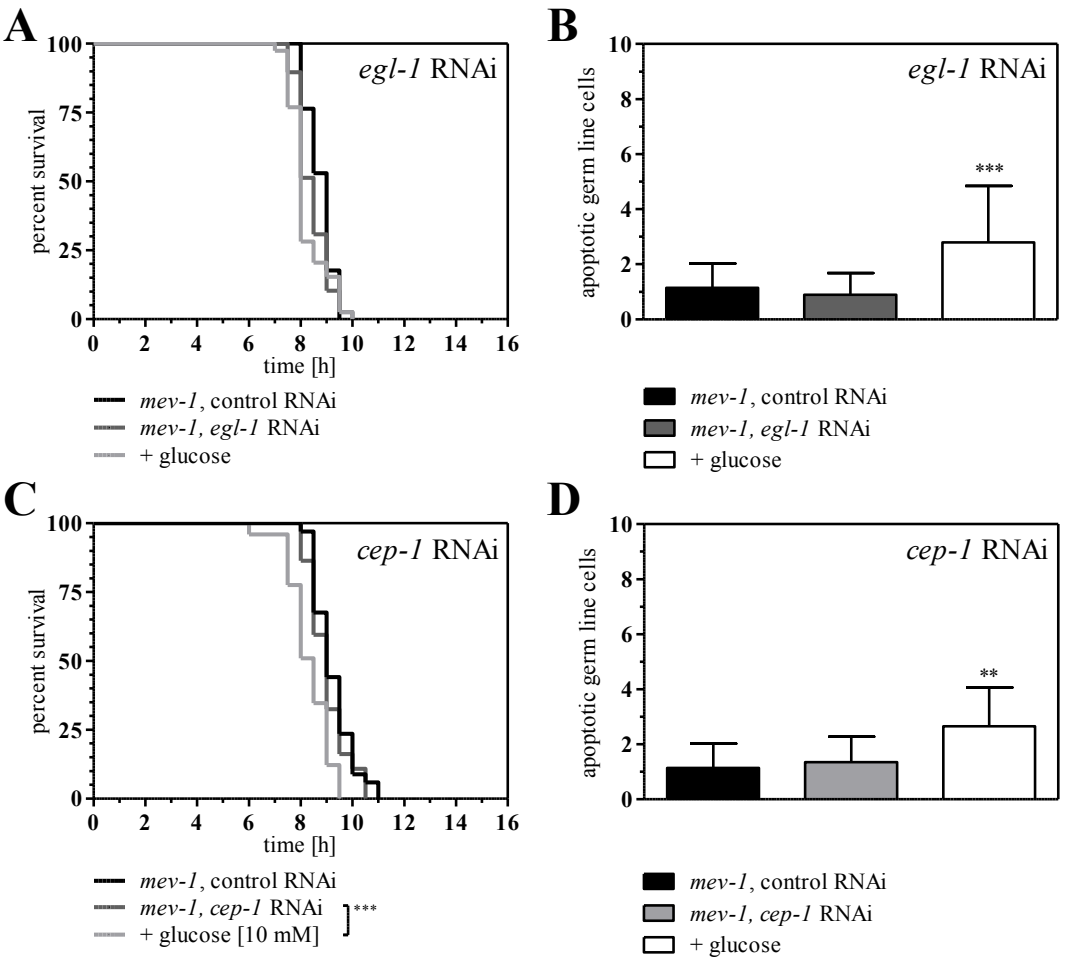

Figure 4-21. Effects of *egl-1* RNAi and *cep-1* RNAi on glucose-induced reduction of life span and apoptosis in *C. elegans* TK22 (*mev-1*).

Young adult nematodes were treated with M9 buffer (control) or 10 mM glucose for 48 h. (A, C) Life span under heat stress of *egl-1* or *cep-1* deficient nematodes was measured at 37 °C. (B, D) Apoptotic cell corpses in *egl-1* or *cep-1* deficient nematodes were stained with the fluorescent dye SYTO12 and quantified microscopically. ** $p < 0.01$, *** $p < 0.001$ compared to control RNAi, control treatment

These results imply that glucose feeding does not lead to apoptosis by induction of DNA damage.

4.4 Activation of Stress Response Pathways by Quercetin

The second part of this work aimed at the activation of stress response pathways to counteract glucose toxicity as stress response has been shown to be an important parameter determining life span. Stress response can be triggered by distinct polyphenols, which are part of the daily human nutrition and have been described as CR-mimetics as well as sirtuin activators. Thus, the potential of the polyphenol quercetin to activate stress response mechanisms and thereby prevent glucose toxicity in *C. elegans* has been studied.

4.4.1 Quercetin Does Not Prolong Life Span in the Absence of Glucose Stress

First of all, the effect of quercetin, a polyphenol occurring in apples and onions, on life span under heat stress was examined in the *mev-1* mutant. Young adult nematodes were treated for 48 h with 1 µM or 100 µM quercetin and afterwards the life span under heat stress was measured. Figure 4-22 shows, that quercetin did not have any effect on life span under these conditions. The mean life span of quercetin treated nematodes in both tested concentrations did not differ from the control group (Table B-12).

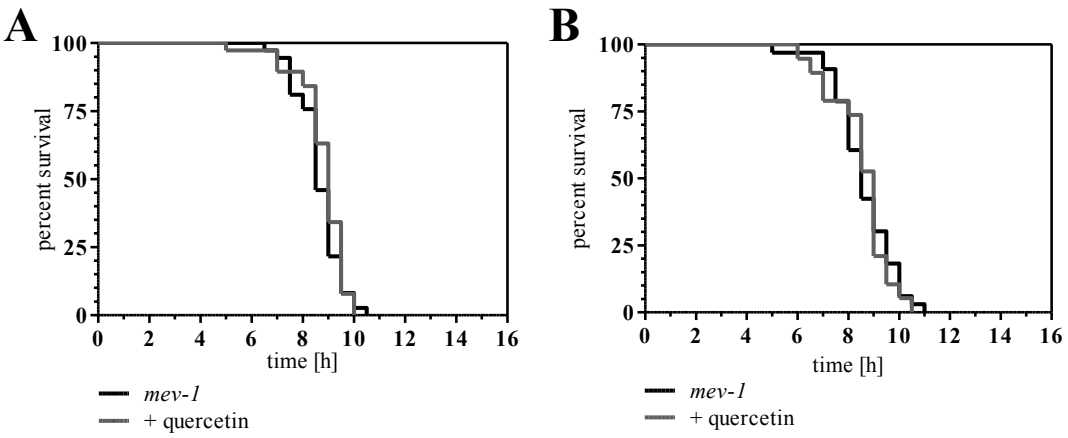

Figure 4-22. Quercetin does not affect the survival of *C. elegans* TK22 (*mev-1*) in the absence of glucose.

Young adult nematodes were treated with (A) 1 µM quercetin or (B) 100 µM quercetin. Subsequently, life span under heat stress was measured at 37 °C.

4.4.2 Quercetin Prevents Glucose Toxicity

Next, the effect of quercetin was studied in *mev-1* nematodes that were simultaneously treated with 10 mM glucose. Figure 4-23 illustrates that quercetin prolonged the life span of glucose fed nematodes. The treatment with 1 µM of the polyphenol sufficed to completely prevent the glucose induced life span reduction. While the average life span of glucose treated worms was reduced by 18% to 33%, the nematodes that had been treated with glucose and quercetin showed mean life spans that were not different to the untreated control group (95 – 104%, Table B-13).

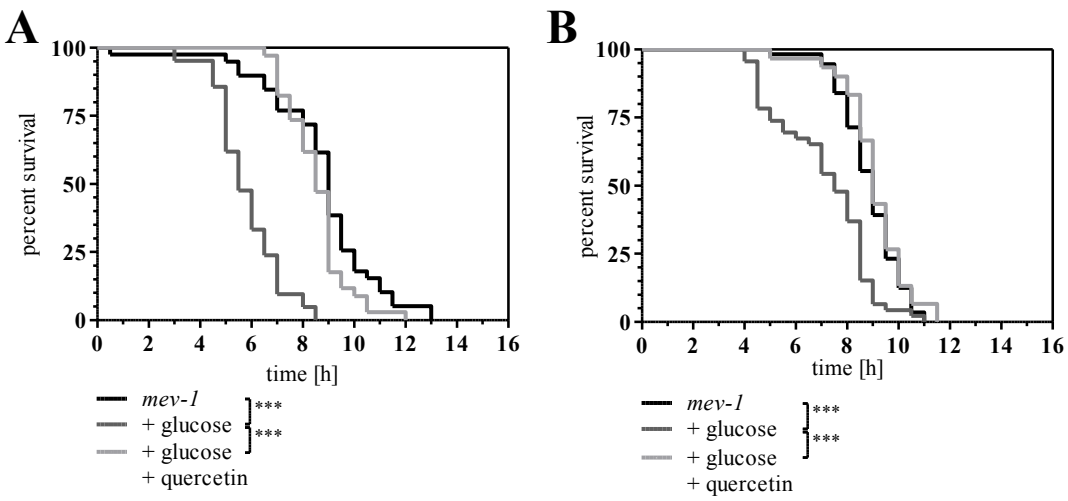

Figure 4-23. Quercetin prevents glucose-induced life span reduction in *C. elegans* TK22 (*mev-1*).

Young adult nematodes were treated with M9 buffer (control), 10 mM glucose, and (A) 10 mM glucose plus 1 µM quercetin or (B) 10 mM glucose plus 100 µM quercetin. Subsequently, life span under heat stress was measured at 37 °C. *** $p < 0.001$

These results imply that quercetin specifically prevents glucose-toxicity, while it does not prolong the life span of the short-lived *mev-1* mutant under unstressed conditions.

4.4.3 The Sirtuin *sir-2.1* Is Essential for the Prevention of Glucose Toxicity by Quercetin

Since quercetin is described as sirtuin activator, the next step was to examine whether the life span-prolonging effect under glucose stress is dependent on sirtuins. Therefore, the four *C. elegans* sirtuin genes *sir-2.1* to *sir-2.4* were knocked down by RNAi. L1 larvae were fed with dsRNA-expressing bacteria to knock down the expression of the desired gene and treated with glucose and quercetin when they had reached the young adult stage. After a 48 hour incubation period life span under heat stress was measured.

While glucose treatment still led to a life span reduction that was compensated by 1 µM quercetin in the control RNAi group (Figure 4-24 A), the addition of quercetin could not reverse this effect in *sir-2.1*-deficient nematodes (Figure 4-24 B). The mean life span of glucose treated nematodes was reduced by 11.5% and 8% for control RNAi and *sir-2.1* RNAi, respectively ($p < 0.01$). The additional application of quercetin increased the mean life span of glucose treated nematodes by 12% in the control RNAi group ($p < 0.01$). In contrast to that, the mean life span of *sir-2.1*-deficient nematodes that were treated with glucose and quercetin was not different to glucose treated nematodes ($p > 0.05$, Table B-14).

In general, polyphenols are described as sirtuin-activators. However, it is also possible that sirtuin expression is decreased by glucose and reactivated by the additional quercetin treatment. To explore this, *sir-2.1* mRNA of glucose or glucose and quercetin treated *mev-1* nematodes was quantified using real time PCR. Figure 4-25 shows that glucose treatment did not reduce *sir-2.1* expression, yet the additional treatment with quercetin resulted in a significant increase of *sir-2.1* mRNA, demonstrating that the polyphenol activates *sir-2.1* also by increasing its expression.

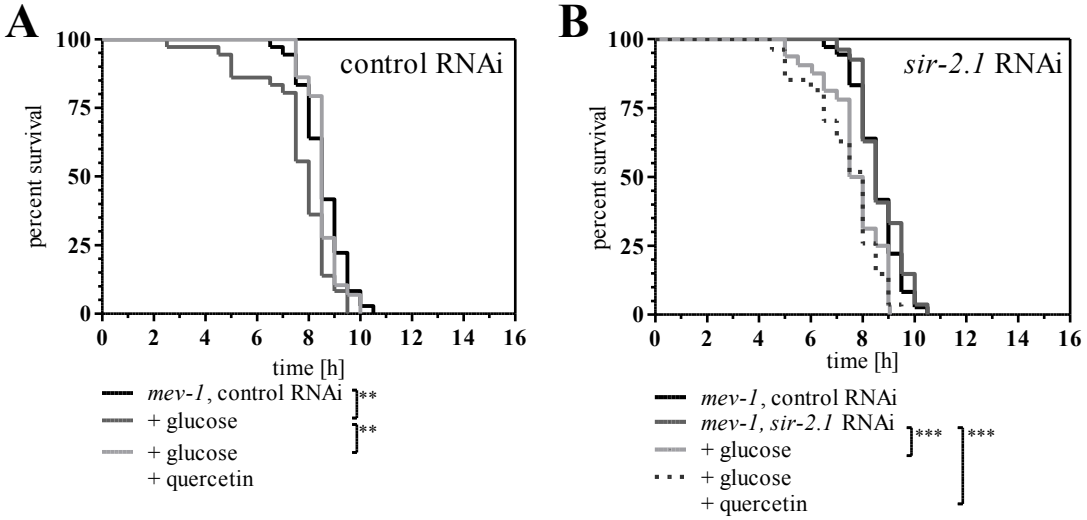

Figure 4-24. The sirtuin *sir-2.1* is essential for the protection from glucose-induced life span reduction by quercetin in *C. elegans* TK22 (*mev-1*).

Nematodes were raised on (A) control RNAi or (B) *sir-2.1* RNAi and treated with M9 buffer (control), 10 mM glucose, or 10 mM glucose plus 1 µM quercetin at the young adult stage. Life span was measured under heat stress at 37 °C. ** $p < 0.01$, *** $p < 0.001$

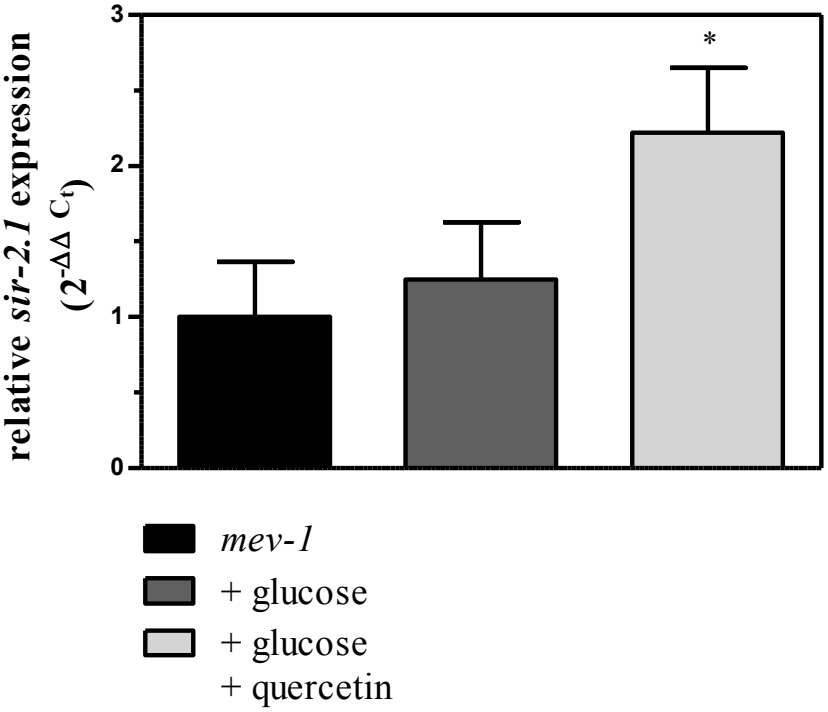

Figure 4-25. Quercetin induces *sir-2.1* mRNA expression in the presence of glucose.

RNA was extracted from young adult *mev-1* nematodes that had been treated with M9 buffer (control), 10 mM glucose, or 10 mM glucose plus 1 µM quercetin at the young adult stage. *Sir-2.1* mRNA expression was determined by quantitative real-time PCR using sir-2.1-fw-201 and sir-2.1-rev-312 primers. * $p < 0.05$ compared to control

The preventive effect of quercetin on glucose-induced life span reduction was not inhibited by a knockdown of the other sirtuins *sir-2.2*, *sir-2.3* or *sir-2.4* (Figure 4-26), indicating that in contrast to *sir-2.1*, other sirtuin members are dispensable for the life-extending effects of quercetin under glucose exposure.

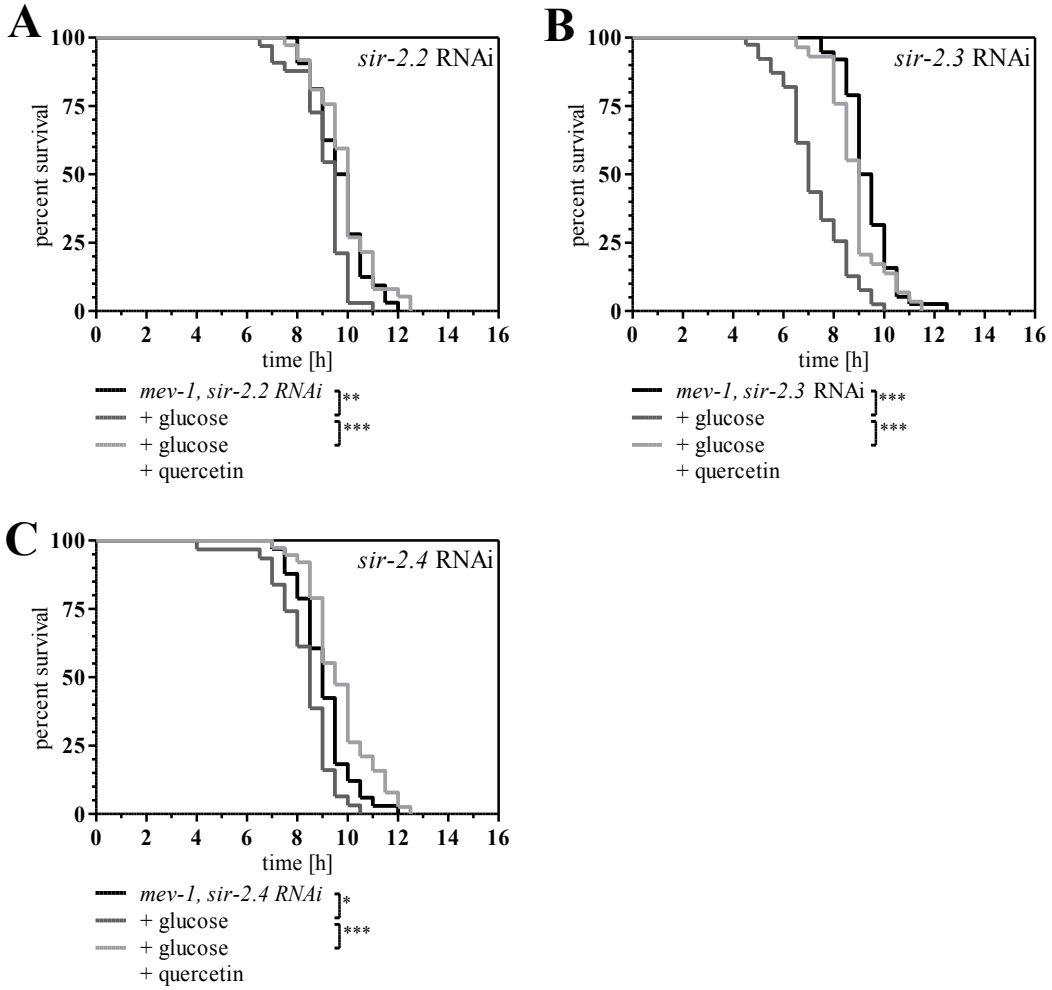

Figure 4-26. *Sir-2.2*, *sir-2.3*, and *sir-2.4* are dispensable for the ability of quercetin to rescue glucose-induced reduction of life span in *C. elegans* TK22 (*mev-1*).

Nematodes were raised on (A) *sir-2.2*, (B) *sir-2.3*, or (C) *sir-2.4* RNAi and treated with M9 buffer, 10 mM glucose, or 10 mM glucose plus 1 µM quercetin at the young adult stage. Life span was measured under heat stress at 37 °C. * $p < 0.05$, ** $p < 0.01$, *** $p < 0.001$

4.4.4 The AMP-Activated Kinase 2 Is Dispensable for the Polyphenol-Induced Inhibition of Glucose Toxicity

The AMP-activated kinase 2 (*aak-2*) functions downstream of energy level signals and positively regulates life span. Although it was shown that 10 mM glucose was without effect on the ATP level (chapter 4.1.2.3), and hence probably

also on the AMP level, the role of *aak-2* in quercetin-induced life span extension in the presence of 10 mM glucose was investigated, because SIR-2.1 can be altered by the NAD^+:NADH ratio, and thus the energy state. Therefore, *aak-2* was knocked down by RNAi in *mev-1* and young adult nematodes were treated for 48 h with 10 mM glucose or 10 mM glucose and additionally 1 µM quercetin. Figure 4-27 shows that the survival under these conditions is significantly reduced by glucose treatment ($p < 0.01$). The reduction of survival was avoided by the combined treatment with glucose and quercetin ($p < 0.01$, Table B-16).

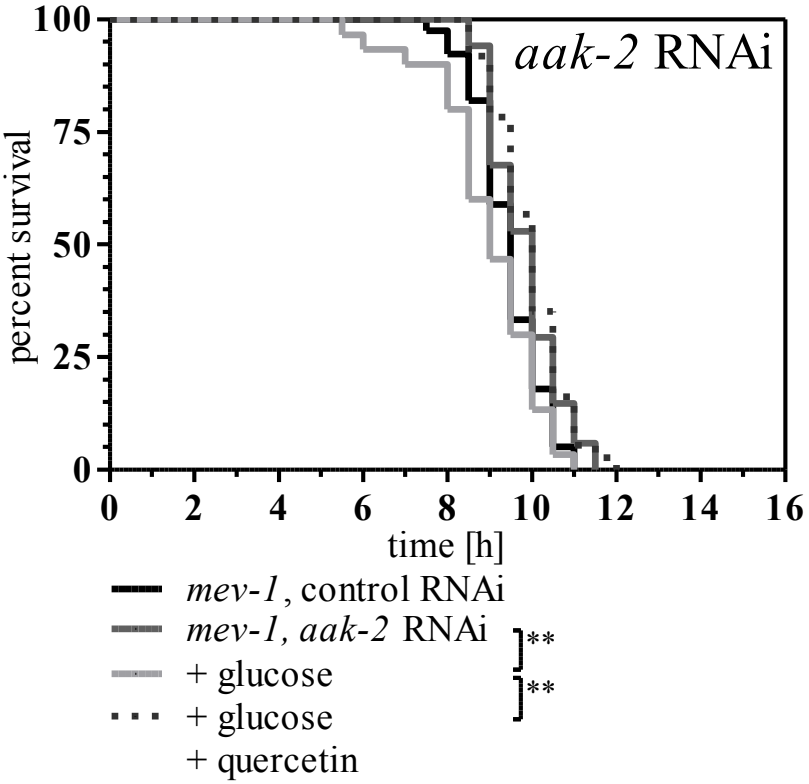

Figure 4-27. Effect of *aak-2* RNAi on the glucose-induced reduction of life span and its rescue by quercetin in *C. elegans* TK22 (*mev-1*).

Nematodes were raised on *aak-2* RNAi and treated with M9 buffer, 10 mM glucose, or 10 mM glucose plus 1 µM quercetin at the young adult stage for 48 h. Life span was measured under heat stress at 37 °C. ** $p < 0.01$

As a conclusion, AAK-2 is not required for the quercetin-induced protection against glucose toxicity.

4.4.5 Quercetin Does Not Interact with the Insulin/IGF-1 Signalling Pathway to Prevent Glucose Toxicity

The life span prolonging effect of caloric restriction in *C. elegans* is mediated by an interaction of sirtuins with the transcription factor DAF-16, regulated by insulin/IGF-1 signalling. To examine if the prevention of glucose toxicity by quercetin also requires the interaction of SIR-2.1 with DAF-16, the localization of DAF-16 in *mev-1* mutants was determined using a transgenic strain that expresses the transgene zIS356[*Pdaf-16::daf-16-gfp; rol-6*] in TK22 (*mev-1*). This revealed that *mev-1* mutants have almost all of their DAF-16 translocated to the nucleus, probably in order to compensate for their increased ROS stress. Even the treatment with glucose, which is supposed to activate insulin/IGF-1 signalling, was not able to influence this condition, and neither was the addition of quercetin under glucose exposure (Figure 4-28). Representative images of control, glucose, or glucose plus quercetin treated animals are shown in Figure 4-29.

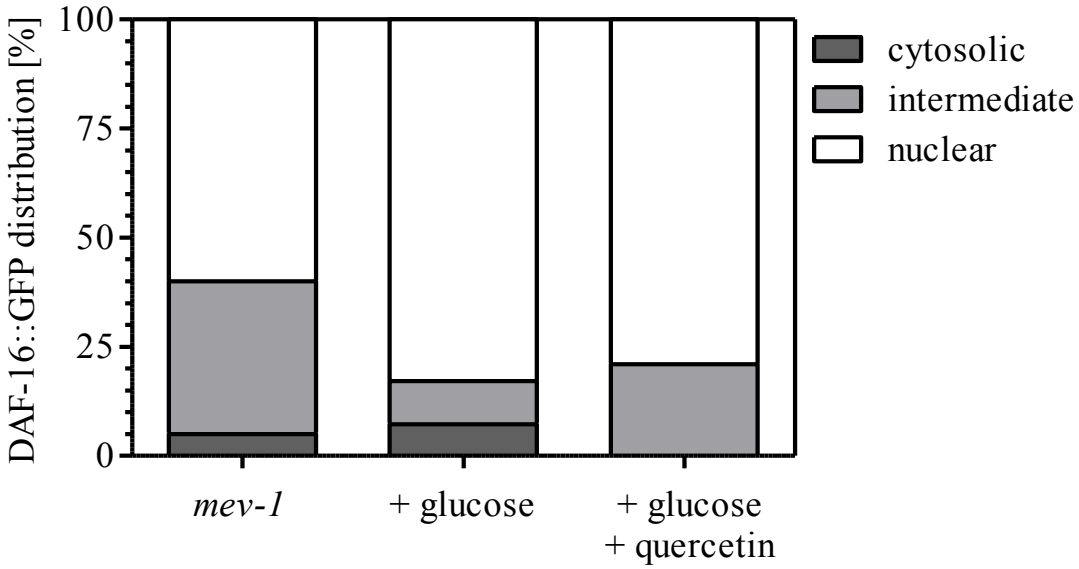

Figure 4-28. Quantification of DAF-16::GFP localization after incubation with glucose and quercetin in transgenic *C. elegans mev-1* nematodes.

Young adult nematodes were treated with M9 buffer (control), 10 mM glucose, or 10 mM glucose plus 1 µM quercetin for 48 h. DAF-16::GFP localization was examined microscopically.

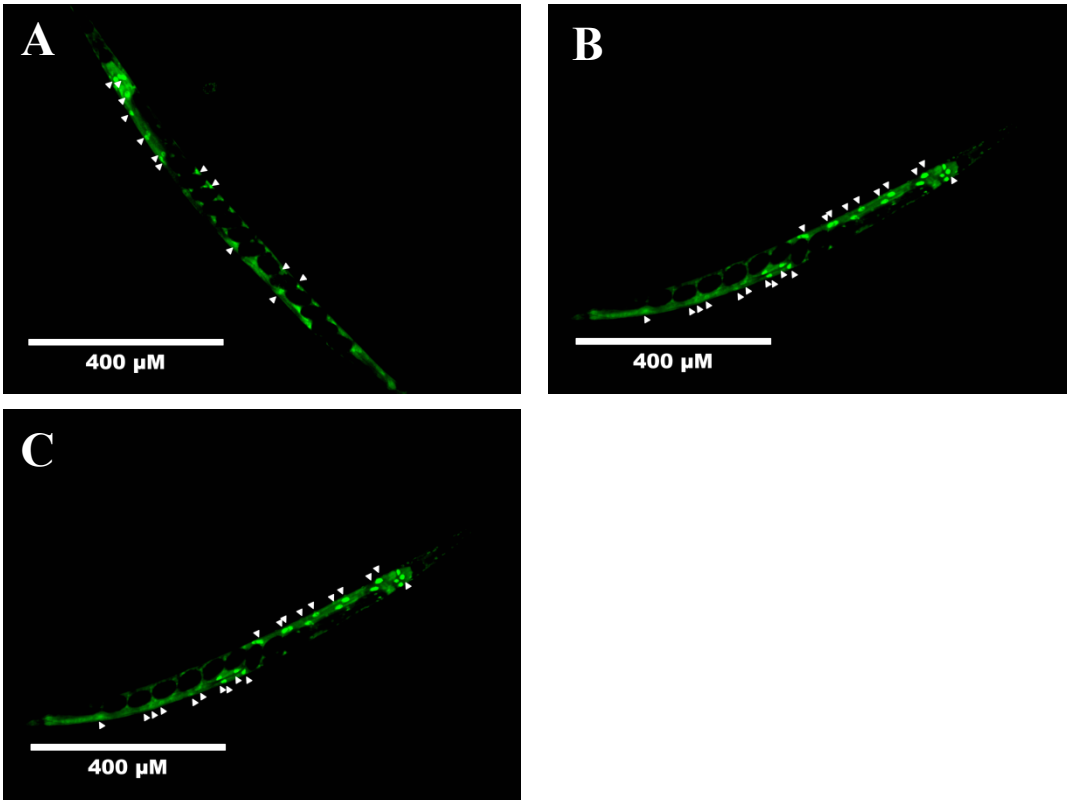

Figure 4-29. Fluorescent microscopic images of DAF-16::GFP localization in transgenic *C. elegans mev-1* nematodes.

Young adult nematodes were treated for 48 h with (A) M9 buffer (control), (B) 10 mM glucose, or (C) 10 mM glucose plus 1 µM quercetin. Arrows exemplarily indicate nuclear localized DAF-16::GFP.

Nevertheless, it could not be excluded that the transcriptional activity of DAF-16 was altered by the treatments. Therefore, the overall meaning of DAF-16 for the life span-rescuing effects of 1 µM quercetin in nematodes exposed to glucose was tested. The knockdown of *daf-16* by RNAi in the *mev-1* mutant showed a mild reduction of mean life span ($p < 0.05$). Moreover, a significant reduction in survival by glucose treatment ($p < 0.001$) that was virtually completely prevented by the additional treatment with quercetin ($p < 0.001$) was observed (Figure 4-30, Table B-17). Similar results were obtained in the *daf-16* mutant strain CF1038 (Table B-18).

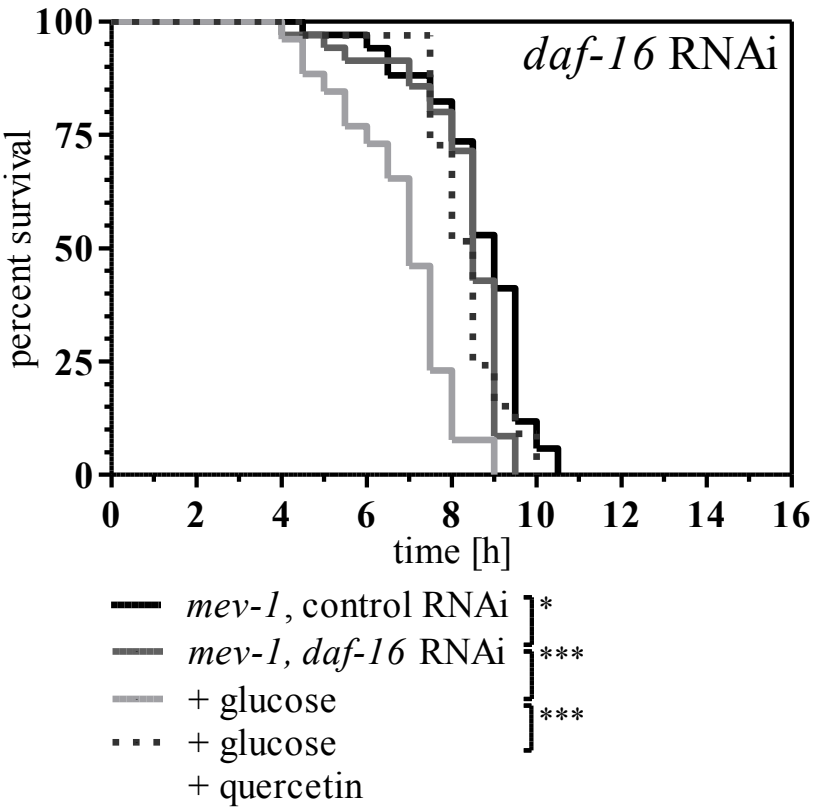

Figure 4-30. Effects of *daf-16* RNAi on glucose-induced life span reduction and its protection by quercetin in *C. elegans* TK22 (*mev-1*).

Nematodes were raised on *daf-16* RNAi and treated with M9 buffer, 10 mM glucose, or 10 mM glucose plus 1 µM quercetin at the young adult stage for 48 h. Life span was measured under heat stress at 37 °C. * $p < 0.01$, *** $p < 0.001$

Although SIR-2.1 and DAF-16 interaction is required for the beneficial effects of caloric restriction, the protection from glucose-induced life span reduction is mediated by SIR-2.1 independently of DAF-16.

4.4.6 The Prevention of Glucose-Induced Life Span Reduction Is Independent of HSF-1, JNK-1, or SKN-1

HSF-1, JNK-1, and SKN-1 represent further factors of stress response that were knocked down to study the effects of glucose toxicity and especially its prevention by quercetin. *Skn-1* and *jnk-1* were knocked down by RNAi in TK22 (*mev-1*). On the contrary, the role of *hsf-1* was studied in the mutant strain PS3551, because *hsf-1* RNAi in the *mev-1* mutant did not lead to a significant reduction of *hsf-1* mRNA. Moreover, the life span reducing effect of 10 mM glucose was studied in wildtype nematodes, for comparison with the *hsf-1* mutant. Similarly to *mev-1*, treatment with 10 mM glucose led to a significant life span reduction in wildtype nematodes and could be prevented by the additional treatment with 10 mM glucose. However, life span reduction was not as strong in the wildtype as in the *mev-1* mutant (data not shown).

Upon knockdown of *skn-1* or *jnk-1* and in the *hsf-1* mutant, the treatment with 10 mM glucose for 48 hours led to a significant reduction of survival, which was effectively prevented by the additional treatment with 1 µM quercetin (Figure 4-31). Moreover, the mean life span of *mev-1* was significantly reduced by knockdown of *skn-1* but not *jnk-1* (Table B-19).

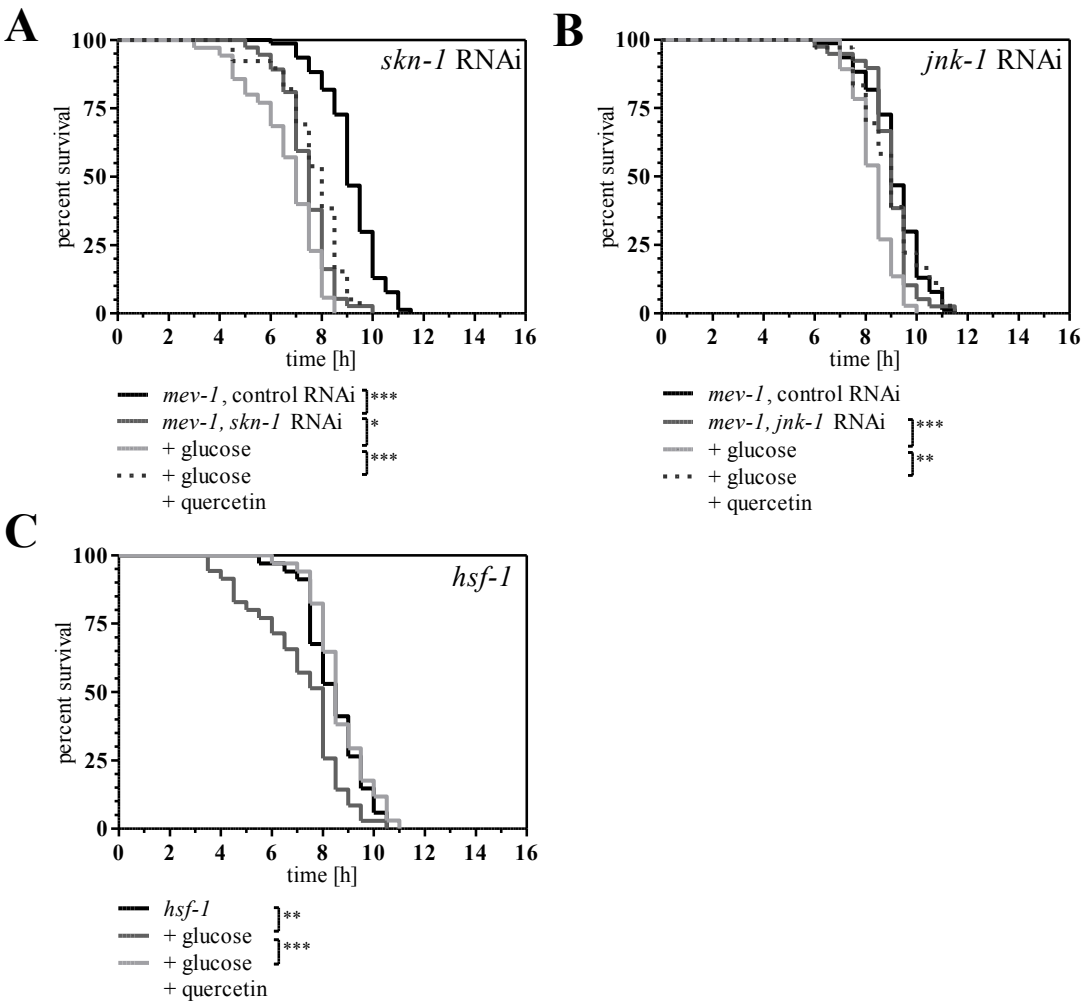

Figure 4-31. Quercetin protects against glucose-induced reduction of life span in *skn-1-*, *jnk-1-*, and *hsf-1*-deficient nematodes.

Young adult nematodes were treated with M9 buffer (control), 10 mM glucose, or 10 mM glucose plus 1 µM quercetin. Subsequently, life span under heat stress was measured. * $p < 0.05$, ** $p < 0.01$, *** $p < 0.001$

In conclusion, neither HSF-1 nor SKN-1 nor JNK-1 interacts with SIR-2.1 to prevent glucose-induced life span reduction.

4.4.7 Influence of Nuclear Hormone Receptors NHR-49 and DAF-12 on the Prevention of Glucose Toxicity

In the following, the focus was shifted towards other proteins for which interactions with sirtuins have been described. Peroxisome proliferator-activated receptors (PPARs) were identified as such targets. Although *C. elegans* possesses numerous nuclear hormone receptors, structural homologues of PPARα or PPARγ do not exist. However, the nuclear hormone receptors DAF-12 and NHR-49 have been described to fulfil similar functions in *C. elegans* to PPARs in humans or mice. Thus, the effects of glucose treatment in the absence or presence of quercetin on *C. elegans* survival were studied in the *nhr-49* mutant strain RB1716 and the *daf-12* mutant strain AA1. The mutant strains were used, because an RNAi clone for *nhr-49* is not available and *daf-12* RNAi led to larval arrest during development.

In the *nhr-49* mutant, a significant reduction of survival was observed by treatment with 10 mM glucose. This was completely prevented by the addition of 1 µM quercetin (Figure 4-32 A). In contrast to this, the addition of 1 µM quercetin could not prevent the glucose-induced life span reduction in the *daf-12* mutant (Figure 4-32 B). Furthermore, the life span reduction of 3.6 hours (34%) by glucose treatment was notably strong (Table B-20), when DAF-12 was functionally absent.

As already done for *sir-2.1* the effects of 1 µM quercetin on DAF-12 expression were studied. In *mev-1*, DAF-12 was detected as a single band at approximately 30 kD, which corresponds to DAF-12 isoform c. The analysis revealed that DAF-12 expression is markedly increased upon treatment with 10 mM glucose but the additional treatment with 1 µM quercetin did not lead to a further alteration of DAF-12 expression (Figure 4-33), indicating that quercetin does not rely on DAF-12 by increased expression but by its activity.

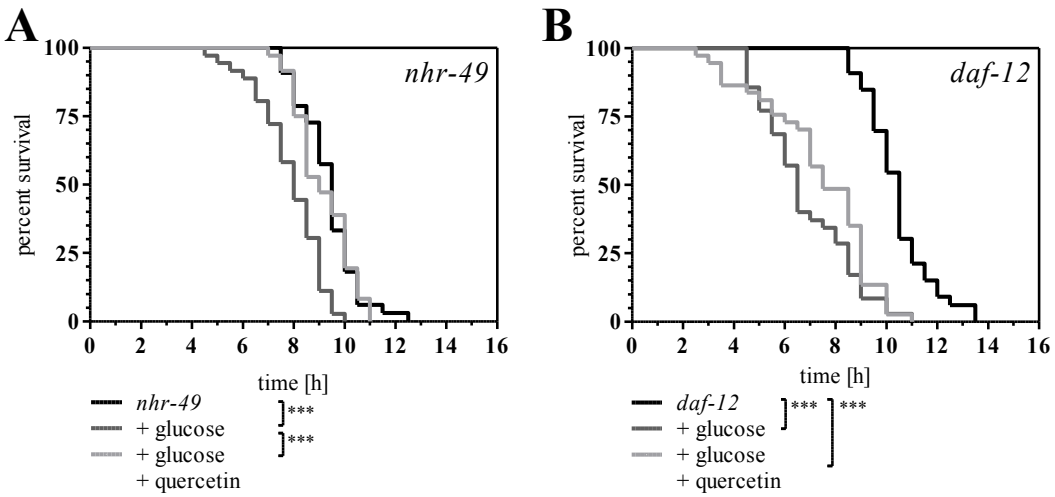

Figure 4-32. Effects of a 48 h treatment with glucose in the absence or presence of quercetin on the life span of *C. elegans* RB1716 (*nhr-49*) and AA1 (*daf-12*).

Young adult (A) *nhr-49* mutant nematodes or (B) *daf-12* mutant nematodes were treated with M9 buffer (control), 10 mM glucose, or 10 mM glucose plus 1 µM quercetin for 48 h. Subsequently, the life span under heat stress (37 °C) was measured. *** $p < 0.001$

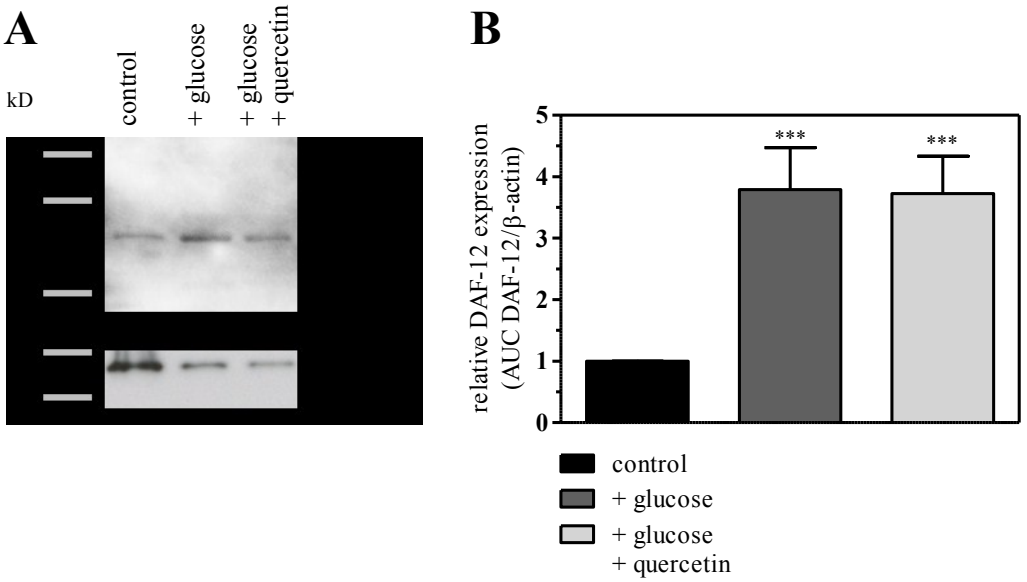

Figure 4-33. Quantification of DAF-12 expression by Western blotting after treatment with glucose or glucose plus quercetin in *C. elegans* TK22 (*mev-1*).

Proteins were extracted from young adult nematodes that had been treated with M9 buffer (control), 10 mM glucose, or 10 mM glucose plus 1 µM quercetin for 48 h and were analysed by Western blotting using rabbit-anti-DAF-12 and goat-anti-rabbit-IgG HRP-conjugated as well as mouse-anti-actin and goat-anti-mouse-IgG HRP-conjugated antibodies. (A) A representative Western blot of DAF-12 with β-actin as reference protein is shown. (B) DAF-12 expression was quantified densitometrically relative to β-actin. AUC: area under curve, *** $p < 0.001$ compared to control

4.4.7.1 DAF-12 Acts Independently of Steroid Signalling to Prevent Glucose Toxicity

DAF-12 is a nuclear hormone receptor that also functions in steroid signalling. In this context it binds dafachronic acids as ligands and promotes reproductive development as well as stress resistance and longevity. These ligands result from the oxidation of cholesterol by DAF-9. Here, it was assessed whether ligand binding to DAF-12 was necessary to increase resistance against glucose toxicity. For this purpose, *mev-1* nematodes were subjected to *daf-9* RNAi to diminish the production of dafachronic acids. From Figure 4-34 it can be concluded that the survival of glucose treated nematodes is reduced, while the combined treatment with glucose and quercetin did not reduce the survival rate compared to control animals (Table B-21).

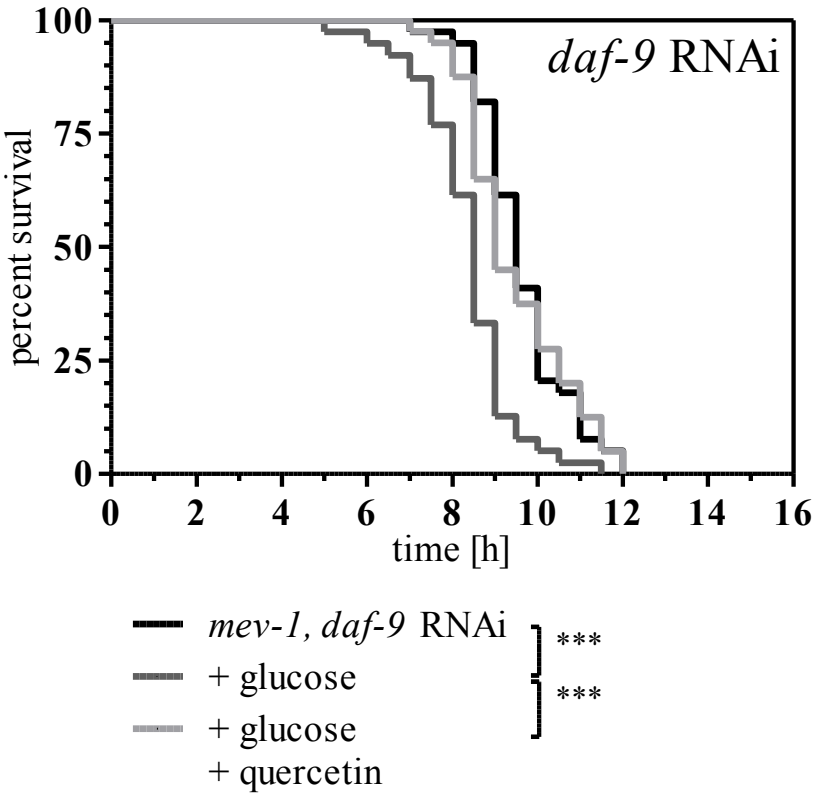

Figure 4-34. *Daf-9* is dispensable for the protection against glucose-induced reduction of life span by quercetin in *C. elegans* TK22 (*mev-1*).

Mev-1 larvae were subjected to *daf-9* RNAi and treated with M9 buffer (control), 10 mM glucose, or 10 mM glucose plus 1 µM quercetin at the young adult stage. Subsequently, life span under heat stress was measured at 37 °C. *** $p < 0.001$

4.4.7.2 The Transcriptional Coactivator MDT-15 Is Required for the Inhibition of Glucose Toxicity by Quercetin

From mammals it is known that PPARs interact with co-activators like PGC-1α. Similar to PPARs, however, a structural homologue of PGC-1α does not exist in *C. elegans*. For the nuclear hormone receptor NHR-49 interactions with the transcriptional co-activator MDT-15 are described in the regulation of fat storage. Moreover, MDT-15 is involved in the regulation of numerous metabolic genes and in mediating the effects of caloric restriction on metabolism. Thus it was asked, whether *mdt-15* is necessary to mediate resistance against glucose-induced life span reduction by quercetin. The knockdown of *mdt-15* led to a reduction of mean life span by 18% ($p < 0.001$, Table B-22). Additionally, Figure 4-35 shows that glucose treatment in *mdt-15*-deficient nematodes led to a significant decrease of survival ($p < 0.001$), which was not be prevented by the simultaneous treatment with 1 µM quercetin ($p = 0.243$), here.

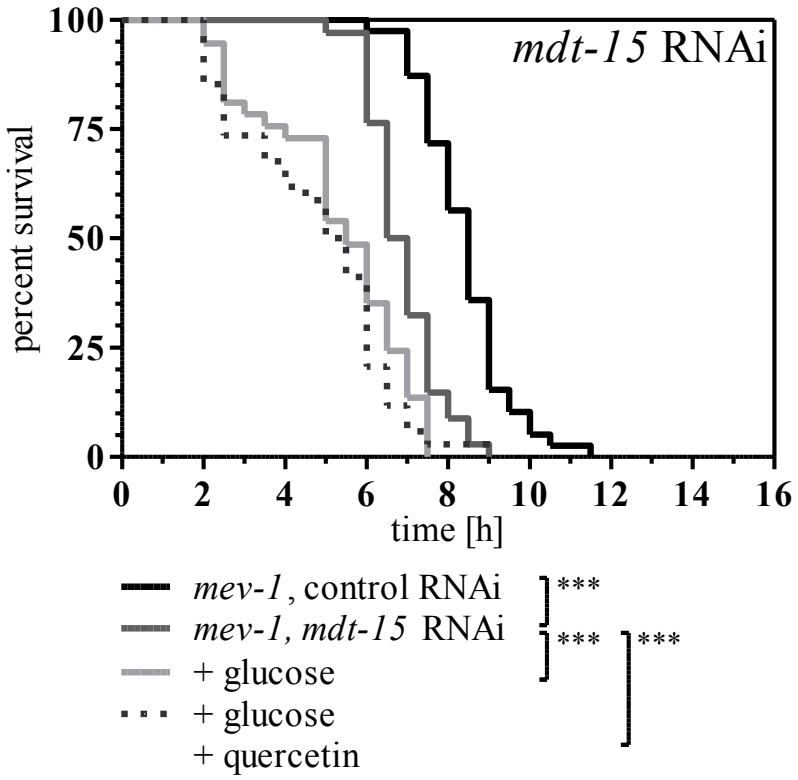

Figure 4-35. *Mdt-15* RNAi abolishes the restoration of life span by quercetin in the presence of glucose in *C. elegans* TK22 (*mev-1*).

Young adult nematodes that had been subjected to *mdt-15* RNAi were treated with M9 buffer (control), 10 mM glucose, or 10 mM glucose plus 1 µM quercetin. Life span under heat stress was measured at 37 °C. *** $p < 0.001$

In summary, the results imply that SIR-2.1, DAF-12, and MDT-15 act in the same pathway to mediate the beneficial effects of quercetin with respect to glucose-induced life span reduction, since the knockdown of either *sir-2.1, daf-12,* or *mdt-15* completely abolishes the life span restoration by quercetin in the presence of glucose.

4.5 Influence of Quercetin on the Protein Quality Control System

In chapter 4.1.4 it was shown that glucose treatment did not further reduce the life span of *mev-1* nematodes if components of the protein quality control system, such as heat shock proteins, mediators of UPR, or ubiquitin, are knocked down. Furthermore, it was found that treatment with glucose or the proteasome inhibitor MG132 had similar but not additive life span reducing effects substantiating that the protein quality control is impaired by glucose. Here it was tested whether quercetin is able to rescue this impairment.

4.5.1 Quercetin Does Not Enhance the Life Span of UPR^{mt}-Deficient Nematodes in the Presence of Glucose

The knockdown of *hsp-6*, *hsp-60*, *dve-1* or *ubl-5* highly significantly reduced the life span of TK22 (*mev-1*) under heat stress. However, the treatment with 10 mM glucose for 48 h did not lead to a further decrease of survival, and the addition of 1 µM quercetin did not extend life span under these conditions (Figure 4-36, Table B-23).

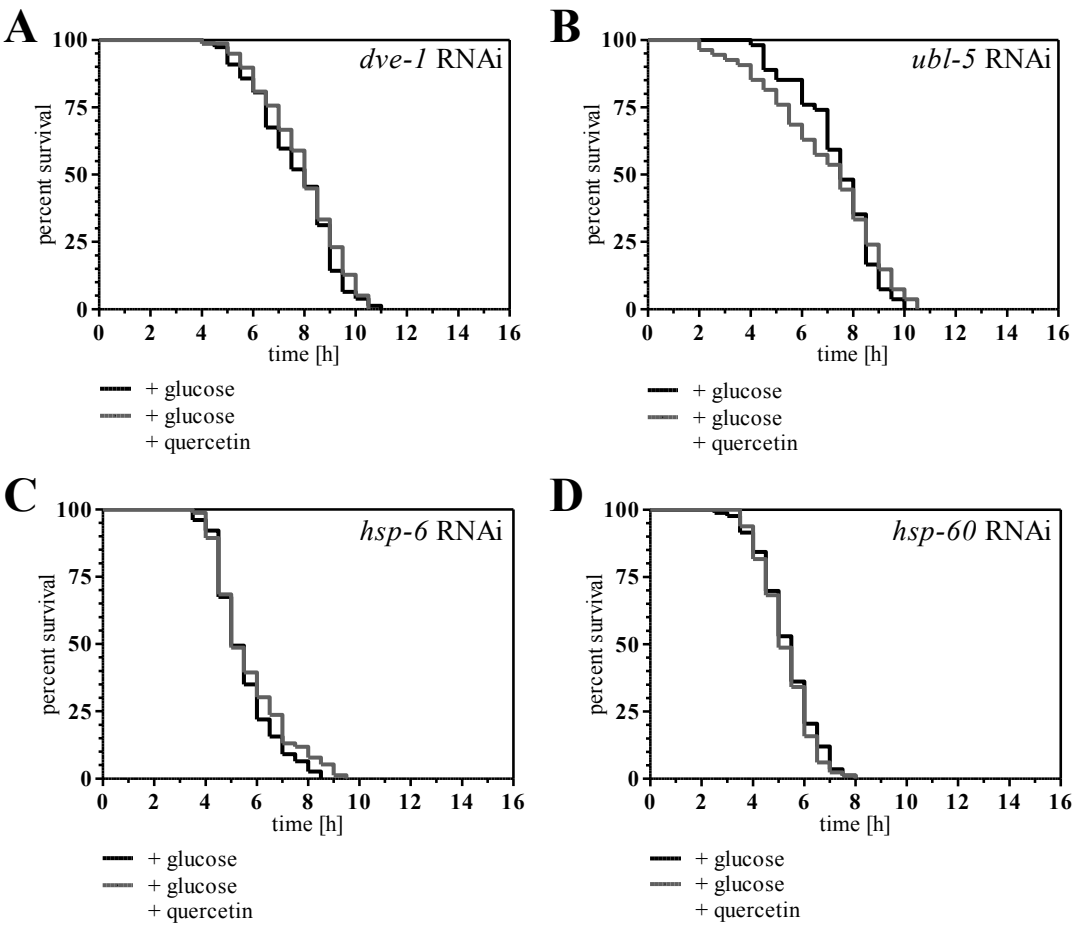

Figure 4-36. Quercetin does not increase the life span of UPR^{mt}-deficient TK22 (*mev-1*) nematodes in the presence of glucose.

Mev-1 nematodes were treated with (A) *dve-1* RNAi, (B) *ubl-5* RNAi, (C) *hsp-6* RNAi, or (D) *hsp-60* RNAi. At the young adult stage nematodes were incubated with 10 mM glucose or 10 mM glucose plus 1 µM quercetin. Life span was measured under heat stress at 37 °C. UPR^{mt}: unfolded protein response in mitochondria

4.5.2 The Life Span of UPR^{ER}-Deficient Nematodes Cannot Be Enhanced by Quercetin in the Presence of Glucose

The same effects were observed upon knockdown of UPR^{ER} components. Similar to the knockdown of mitochondrial chaperones, *xbp-1*, *abu-1*, or *abu-11* RNAi resulted in reduced survival of the *mev-1* mutant, which was not further reduced by glucose treatment (Table B-24). Under neither condition, the addition of quercetin was able to enhance the survival (Figure 4-37) suggesting that quercetin activates UPR in mitochondria and the ER in a *sir-2.1*, *daf-12*, and *mdt-15*-dependent manner.

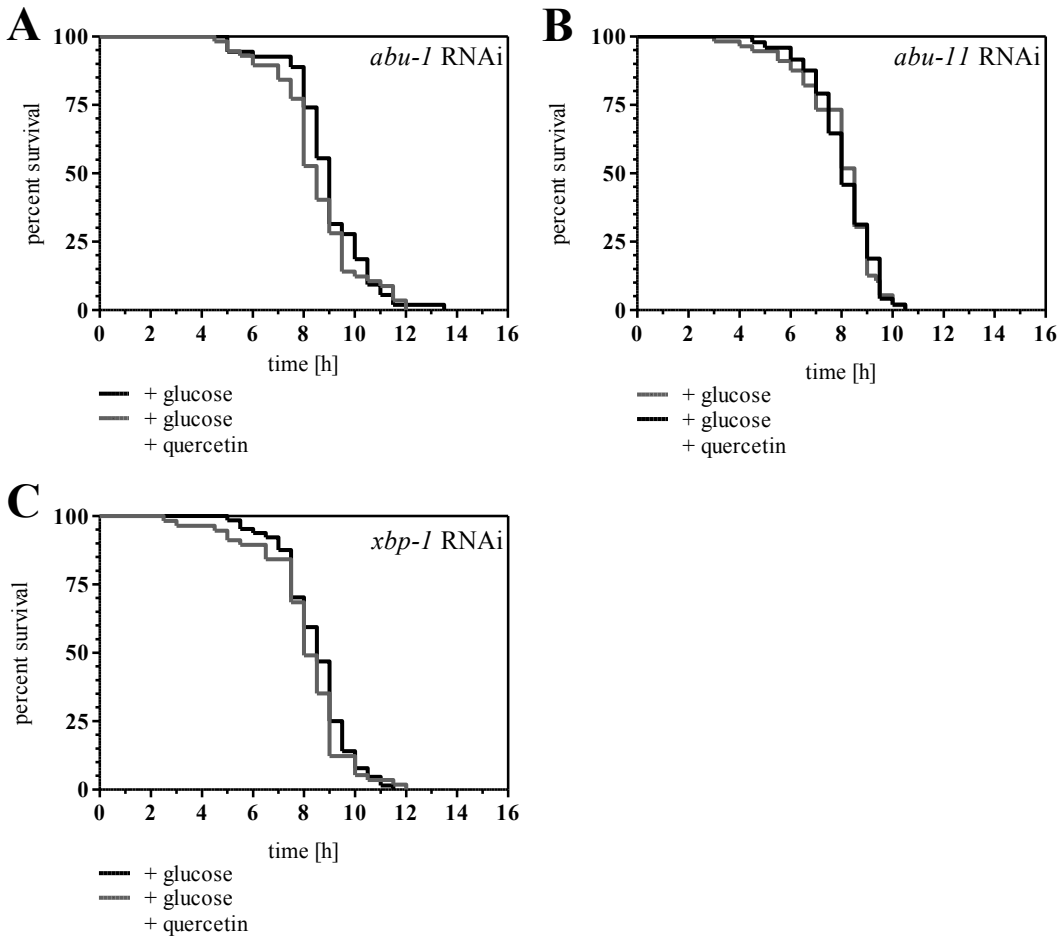

Figure 4-37. Quercetin does not increase the life span of UPR^{ER}-deficient TK22 (*mev-1*) nematodes in the presence of glucose.

Mev-1 nematodes were treated with (A) *abu-1* RNAi, (B) *abu-11* RNAi, or (C) *xbp-1* RNAi. At the young adult stage nematodes were incubated with 10 mM glucose or 10 mM glucose plus 1 µM quercetin. Life span was measured under heat stress at 37 °C. UPR^{ER}: unfolded protein response in the endoplasmic reticulum

4.5.3 Effects of Quercetin on the Ubiquitin-Proteasome System in the Presence of Glucose

As indicated in Table B-25, *ubq-1* and *uba-1* RNAi led to a significant life span reduction under heat stress. The survival of RNAi treated nematodes was not further decreased by the application of 10 mM glucose and could not be increased by the addition of 1 µM quercetin either (Figure 4-38).

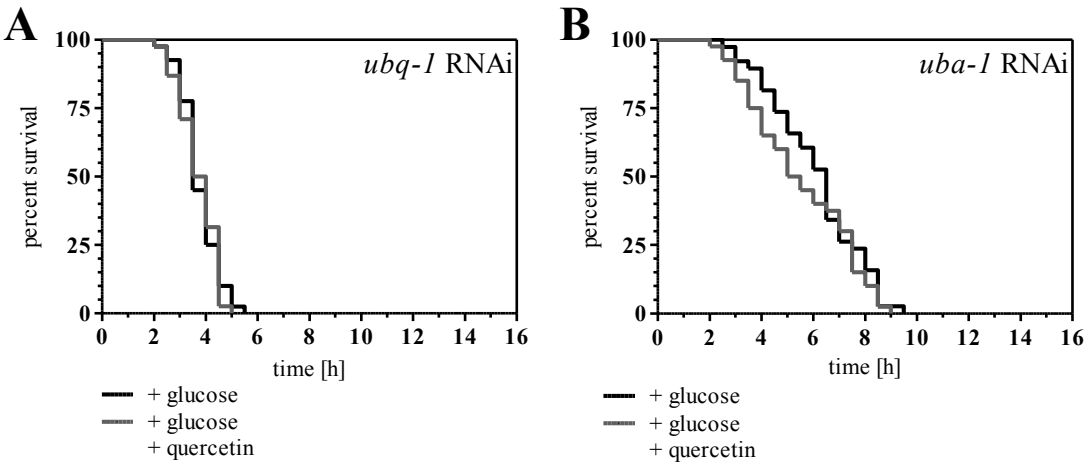

Figure 4-38. Life span of *ubq-1* or *uba-1* RNAi treated nematodes is not prolonged by quercetin in the presence of glucose.

Nematodes were raised on control RNAi. At the young adult stage they were transferred to (A) *ubq-1* or (B) *uba-1* RNAi and treated with 10 mM glucose or 10 mM glucose plus 1 µM quercetin. Subsequently, the life span under heat stress (37 °C) was measured.

On the contrary, the life span reduction by treatment with the proteasome inhibitor MG132 could be entirely reversed by the addition of 1 µM quercetin (Figure 4-39 A). However, the additional treatment with 1 µM quercetin did not prevent the decreased survival that resulted from the simultaneous treatment with 10 mM glucose and 200 µM MG132 (Figure 4-39 B), suggesting first of all that the proteasome inhibition by MG132 is not irreversible and secondly, that inhibition by MG132 plus glucose becomes too severe to be compensated by quercetin.

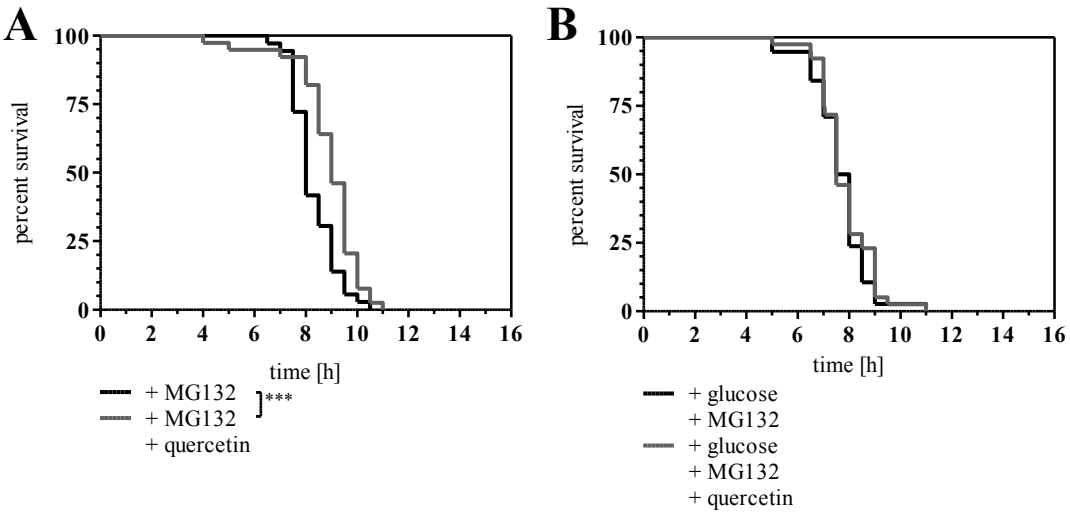

Figure 4-39. Inhibition of the proteasome by MG132 reduces the life span *C. elegans* TK22 (*mev-1*) similar to glucose and is reversed by quercetin.

Young adult nematodes were treated with (A) 200 µM MG132 or 200 µM MG132 plus 1 µM quercetin, or (B) 10 mM glucose plus 200 µM MG132 or 10 mM glucose, 200 µM MG132, and 1 µM quercetin. Life span was measured under heat stress at 37 °C. *** $p < 0.001$

In summary these results imply that the proteasome inhibition by glucose can be overcome by the addition of 1 µM quercetin.

4.6 Quercetin Reduces Apoptosis

The apoptotic programme is among others initiated, if proteostasis is severely impaired and cannot be restored by the activation of the different quality control mechanisms. In chapter 4.3 it was shown that this is the case in glucose-treated nematodes. Here it was examined whether additional treatment with 1 µM quercetin had any influence on glucose-induced apoptosis. From Figure 4-40 follows that quercetin effectively suppressed the increase of germ line apoptosis that was observed upon glucose treatment. Again, these results were confirmed in the *ced-1* mutant.

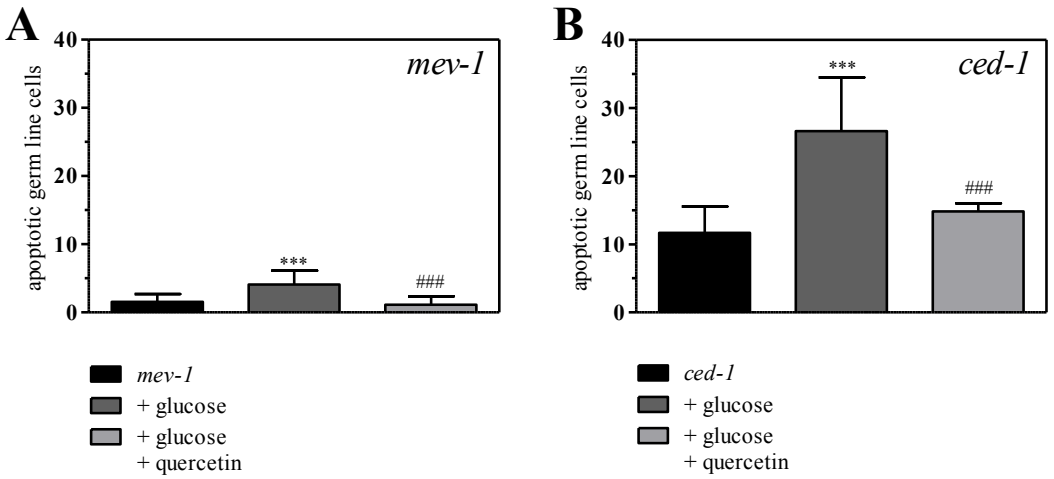

Figure 4-40. Quercetin reduces glucose induced apoptosis in *C. elegans* TK22 (*mev-1*) and CB3203 (*ced-1*).

(A) Young adult *mev-1* or (B) *ced-1* nematodes were treated with M9 buffer (control), 10 mM glucose, or 10 mM glucose plus 1 µM quercetin. Apoptotic cell corpses were stained with the fluorescent dye SYTO12 and quantified microscopically. *** $p < 0.001$ compared to control, ### $p < 0.001$ compared to glucose treatment

4.7 Effects of Quercetin on Autophagy

Autophagy is a conserved cellular process for the degradation of cytoplasmic constituents and contributes to proteostasis. Moreover, it plays a role in programmed cell death whereupon it can act both agonistic and antagonistic to apoptosis. To study the influence of autophagy on glucose-induced life span reduction in *C. elegans*, TK22 *(mev-1)* nematodes were subjected to *bec-1* RNAi. Since BEC-1 is essential for autophagosome formation, autophagy is prevented by knockdown of *bec-1*. Figure 4-41 A indicates that knockdown of *bec-1* did not influence the survival of *C. elegans* TK22 *(mev-1)*. Moreover, autophagy-deficient nematodes were protected from life span reduction by glucose treatment, suggesting that glucose activates apoptosis by autophagosome-related pathways. This was finally verified by the determination of germ line apoptosis upon *bec-1* RNAi. Under these conditions glucose treatment did not lead to increased apoptosis. The additional application of quercetin did not affect apoptosis either (Figure 4-41 B).

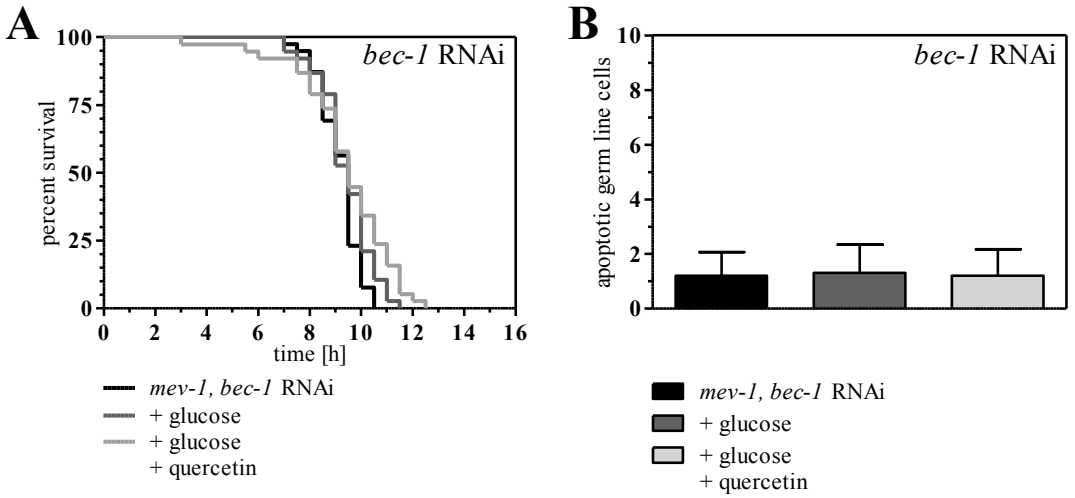

Figure 4-41. Effect of *bec-1* RNAi on glucose-induced reduction of life span and apoptosis in *C. elegans* TK22 (*mev-1*) in the absence or presence of quercetin.

Young adult nematodes that had been treated with *bec-1* RNAi were incubated with M9 buffer (control), 10 mM glucose, or 10 mM glucose plus 1 µM quercetin for 48 h. (A) Life span was measured under heat stress at 37 °C. (B) Apoptotic cell corpses were stained with the fluorescent dye SYTO12 and quantified microscopically.

5 DISCUSSION

The question, why people age, has been a topic of biologic research for decades. While mean life span has largely increased over time, only small changes in maximum life span were observed. This indicates the existence of parameters that limit the maximum life span in humans [202]. Moreover, the life expectancy of 75 year old people did not increase over time. Thus it is assumed that adaption to environmental stress factors results in reduced mortality. The focus is not only on factors that determine life span but also on such parameters that contribute to the development of age-associated pathologies and lead to decreased health and ability as age increases.

Age-related, physiological changes begin already at the age of 20 to 30 years. The speed of progression varies among different organ systems and individuals. An example for such age-related changes is the development of impaired glucose tolerance, which occurs more frequently in elderly people.

The nematode *C. elegans* is ideally suited as model organism to study the consequences of environmental stressors, such as a high-caloric diet and hyperglycaemia, as well as the relevance of different stress resistance mechanisms in response to those disturbances. Its relatively short life cycle allows the examination of life span-modulating agents within a short period of time. Moreover, the transparent body permits the use of fluorescence-based techniques to study, e.g. protein expression and localization *in vivo*. The availability of the completely sequenced *C. elegans* genome furthermore offers the application of versatile genetic analysis tools.

In the course of this work, the mechanisms of a glucose-triggered life span reduction were studied. In doing so, mitochondria-associated parameters as well as modifications of proteins by oxidation and carbonylation were determined. Additionally, the activation of stress resistance mechanisms by quercetin, a polyphenol occurring mainly in apple skin and onions, was examined.

5.1 A Number of Parameters Discussed to Be Relevant for Glucose Toxicity Cannot Explain the Life Span Reduction in *mev*-1 Mutants by Feeding High Glucose Concentrations

In the present work, *C. elegans* was incubated with glucose to study the effects of a high-caloric diet on ageing and life span. While caloric restriction has been shown to slow the ageing process and extend life span in many organisms, a high caloric diet is associated with accelerated ageing and increased mortality [203]. The *C. elegans* mutant strain TK22 (*mev-1*) was used as model organism, because it is closely related to the metabolic situation of diabetic patients (chapter 1.8). *Mev-1* nematodes are short-lived and suffer from increased endogenous ROS production due to a mutation in complex II of the electron transport chain. To simulate a mild hyperglycaemia [201], which could appear as a consequence of ageing or hypercaloric nutrition and is present in diabetes, nematodes were incubated in liquid NGM containing *E. coli* as food source and additionally 10 mM glucose. The adequate uptake of glucose by *C. elegans* was ensured by using a liquid culture medium that, according to the pumping activity of the pharynx, causes a continuous delivery of dissolved compounds to the intestinal tract [204, 205].

First of all, the effect of glucose feeding on life span under heat stress was studied. Therefore, wildtype and *mev-1* mutant nematodes were treated with glucose, in a range of 10 mM to 250 mM. In both strains the application of 10 mM glucose for 48 h hours resulted in a highly significant life span reduction that was not further decreased by higher glucose concentrations. A life span shortening effect of glucose was also reported by Lee *et al*. and Schlotterer *et al.* [201, 206]. Since glucose was applied in addition to *E. coli*, which serves as the natural food source, the observed life span reduction is not a result of malnutrition. Moreover, *E. coli* were inactivated by antibiotics to circumvent bacterial glucose metabolism. Consequently, glucose-metabolites generated by *E. coli* cannot account for the life span reduction in *C. elegans*. Hence, glucose functions as stressor, against which *C. elegans* has not developed successful stress resistance mechanisms.

Increased glucose metabolism, i. e. increased flux through glycolysis and TCA cycle, leads to the formation of reactive oxygen species in the mitochondrial

electron transport chain [11]. Already in 1956 D. Harman presented the free radical theory of ageing, proposing that deleterious effects of free radicals on cell constituents contribute to the ageing process [207]. Today, the free radical theory is still a point of interest and controversially discussed [208]. On the one hand, it has been reported that long-lived *daf-2* mutants show elevated expression of *sod-3* and are resistant to ROS [209, 210]. Moreover, life span extension by *daf-2* mutation is suppressed by decreased expression of a cytosolic catalase [211]. On the other hand, other long-lived mutants, such as *isp-1* and *nuo-6* mutants, have elevated ROS levels [212]. Additionally, the treatment with ROS-generating agents, like juglone or paraquat, increases the life span of wildtype nematodes [204, 209, 210].

In the present work it was shown that incubation with 10 mM glucose increases ROS production in *mev-1* by 45%. In wildtype nematodes, which have lower endogenous ROS production compared to *mev-1*, the ROS production was more than 2fold enhanced upon glucose feeding (data not shown, [201]).

To examine whether a causal link exists between increased ROS production and life span reduction in glucose treated *mev-1* nematodes, the antioxidant ascorbic acid was applied simultaneously with glucose. It was shown that 250 µM ascorbic acid efficiently suppressed the increase in ROS production upon glucose feeding. However, the treatment with ascorbic acid displayed no influence at all on survival at 37 °C, demonstrating that ROS formation cannot account for the reduced life span upon glucose feeding to *mev-1* in the present study.

Hyperglycaemia is not only associated with increased oxidative stress but also with mitochondrial dysfunction in a more general view. For example, the coupling of oxygen consumption and ATP production, mitochondrial integrity, and capacity of the electron transport chain were decreased, while mitochondrial dyscoupling was increased in isolated heart mitochondria of diabetic Wistar rats [213]. Thus, the effects of glucose on mitochondrial function beyond ROS formation were examined in *mev-1* mutants. In doing so, it was shown that both the quantity of mitochondrial activity and mass were increased upon treatment with 10 mM glucose. To examine, whether increased quantity of respiring mitochondria was merely a consequence of changes in mitochondrial mass, the ratio of both parameters was calculated. This revealed a small decrease of that ratio, indicating a functional impairment of mitochondria by glucose. Additionally

the effects of glucose on oxygen consumption and ATP production were determined as further parameters of metabolic activity. It was found that oxygen consumption significantly increased but did not result in more ATP production. Increased oxygen consumption that does not result in enhanced ATP formation might be the result of mitochondrial uncoupling. However, this is unlikely because this would dissipate the mitochondrial membrane potential and thus could not lead to increased mitochondrial activity as detected by staining with CM-XRos. Moreover, the "uncoupling to survive" theory proposes that uncoupling of mitochondrial respiration from energy production decreases ROS production and could increase life span [214]. Indeed lower mitochondrial membrane potential was recently associated with increased life span in long-lived *C. elegans* mutants, such as *daf-2*, *age-1*, and *eat-2* [215].

It could be hypothesized that glucose induces mitochondrial biogenesis and leads to an increase of mitochondrial mass. Although mitochondrial activity increases as well, the ratio of active, respiring mitochondria to mitochondrial mass drops due to increased ROS production, while oxygen consumption is only temporarily increased and ATP production remains unchanged. These results were supported by experiments in which nematodes were treated with 100 mM glucose (data not shown). Although no significant increase of mitochondrial activity or mass was observed after treatment with 100 mM glucose, the ratio was decreased by 10 %. Again, oxygen consumption was significantly increased but did not result in enhanced ATP levels.

Advanced glycation end products result from the non-enzymatic addition of reducing sugars or reactive carbonyls to proteins and other macromolecules [2]. The accumulation of AGEs during ageing has been described in numerous species, including rats [19], mice, monkeys [216], and humans [216, 217]. Moreover, Sell *et al.* demonstrated a correlation of AGE accumulation with overall longevity as AGE accumulation is slower in long-lived species, e.g. monkeys and humans, compared to shorter-lived species, such as cows and dogs [216]. Additionally, the progression of AGE accumulation is accelerated by hyperglycaemia in diabetes. For example, AGEs were shown to accumulate in the retinal vasculature of diabetic rats, while no AGEs were observed in non-diabetic controls [218]. Since protein carbonylation precedes the formation of AGEs, the entity of carbonylated

proteins was determined by us of the Oxy Blot kit. A significant increase of protein carbonylation was found upon incubation with 100 mM glucose, but not after application of 10 m glucose.

In *C. elegans* the feeding of 40 mM glucose increases the accumulation of methylglyoxal derived AGEs and leads to a life span reduction [(201)]. Overexpression of glyoxalase-1, a methylglyoxal-detoxifying enzyme, attenuated both AGE accumulation and life span reduction, while knockdown of glyoxalase-1 by RNAi reduced the survival of control and glucose-treated nematodes to a similar extend [(201)].

In the present work it was examined whether also lower glucose concentrations (10 mM) increase the formation of MG-derived AGEs and may cause the glucose-induced life span reduction. Although treatment with 500 µM MG resulted in a significant decrease of survival (data not shown), MG-derived AGE formation cannot be the cause of glucose-induced life span reduction, since the feeding of 10 mM glucose did not lead to a detectable increase of MG-AGEs in wildtype or *mev-1* nematodes. On the contrary, the treatment with 100 mM glucose led to a 4fold increase of MG-AGEs in the *mev-1* mutant although the two concentrations did not affect life span differently.

Nevertheless, it is conceivable that AGEs derived from N^{ε}-(carboxymethyl) lysine, N^{ε}-(carboxyethyl) lysine, and pentosidine might play a role and that it is rather the sum of AGE formation that causes the life span reduction. To test this hypothesis, the AGE-breaker pyridoxamine was applied in combination with glucose in life span experiments. Pyridoxamine has been shown to inhibit AGE formation from glucose-incubated BSA and human methemoglobin *in vitro* [(219)]. Moreover the prevention of collagen glycation by pyridoxamine *in vivo* has been reported in Fisher rats [(220)] and streptozotocin-diabetic rats [(221)]. Indeed it was found that the co-incubation with 10 mM glucose and 50 mM pyridoxamine entirely prevented glucose-induced life span reduction of *mev-1* mutants.

Taken together, direct evidence that glucose-induced life span reduction is caused by AGEs was not found. Yet, the beneficial impact of pyridoxamine implies that the formation of certain AGEs, which are non-MG derived and cannot be detected by Oxy blotting, does play a role and is probably linked to more subtle mechanisms that affect for instance proteostasis.

5.2 Glucose Interferes with the Protein Quality Control System

The maintenance of proteostasis is essential for normal cellular functions and viability. During ageing, the efficiency of proteostasis declines, on the one hand, and the accumulation of misfolded or damaged proteins challenges the proteostasis network, on the other hand. Disturbed proteostasis is associated with the development of diseases [222]. These include not only neurodegenerative diseases, like Alzheimer's disease, Parkinson's disease and Huntington's disease but also type 2 diabetes mellitus [30]. For example, genes involved in UPR^{ER} have been shown to be upregulated in kidney tubuli of patients with diabetic nephropathy. Additionally, hyperglycaemia induced the expression of UPR^{ER} genes in HK-2 cells [223]. In the present work various components of the proteostasis network were knocked down or inhibited to study the mechanisms of glucose-induced life span reduction.

Heat shock proteins function as chaperones that are required for correct and efficient protein folding. The expression of many heat shock proteins, especially of the HSP70 family (e.g. *hsp-1* to *hsp-4*), decreases during ageing of *C. elegans* [224]. The *C. elegans* proteins HSP-6 and HSP-60 are chaperones that are involved in the handling of mitochondrial stress, and their expression has been shown to decline with age. Additionally, knockdown of *hsp-6* by RNAi also decreases the expression of *hsp-60* and leads to life span reduction [147]. DVE-1 is a transcription factor involved in mitochondrial stress response. Upon mitochondrial stress *hsp-60* and *hsp-6* are upregulated in a DVE-1 dependent manner. Benedetti *et al.* identified *ubl-5* as regulator of *hsp-6* and *hsp-60* using *hsp-6::gfp* and *hsp-60::gfp* transgenic nematodes [225]. Similarly, *dve-1* was discovered as an inducer of *hsp-6* and *hsp-60* under conditions of mitochondrial unfolded protein stress [151], as evidenced additionally by the binding of DVE-1 to *hsp-6* and *hsp-60* promoters [151]. Haynes *et al.* hypothesized that UBL-5 and DVE-1 form a nuclear complex that facilitates or permits the association of DVE-1 with promoter regions of genes involved in mitochondrial unfolded protein response [151]. A role of UBL-5 in UPR^{mt} has not been reported in other organisms than *C. elegans*. However, polymorphisms in human UBL5 have been

linked to obesity and diabetes [226] and UBL5 is highly conserved among eukaryotic organisms.

Knockdown of *hsp-6* resulted in a highly significant life span reduction in the present work. Because *hsp-6* RNAi has been described to be embryonically lethal, Kimura *et al.* started RNAi after nematodes had reached adulthood [147]. In the course of this work, *hsp-6* RNAi was applied to L1 larvae. Although nematodes were obviously retarded in development, remained small in body size, and did not produce progeny, larval lethality was not observed. Here, RNAi of *hsp-6* reduced mean life span by 38% compared to control animals. Upon *hsp-60* RNAi the life span reduction was even stronger, leading to a decline of mean survival by 46%. Although it has been reported that DVE-1 and UBL-5 are involved in the transcriptional regulation of *hsp-6* and *hsp-60*, the life span reduction upon *dve-1* RNAi or *ubl-5* RNAi was not as strong as upon knockdown of *hsp-6* or *hsp-60*, indicating that *hsp-6* and *hsp-60* are likely to be regulated by other transcription factors as well. This is in agreement with the results generated by Benedetti *et al.* and Haynes *et al.*, who also detected some remaining *hsp-60::gfp* expression upon *dve-1* RNAi or *ubl-5* RNAi [151, 225]. Interestingly, neither upon knockdown of *hsp-6* or *hsp-60* nor *dve-1* or *ubl-5* the treatment with glucose led to an additional life span reduction, indicating that glucose diminishes the life span of *C. elegans mev-1* mutants by blocking UPR^{mt} in the same manner as knockdown of *hsp-6*, *hsp-60*, *dve-1*, or *ubl-5* did.

To elucidate how glucose interferes with the proteostasis network, also factors of the UPR^{ER} were knocked down by RNAi. ER stress leads to the activation of the bZip transcription factor *xbp-1* by IRE-1-mediated, alternative splicing. Also under physiological conditions *xbp-1* is required to maintain ER homoeostasis and the knockdown of *xpb-1* leads to constitutive ER stress resembled by activation of IRE-1 and PEK-1 [227]. Moreover, the *xbp-1* mutant is also more sensitive to exogenously administered ER stress [227]. Increased sensitivity to ER stress is likely the result of missing upregulation of *xbp-1* target genes [154]. Recently it was shown that *xbp-1*, together with *ire-1*, contributes to longevity in the *daf-2* mutant. Yet, the *xbp-1* mutant displayed a similar life span as wildtype nematodes [153] in the absence of an exogenous stressor. Here it was demonstrated that *xpb-1* RNAi significantly reduced the survival of *mev-1* mutants, which could be due to

enhanced ER stress in *mev-1* nematodes. Urano *et al.* identified the *abu* family that is upregulated in *xbp-1* mutants to compensate for enhanced ER stress due to *xbp-1* deficiency [154]. Furthermore, they have shown that knockdown of *abu-1* strongly induces the ER stress reporter gene *hsp-4::gfp* and leads to reduced survival of *xbp-1* mutants. On the other hand, *abu-1* RNAi did not affect survival of wildtype nematodes [154]. In *mev-1* mutants the knockdown of *abu-1* or *abu-11* resulted in a significant reduction of survival, suggesting that their presence becomes especially important for survival under stress conditions. In case of *abu-1* RNAi this was similar to the decrease of survival by *xbp-1* RNAi (10%); *abu-11* RNAi decreased life span even stronger (17%). When RNAi-treated nematodes were incubated with glucose, like to the knockdown of key proteins involved in UPR^{mt}, no additional life span reduction was observed. These results corroborate the adverse effects of glucose on proteostasis.

The impact of proteasomal degradation on life span was studied, on the one hand, by knockdown of *ubq-1*, which tags proteins for proteasomal degradation, and *uba-1*, which is required for ubiquitin attachment to proteins, and, on the other hand, by inhibition of the proteasomal catalytic activity using the inhibitor MG132. Both *ubq-1* RNAi and *uba-1* RNAi resulted in a strong reduction of mean life span (23% by *uba-1* RNAi, 55% by *ubq-1* RNAi). The inhibition of the proteasome by MG132 also led to decreased life span, although to a much lesser extent (10%). Again, the incubation of RNAi-treated nematodes with glucose did not reduce survival compared to RNAi exposure alone. Neither did the combined treatment with glucose and MG132 result in additional effects on life span.

Since, glucose did not lead to a further life span reduction if either UPR^{mt} or UPR^{ER} or the ubiquitin-proteasome system are disturbed, it may be assumed that glucose overloads the proteostasis network and thereby affects the three named signalling pathways simultaneously. Upon ER stress not only the UPR^{ER} is induced but also ER-associated protein degradation. The ERAD pathway recognizes proteins that are unable to pass the ER quality control. They are retranslocated to the cytosol, ubiquitinated and degraded by the proteasome [32, 34]. Of course such mechanisms would be triggered in case of increased protein damage. A similar link of UPR^{mt} and the ubiquitin-proteasome system has not yet been reported so far. However, the existence of the UPR^{mt} was only recently

proposed [31] and is less well understood than UPR^{ER} or cytosolic heat shock response [32]. UPR^{mt} has been suggested to be conceptually similar to UPR^{ER} and heat shock response [32]. Moreover, cross-talk between mitochondria and ER during stress conditions has been assumed [31]. Therefore, it seems conceivable that prolonged activation of UPR^{mt} also leads to increased protein degradation via the ubiquitin-proteasome system.

5.3 Glucose Induces Apoptosis

Proteasome inhibition results in protein accumulation [228-230] and induces apoptosis [228, 229]. Moreover, apoptosis seems to play a role in the development of diabetic complications. Several studies using rat models reported increased cell deaths in pericyte and endothelial cells of diabetic animals [231-233]. Increased death of pericytes and endothelial cells were also found in diabetic patients [231]. Additionally it was reported that inhibition of AGE formation ameliorated the increase of apoptosis [232], while the chronic exposure of pericytes to AGEs resulted in a 3fold increase of apoptotic cell death [234]. Apoptosis is a tightly regulated mechanism that is essential for the removal of damaged or degenerated cells. Both, insufficient and excessive apoptosis can result in dysfunction and severe diseases and eventually reduced life span.

In the following it was shown that treatment with 10 mM glucose significantly induced germ line apoptosis in *C. elegans* TK22 *(mev-1)*. Both developmental and germ line apoptosis can be prevented by the knockdown of *ced-3* or *ced-4*, which are components of the core apoptotic machinery [165]. As expected, it was demonstrated here that *ced-3* or *ced-4* RNAi-treated nematodes displayed significantly less germ line apoptosis than control RNAi-treated animals. Moreover, glucose treatment did no longer increase apoptosis upon RNAi knockdown of these pro-apoptotic factors. Consistent with this, incubation with glucose did no longer result in a life span reduction in *ced-3* or *ced-4* RNAi treated animals, which has also been reported by S. Choi [125]. Unexpectedly however, *ced-3* RNAi itself led to a significant decrease of survival, while *ced-4*

RNAi did not affect life span, suggesting that CED-3 has pro-survival activities as well.

Depending on the kind of stressor, *C. elegans* uses different pathways to trigger apoptosis. While *cep-1* and *egl-1* are required for DNA damage-induced apoptosis, they are dispensable for apoptosis induced by environmental insults. The latter initiate apoptosis via MAPK signalling and rely on *mek-1*, *jnk-1*, *sek-1*, *pmk-1* [178].

The examination of germ line apoptosis upon *cep-1* and *egl-1* RNAi revealed that, in contrast to *ced-3* or *ced-4* RNAi, *cep-1* or *egl-1* are without influence on glucose-induced apoptosis. Hence it can be concluded that induction of apoptosis upon glucose treatment is not the result of increased DNA damage. Moreover, incubation with glucose significantly reduced the survival of *cep-1* RNAi treated animals; whereas it did not reduce the survival of *egl-1* RNAi treated nematodes.

5.4 Overburdening Autophagy Causes Glucose-Induced Life Span Reduction

Autophagy is a ubiquitous, cellular process that is required for the maintenance of cellular homoeostasis, on the one hand, but can also contribute to cell death, on the other hand. As impaired protein homoeostasis and increased programmed cell death are the main contributors for glucose-induced life span reduction in *C. elegans* it seemed conceivable that autophagy may also be involved. Inhibition of autophagy increases the susceptibility to apoptosis, indicating its pro-survival function [235]. However, as mentioned above, apoptosis and autophagy can also act as cooperative cell death inducers [236]; and regulators such as DAP and JNK kinases have been identified to be crucial for this cooperativity [54, 237]. In the present work, autophagy was inhibited in *mev-1* mutants by knockdown of *bec-1*, which is essential for autophagosome formation. *Bec-1*-deficient nematodes lived as long as control animals and did not display increased apoptosis. However, inhibition of autophagy prevented life span reduction and enhanced apoptosis upon glucose treatment, demonstrating that autophagy is a prerequisite to induce apoptosis in *mev-1* by glucose treatment.

It was described above that knockdown of *egl-1* prevents life span reduction but not increased apoptosis by glucose treatment. Additionally, *ced-3*-deficient nematodes were protected from apoptosis, yet lived shorter than control animals. These results are out of tune with the hypothesis that apoptosis alone is the cause of reduced survival upon glucose treatment. However, they can be explained taking the role of autophagy into account. EGL-1 cannot only induce apoptosis but also autophagy. Maiuri *et al.* have shown that an *egl-1* gain-of-function mutation increased constitutive autophagy, while loss of *egl-1* prevented starvation-induced autophagy. Moreover, starvation did not further increase autophagy in the *egl-1* gain-of-function mutant [(50)]. Hence, the missing life span reduction upon glucose-treatment in *egl-1*-deficient nematodes may be the result of inhibiting the induction of autophagy.

In a mammalian cell culture model Beclin1 was shown to be cleaved by caspase-3, resulting in reduced autophagosome formation [(53)]. Beclin1 Asp149 was identified as conserved caspase cleavage site [(53)]. Basic Local Alignment of human Beclin1 and *C. elegans* BEC-1 revealed that Asp149 is conserved in *C. elegans*, too, thus offering the opportunity that also in the nematode BEC-1 may be a substrate for caspase-dependent cleavage. Suggesting that CED-3 does cleave BEC-1, the reduced survival upon *ced-3* RNAi could be the result of increased *bec-1*-dependent autophagy. That glucose does not further reduce the life span of *ced-3*-deficient nematodes implies that glucose treatment leads to the induction of autophagy in *mev-1* mutants but does not further enhance autophagy in *ced-3* RNAi treated nematodes.

Finally the question should be addressed, why knockdown of *ced-4*, causing the inhibition of CED-3, prevents glucose-induced life span reduction and apoptosis likewise to *ced-3* RNAi, but does not reduce the life span of control treated animals. CED-4 is essential for CED-3 activation during apoptosis [(238)], which is consistent with the observation that germ line apoptosis is absent in both *ced-3* and *ced-4* deficient nematodes. It has been supposed that the release of CED-4 from a CED-9/CED-4 complex [(239)] leads to CED-4 perinuclear translocation and self-oligomerization [(240)], which might bring CED-3 zymogens to close proximity and allow self-activation of CED-3 [(241)]. However, CSP-1B has been shown to cleave the CED-3 proprotein as well [(242)], offering an opportunity for CED-4-

independent activation of CED-3 in analogy to caspase-3 and -6 activation by caspase-8 or -9 in mammalian cells [243]. Hence, in *ced-4*-deficient nematodes, CED-3 may be activated by CSP-1B and be able to cleave BEC-1 to inhibit autophagy. This would prevent a lifespan reduction by *ced-4* RNAi and also by the application of glucose.

5.5 Activation of Stress Response Pathways by Quercetin Prevents Glucose-Induced Life Span Reduction and Apoptosis

The second part of this work aimed at the activation of stress response pathways to counteract glucose toxicity. For many species caloric restriction has been shown to slow the ageing process and extend life span [63-67]; and activation of stress response appears as a key mechanism to provide finally hormesis.

Sirtuins have been shown to mediate CR-induced longevity in *S. cerevisiae* [244], *D. melanogaster* [245], and in the *C. elegans eat-2* mutant [190]. Moreover, mammalian sirtuins are implicated in the regulation of CR responses, such as glucose homoeostasis in mice [91], stress resistance [246], and survival [85, 247].

The association of sirtuins with ageing processes and CR has initiated the search for sirtuin-activators that act as CR mimetics. Quercetin is a secondary plant compound that was formerly shown to be a sirtuin-activating compound [189, 248].

Incubation of *mev-1* with 1 µM or 100 µM quercetin did not affect life span in the absence of glucose. However, in combination with glucose treatment quercetin prevented the life span reduction induced by glucose completely. These results indicate that quercetin selectively increases stress resistance to provoke its hormetic, life span extending effects.

Due to the necessity of *sir-2.1* for activation of several pathways and findings showing that SIRT1 expression in human monocytes and endothelial cells was decreased under high glucose treatment, including its reversal by polyphenols [249, 250], this factor came into focus. Interestingly, others found life span extending effects of quercetin in the absence of a stressor that were

independent of *sir-2.1* [251]. In the course of this work, however, it was found that the prevention of glucose-induced life span reduction by quercetin is absolutely dependent on *sir-2.1* in the *mev-1* mutant. Moreover, a significant induction of *sir-2.1* expression in glucose-treated nematodes was demonstrated to occur by the addition of quercetin, while the treatment with glucose alone had no effect of *sir-2.1* expression. This could be due to a comparably high *sir-2.1* expression in *mev-1* mutants according to their increased stress conditions.

The insulin/IGF-1 signalling pathway in *C. elegans* has been described to essentially affect stress response and life span, with DAF-16 increasing both parameters when translocated to the nucleus in the absence of extracellular ligands. Moreover, *daf-16* is needed for the life span prolonging effects of *sir-2.1* overexpression [192]. Hormetic effects in response to treatment with the ROS generating agent juglone, also require both *daf-16* and sir-*2.1* [204]. However, DAF-16 is not required for *sir-2.1*-dependent life span extension by caloric restriction in *unc-13* mutants [252] indicating that *sir-2.1* has also *daf-16* independent functions.

The localization of DAF-16 was studied in a transgenic line that expresses the DAF-16::GFP fusion protein in a *mev-1* background. In wildtype nematodes DAF-16 is found to be predominantly cytosolic, yet rapidly translocates to the nucleus in response to environmental stressors, such as heat stress or oxidative stress [253] and then activates the transcription of target genes, which promote stress resistance and longevity [254, 255]. Consistent with Kondo *et al.* [256] most DAF-16 was found to be nuclear in *mev-1* mutants even under control conditions, which is probably due to increased endogenous stress. Treatment with glucose alone and in addition to quercetin did not alter DAF-16 localization.

In contrast to a previously published report, stating that glucose shortens *C. elegans* life span by downregulation of DAF-16 and the heat shock factor HSF-1 [206], a highly significant life span reduction due to glucose feeding was found in *daf-16* RNAi treated *mev-1* nematodes. These results were also confirmed in the *daf-16* mutant strain CF1038 that was unresponsive to glucose in the other study [206]. A possible explanation for this is the use of liquid medium in the present work, which increases the availability of dissolved compounds [204, 205].

The glucose-induced life span reduction was reversed by the additional treatment with quercetin in both the *daf-16* mutant strain and in *daf-16* RNAi-treated *mev-1* animals indicating that quercetin acts on *sir-2.1* in a *daf-16* independent fashion to prevent the life span reducing effect of glucose.

Since, overexpression of *sir-2.1* leads to aak-2-dependent longevity, the AMP-activated protein kinase was a candidate to contribute to the rescuing effects of quercetin on glucose-caused reduction of life span. Moreover, according to the hypothesis that increased stress response is responsible for hormetic effects of quercetin under glucose exposure, the stress response factors HSF-1, JNK-1, and SKN-1 were looked at, additionally. That those factors are able to influence ageing in general has been shown in various studies. E.g. *aak-2* has been previously reported to act as an energy sensor and regulate life span. Similarly to *daf-16*, *aak-2* is required for the longevity phenotype of *daf-2* mutants [257] and *sir-2.1* overexpression [258]. Additionally, *aak-2* is required for some regimens of CR [188, 259], yet dispensable for others [188, 258]. Here it was found that quercetin can prevent the reduction of life span imposed by glucose feeding independent of *aak-2*, analogously to *daf-16*.

With respect to *hsf-1*, knockdown shortens life span [135, 260] and accelerates tissue disintegration [260], while overexpression extends the life span of *C. elegans* [135]. Furthermore, the life span prolongation by *hsf-1* overexpression was shown to be completely dependent on *daf-16*; and it was found that *hsf-1* and *daf-16* both are required for the increased expression of small heat shock proteins upon heat shock, indicating overlapping functions of DAF-16 and HSF-1 [135]. This is consistent with the results presented in this work, indicating that quercetin does not increase heat shock resistance to prevent the life span reduction induced by glucose feeding.

SKN-1 is another *C. elegans* transcription factor and is responsible for resistance against oxidative stress. An and Blackwell [126] have shown that *skn-1* mutant strains are short-lived and sensitive to paraquat, a ROS generating agent. Upon stress SKN-1 accumulates in intestinal nuclei and activates xenobiotic metabolism [136]. It is noteworthy that SKN-1 is inhibited by kinases of the insulin-like signalling cascade and contributes to stress resistance and longevity of *daf-2* mutants [139]. Similar to *hsf-1*, expression of some *skn-1* target genes also requires

daf-16, and *daf-16* RNAi suppresses the life span extension observed in a SKN-1 transgenic strain [139]. With respect to quercetin-mediated life span extension of glucose-fed nematodes, *skn-1* was found to be dispensable indicating that quercetin acts in a pathway different from that typically activated by oxidative stress. This is in agreement with the fact that reducing oxidative stress by treatment with ascorbic acid in the present study did not prolong life span of *mev-1* nematodes that were exposed to glucose.

The *C. elegans* protein JNK-1 is a transcription factor of the MAPK superfamily. From mammalian systems it is known that JNK signalling is also linked to the insulin/IGF-1 pathway [261, 262] and is implicated in development, apoptosis and survival [263]. Very similar to what is reported for *hsf-1* and *skn-1*, knockdown of *jnk-1* leads to reduced survival of *C. elegans*; and overexpression of *jnk-1* increases life span [134]. Moreover, life span extension by *jnk-1* overexpression is suppressed by *daf-16* RNAi. Consistently, *jnk-1* transgenic lines are resistant to heat stress and oxidative stress, while loss of *jnk-1* increases stress sensitivity [134]. However, quercetin also prolongs the life span of glucose-fed *mev-1* nematodes that were treated with *jnk-1* RNAi indicating that quercetin does not act via an increase of stress resistance in a *jnk-1*-dependent pathway.

The effects of mammalian SIRT1 in metabolism are manifold and well characterized. Targets of SIRT1 deacetylation are for example PPARγ, PPARα, PGC-1α, and FOXO transcription factors. SIRT1 regulates insulin secretion [90], gluconeogenesis [91], and fatty acid oxidation [92]. PPARs are nuclear receptors that regulate adipogenesis and fat storage in white adipose tissue. For example, PPAR-dependent release of free fatty acids from visceral white adipose tissue contributes to the development of insulin resistance [264].

In mouse fibroblasts SIRT1 regulates adipogenesis and triglyceride accumulation by repressing PPARγ activity. Similarly, incubation with resveratrol was shown to reduce fat accumulation in differentiated adipocytes in a SIRT1-dependent manner [92]. Moreover, resveratrol increases SIRT1 mRNA expression and reduces PPARγ expression in human visceral adipocytes *in vitro* [265]. However, the effects of PPARγ exerted under caloric restriction and SIRT1 activation are less clear. While short term fasting was reported to increase PPARγ expression in rat visceral adipose tissue [266], 1 to 16 weeks caloric restriction

resulted in decreased PPARγ expression in mouse liver [267]. No changes of PPARγ expression in mouse liver were observed after 5 months of caloric restriction [268]. Also longer periods of caloric restriction, i. e. 16 months, did not alter PPARγ mRNA or protein expression in mouse liver [269].

Similar to PPARγ, PPARα was shown to be significantly increased by 24 h fasting in the liver [270]. Long term caloric restriction (16 months) increased PPARα mRNA in mouse liver, but did not change protein levels of PPARα [269]. Moreover it was shown, that glucose treatment reduces PPARα mRNA expression and DNA binding activity in rat islets and INS(832/13) β-cells [271]. Resveratrol, on the other hand, was shown to increase PPARα activity [272].

C. elegans possesses 284 nuclear hormone receptors [273], yet no clear structural homologues of PPARα or PPARγ. Nevertheless, two *C. elegans* NHRs, *nhr-49* and *daf-12*, have been proposed to play similar roles in fat metabolism like PPARs in mammals [274, 275].

Hence, the roles of *nhr-49* and *daf-12* in glucose-induced life span reduction and its prevention by quercetin were examined in this work. In doing so, it was found that *nhr-49* is not required to prevent glucose-induced life span reduction by the additional treatment with quercetin, whereas in *daf-12* mutants the reversal of life span reduction was absent. Moreover, the glucose-dependent reduction in survival was extraordinarily strong in these animals, stressing that DAF-12 is important to counteract glucose-toxicity. Accordingly, the increased expression of DAF-12 in glucose-treated nematodes must be interpreted as a reasonable response. However, the combined treatment with glucose and quercetin did not increase DAF-12 expression further, indicating that the prevention of glucose-induced life span reduction is not the result of simply upregulating DAF-12.

DAF-12 also plays a role in steroid signalling in *C. elegans*. In this pathway DAF-12 binds dafachronic acids, which are produced from cholesterol by DAF-36 and DAF-9. Depending on the signalling context DAF-12 has different effects on life span. On the one hand, ligand-bound DAF-12 promotes longevity in the absence of signals from the germ line. On the other hand, it promotes reproductive development and inhibits longevity in the dauer pathway, while ligand-free DAF-12 increases stress resistance and longevity under these conditions [276]. In *daf-9* mutant animals no DAF-12 ligand is formed due to

inhibition of dafachronic acid production [276]. Since quercetin was able to prevent glucose-induced life span reduction in *daf-9*-deficient nematodes, it can be concluded that DAF-12 acts on longevity in glucose-exposed *mev-1* mutants independent of steroid signalling.

Many nuclear hormone receptors interact with co-activator or co-repressor molecules to regulate transcription [277]. PGC-1α is such a co-activator molecule that has been shown to cooperate with PPARγ and PPARα [278, 279]. It is moreover a central metabolic regulator that controls glucose and fatty acid metabolisms as well as mitochondrial biogenesis [96-98]. Similar to PPARs, the *C. elegans* genome seems to lack a structural PGC-1 orthologue [144]. However, MDT-15, a subunit of the *C. elegans* mediator complex, has been described to have partially overlapping functions with PGC-1α. MDT-15 physically interacts with NHR-49 and is a transcriptional co-activator of NHR-49 target genes. Yet, no physical interaction between MDT-15 and DAF-12 has been found so far [145]. In the present work it was shown that besides *sir-2.1* and *daf-12* also *mdt-15* was required to prevent glucose-induced life span reduction by quercetin. Rodgers *et al.* have proposed a model that implies SIRT1, PGC-1α, and PPARα in nutrient signalling: In response to fasting, NAD^+ levels increase leading to enhanced SIRT1 protein expression and activity. Active SIRT1 is proposed to deacetylate PGC-1α, which interacts with transcription factors and nuclear hormone receptors, i. e. FoxO1, HNF4α, and PPARα, to regulate glucose, lipid and mitochondrial metabolism [280]. In analogy it may be hypothesized that in *C. elegans* SIR-2.1 deacetylates MDT-15, which probably indirectly interacts with DAF-12 [145] to promote increased stress resistance and longevity.

It was discussed above (chapter 5.2) that glucose may act as proteasome inhibitor and that life span reduction upon glucose treatment is the result of increased autophagy triggered by prolonged impairment of proteostasis. Because the activation of the SIR-2.1/DAF-12 pathway by quercetin does not prolong life span *per se* but selectively inhibits life span reduction after incubation with glucose it seems conceivable that the life-extending effects of quercetin are mediated by a direct link between SIR-2.1/DAF-12 and proteostasis. Indeed the proteasome activator PA28 is a down-stream target of DAF-12 [281], which could provide such a link.

In chapter 5.2 the role of glucose in causing a proteasome overload by increasing the number of aged proteins marked for degradation has been discussed. This hypothesis was based on the observation that both glucose and the proteasome inhibitor MG132 reduce the life span of *C. elegans*, but the combined treatment with glucose and MG132 did not result in additional effects on life span reduction. Likewise, the knockdown of various upstream proteasome components resulted each in a significantly decreased survival that was not further reduced by glucose treatment.

Whereas the life span reductions achieved by RNAi of proteasomal components could not be extended by additional treatment with quercetin, effects of glucose or MG132 on life span were reversible. These results are in agreement with the idea that quercetin either reduces the delivery of aged proteins to the proteasome or increases its catalytic activity. The latter suggestion of proteasomal activation is supported by the fact that quercetin reverts the life span-reducing activities of MG132. Consistent with this, it was reported that quercetin reversed MG132-mediated effects on heat shock response and apoptosis in lens epithelial cells [(282)].

In consequence of impaired proteostasis cells undergo apoptosis. Moreover, autophagy is probably increased leading to apoptotic or necrotic cell death [(48)]. As discussed above, the life span reduction by glucose treatment is presumably the result of proteasome inhibition that eventually increases autophagy and apoptosis as proteostasis cannot be restored. Consistently, quercetin treatment did not only prevent glucose- or MG132-induced life span reduction but also inhibited the induction of apoptosis. Whether quercetin also inhibits the induction of autophagy has not been determined in the course of this work. However, the demonstration that *sir-2.1* [(283)] or resveratrol [(284)] induce autophagy in *C. elegans* and that inhibition of autophagy by knockdown of *bec-1* suppressed longevity caused by *sir-2.1* overexpression [(187)] or resveratrol treatment [(283)] clearly indicates that autophagy needs to be finely tuned in order to be cytoprotective and that both inhibition or activation can be life-shortening depending on the conditions.

6 SUMMARY

Ageing is an inevitable process that is often accompanied by the development of mild hyperglycaemia. Besides this physiological type of hyperglycaemia, pathological, more pronounced hyperglycaemia is a hallmark of diabetes mellitus and responsible for its late-onset complications. Polyphenols are a group of secondary plant compounds with preventive effects against glucose-induced degenerative processes.

In the present work the *mev-1* mutant of the nematode *Caenorhabditis elegans* was used as model organisms to study the effects of glucose as well as protective effects of the polyphenol quercetin at the molecular level. The *mev-1* mutant was used since it displays elevated mitochondrial superoxide generation, which is typical for diabetes, too.

It was found that glucose in a concentration of 10 mM significantly reduced the life span measured under heat stress at 37 °C. Although glucose led to enhanced generation of reactive oxygen species (ROS) in mitochondria, the scavenging of ROS by ascorbic acid did not prolong life span. Further processes that are discussed to play a role in glucose-induced damage, such as protein carbonylation and formation of advanced glycation end products (AGEs) were not affected by 10 mM glucose.

A substantial reduction of the P/O ratio pointed to a reduction of mitochondrial efficiency by glucose. To prove functional losings of mitochondrial proteins, the expression of key proteins of the mitochondrial unfolded protein response (UPR^{mt}) was reduced by RNA interference (RNAi). For example, the knockdown of heat shock proteins HSP-6 and HSP-60, respectively, strongly shortened the life span of *mev-1,* yet glucose did not cause an additional reduction. It may be concluded that the inhibition of those proteins by glucose is the reason for the observed reduction of life span. Similar results were found after RNAi of proteins of the unfolded protein response in the endoplasmic reticulum (UPR^{ER}) or proteasomal protein degradation. Interestingly, RNAi against BEC-1, which is essential for the formation of autophagosomes, completely prevented glucose

toxicity but did not affect life span in absence of glucose. It may be assumed that the inhibition of autophagy enhances proteasomal degradation.

Apoptosis, on the contrary, does not seem to be relevant for the life span reduction by glucose. This is supported by the finding that RNAi against the Bcl homologue EGL-1 prevents the life span reduction by glucose but does not affect glucose-induced apoptosis.

The plant polyphenol quercetin at a concentration of 1 µM prevented the glucose-induced life span reduction completely. RNAi against the identified targets of glucose with respect to life span finally inhibited the life span prolongation by quercetin as well. The Sirtuin SIR-2.1, the nuclear hormone receptor DAF-12 and its putative co-activator MDT-15 were identified as upstream regulators of UPR^{mt}, UPR^{ER}, and proteasomal and autophagosomal degradation and are activated by quercetin.

In conclusion, the present work demonstrates that enhanced glucose concentrations reduce the life span of the model organism *C. elegans*. Whereas the formation of ROS, mitochondrial dysfunction, protein carbonylation and generation of AGEs were ruled out as a cause, impairments of proteostasis were identified to be crucial. Quercetin at low micromolar concentrations completely reversed the life span reduction by glucose depending on SIR-2.1, DAF-12, and MDT-15. Those cellular regulators appear to activate the proteostasis network and thereby inhibit the accumulation of proteins damaged by glucose.

7 ZUSAMMENFASSUNG

Alterung ist ein unausweichlicher Prozess der oftmals mit der Entwicklung einer milden Hyperglykämie einhergeht. Neben dieser physiologischen Art der Hyperglykämie, ist die pathologische, stärker ausgeprägte Hyperglykämie ein Kennzeichen des Diabetes mellitus und verantwortlich für dessen Spätfolgen. Polyphenole sind eine Gruppe sekundärer Pflanzeninhaltsstoffe, denen präventive Wirkungen im Rahmen Glukose-induzierter degenerativer Prozesse zugesprochen werden. In der vorliegenden Arbeit wurde die *mev-1* Mutante des Fadenwurms *Caenorhabditis elegans* als Modellorganismus verwendet, um die Effekte der Glukose sowie protektive Wirkungen des Polyphenols Quercetins auf molekularer Ebene zu untersuchen. Die *mev-1* Mutante wurde verwendet, da sie vermehrte mitochondriale Superoxid-Bildung aufweist, die auch typisch für Diabetes ist.

Es konnte gezeigt werden, dass Glukose ab einer Konzentration von 10 mM die Lebensspanne unter Hitzestress bei 37 °C signifikant verminderte. Glukose führte zwar zur erhöhten Bildung reaktiver Sauerstoffspezies in Mitochondrien, deren Abfangen durch Zugabe von Ascorbinsäure bewirkte allerdings keine Lebensverlängerung. Weitere im Rahmen Glukose-bedingter Schädigung diskutierte Prozesse, wie Proteincarbonylierung und die Bildung von *advanced glycation end products* (AGEs), wurden durch 10 mM Glukose nicht beeinflusst.

Eine deutliche Abnahme des P/O-Quotienten wies auf eine Reduktion mitochondrialer Effizienz durch Glukose hin. Um funktionelle Einbußen mitochondrialer Proteine durch Glukose nachzuweisen wurden zentrale Proteine der mitochondrialen *unfolded protein response* (UPR^{mt}) in ihrer Expression mittels RNA-Interferenz (RNAi) reduziert. Dabei zeigte sich beispielsweise, dass der *knockdown* der Hitzeschockproteine HSP-6 bzw. HSP-60 die Lebensspanne von *mev-1* drastisch reduzierte, Glukose aber keine weitere Verkürzung der Lebensdauer bewirkte. Daraus lässt sich schließen, dass eine Hemmung solcher Proteine durch Glukose die beobachtete Lebenszeitverkürzung bewirkt. Ähnliche Ergebnisse ergaben sich nach RNAi von Proteinen der *unfolded protein response* im endoplasmatischen Retikulum (UPR^{ER}) oder des proteasomalen Abbaus. Interessanterweise verhinderte RNAi gegenüber dem für die

Autophagosomenbildung essentiellen Faktor BEC-1 vollständig die Glukosetoxizität ohne die Lebensspanne in Abwesenheit von Glukose zu beeinflussen. Vermutet werden kann eine Steigerung des proteasomalen Abbaus bei Hemmung der Autophagosomenbildung.

Apoptose scheint hingegen keine Bedeutung für die Lebenszeitverkürzung durch Glukose zu spielen. Dafür spricht, dass die Verminderung der Expression des Bcl-Homologs EGL-1 die Lebenszeitverkürzung durch Glukose verhinderte ohne die Glukose-induzierte Apoptose zu beeinflussen.

Das Pflanzenpolyphenol Quercetin unterdrückte in einer Konzentration von 1 µM die Glukose-induzierte Lebenszeitverkürzung vollständig. RNAi identifizierter Zielproteine der Glukose mit Relevanz für die Lebensspanne verhinderte schließlich auch die Lebensverlängerung durch Quercetin. Als übergeordnete Regulatoren der UPR^{mt}, UPR^{ER} sowie des proteasomalen und autophagosomalen Abbaus, die durch Quercetin aktiviert werden, konnten das Sirtuin SIR-2.1, der nukleäre Hormonrezeptor DAF-12 sowie dessen putativer Co-Aktivator MDT-15 identifiziert werden.

Zusammenfassend wurde in der vorliegenden Arbeit gezeigt, dass erhöhte Glukosekonzentrationen die Lebensspanne des Modellorganismus *C. elegans* vermindern. Während die Bildung reaktiver Sauerstoffspezies, mitochondriale Dysfunktion, Proteincarbonylierung und AGE-Bildung als Ursache der Lebensverkürzung ausgeschlossen werden konnten, wurde die Störung der Proteostase als essentiell dafür identifiziert. Mikromolare Quercetin-konzentrationen verhinderten die Verkürzung der Lebensspanne durch Glukose vollständig in Abhängigkeit von SIR-2.1, DAF-12 und MDT-15. Diese zellulären Regulatoren aktivieren offensichtlich das Proteostase-Netzwerk und verhindern dadurch die Akkumulation Glukose-geschädigter Proteine.

8 REFERENCE LIST

1. Statistisches Bundesamt (ed.) (2006 Apr. 12) Generationen-Sterbetafeln für Deutschland - Modellrechnungen für die Geburtsjahrgänge 1871 - 2004. Statistisches Bundesamt, *www.destatis.de* (2012 June 1)
2. Braeckman BP, Houthoofd K, and Vanfleteren JR (2001) Insulin-like signaling, metabolism, stress resistance and aging in *Caenorhabditis elegans*. *Mech Ageing Dev* **122(7):673-693**
3. Hughes KA and Reynolds RM (2005) Evolutionary and mechanistic theories of aging. *Annu Rev Entomol* **50(1):421-445**
4. Kavanagh K, Wylie AT, Chavanne TJ, Jorgensen MJ, Voruganti VS *et al*. (2012) Aging does not reduce heat shock protein 70 in the absence of chronic insulin resistance. *J Gerontol A Biol Sci Med Sci* **67(10):1014-1021**
5. Carrascosa JM, Andres A, Ros M, Bogonez E, Arribas C *et al*. (2011) Development of insulin resistance during aging: involvement of central processes and role of adipokines. *Curr Protein Pept Sci* **12:305-315**
6. Fu Z, Gilbert ER, Pfeiffer L, Zhang Y, Fu Y *et al*. (2012) Genistein ameliorates hyperglycemia in a mouse model of nongenetic type 2 diabetes. *Appl Physiol Nutr Metab* **37(3):480-488**
7. Leem J and Koh EH (2012) Interaction between mitochondria and the endoplasmic reticulum: implications for the pathogenesis of type 2 diabetes mellitus. *Exp Diabetes Res* **2012**, Article ID 242984, **8 pages**, **doi:10.1155/2012/242984**
8. Eckel RH, Kahn SE, Ferrannini E, Goldfine AB, Nathan DM *et al*. (2011) Obesity and type 2 diabetes: what can be unified and what needs to be individualized? *J Clin Endocrinol Metab* **96(6):1654-1663**
9. Ihm SH, Moon HJ, Kang JG, Park CY, Oh KW *et al*. (2007) Effect of aging on insulin secretory function and expression of beta cell function-related genes of islets. *Diabetes Res Clin Pract* **77(3, Supplement):S150-S154**
10. Gu Z, Du Y, Liu Y, Ma L, Li L *et al*. (2012) Effect of aging on islet beta-cell function and its mechanisms in Wistar rats. *Age (Dordr)* **34(6):1393-1403**
11. Giacco F and Brownlee M (2010) Oxidative stress and diabetic complications. *Circ Res* **107(9):1058-1070**
12. Luoma JS, Strålin P, Marklund SL, Hiltunen TP, Särkioja T *et al*. (1998) Expression of extracellular SOD and iNOS in macrophages and smooth muscle cells in human and rabbit atherosclerotic lesions: colocalization with epitopes characteristic of oxidized LDL and peroxynitrite-modified proteins. *Arterioscler Thromb Vasc Biol* **18(2):157-167**
13. Vikramadithyan RK, Hu Y, Noh H-L, Liang C-P, Hallam K *et al*. (2005) Human aldose reductase expression accelerates diabetic atherosclerosis in transgenic mice. *J Clin Invest* **115(9):2434-2443**
14. Geraldes P and King GL (2010) Activation of protein kinase C isoforms and its impact on diabetic complications. *Circ Res* **106(8):1319-1331**

15. Sayeski PP and Kudlow JE (1996) Glucose metabolism to glucosamine is necessary for glucose stimulation of transforming growth factor-α gene transcription. *J Biol Chem* **271(25):15237-15243**
16. Kolm-Litty V, Sauer U, Nerlich A, Lehmann R, and Schleicher E (1998) High glucose-induced transforming growth factor beta1 production is mediated by the hexosamine pathway in porcine glomerular mesangial cells. *J Clin Invest* **101(1):160-169**
17. Chen YQ, Su M, Walia RR, Hao Q, Covington JW *et al*. (1998) Sp1 sites mediate activation of the plasminogen activator inhibitor-1 promoter by glucose in vascular smooth muscle cells. *J Biol Chem* **273(14):8225-8231**
18. Musicki B, Kramer MF, Becker RE, and Burnett AL (2005) Inactivation of phosphorylated endothelial nitric oxide synthase (Ser-1177) by O-GlcNAc in diabetes-associated erectile dysfunction. *Proc Natl Acad Sci U S A* **102(33):11870-11875**
19. Dammann P, Sell DR, Begall S, Strauch C, and Monnier VM (2012) Advanced glycation end-products as markers of aging and longevity in the long-lived Ansell's mole-rat *(Fukomys anselli)*. *J Gerontol A Biol Sci Med Sci* **67(6):573-583**
20. Li J and Schmidt AM (1997) Characterization and functional analysis of the promoter of RAGE, the receptor for advanced glycation end products. *J Biol Chem* **272(26):16498-16506**
21. Lander HM, Tauras JM, Ogiste JS, Hori O, Moss RA *et al*. (1997) Activation of the receptor for advanced glycation end products triggers a p21 ras-dependent mitogen-activated protein kinase pathway regulated by oxidant stress. *J Biol Chem* **272(28):17810-17814**
22. Yamagishi S, Fujimori H, Yonekura Y, and Yamamoto H (1998) Advanced glycation endproducts inhibit prostacyclin production and induce plasminogen activator inhibitor-1 in human microvascular endothelial cells. *Diabetologia* **41(12):1435-1441**
23. Vlassara H, Fuh H, Donnelly T, and Cybulsky M (1995) Advanced glycation endproducts promote adhesion molecule (VCAM-1, ICAM-1) expression and atheroma formation in normal rabbits. *Mol Med* **1(4):447-456**
24. Schmidt AM, Crandall J, Hori O, Cao R, and Lakatta E (1996) Elevated plasma levels of vascular cell adhesion molecule-1 (VCAM-1) in diabetic patients with microalbuminuria: a marker of vascular dysfunction and progressive vascular disease. *Br J Haematol* **92(3):747-750**
25. Bierhaus A, Humpert P, Morcos M, Wendt T, Chavakis T *et al*. (2005) Understanding RAGE, the receptor for advanced glycation end products. *Mol Med* **83(11):876-886**
26. Queisser MA, Yao D, Geisler S, Hammes HP, Lochnit G *et al*. (2010) Hyperglycemia impairs proteasome function by methylglyoxal. *Diabetes* **59(3):670-678**
27. Gidalevitz T, Prahlad V, and Morimoto RI (2011) The stress of protein misfolding: from single cells to multicellular organisms. *Cold Spring Harb Perspect Biol* **3(6):a009704**
28. Stolz A and Wolf DH (2010) Endoplasmic reticulum associated protein degradation: A chaperone assisted journey to hell. *Biochim Biophys Acta* **1803(6):694-705**

29. Yoneda T, Benedetti C, Urano F, Clark SG, Harding HP *et al*. (2004) Compartment-specific perturbation of protein handling activates genes encoding mitochondrial chaperones. *J Cell Sci* **117(18):4055-4066**
30. Hartl FU and Hayer-Hartl M (2002) Molecular chaperones in the cytosol: from nascent chain to folded protein. *Science* **295(5561):1852-1858**
31. Hu F and Liu F (2011) Mitochondrial stress: A bridge between mitochondrial dysfunction and metabolic diseases? *Cell Signal* **23(10):1528-1533**
32. Pellegrino MW, Nargund AM, and Haynes CM (2012 Mar 14) Signaling the mitochondrial unfolded protein response. *Biochim Biophys Acta* [Epub ahead of print]
33. Walter P and Ron D (2011) The unfolded protein response: from stress pathway to homeostatic regulation. *Science* **334(6059):1081-1086**
34. Brodsky JL and Skach WR (2011) Protein folding and quality control in the endoplasmic reticulum: Recent lessons from yeast and mammalian cell systems. *Curr Opin Cell Biol* **23(4):464-475**
35. Uchiki T, Weikel KA, Jiao W, Shang F, Caceres A *et al*. (2012) Glycation-altered proteolysis as a pathobiologic mechanism that links dietary glycemic index, aging, and age-related disease (in nondiabetics). *Aging Cell* **11(1):1-13**
36. Kriegenburg F, Ellgaard L, and Hartmann-Petersen R (2012) Molecular chaperones in targeting misfolded proteins for ubiquitin-dependent degradation. *FEBS Journal* **279(4):532-542**
37. Ciechanover A and Brundin P (2003) The ubiquitin proteasome system in neurodegenerative diseases: sometimes the chicken, sometimes the egg. *Neuron* **40(2):427-446**
38. Pickart CM and Eddins MJ (2004) Ubiquitin: structures, functions, mechanisms. *Biochim Biophys Acta* **1695(1–3):55-72**
39. Glickman MH and Ciechanover A (2002) The ubiquitin-proteasome proteolytic pathway: destruction for the sake of construction. *Physiol Rev* **82(2):373-428**
40. Adams J (2003) The proteasome: structure, function, and role in the cell. *Cancer Treatment Reviews* **29(Supplement 1):3-9**
41. Voges D, Zwickl P, and Baumeister W (1999) The 26S proteasome: a molecular machine designed for controlled proteolysis. *Annu Rev Biochem* **68(1):1015-1068**
42. Szweda PA, Friguet B, and Szweda LI (2002) Proteolysis, free radicals, and aging. *Free Radic Biol Med* **33(1):29-36**
43. Dasuri K, Zhang L, Ebenezer P, Liu Y, Fernandez-Kim SO *et al*. (2009) Aging and dietary restriction alter proteasome biogenesis and composition in the brain and liver. *Mech Ageing Dev* **130(11–12):777-783**
44. Montenarh M (2007) Replikation und Gentechnik. In Löffler G, Heinrich P, and Petrides P (Eds.), *Biochemie und Pathobiochemie* (pp. 219-253). Heidelberg: Springer Medizin, 8. ed.
45. Adams JM (2003) Ways of dying: multiple pathways to apoptosis. *Genes Dev* **17(20):2481-2495**
46. Hetz C (2012) The unfolded protein response: controlling cell fate decisions under ER stress and beyond. *Nat Rev Mol Cell Biol* **13(2):89-102**

47. Levine B and Kroemer G (2008) Autophagy in the pathogenesis of disease. *Cell* **132(1):27-42**
48. Fimia GM and Piacentini M (2010) Regulation of autophagy in mammals and its interplay with apoptosis. *Cell Mol Life Sci* **67(10):1581-1588**
49. Florez-McClure ML, Hohsfield LA, Fonte G, Bealor MT, and Link CD (2007) Decreased Insulin-Receptor Signaling Promotes the Autophagic Degradation of β-Amyloid Peptide in *C. elegans*. *Autophagy* **3(6):569-580**
50. Maiuri MC, Le Toumelin G, Criollo A, Rain JC, Gautier F *et al*. (2007) Functional and physical interaction between Bcl-XL and a BH3-like domain in Beclin-1. *EMBO J* **26(10):2527-2539**
51. Wei Y, Pattingre S, Sinha S, Bassik M, and Levine B (2008) JNK1-mediated phosphorylation of Bcl-2 regulates starvation-induced autophagy. *Mol Cell* **30(6):678-688**
52. Zalckvar E, Berissi H, Mizrachy L, Idelchuk Y, Koren I *et al*. (2009) DAP-kinase-mediated phosphorylation on the BH3 domain of beclin 1 promotes dissociation of beclin 1 from Bcl-XL and induction of autophagy. *EMBO Rep* **10(3):285-292**
53. Luo S and Rubinsztein DC (2009) Apoptosis blocks Beclin 1-dependent autophagosome synthesis: an effect rescued by Bcl-xL. *Cell Death Differ* **17(2):268-277**
54. Gozuacik D, Bialik S, Raveh T, Mitou G, Shohat G *et al*. (2008) DAP-kinase is a mediator of endoplasmic reticulum stress-induced caspase activation and autophagic cell death. *Cell Death Differ* **15(12):1875-1886**
55. Kihara A, Kabey Y, Ohsumi Y, and Yoshimori T (2001) Beclin-phosphatidylinositol 3-kinase complex functions at the *trans*-Golgi network. *EMBO Rep* **2(4):330-335**
56. Axe EL, Walker SA, Manifava M, Chandra P, Roderick HL *et al*. (2008) Autophagosome formation from membrane compartments enriched in phosphatidylinositol 3-phosphate and dynamically connected to the endoplasmic reticulum. *J Cell Biol* **182(4):685-701**
57. Suzuki K, Kubota Y, Sekito T, and Ohsumi Y (2007) Hierarchy of Atg proteins in pre-autophagosomal structure organization. *Genes Cells* **12(2):209-218**
58. Takeuchi H, Kondo Y, Fujiwara K, Kanzawa T, Aoki H *et al*. (2005) Synergistic augmentation of rapamycin-induced autophagy in malignant glioma cells by phosphatidylinositol 3-kinase/protein kinase B inhibitors. *Cancer Res* **65(8):3336-3346**
59. Inoki K, Zhu T, and Guan KL (2003) TSC2 mediates cellular energy response to control cell growth and survival. *Cell* **115(5):577-590**
60. Sánchez-Margalet V, Zoratti R, and Sung CK (1995) Insulin-like growth factor-1 stimulation of cells induces formation of complexes containing phosphatidylinositol-3-kinase, guanosine triphosphatase-activating protein (GAP), and p62 GAP-associated protein. *Endocrinology* **136(1):316-321**
61. Chan EYW, Kir S, and Tooze SA (2007) siRNA screening of the kinome identifies ULK1 as a multidomain modulator of autophagy. *J Biol Chem* **282(35):25464-25474**
62. Juhász G, Hill JH, Yan Y, Sass M, Baehrecke EH *et al*. (2008) The class III PI(3)K Vps34 promotes autophagy and endocytosis but not TOR signaling in *Drosophila*. *J Cell Biol* **181(4):655-666**

63. Herranz D and Serrano M (2010) SIRT1: recent lessons from mouse models. *Nat Rev Cancer* **10(12):819-823**
64. Jiang JC, Jaruga E, Repnevskaya MV, and Jazwinski SM (2000) An intervention resembling caloric restriction prolongs life span and retards aging in yeast. *FASEB J* **14(14):2135-2137**
65. Lakowski B and Hekimi S (1998) The genetics of caloric restriction in *Caenorhabditis elegans*. *Proc Natl Acad Sci U S A* **95(22):13091-13096**
66. Weindruch R and Walford RL (1982) Dietary restriction in mice beginning at 1 year of age: effect on life-span and spontaneous cancer incidence. *Science* **215(4538):1415-1418**
67. Mair W, Goymer P, Pletcher SD, and Partridge L (2003) Demography of dietary restriction and death in *Drosophila*. *Science* **301(5640):1731-1733**
68. Bodkin NL, Alexander TM, Ortmeyer HK, Johnson E, and Hansen BC (2003) Mortality and Morbidity in Laboratory-maintained Rhesus Monkeys and Effects of Long-term Dietary Restriction. *J Gerontol A Biol Sci Med Sci* **58(3):B212-B219**
69. Zheng Y, Zhang W, Pendleton E, Leng S, Wu J *et al*. (2009) Improved insulin sensitivity by calorie restriction is associated with reduction of ERK and p70S6K activities in the liver of obese Zucker rats. *J Endocrinol* **203(3):337-347**
70. Licastro F, Weindruch R, Davis L, and Walford R (1988) Effect of dietary restriction upon the age-associated decline of lymphocyte DNA repair activity in mice. *Age (Dordr)* **11(2):48-52**
71. Tilley R, Miller S, Srivastava V, and Busbee D (1992) Enhanced unscheduled DNA synthesis by secondary cultures of lung cells established from calorically restricted aged rats. *Mech Ageing Dev* **63(2):165-176**
72. Spaulding CC, Walford RL, and Effros RB (1997) Calorie restriction inhibits the age-related dysregulation of the cytokines TNF-α and IL-6 in C3B10RF1 mice. *Mech Ageing Dev* **93(1–3):87-94**
73. Fernandes G, Venkatraman JT, Turturro A, Attwood VG, and Hart RW (1997) Effect of food restriction on life span and immune functions in long-lived Fischer-344 x Brown Norway F1 rats. *J Clin Immunol* **17(1):85-95**
74. Aksenova MV, Aksenov MY, Carney JM, and Butterfield DA (1998) Protein oxidation and enzyme activity decline in old brown Norway rats are reduced by dietary restriction. *Mech Ageing Dev* **100(2):157-168**
75. Radák Z, Takahashi R, Kumiyama A, Nakamoto H, Ohno H *et al*. (2002) Effect of aging and late onset dietary restriction on antioxidant enzymes and proteasome activities, and protein carbonylation of rat skeletal muscle and tendon. *Exp Gerontol* **37(12):1423-1430**
76. Gugliucci A, Kotani K, Taing J, Matsuoka Y, Sano Y *et al*. (2009) Short-term low calorie diet intervention reduces serum advanced glycation end products in healthy overweight or obese adults. *Ann Nutr Metab* **54(3):197-201**
77. Sohal RS, Ku HH, Agarwal S, Forster MJ, and Lal H (1994) Oxidative damage, mitochondrial oxidant generation and antioxidant defenses during aging and in response to food restriction in the mouse. *Mech Ageing Dev* **74(1–2):121-133**

78. Haigis MC and Sinclair DA (2010) Mammalian sirtuins: biological insights and disease relevance. *Annu Rev Pathol Mech Dis* **5(1):253-295**
79. Imai Si, Armstrong CM, Kaeberlein M, and Guarente L (2000) Transcriptional silencing and longevity protein Sir2 is an NAD-dependent histone deacetylase. *Nature* **403(6771):795-800**
80. Frye RA (1999) Characterization of five human cDNAs with homology to the yeast SIR2 gene: Sir2-like proteins (sirtuins) metabolize NAD and may have protein ADP-ribosyltransferase activity. *Biochem Biophys Res Commun* **260(1):273-279**
81. Frye RA (2000) Phylogenetic classification of prokaryotic and eukaryotic Sir2-like proteins. *Biochem Biophys Res Commun* **273(2):793-798**
82. Haigis MC and Guarente LP (2006) Mammalian sirtuins - emerging roles in physiology, aging, and calorie restriction. *Genes Dev* **20(21):2913-2921**
83. Michishita E, Park JY, Burneskis JM, Barrett JC, and Horikawa I (2005) Evolutionarily conserved and nonconserved cellular localizations and functions of human SIRT proteins. *Mol Biol Cell* **16(10):4623-4635**
84. North BJ and Verdin E (2007) Interphase nucleo-cytoplasmic shuttling and localization of SIRT2 during mitosis. *PLoS ONE* **2(8):e784**
85. Cohen HY, Miller C, Bitterman KJ, Wall NR, Hekking B *et al*. (2004) Calorie restriction promotes mammalian cell survival by inducing the SIRT1 deacetylase. *Science* **305(5682):390-392**
86. Bordone L, Cohen D, Robinson A, Motta MC, Van Veen E *et al*. (2007) SIRT1 transgenic mice show phenotypes resembling calorie restriction. *Aging Cell* **6(6):759-767**
87. Banks AS, Kon N, Knight C, Matsumoto M, Gutiérrez-Juárez R *et al*. (2008) SirT1 gain of function increases energy efficiency and prevents diabetes in mice. *Cell Metab* **8(4):333-341**
88. Herranz D, Munoz-Martin M, Canamero M, Mulero F, Martinez-Pastor B *et al*. (2010) Sirt1 improves healthy ageing and protects from metabolic syndrome-associated cancer. *Nat Commun* **1:3**
89. Pfluger PT, Herranz D, Velasco-Miguel S, Serrano M, and Tschöp MH (2008) Sirt1 protects against high-fat diet-induced metabolic damage. *Proc Natl Acad Sci U S A* **105(28):9793-9798**
90. Bordone L, Motta MC, Picard F, Robinson A, Jhala US *et al*. (2005) Sirt1 regulates insulin secretion by repressing UCP2 in pancreatic β–cells. *PLoS Biol* **4(2):e31**
91. Rodgers JT, Lerin C, Haas W, Gygi SP, Spiegelman BM *et al*. (2005) Nutrient control of glucose homeostasis through a complex of PGC-1α and SIRT1. *Nature* **434(7029):113-118**
92. Picard F, Kurtev M, Chung N, Topark-Ngarm A, Senawong T *et al*. (2004) Sirt1 promotes fat mobilization in white adipocytes by repressing PPARγ. *Nature* **429(6993):771-776**
93. Li X, Zhang S, Blander G, Tse JG, Krieger M *et al*. (2007) SIRT1 deacetylates and positively regulates the nuclear receptor LXR. *Mol Cell* **28(1):91-106**
94. Kemper JK, Xiao Z, Ponugoti B, Miao J, Fang S *et al*. (2009) FXR acetylation is normally dynamically regulated by p300 and SIRT1 but constitutively elevated in metabolic disease States. *Cell Metab* **10(5):392-404**

95. Ponugoti B, Kim DH, Xiao Z, Smith Z, Miao J *et al*. (2010) SIRT1 deacetylates and inhibits SREBP-1C activity in regulation of hepatic lipid metabolism. *J Biol Chem* **285(44):33959-33970**
96. Kong X, Wang R, Xue Y, Liu X, Zhang H *et al*. (2010) Sirtuin 3, a new target of PGC-1α, plays an important role in the suppression of ROS and mitochondrial biogenesis. *PLoS ONE* **5(7):e11707**
97. Lagouge M, Argmann C, Gerhart-Hines Z, Meziane H, Lerin C *et al*. (2006) Resveratrol improves mitochondrial function and protects against metabolic disease by activating SIRT1 and PGC-1α. *Cell* **127(6):1109-1122**
98. Herzig S, Long F, Jhala US, Hedrick S, Quinn R *et al*. (2001) CREB regulates hepatic gluconeogenesis through the coactivator PGC-1. *Nature* **413(6852):179-183**
99. Canto C, Gerhart-Hines Z, Feige JN, Lagouge M, Noriega L *et al*. (2009) AMPK regulates energy expenditure by modulating NAD^+ metabolism and SIRT1 activity. *Nature* **458(7241):1056-1060**
100. Mercken EM, Carboneau BA, Krzysik-Walker SM, and de Cabo R (2012) Of mice and men: The benefits of caloric restriction, exercise, and mimetics. *Ageing Research Reviews* **11(3):390-398**
101. Kennedy DO and Wightman EL (2011) Herbal extracts and phytochemicals: plant secondary metabolites and the enhancement of human brain function. *Adv Nutr* **2(1):32-50**
102. Pietta PG (2000) Flavonoids as antioxidants. *J Nat Prod* **63(7):1035-1042**
103. Beecher GR (2003) Overview of dietary flavonoids: nomenclature, occurrence and intake. *J Nutr* **133(10):3248S-3254S**
104. Scalbert A, Manach C, Morand C, Rémésy C, and Jiménez L (2005) Dietary polyphenols and the prevention of diseases. *Crit Rev Food Sci Nutr* **45(4):287-306**
105. D'Archivio M, Filesi C, Di Benedetto R, Gargiulo R, Giovannini C *et al*. (2007) Polyphenols, dietary sources and bioavailability. *Ann Ist Super Sanita* **43(3):348-361**
106. Williams RJ, Spencer JPE, and Rice-Evans C (2004) Flavonoids: antioxidants or signalling molecules? *Free Radic Biol Med* **36(7):838-849**
107. Poinar GO (1983) *The natural history of nematodes*. New Jersey: Prentice-Hall, Inc.
108. Lucius R and Loos-Frank B (2008) *Biologie der Parasiten*. Berlin: Springer, 2. ed.
109. Nicholas WL (1984) *The biology of free-living nematodes*. Oxford: Clarendon Press, 2. ed.
110. Brenner S (1974) The genetics of *Caenorhabditis elegans*. *Genetics* **77(1):71-94**
111. Corsi AK (2006) A biochemist's guide to *Caenorhabditis elegans*. *Anal Biochem* **359(1):1-17**
112. Altun ZF, Herndon LA, Crocker C, Lints R, and Hall DH (eds.) (2002) WormAtlas., *http://wormatlas.org* (2012 June 1)
113. The C. elegans Sequencing Consortium (1998) Genome sequence of the nematode *C. elegans*: a platform for investigating biology. *Science* **282(5396):2012-2018**

114. Stiernagle T (1999) Maintenance of *C. elegans*. In Hope IA (Ed.), *C. elegans: A practical approach* (pp. 51-67). Oxford: Oxford University Press
115. Ambros V (2000) Control of developmental timing in *Caenorhabditis elegans*. *Curr Opin Genet Dev* **10(4):428-433**
116. Sulston JE and Horvitz HR (1977) Post-embryonic cell lineages of the nematode *Caenorhabditis elegans*. *Dev Biol* **56(1):110-156**
117. Sulston JE (1988) Cell lineage. In Wood WB (Ed.), *The nematode Caenorhabditis elegans* (pp. 123-156). New York: Cold Spring Harbor Laboratory Press
118. Johnson TE, Mitchell DH, Kline S, Kemal R, and Foy J (1984) Arresting development arrests aging in the nematode *Caenorhabditis elegans*. *Mech Ageing Dev* **28(1):23-40**
119. White JG (1988) The anatomy. In Wood WB (Ed.), *The nematode C. elegans* (pp. 81-122). New York: Cold Spring Harbor
120. Ishii T, Miyazawa M, Hartman PS, and Ishii N (2011) Mitochondrial superoxide anion (O_2^-) inducible "mev-1" animal models for aging research. *BMB Rep* **44(5):298-305**
121. Baumeister R, Schaffitzel E, and Hertweck M (2006) Endocrine signaling in *Caenorhabditis elegans* controls stress response and longevity. *J Endocrinol* **190(2):191-202**
122. Ishii N, Takahashi K, Tomita S, Keino T, Honda S *et al*. (1990) A methyl viologen-sensitive mutant of the nematode *Caenorhabditis elegans*. *Mutat Res* **237(3-4):165-171**
123. Nishikawa T, Edelstein D, Du XL, Yamagishi Si, Matsumura T *et al*. (2000) Normalizing mitochondrial superoxide production blocks three pathways of hyperglycaemic damage. *Nature* **404(6779):787-790**
124. Ishii N, Fujii M, Hartman PS, Tsuda M, Yasuda K *et al*. (1998) A mutation in succinate dehydrogenase cytochrome b causes oxidative stress and ageing in nematodes. *Nature* **394(6694):694-697**
125. Choi SS (2011) High glucose diets shorten lifespan of *Caenorhabditis elegans* via ectopic apoptosis induction. *Nutr Res Pract* **5(3):214-218**
126. An JH and Blackwell TK (2003) SKN-1 links *C. elegans* mesendodermal specification to a conserved oxidative stress response. *Genes Dev* **17(15):1882-1893**
127. Morris JZ, Tissenbaum HA, and Ruvkun G (1996) A phosphatidylinositol-3-OH kinase family member regulating longevity and diapause in *Caenorhabditis elegans*. *Nature* **382(6591):536-539**
128. Paradis S and Ruvkun G (1998) *Caenorhabditis elegans* Akt/PKB transduces insulin receptor-like signals from AGE-1 PI3 kinase to the DAF-16 transcription factor. *Genes Dev* **12(16):2488-2498**
129. Hertweck M, Göbel C, and Baumeister R (2004) *C. elegans* SGK-1 is the critical component in the Akt/PKB kinase complex to control stress response and life span. *Dev Cell* **6(4):577-588**
130. Lee RYN, Hench J, and Ruvkun G (2001) Regulation of *C. elegans* DAF-16 and its human ortholog FKHRL1 by the *daf-2* insulin-like signaling pathway. *Curr Biol* **11(24):1950-1957**
131. Tatar M, Bartke A, and Antebi A (2003) The endocrine regulation of aging by insulin-like signals. *Science* **299(5611):1346-1351**

132. Finch CE and Ruvkun G (2001) The genetics of aging. *Annu Rev Genom Human Genet* **2(1):435-462**
133. Kenyon C, Chang J, Gensch E, Rudner A, and Tabtiang R (1993) A *C. elegans* mutant that lives twice as long as wild type. *Nature* **366(6454):461-464**
134. Oh SW, Mukhopadhyay A, Dixit BL, Raha T, Green MR *et al*. (2006) Identification of direct DAF-16 targets controlling longevity, metabolism and diapause by chromatin immunoprecipitation. *Nat Genet* **38(2):251-257**
135. Hsu AL, Murphy CT, and Kenyon C (2003) Regulation of aging and age-related disease by DAF-16 and heat-shock factor. *Science* **300(5622):1142-1145**
136. An JH, Vranas K, Lucke M, Inoue H, Hisamoto N *et al*. (2005) Regulation of the *Caenorhabditis elegans* oxidative stress defense protein SKN-1 by glycogen synthase kinase-3. *Proc Natl Acad Sci U S A* **102(45):16275-16280**
137. Morley JF and Morimoto RI (2004) Regulation of longevity in *Caenorhabditis elegans* by heat shock factor and molecular chaperones. *Mol Biol Cell* **15(2):657-664**
138. Chiang WC, Ching TT, Lee HC, Mousigian C, and Hsu AL (2012) HSF-1 regulators DDL-1/2 link insulin-like signaling to heat-shock responses and modulation of longevity. *Cell* **148(1–2):322-334**
139. Tullet JMA, Hertweck M, An JH, Baker J, Hwang JY *et al*. (2008) Direct inhibition of the longevity-promoting factor SKN-1 by insulin-like signaling in *C. elegans*. *Cell* **132(6):1025-1038**
140. Inoue H, Hisamoto N, An JH, Oliveira RP, Nishida E *et al*. (2005) The *C. elegans* p38 MAPK pathway regulates nuclear localization of the transcription factor SKN-1 in oxidative stress response. *Genes Dev* **19(19):2278-2283**
141. Beckstead RB and Thummel CS (2006) Indicted: worms caught using steroids. *Cell* **124(6):1137-1140**
142. Dowell P, Otto TC, Adi S, and Lane MD (2003) Convergence of peroxisome proliferator-activated receptor γ and Foxo1 signaling pathways. *J Biol Chem* **278(46):45485-45491**
143. Sugden MC, Caton PW, and Holness MJ (2010) PPAR control: it's SIRTainly as easy as PGC. *J Endocrinol* **204(2):93-104**
144. Knutti D, Kaul A, and Kralli A (2000) A tissue-specific coactivator of steroid receptors, identified in a functional genetic screen. *Molecular and Cellular Biology* **20(7):2411-2422**
145. Taubert S, Van Gilst MR, Hansen M, and Yamamoto KR (2006) A mediator subunit, MDT-15, integrates regulation of fatty acid metabolism by NHR-49-dependent and -independent pathways in *C. elegans*. *Genes Dev* **20(9):1137-1149**
146. Schleit J, Wall VZ, Simko M, and Kaeberlein M (2011) The MDT-15 subunit of mediator interacts with dietary restriction to modulate longevity and fluoranthene toxicity in *Caenorhabditis elegans*. *PLoS ONE* **6(11):e28036**
147. Kimura K, Tanaka N, Nakamura N, Takano S, and Ohkuma S (2007) Knockdown of mitochondrial heat shock protein 70 promotes progeria-like phenotypes in *Caenorhabditis elegans*. *J Biol Chem* **282(8):5910-5918**

148. Morley JF, Brignull HR, Weyers JJ, and Morimoto RI (2002) The threshold for polyglutamine-expansion protein aggregation and cellular toxicity is dynamic and influenced by aging in *Caenorhabditis elegans*. *Proc Natl Acad Sci U S A* **99(16):10417-10422**
149. Singh V and Aballay A (2006) Heat-shock transcription factor (HSF)-1 pathway required for *Caenorhabditis elegans* immunity. *Proc Natl Acad Sci U S A* **103(35):13092-13097**
150. Steinkraus KA, Smith ED, Davis C, Carr D, Pendergrass WR *et al*. (2008) Dietary restriction suppresses proteotoxicity and enhances longevity by an *hsf-1*-dependent mechanism in *Caenorhabditis elegans*. *Aging Cell* **7(3):394-404**
151. Haynes CM, Petrova K, Benedetti C, Yang Y, and Ron D (2007) ClpP mediates activation of a mitochondrial unfolded protein response in *C. elegans*. *Dev Cell* **13(4):467-480**
152. Shen X, Ellis RE, Lee K, Liu CY, Yang K *et al*. (2001) Complementary signaling pathways regulate the unfolded protein response and are required for *C. elegans* development. *Cell* **107(7):893-903**
153. Henis-Korenblit S, Zhang P, Hansen M, McCormick M, Lee SJ *et al*. (2010) Insulin/IGF-1 signaling mutants reprogram ER stress response regulators to promote longevity. *Proc Natl Acad Sci U S A* **107(21):9730-9735**
154. Urano F, Calfon M, Yoneda T, Yun C, Kiraly M *et al*. (2002) A survival pathway for *Caenorhabditis elegans* with a blocked unfolded protein response. *J Cell Biol* **158(4):639-646**
155. Graham RW, Jones D, and Candido EP (1989) UbiA, the major polyubiquitin locus in *Caenorhabditis elegans*, has unusual structural features and is constitutively expressed. *Mol Cell Biol* **9(1):268-277**
156. Schlesinger M and Bond U (1987) Ubiquitin genes. *Oxf Surv Eukaryot Genes* **4:77-91**
157. Johnston SC, Riddle SM, Cohen RE, and Hill CP (1999) Structural basis for the specificity of ubiquitin C-terminal hydrolases. *EMBO J* **18(14):3877-3887**
158. Jones D and Candido EP (1993) Novel ubiquitin-like ribosomal protein fusion genes from the nematodes *Caenorhabditis elegans* and *Caenorhabditis briggsae*. *J Biol Chem* **268(26):19545-19551**
159. Gonczy P, Echeverri C, Oegema K, Coulson A, Jones SJM *et al*. (2000) Functional genomic analysis of cell division in *C. elegans* using RNAi of genes on chromosome III. *Nature* **408(6810):331-336**
160. Piano F, Schetter AJ, Morton DG, Gunsalus KC, Reinke V *et al*. (2002) Gene clustering based on RNAi phenotypes of ovary-enriched genes in *C. elegans*. *Curr Biol* **12(22):1959-1964**
161. Kipreos ET (2005 Dec 1) Ubiquitin-mediated pathways in *C. elegans*. In The C.elegans Research Community (Ed.), *WormBook*, doi/10.1895/woormbook.1.36.1, http://www.wormbook.org
162. Davy A, Bello P, Thierry-Mieg N, Vaglio P, Hitti J *et al*. (2001) A protein-protein interaction map of the *Caenorhabditis elegans* 26S proteasome. *EMBO Rep* **2(9):821-828**

163. Takahashi M, Iwasaki H, Inoue H, and Takahashi K (2005) Reverse genetic analysis of the *Caenorhabditis elegans* 26S proteasome subunits by RNA interference. *Biol Chem* **383(7-8):1263-1266**
164. Sulston JE, Schierenberg E, White JG, and Thomson JN (1983) The embryonic cell lineage of the nematode *Caenorhabditis elegans*. *Dev Biol* **100(1):64-119**
165. Gumienny TL, Lambie E, Hartwieg E, Horvitz HR, and Hengartner MO (1999) Genetic control of programmed cell death in the *Caenorhabditis elegans* hermaphrodite germline. *Development* **126(5):1011-1022**
166. Conradt B and Xue D (2005 Oct 6) Programmed cell death. In The C.elegans Research Community (Ed.), *WormBook*, doi/10.1895/wormbook.1.32.1, http://www.wormbook.org
167. Hengartner MO, Ellis R, and Horvitz R (1992) *Caenorhabditis elegans* gene *ced-9* protects cells from programmed cell death. *Nature* **356(6369):494-499**
168. Hengartner MO and Horvitz HR (1994) *C. elegans* cell survival gene *ced-9* encodes a functional homolog of the mammalian proto-oncogene bcl-2. *Cell* **76(4):665-676**
169. Bouillet P and Strasser A (2002) BH3-only proteins - evolutionarily conserved proapoptotic Bcl-2 family members essential for initiating programmed cell death. *J Cell Sci* **115(8):1567-1574**
170. Conradt B and Horvitz HR (1998) The *C. elegans* protein EGL-1 is required for programmed cell death and interacts with the Bcl-2-like protein CED-9. *Cell* **93(4):519-529**
171. Yuan J, Shaham S, Ledoux S, Ellis HM, and Horvitz HR (1993) The *C. elegans* cell death gene *ced-3* encodes a protein similar to mammalian interleukin-1-converting enzyme. *Cell* **75(4):641-652**
172. Alnemri ES, Livingston DJ, Nicholson DW, Salvesen G, Thornberry NA *et al*. (1996) Human ICE/CED-3 protease nomenclature. *Cell* **87(2):171**
173. Xue D, Shaham S, and Horvitz HR (1996) The *Caenorhabditis elegans* cell-death protein CED-3 is a cysteine protease with substrate specificities similar to those of the human CPP32 protease. *Genes Dev* **10(9):1073-1083**
174. Yuan J and Horvitz HR (1992) The *Caenorhabditis elegans* cell death gene *ced-4* encodes a novel protein and is expressed during the period of extensive programmed cell death. *Development* **116(2):309-320**
175. Zou H, Henzel WJ, Liu X, Lutschg A, and Wang X (1997) Apaf-1, a Human Protein Homologous to *C. elegans* CED-4, participates in cytochrome c-dependent activation of caspase-3. *Cell* **90(3):405-413**
176. Zhou Z, Hartwieg E, and Horvitz HR (2001) CED-1 Is a transmembrane receptor that mediates cell corpse engulfment in *C. elegans*. *Cell* **104(1):43-56**
177. Hedgecock EM, Sulston JE, and Thomson JN (1983) Mutations affecting programmed cell deaths in the nematode *Caenorhabditis elegans*. *Science* **220(4603):1277-1279**
178. Gartner A, Boag PR, and Blackwell TK (2008 Sep 4) Germline survival and apoptosis. In The C.elegans Research Community (Ed.), *WormBook*, doi/10.1895/wormbook.1.145.1, http://www.wormbook.org

179. Lettre G and Hengartner MO (2006) Developmental apoptosis in *C. elegans*: a complex CEDnario. *Nat Rev Mol Cell Biol* **7(2):97-108**
180. Meléndez A and Levine B (2009) Autophagy in *C. elegans*. In The C.elegans Research Community (Ed.), *WormBook*, doi/10.1895/wormbook.1.147.1, http://www.wormbook.org
181. Takacs-Vellai K, Vellai T, Puoti A, Passannante M, Wicky C *et al*. (2005) Inactivation of the autophagy gene *bec-1* triggers apoptotic cell death in *C. elegans*. *Curr Biol* **15(16):1513-1517**
182. Meléndez A, Tallóczy Z, Seaman M, Eskelinen EL, Hall DH *et al*. (2003) Autophagy genes are essential for dauer development and life-span extension in *C. elegans*. *Science* **301(5638):1387-1391**
183. Hansen M, Chandra A, Mitic LL, Onken B, Driscoll M *et al*. (2008) A role for autophagy in the extension of lifespan by dietary restriction in *C. elegans*. *PLoS Genet* **4(2):e24**
184. Toth ML, Sigmond T, Borsos E, Barna J, Erdelyi P *et al*. (2008) Longevity pathways converge on autophagy genes to regulate life span in *Caenorhabditis elegans*. *Autophagy* **4(3):330-338**
185. Tavernarakis N, Pasparaki A, Tasdemir E, Maiuri MC, and Kroemer G (2008) The effects of p53 on whole organism longevity are mediated by autophagy. *Autophagy* **4(7):870-873**
186. Lee IH, Cao L, Mostoslavsky R, Lombard DB, Liu J *et al*. (2008) A role for the NAD-dependent deacetylase Sirt1 in the regulation of autophagy. *Proc Natl Acad Sci U S A* **105(9):3374-3379**
187. Morselli E, Maiuri MC, Markaki M, Megalou E, Pasparaki A *et al*. (2010) Caloric restriction and resveratrol promote longevity through the Sirtuin-1-dependent induction of autophagy. *Cell Death and Dis* **1(1):e10**
188. Greer EL and Brunet A (2009) Different dietary restriction regimens extend lifespan by both independent and overlapping genetic pathways in *C. elegans*. *Aging Cell* **8(2):113-127**
189. Wood JG, Rogina B, Lavu S, Howitz K, Helfand SL *et al*. (2004) Sirtuin activators mimic caloric restriction and delay ageing in metazoans. *Nature* **430(7000):686-689**
190. Wang Y and Tissenbaum HA (2006) Overlapping and distinct functions for a *Caenorhabditis elegans* SIR2 and DAF-16/FOXO. *Mech Ageing Dev* **127(1):48-56**
191. Blagosklonny MV (2010) Linking calorie restriction to longevity through sirtuins and autophagy: any role for TOR. *Cell Death and Dis* **1:e12**
192. Tissenbaum HA and Guarente L (2001) Increased dosage of a sir-2 gene extends lifespan in *Caenorhabditis elegans*. *Nature* **410(6825):227-230**
193. Lewis JA and Fleming JT (1995) Basic culture methods. In Epstein HF and Shakes DC (Eds.), *Methods in Cell Biology (Volume 48) Caenorhabditis elegans: Modern Biologcal Analysis of an Organism* (pp. 3-29). San Diego, CA: Academic Press
194. Kamath RS, Martinez-Campos M, Zipperlen P, Fraser AG, and Ahringer J (2000) Effectiveness of specific RNA-mediated interference through ingested double-stranded RNA in *Caenorhabditis elegans*. *Genome Biol* **2(1):research0002.1-research0002.10**
195. Altincicek B, Fischer M, Fischer M, Luersen K, Boll M *et al*. (2010) Role of matrix metalloproteinase ZMP-2 in pathogen resistance and

development in Caenorhabditis elegans. *Dev Comp Immunol* **34(11):1160-1169**
196. Gill MS, Olsen A, Sampayo JN, and Lithgow GJ (2003) An automated high-throughput assay for survival of the nematode *Caenorhabditis elegans*. *Free Radic Biol Med* **35(6):558-565**
197. Bradford MM (1976) A rapid and sensitive method for the quantitation of microgram quantities of protein utilizing the principle of protein-dye binding. *Anal Biochem* **72(1–2):248-254**
198. Kamath RS, Fraser AG, Dong Y, Poulin G, Durbin R *et al*. (2003) Systematic functional analysis of the Caenorhabditis elegans genome using RNAi. *Nature* **421(6920):231-237**
199. Bustin SA and Mueller R (2005) Real-time reverse transcription PCR (qRT-PCR) and its potential use in clinical diagnosis. *Clin Sci* **109(4):365-379**
200. Pfaffl MW (2001) A new mathematical model for relative quantification in real-time RT-PCR. *Nucleic Acids Research* **29(9):e45**
201. Schlotterer A, Kukudov G, Bozorgmehr F, Hutter H, Du X *et al*. (2009) *C. elegans* as model for the study of high glucose–mediated life span reduction. *Diabetes* **58(11):2450-2456**
202. Ruiz-Torres A and Beier W (2005) On maximum human life span: interdisciplinary approach about its limits. *Adv Gerontology* **16:14-20**
203. Baur JA, Pearson KJ, Price NL, Jamieson HA, Lerin C *et al*. (2006) Resveratrol improves health and survival of mice on a high-calorie diet. *Nature* **444(7117):337-342**
204. Heidler T, Hartwig K, Daniel H, and Wenzel U (2010) *Caenorhabditis elegans* lifespan extension caused by treatment with an orally active ROS-generator is dependent on DAF-16 and SIR-2.1. *Biogerontology* **11(2):183-195**
205. Hartwig K, Heidler T, Moch J, Daniel H, and Wenzel U (2009) Feeding a ROS-generator to Caenorhabditis elegans leads to increased expression of small heat shock protein HSP-16.2 and hormesis. *Genes & Nutrition* **4(1):59-67**
206. Lee SJ, Murphy CT, and Kenyon C (2009) Glucose shortens the life span of *C. elegans* by downregulating DAF-16/FOXO activity and aquaporin gene expression. *Cell Metab* **10(5):379-391**
207. Harman D (1956) Aging: a theory based on free radical and radiation chemistry. *J Gerontol* **11(3):298-300**
208. Gruber J, Schaffer S, and Halliwell B (2008) The mitochondrial free radical theory of ageing--where do we stand? *Front Biosci* **13:6554-6579**
209. Honda Y and Honda S (1999) The *daf-2* gene network for longevity regulates oxidative stress resistance and Mn-superoxide dismutase gene expression in *Caenorhabditis elegans*. *FASEB J* **13(11):1385-1393**
210. Vanfleteren JR and Braeckman BP (1999) Mechanisms of life span determination in *Caenorhabditis elegans*. *Neurobiol Aging* **20(5):487-502**
211. Taub J, Lau JF, Ma C, Hahn JH, Hoque R *et al*. (1999) A cytosolic catalase is needed to extend adult lifespan in *C. elegans daf-C* and *clk-1* mutants. *Nature* **399(6732):162-166**
212. Yang W and Hekimi S (2010) A mitochondrial superoxide signal triggers increased longevity in *Caenorhabditis elegans*. *PLoS Biol* **8(12):e1000556**

213. Labieniec-Watala M, Siewiera K, and Jozwiak Z (2011) Resorcylidene Aminoguanidine (RAG) improves cardiac mitochondrial bioenergetic impaired by hyperglycaemia in a model of experimental diabetes. *Int J Mol Sci* **12(11):8013-8026**
214. Brand MD (2000) Uncoupling to survive? The role of mitochondrial inefficiency in ageing. *Exp Gerontol* **35(6–7):811-820**
215. Lemire BD, Behrendt M, DeCorby A, and Gásková D (2009) *C. elegans* longevity pathways converge to decrease mitochondrial membrane potential. *Mech Ageing Dev* **130(7):461-465**
216. Sell DR, Lane MA, Johnson WA, Masoro EJ, Mock OB *et al*. (1996) Longevity and the genetic determination of collagen glycoxidation kinetics in mammalian senescence. *Proc Natl Acad Sci U S A* **93(1):485-490**
217. Uribarri J, Cai W, Peppa M, Goodman S, Ferrucci L *et al*. (2007) Circulating glycooxins and dietary advanced glycation endproducts: two links to inflammatory response, oxidative stress, and aging. *J Gerontol A Biol Sci Med Sci* **62(4):427-433**
218. Stitt AW, Li YM, Gardiner TA, Bucala R, Archer DB *et al*. (1997) Advanced glycation end products (AGEs) co-localize with AGE receptors in the retinal vasculature of diabetic and of AGE-infused rats. *Am J Pathol* **150(2):523-531**
219. Booth AA, Khalifah RG, and Hudson BG (1996) Thiamine pyrophosphate and pyridoxamine inhibit the formation of antigenic advanced glycation end-products: comparison with aminoguanidine. *Biochem Biophys Res Commun* **220(1):113-119**
220. Wu ET, Liang JT, Wu MS, and Chang KC (2011) Pyridoxamine prevents age-related aortic stiffening and vascular resistance in association with reduced collagen glycation. *Exp Gerontol* **46(6):482-488**
221. Degenhardt TP, Alderson NL, Arrington DD, Beattie RJ, Basgen JM *et al*. (2002) Pyridoxamine inhibits early renal disease and dyslipidemia in the streptozotocin-diabetic rat. *Kidney Int* **61(3):939-950**
222. Hartl FU, Bracher A, and Hayer-Hartl M (2011) Molecular chaperones in protein folding and proteostasis. *Nature* **475(7356):324-332**
223. Lindenmeyer MT, Rastaldi MP, Ikehata M, Neusser MA, Kretzler M *et al*. (2008) Proteinuria and hyperglycemia induce endoplasmic reticulum stress. *J Am Soc Nephrol* **19(11):2225-2236**
224. Lund J, Tedesco P, Duke K, Wang J, Kim SK *et al*. (2002) Transcriptional profile of aging in *C. elegans*. *Curr Biol* **12(18):1566-1573**
225. Benedetti C, Haynes CM, Yang Y, Harding HP, and Ron D (2006) Ubiquitin-like protein 5 positively regulates chaperone gene expression in the mitochondrial unfolded protein response. *Genetics* **174(1):229-239**
226. Jowett JB, Elliott KS, Curran JE, Hunt N, Walder KR *et al*. (2004) Genetic variation in BEACON influences quantitative variation in metabolic syndrome–related phenotypes. *Diabetes* **53(9):2467-2472**
227. Richardson CE, Kinkel S, and Kim DH (2011) Physiological IRE-1-XBP-1 and PEK-1 signaling in *Caenorhabditis elegans* larval development and immunity. *PLoS Genet* **7(11):e1002391**
228. An WG, Hwang SG, Trepel JB, and Blagosklonny MV (2000) Protease inhibitor-induced apoptosis: accumulation of wt p53, $p21^{WAF1/CIP1}$, and

induction of apoptosis are independent markers of proteasome inhibition. *Leukemia* **14(7):1276-1283**
229. Kudo Y, Takata T, Ogawa I, Kaneda T, Sato S *et al*. (2000) p27Kip1 accumulation by inhibition of proteasome function induces apoptosis in oral squamous cell carcinoma cells. *Clin Cancer Res* **6(3):916-923**
230. van Eersel J, Ke YD, Gladbach A, Bi M, Götz J *et al*. (2011) Cytoplasmic accumulation and aggregation of TDP-43 upon proteasome inhibition in cultured neurons. *PLoS ONE* **6(7):e22850**
231. Mizutani M, Kern TS, and Lorenzi M (1996) Accelerated death of retinal microvascular cells in human and experimental diabetic retinopathy. *J Clin Invest* **97(12):2883-2890**
232. Yatoh S, Mizutani M, Yokoo T, Kozawa T, Sone H *et al*. (2006) Antioxidants and an inhibitor of advanced glycation ameliorate death of retinal microvascular cells in diabetic retinopathy. *Diabetes Metab Res Rev* **22(1):38-45**
233. Kern TS, Tang J, Mizutani M, Kowluru RA, Nagaraj RH *et al*. (2000) Response of capillary cell death to aminoguanidine predicts the development of retinopathy: comparison of diabetes and galactosemia. *Invest Ophthalmol Vis Sci* **41(12):3972-3978**
234. Denis U, Lecomte M, Paget C, Ruggiero D, Wiernsperger N *et al*. (2002) Advanced glycation end-products induce apoptosis of bovine retinal pericytes in culture: involvement of diacylglycerol/ceramide production and oxidative stress induction. *Free Radic Biol Med* **33(2):236-247**
235. Ullman E, Fan Y, Stawowczyk M, Chen HM, Yue Z *et al*. (2007) Autophagy promotes necrosis in apoptosis-deficient cells in response to ER stress. *Cell Death Differ* **15(2):422-425**
236. Yousefi S, Perozzo R, Schmid I, Ziemiecki A, Schaffner T *et al*. (2006) Calpain-mediated cleavage of Atg5 switches autophagy to apoptosis. *Nat Cell Biol* **8(10):1124-1132**
237. Wei Y, Sinha SC, and Levine B (2008) Dual role of JNK1-mediated phosphorylation of Bcl-2 in autophagy and apoptosis regulation. *Autophagy* **4(7):949-951**
238. Seshagiri S and Miller LK (1997) *Caenorhabditis elegans* CED-4 stimulates CED-3 processing and CED-3-induced apoptosis. *Curr Biol* **7(7):455-460**
239. Spector MS, Desnoyers S, Hoeppner DJ, and Hengartner MO (1997) Interaction between the *C. elegans* cell-death regulators CED-9 and CED-4. *Nature* **385(6617):653-656**
240. Chen F, Hersh BM, Conradt B, Zhou Z, Riemer D *et al*. (2000) Translocation of *C. elegans* CED-4 to nuclear membranes during programmed cell death. *Science* **287(5457):1485-1489**
241. Yang X, Chang HY, and Baltimore D (1998) Essential role of CED-4 oligomerization in CED-3 activation and apoptosis. *Science* **281(5381):1355-1357**
242. Shaham S (1998) Identification of multiple *Caenorhabditis elegans* caspases and their potential roles in proteolytic cascades. *J Biol Chem* **273(52):35109-35117**

243. Budihardjo I, Oliver H, Lutter M, Luo X, and Wang X (1999) Biochemical pathways of caspase activation during apoptosis. *Annu Rev Cell Dev Biol* **15(1):269-290**
244. Lin SJ, Defossez PA, and Guarente L (2000) Requirement of NAD and SIR2 for life-span extension by calorie restriction in *Saccharomyces cerevisiae*. *Science* **289(5487):2126-2128**
245. Rogina B and Helfand SL (2004) Sir2 mediates longevity in the fly through a pathway related to calorie restriction. *Proc Natl Acad Sci U S A* **101(45):15998-16003**
246. Brunet A, Sweeney LB, Sturgill JF, Chua KF, Greer PL *et al*. (2004) Stress-dependent regulation of FOXO transcription factors by the SIRT1 deacetylase. *Science* **303(5666):2011-2015**
247. Luo J, Nikolaev AY, Imai Si, Chen D, Su F *et al*. (2001) Negative control of p53 by Sir2 promotes cell survival under stress. *Cell* **107(2):137-148**
248. Howitz KT, Bitterman KJ, Cohen HY, Lamming DW, Lavu S *et al*. (2003) Small molecule activators of sirtuins extend *Saccharomyces cerevisiae* lifespan. *Nature* **425(6954):191-196**
249. Yang J, Wang N, Zhu Y, and Feng P (2011) Roles of SIRT1 in high glucose-induced endothelial impairment: association-with diabetic atherosclerosis. *Arch Med Res* **42(5):354-360**
250. Yun JM, Chien A, Jialal I, and Devaraj S (2011) Resveratrol up-regulates SIRT1 and inhibits cellular oxidative stress in the diabetic milieu: mechanistic insights. *J Nutr Biochem* **23(7):699-705**
251. Pietsch K, Saul N, Menzel R, Stürzenbaum SR, and Steinberg CEW (2009) Quercetin mediated lifespan extension in *Caenorhabditis elegans* is modulated by *age-1, daf-2, sek-1* and *unc-43*. *Biogerontology* **10(5):565-578**
252. Wang Y, Oh SW, Deplancke B, Luo J, Walhout AJM *et al*. (2006) *C. elegans* 14-3-3 proteins regulate life span and interact with SIR-2.1 and DAF-16/FOXO. *Mech Ageing Dev* **127(9):741-747**
253. Henderson ST and Johnson TE (2001) *daf-16* integrates developmental and environmental inputs to mediate aging in the nematode *Caenorhabditis elegans*. *Curr Biol* **11(24):1975-1980**
254. Lee SS, Kennedy S, Tolonen AC, and Ruvkun G (2003) DAF-16 target genes that control *C. elegans* life-span and metabolism. *Science* **300(5619):644-647**
255. Murphy CT, McCarroll SA, Bargmann CI, Fraser A, Kamath RS *et al*. (2003) Genes that act downstream of DAF-16 to influence the lifespan of *Caenorhabditis elegans*. *Nature* **424(6946):277-283**
256. Kondo M, Senoo-Matsuda N, Yanase S, Ishii T, Hartman PS *et al*. (2005) Effect of oxidative stress on translocation of DAF-16 in oxygen-sensitive mutants, *mev-1* and *gas-1* of *Caenorhabditis elegans*. *Mech Ageing Dev* **126(6–7):637-641**
257. Apfeld J, O'Connor G, McDonagh T, DiStefano PS, and Curtis R (2004) The AMP-activated protein kinase AAK-2 links energy levels and insulin-like signals to lifespan in *C. elegans*. *Genes Dev* **18(24):3004-3009**
258. Curtis R, O'Connor G, and DiStefano PS (2006) Aging networks in *Caenorhabditis elegans*: AMP-activated protein kinase (*aak-2*) links multiple aging and metabolism pathways. *Aging Cell* **5(2):119-126**

259. Greer EL, Dowlatshahi D, Banko MR, Villen J, Hoang K *et al*. (2007) An AMPK-FOXO pathway mediates longevity induced by a novel method of dietary restriction in *C. elegans*. *Curr Biol* **17(19):1646-1656**
260. Garigan D, Hsu AL, Fraser AG, Kamath RS, Ahringer J *et al*. (2002) Genetic analysis of tissue aging in *Caenorhabditis elegans*: a role for heat-shock factor and bacterial proliferation. *Genetics* **161(3):1101-1112**
261. Aguirre V, Uchida T, Yenush L, Davis R, and White MF (2000) The c-Jun NH2-terminal kinase promotes insulin resistance during association with insulin receptor substrate-1 and phosphorylation of Ser307. *J Biol Chem* **275(12):9047-9054**
262. Kim AH, Yano H, Cho H, Meyer D, Monks B *et al*. (2002) Akt1 regulates a JNK scaffold during excitotoxic apoptosis. *Neuron* **35(4):697-709**
263. Davis RJ (2000) Signal transduction by the JNK group of MAP kinases. *Cell* **103(2):239-252**
264. Koo S-H, Satoh H, Herzig S, Lee C-H, Hedrick S *et al*. (2004) PGC-1 promotes insulin resistance in liver through PPAR-α-dependent induction of TRB-3. *Nature Medicine* **10:530-534**
265. Costa Cdos S, Rohden F, Hammes T, Margis R, Bortolotto J *et al*. (2011) Resveratrol upregulated SIRT1, FOXO1, and adiponectin and downregulated PPARγ1-3 mRNA expression in human visceral adipocytes. *Obes Surg* **21(3):356-361**
266. Li Y, Bujo H, Takahashi K, Shibasaki M, Zhu Y *et al*. (2003) Visceral fat: higher responsiveness of fat mass and gene expression to calorie restriction than subcutaneous fat. *Exp Biol Med* **228(10):1118-1123**
267. Mulligan JD, Stewart AM, and Saupe KW (2008) Downregulation of plasma insulin levels and hepatic PPARγ expression during the first week of caloric restriction in mice. *Exp Gerontol* **43(3):146-153**
268. Rahman M, Halade GV, Bhattacharya A, and Fernandes G (2009) The *fat-1* transgene in mice increases antioxidant potential, reduces pro-inflammatory cytokine levels, and enhances PPARγ and SIRT-1 expression on a calorie restricted diet. *Oxid Med Cell Longev* **2(5):307-316**
269. Masternak MM, Al-Regaiey K, Bonkowski MS, Panici J, Sun L *et al*. (2004) Divergent effects of caloric restriction on gene expression in normal and long-lived mice. *J Gerontol A Biol Sci Med Sci* **59(8):B784-B788**
270. Hayashida S, Arimoto A, Kuramoto Y, Kozako T, Honda Si *et al*. (2010) Fasting promotes the expression of SIRT1, an NAD^+-dependent protein deacetylase, via activation of PPARγ in mice. *Mol Cell Biochem* **339(1):285-292**
271. Roduit R, Morin J, Massé F, Segall L, Roche E *et al*. (2000) Glucose down-regulates the expression of the peroxisome proliferator-activated receptor-α gene in the pancreatic β–cell. *J Biol Chem* **275(46):35799-35806**
272. Inoue H, Jiang XF, Katayama T, Osada S, Umesono K *et al*. (2003) Brain protection by resveratrol and fenofibrate against stroke requires peroxisome proliferator-activated receptor γ in mice. *Neurosci Lett* **352(3):203-206**

273. Sluder AE, Mathews SW, Hough D, Yin VP, and Maina CV (1999) The nuclear receptor superfamily has undergone extensive proliferation and diversification in nematodes. *Genome Res* **9(2):103-120**
274. Gilst MRV, Hadjivassiliou H, Jolly A, and Yamamoto KR (2005) Nuclear hormone receptor NHR-49 controls fat consumption and fatty acid composition in *C. elegans*. *PLoS Biol* **3(2):e53**
275. Van Gilst MR, Hadjivassiliou H, and Yamamoto KR (2005) A *Caenorhabditis elegans* nutrient response system partially dependent on nuclear receptor NHR-49. *Proc Natl Acad Sci U S A* **102(38):13496-13501**
276. Gerisch B, Rottiers V, Li D, Motola DL, Cummins CL *et al*. (2007) A bile acid-like steroid modulates *Caenorhabditis elegans* lifespan through nuclear receptor signaling. *Proc Natl Acad Sci U S A* **104(12):5014-5019**
277. Janknecht R and Hunter T (1996) A growing coactivator network. *Nature* **383(6595):22-23**
278. Vega RB, Huss JM, and Kelly DP (2000) The coactivator PGC-1 cooperates with peroxisome proliferator-activated receptor α in transcriptional control of nuclear genes encoding mitochondrial fatty acid oxidation Enzymes. *Molecular and Cellular Biology* **20(5):1868-1876**
279. Puigserver P, Wu Z, Park CW, Graves R, Wright M *et al*. (1998) A cold-inducible coactivator of nuclear receptors linked to adaptive thermogenesis. *Cell* **92(6):829-839**
280. Rodgers JT, Lerin C, Gerhart-Hines Z, and Puigserver P (2008) Metabolic adaptations through the PGC-1α and SIRT1 pathways. *FEBS Lett* **582(1):46-53**
281. Minami M, Shinozaki F, Suzuki M, Yoshimatsu K, Ichikawa Y *et al*. (2006) The proteasome activator PA28 functions in collaboration with Hsp90 in vivo. *Biochem Biophys Res Commun* **344(4):1315-1319**
282. Awasthi N and Wagner BJ (2005) Upregulation of heat shock protein expression by proteasome inhibition: an antiapoptotic mechanism in the lens. *Invest Ophthalmol Vis Sci* **46(6):2082-2091**
283. Morselli E, Maiuri MC, Markaki M, Megalou E, Pasparaki A *et al*. (2010) The life span-prolonging effect of Sirtuin-1 is mediated by autophagy. *Autophagy* **6(1):186-188**
284. Scarlatti F, Maffei R, Beau I, Ghidoni R, and Codogno P (2008) Non-canonical autophagy: An exception or an underestimated form of autophagy? *Autophagy* **4(8):1083-1085**
285. Timmons L and Fire A (1998) Specific interference by ingested dsRNA. *Nature* **395(6705):854-854**
286. Antebi A, Culotti JG, and Hedgecock EM (1998) *daf-12* regulates developmental age and the dauer alternative in *Caenorhabditis elegans*. *Development* **125(7):1191-1205**
287. Horvitz H, Sternberg P, Greenwald I, Fixsen W, and Ellis HM (1983) Mutations that affect neural cell lineages and cell fates during the development of the nematode *Caenorhabditis elegans*. *Cold Spring Harb Symp Quant Biol* **48(Pt 2):453-463**
288. Lin K, Dorman JB, Rodan A, and Kenyon C (1997) *daf-16*: An HNF-3/forkhead family member that can function to double the life-span of *Caenorhabditis elegans*. *Science* **278(5341):1319-1322**

289. Hajdu-Cronin YM, Chen WJ, and Sternberg PW (2004) The L-Type cyclin CYL-1 and the heat-shock-factor HSF-1 are required for heat-shock-induced protein expression in *Caenorhabditis elegans*. *Genetics* **168(4):1937-1949**
290. The C.elegans gene knockout consortium (ed.), *www.celeganskocosortium.omrf.org* (2012 June 1)
291. Takiff HE, Chen SM, and Court DL (1989) Genetic analysis of the rnc operon of *Escherichia coli*. *J Bacteriol* **171(5):2581-2590**

A APPENDIX: MATERIAL

A.1 Consumables

Consumable material (Table A-1) was purchased from Brand GmbH (Wertheim, D), Carl Roth GmbH & Co. KG (Karlsruhe, D), Duran Group GmbH (Wertheim/Main, D), GE Healthcare (München, D), Gilson Inc. (Middleton, WI, USA), Greiner Bio-One GmbH (Frickenhausen, D), Nalgene® Labware (Langenselbold, D), Pechiney (Chicago, USA), PreSens (Regensburg, D), Sarstedt AG & Co. (Nürnbrecht, D), and Whatman GmbH (Dassel, D).

Table A-1. List of consumables and manufacturers.

Material	Manufacturer
Amersham Hyperfilm ™ ECL	GE Healthcare
Beakers	Duran
Blotting Paper 3MM Chr	Whatman
Cell culture microplates 96 well, 24 well	Greiner Bio-One
Cell culture tubes	Greiner Bio-One
Cover slips	Carl Roth
Cryo 1 °C Freezing Container	Nalgene® Labware
Distritips® for Distriman®	Gilson
Erlenmeyer flasks	Duran
Laboratory glass bottles	Duran
Lid for BRAND plates® 384 well	Brand
Measuring cylinders	Brand
Micro tubes (1.5 ml, 2 ml)	Sarstedt
Microplate 384 well	Greiner Bio-One
Microscope slides standard	Carl Roth
Oxoplate® OP96U	PreSens
Parafilm® M	Pechiney Plastic Packaging
Pasteur pipettes (150 mm)	Carl Roth
Petri dishes	Carl Roth
Pipette tips (10 µl, 200 µl, 1000 µl)	Sarstedt
PVDF Membrane	Carl Roth
Reagent and centrifuge tube (15 ml, 50 ml)	Sarstedt

Material	Manufacturer
Rotilabo®-aluminium foils	Carl Roth
Rotilabo®-cryo boxes	Carl Roth
Rotilabo®-disposable cuvettes semi-micro	Carl Roth
Rotilabo®-inoculating loops	Carl Roth
Scalpel	Carl Roth
Sealing film	Carl Roth
Serological pipette (2, 5, 10, 25 ml)	Sarstedt
Steristoppers®	Carl Roth
Toothpicks	Carl Roth
Reaction tube (1.5 ml, 2 ml)	Sarstedt
8-cap strips for RT-PCR	Greiner Bio-One
8-tube strips (0.2 ml)	Greiner Bio-One
Reaction tube (0.2 ml)	Greiner Bio-One

A.2 Instruments

Instruments that were used in the present work are listed in Table A-2.

Table A-2. List of instruments and manufacturers.

Instrument	Manufacturer
Autoclave systec DB23	Systec (Wettenberg, D)
Axioskop 2 MOT microscope	Carl Zeiss GmbH (Jena, D)
Benchtop centrifuge universal 320R	Hettich (Tuttlingen, D)
Biophotometer Plus	Eppendorf (Hamburg, D)
CFX™real-time-PCR detection system	Bio-Rad (Hercules, USA)
Cold light source KL200	Schott AG (Mainz, D)
Distriman®	Gilson (Bad Camberg, D)
Fluoroskan Ascent FL	Thermo Labsystems (Bornheim, D)
HERAsafe® KS safety cabinet	Heraeus (Hanau, D)
Incubator	Lovibond (Dortmund, D)
Incubator	Binder (Tuttlingen, D)
Microliter centrifuge mikro 120	Hettich (Tuttlingen, D)
Microwave	Cinex (Ascheberg, D)
Mini PROTEAN 3 system	Bio-Rad (Hercules, USA)
Moticam 2500 USB 2.0	Bayersdörfer (Saarbrücken, Eschringen, D)
Multiskan EX	Thermo Labsystems (Bornheim, D)

Instrument	Manufacturer
Nano-Drop spectrophotometer	Peqlab (Erlangen, D)
Optimax X-Ray film processor	Protec Medizintechnik (Oberstenfeld, D)
PerfectBlue™ gel system	Peqlab (Erlangen, D)
pH meter	Schott Instruments (Mainz, D)
Pipetman® P	Gilson (Bad Camberg, D)
Pipetus®	Hirschmann (Eberstadt, D)
Precision balance	Kern & Sohn (Bailingen, D)
Primus 25 advanced thermocycler	PeqLab (Erlangen, D)
Rotating shaker	neoLab (Heidelberg, D)
Semi-dry blotter HEP1	Owl (Porthsmouth, USA)
Shakers unimax 1010	Heidolph (Hamburg, D)
Sonoplus HD2070	Bandelin electronic (Berlin, D)
Sonotrode Uw2070	Bandelin electronic (Berlin, D)
Stereo microscope	Breukhoven Microscope Systems (Capelle a/d IJssl, NL)
Sterilising oven	WTB Binder (Tuttlingen, D)
Transferpette® S -8	Brand (Wertheim, D)
Ultrasonic bath	Bandelin electronic (Berlin, D)
Ultrospec UV/Visible spectrophotometer	Amersham Pharmacia (Nürnbrecht, D)
UV transilluminator	Fröbel (Chemnitz, D)
Vacuum pump	neoLab (Heidelberg, D)
Vortex mixer REAX control	Heidolph Instruments (Schwabach, D)
Water bath	Bandelin electronic (Berlin, D)

A.3 Chemicals and Reagents

Chemicals and reagents (Table A-3) were purchased from Bio-Rad Laboratories GmbH (München, D), Biomol GmbH (Hamburg, D), Carl Roth GmbH & Co. KG (Karlsruhe, D), Fermentas (St. Leon-Rot, D), Fisher Scientific (Schwerte, D), Life Technologies GmbH (Darmstadt, D), Merck KGaA (Darmstadt, D), New England Biolabs (Frankfurt am Main, D), Oxoid (Cambridge, UK), Sigma-Aldrich Chemie GmbH (München, D), and Serva Electrophoresis GmbH (Heidelberg, D).

Table A-3. List of chemicals and reagents with order number and manufacturer.

Product	Order No.	Manufacturer
1,4-Dithiothreitol (DTT)	6908.1	Carl Roth
1-Methyl-2-propanol	58460	Sigma-Aldrich
2x YT-Medium	X966.1	Carl Roth
2-Mercaptoethanol	4227.3	Carl Roth
Acetic acid	7332.1	Carl Roth
Acrylamide solution (30%)	3029.1	Carl Roth
Agar Agar SERVA Kobe I	11392	Serva Electrophoresis
Agarose broad range	T846.2	Carl Roth
Albumin Fraction V (BSA)	8076.1	Carl Roth
Ammonium peroxydisulphate (APS)	9592.3	Carl Roth
Ampicillin sodium salt	K029.1	Carl Roth
Ascorbic acid	3525.1	Carl Roth
Bio-Rad Protein Assay Dye Reagent Concentrate	500-0006	Bio-Rad
Bromophenol blue	32768	Sigma-Aldrich
Calcium chloride dihydrat ($CaCl_2 \cdot 2\ H_2O$)	5239.2	Carl Roth
Carbenicillin disodium salt	C1389	Sigma-Aldrich
Chloroform (> 99.9%)	3313.1	Carl Roth
Cholesterol	C8667	Sigma-Aldrich
Dimethyl sulphoxid, DMSO (C_2H_6OS)	4720.2	Carl Roth
di-Potassium hydrogen phosphate (K_2HPO_4)	P749.2	Carl Roth
di-Sodium hydrogen phosphate (Na_2HPO_4)	P030.1	Carl Roth
DNA Loading Dye (6x)	R0611	Fermentas
dNTP-Mix, 10 mM each	R0191	Fermentas
Ethanol (> 99.5%)	5054.3	Carl Roth
Ethanol (70%, denatured)	T913.3	Carl Roth
Ethylenediamine tetraacetic acid (EDTA)	CN06.1	Carl Roth
Gene Ruler^{TM} 100 bp Plus DNA Ladder	SM0321	Fermentas
Glycerol	3783.1	Carl Roth
Glycine	3908.2	Carl Roth
Hydrogen peroxide (H_2O_2, 35%)	9683.1	Carl Roth
Isopropanol (2-Propanol, 99.8%)	6752.3	Carl Roth
Isopropyl-β-D-thiogalactopyranoside (IPTG)	59740	Sigma-Aldrich
Levamisol hydrochloride	46944	Sigma-Aldrich
Luminol	4203.1	Carl Roth
Magnesium chloride hexahydrate ($MgCl_2 \cdot 6\ H_2O$)	2189.1	Carl Roth
Magnesium sulphate heptahydrate ($MgSO_4 \cdot 7\ H_2O$)	P027.2	Carl Roth

Product	Order No.	Manufacturer
Methanol	4627.4	Carl Roth
MG132	Cay13697	Biomol
MitoTracker® Green FM	M7514	Life Technologies
MitoTracker® Red CM-H_2XRos	M7513	Life Technologies
MitoTracker® Red CM-XRos	M7512	Life Technologies
N,N,N‘,N‘-Tetramethylethylenediamine (TEMED)	2367.3	Carl Roth
Nystatin Suspension	N1683	Sigma
p-Coumaric acid	C9008	Sigma-Aldrich
Peptone ex soya	2365.1	Carl Roth
Peptone from Casein (Tryptone)	111931	Merck
Perfect DNA™ 1 kbp Ladder	70537	Merck
Phenylmethansulfonyl fluoride (PMSF)	78830	Sigma-Aldrich
Potassium dihydrogen phosphate (KH_2PO_4)	3904.1	Carl Roth
Potassium hydroxide (KOH)	6751.1	Carl Roth
Powdered milk	T145.1	Carl Roth
Pyridoxamine dihydrochloride	5254.1	Carl Roth
Quercetin Dihydrate	69249	Sigma-Aldrich
Resveratrol	R5010	Sigma-Aldrich
RNAsin® Plus RNAse inhibitor	N2615	Promega
SOC Medium	B9020S	New England BioLabs
Sodium chloride (NaCl)	3957.1	Carl Roth
Sodium dodecyl sulphate (SDS)	4360.2	Carl Roth
Sodium hydroxide (NaOH)	677.1	Carl Roth
Sodium hypochlorite solution (NaClO in H_2O, 12% Cl)	9062.3	Carl Roth
Sodium sulphite	P033.1	Carl Roth
Sucrose	4621.1	Carl Roth
SYBR Safe	S33102	Life Technologies
SYTO12	S7574	Life Technologies
SYTOX® Green nucleic acid stain	S7020	Life Technologies
Tetracycline hydrochloride	T7660	Sigma-Aldrich
Total RNA Isolation reagent (TRI reagent)	AB-0303	Fisher Scientific
Tris(hydroxmethyl)-aminomethane (TRIS)	4855.2	Carl Roth
TRIS-HCl	9090.3	Carl Roth
TWEEN® 20	P2287	Sigma-Aldrich
α-D(+)-Glucose monohydrate	6780.1	Carl Roth

A.4 Kits

Kits that were used in this work are listed in Table A-4.

Table A-4. List of utilized kits, order number, and manufacturer.

Kit	Order No.	Manufacturer
ATP Bioluminescence Assay Kit CLS II	11699695001	Roche
Brilliant II SYBR® Green QRT-PCR Master Mix Kit, 1-Step	600825	Agilent Technologies
FastPlasmid™ Mini Kit	2300000	5Prime
GenElute Mammalian Genomic DNA Miniprep	G1N10	Sigma-Aldrich
OxiSelect™ Methylglyoxal (MG) ELISA Kit	STA-311	Cell Biolabs
OxyBlot™ Protein Oxidation Detection Kit	S7150	Millipore
peqGOLD Gel Extraction Kit	12-2500-00	Peqlab
Plasmid Midi Kit	12145	Qiagen
Rapid DNA Ligation Kit	K1422	Fermentas
RevertAid™ First Strand cDNA Synthesis Kit	K1621	Fermentas
TOPO TA Cloning® Kit	45-0641	Life Technologies

A.5 Enzymes and Antibodies

Utilized enzymes and antibodies are listed in Table A-5 and Table A-6.

Table A-5. List of utilized enzymes with recognition sequences for restriction enzymes, order number, and manufacturer.

Enzyme	Recognition Sequence	Order No.	Manufacturer
T4 DNA Ligase		11000321	Roche
Taq DNA Polymerase (recombinant)		EP0401	Fermentas
HindIII	5'...A↓AGCT T...3' 3'...T TCGA↑A...5'	ER0501	Fermentas
XhoI	5'...C↓TCGA G...3' 3'...G AGCT↑C...5'	ER0691	Fermentas

Table A-6. List of utilized antibodies, order number, and manufacturer.

Antibody	Order No.	Manufacturer
Western Blot		
Rabbit-anti-DAF-12 (polyclonal)	SC-50481	Santa Cruz
Mouse-anti-actin (polyclonal)	DLN-07273	Dianova
Goat-anti-rabbit-IgG, HRP conjugated (polyclonal)	SC-2004	Santa Cruz
Goat-anti-mouse-IgG, HRP conjugated (polyclonal)	SC-2005	Santa Cruz
OxyBlot		
Rabbit-anti-DNP	90451	Millipore
Goat-anti-rabbit-IgG, HRP conjugated	90452	Millipore

A.6 Oligonucleotides

Oligonucleotides were designed using the Eurofins PCR primer tool and ordered from Eurofins MWG Operon (Ebersberg, D). Sequences and melting temperatures of utilized oligonucleotides are listed in Table A-7.

Table A-7. Sequences (5' → 3') of utilized oligonucleotides.

	sequence (5' → 3')	T_m (°C)
18S rRNA-fw	ATG GTT GCA AAG CTG AAA CT	53.2
18S rRNA-rev	TCC CGT GTT GAG TCA AAT TA	53.2
abu-11-fw-699-1	TCA ATC GTG CCA GCC ACA ATG	59.8
abu-11-r-1198-1	AAG CCG AAC AAC TCT GCT GAC	59.8
abu-11-fw-184-2	ACC GCC CAA CAA TCT TGC TCC	61.8
abu-11-r-683-2	CAC TGT TGC ACT GGC TGC TG	61.4
abu-11-fw-343-3	TGC TCT TCC ACT TGC CAG TCC	61.8
abu-11-r-842-3	TGG GAA GCT CCT TGG TAT GAT GG	62.4
abu-11-fw-190-4	CAA CAA TCT TGC TCC TGC GCT C	62.1
abu-11-r-689-4	GAT TGG CAC TGT TGC ACT GGC	61.8
sir-2.1-qPCR-fw-201	GAC AAA GAA CAG AAA GTA CAA CCA G	52.6
sir-2.1-qPCR-rev-312	GGA GTG GCA CCA TCA TCA AG	52.8
sir-2.4-fw-282	GGA CTT TCA AGT TGC TCG TCC C	62.4
sir-2.4-fw-328	GCA CTT CAC AAG GCG GTT AC	61.8
sir-2.4-rev-857	TCT CCA AGA TCA ACA TTC ACT CCA	59.3
sir-2.4-rev-878	GGC ACT TCA TCC GGT AGA TCA TC	62.1
Oligo$(dT)_{18}$ Primer*	TTT TTT TTT TTT TTT TTT	

T_m: melting temperature, * Oligo$(dT)_{18}$ Primer were purchased from Fermentas.

A.7 Plasmids and Vectors

Vectors that were used for cloning are listed in Table A-8. Figure A-1 and Figure A-2 show schematic diagrams of the vectors with relevant features.

Table A-8. List of utilized vectors.

Vectors	Reference
pPD129.36 (L4440)	(285)
pCR®2.1-TOPO®	Life Technologies

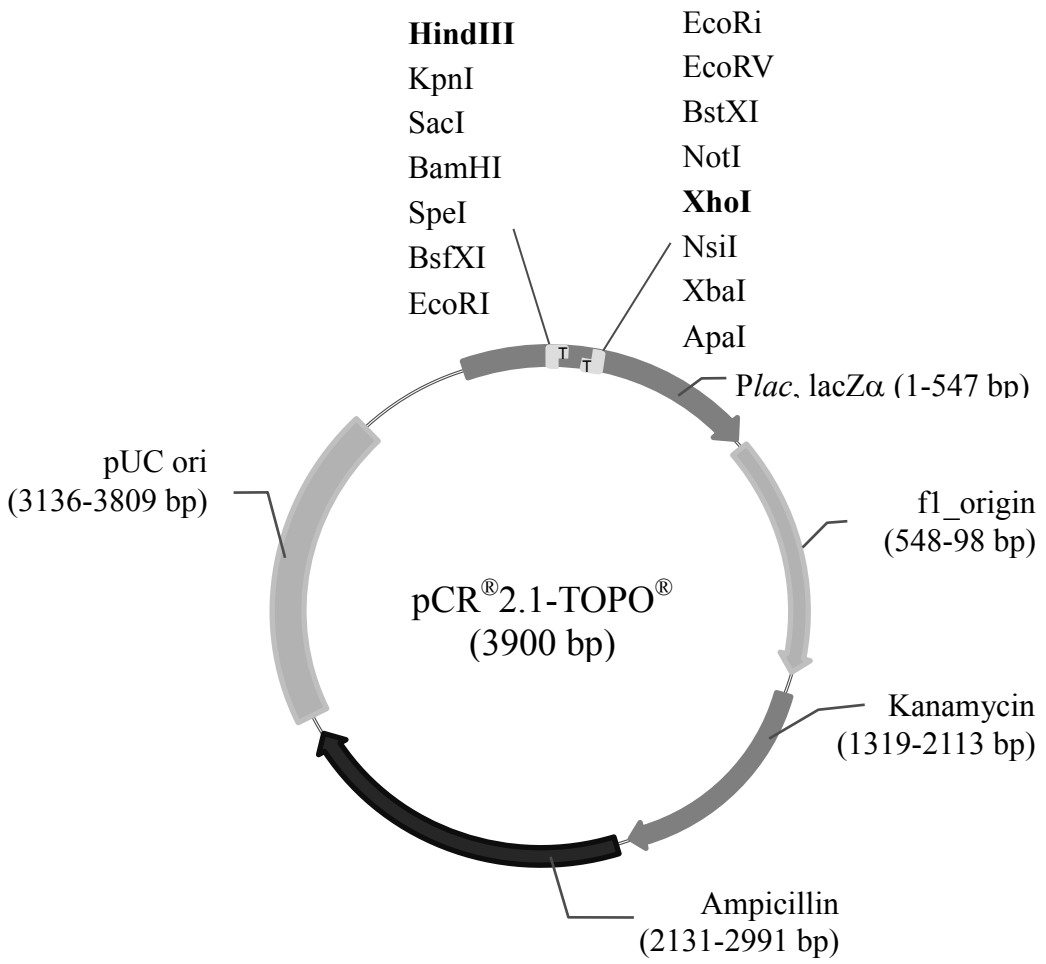

Figure A-1. Schematic diagram of the pCR®2.1-TOPO® vector.

The pCR®2.1-TOPO® vector is characterized by 3'-T overhang for direct ligation of *Taq*-amplified PCR products, T7 promoter for *in vitro* RNA transcription and sequencing as well as M13 forward (391-406 bp) and reverse primer sites (205-221 bp) for sequencing. It includes kanamycin and ampicillin resistance genes and is suitable for blue/white screening.

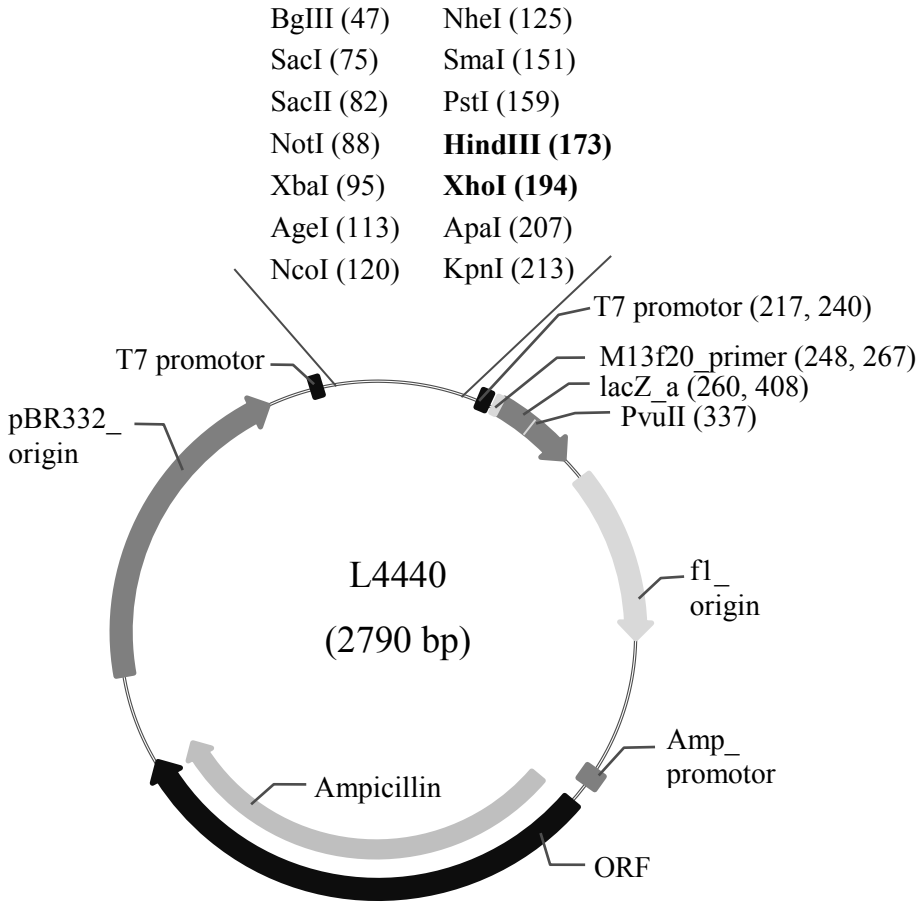

Figure A-2. Schematic diagram of the L4440 plasmid vector.

The multiple cloning site of the L4440 plasmid vector is flanked by two convergent T7 polymerase promoters in opposite orientation. This allows the expression of dsRNA.

RNAi clones (Table A-9) were purchased from Source Bioscience, Cambridge, UK. The *sir-2.4* and *abu-11* clones were constructed as described in chapter 3.3.1. RNAi clones consist of the pPD129.36 (L4440) plasmid transformed into *E. coli* HT115. Each plasmid carries part of the sequence of the gene that is to be knocked down.

Table A-9. List of utilized RNAi clones.

Gene name	Sequence name	Description
aak-2	T01C8.1	AMP activated kinase
abu-1	AC3.3	activated in blocked unfolded protein response
*abu-11**	T01D1.6	activated in blocked unfolded protein response
bec-1	T19E7.3	Beclin1
ced-3	C48D1.2	cell death abnormality
ced-4	C35D10.9	cell death abnormality
daf-9	T13C5.1	abnormal dauer formation
daf-16	R13H8.1	abnormal dauer formation
dve-1	ZK1193.5	defective proventriculus in *Drosophila* homologue
hsf-1	Y53C10A.12	heat shock factor
hsp-6	C37H5.8	heat shock protein
hsp-60	Y22D7AL.5	heat shock protein
jnk-1	B0478.1	c-jun kinase
mdt-15	R12B2.5	mediator
sir-2.1	R11A8.4	yeast SIR related
sir-2.2	F46G10.7	yeast SIR related
sir-2.3	F46G10.3	yeast SIR related
*sir-2.4**	C06A5.11	yeast SIR related
skn-1	T19E7.2	skinhead
uba-1	C47E12.5	human ubiquitin related
ubl-5	F46F11.4	ubiquitin-like family
ubq-1	F25B5.4	ubiquitin
xbp-1	R74.3	x-box binding protein homologue
zmp-2	H19M22.3	zinc matrix metalloproteases

* *sir-2.4* and *abu-11* RNAi clones have been constructed as part of the present work.

Each RNAi clone has been verified by sequencing before it was used in experiments. Therefore plasmid preparation from an overnight culture was performed as described in chapter 3.3.9. The plasmid DNA was sequenced by the sequencer lab of the Interdisciplinary Research Center, University of Gießen using universal M13-forward primer.

A.8 *C. elegans* Strains

The *C. elegans* stocks (Table A-10) were purchased from Caenorhabditis Genetics Center (CGC) University of Minnesota, Minneapolis, USA. *Mev-1; daf-16*::gfp was constructed in the lab of Dr. Kai Lüersen, University of Kiel.

Table A-10. List of the utilized *C. elegans* strains with genotype and reference.

Strain	Genotype	Reference
N2	Wildtype	(110)
AA1	*daf-12 (rh257)*	(286)
CB3203	*ced-1 (e1735)*	(287)
CF1038	*daf-16 (mu86)*	(288)
PS3551	*hsf-1 (sy441)*	(289)
RB1716	*nhr-49 (ok2165)*	(290)
TJ356	*zIs356 [Pdaf-16::daf-16-gfp; rol-6(su1006)]*	(253)
TK22	*mev-1 (kn1)*	(122)
	mev-1(kn1);[Pdaf-16::daf-16-gfp;rol-6(su1006)]	Dr. Kai Lüersen, Kiel University

A.9 Bacteria Strains

In Table A-11 the used bacteria strains are listed. Starter cultures of *E. coli* were obtained from the CGC.

Table A-11. List of the utilized *E. coli* strains with genotype and reference.

Strain	Genotype	Reference
E. coli OP50	ura-	(110)
E. coli HT115	*F-, mcrA, mcrB, IN(rrnD-rrnE)1, lambda$^-$, rnc14::Tn10(DE3 lysogen: lavUV5 promoter -T7 polymerase)*	(291)
NovaBlue Giga Singles (*E. coli*)	*endA1 hsdR17* (r_{K12}^- m_{K12}^+) *supE44 thi-1 recA1 gyrA96 relA1 lac* F′[*proA*$^+$*B*$^+$ *lacI*^{q}*ZΔM15*::Tn*10*] (Tet^R)	Merck

A.10 Buffers and Solutions

Table A-12. NaCl-peptone.

NaCl-peptone	
Peptone	2.5 g
NaCl	3 g
H_2O	ad 1 l
→ autoclave	

NaCl-peptone was stored at room temperature after autoclaving.

Table A-13. M9 buffer.

M9 buffer	
KH_2PO_4	3 g
Na_2HPO_4	6 g
NaCl	5 g
H_2O	ad 999 ml
→ autoclave, chill to 60 °C	
$MgSO_4$ (1 M)	1 ml

M9 buffer has a pH of 7.0 and was stored at room temperature.

Table A-14. M9:TWEEN®20 buffer.

M9:TWEEN®20 buffer	
M9 buffer	990 ml
TWEEN®20	10 ml

The buffer was stored at room temperature.

Table A-15. Bleaching solution.

Bleaching solution	
KOH (5 N)	2.5 ml
NaClO (12% Cl)	3 ml
H_2O	19.5 ml

Bleaching solution was used for the synchronization of worms and prepared freshly every time.

Table A-16. Ethanol:TWEEN®20.

Ethanol:TWEEN®20	
Ethanol	92 ml
Tween®20	8 ml

The solution was stored at 4 °C.

Table A-17. Freezing buffer A.

Freezing buffer A	
K_2HPO_4	8.7 g
KH_2PO_4	6.8 g
NaCl	2.9 g
H_2O	ad 500 ml
→ pH 5.95	
→ autoclave	

Table A-18. Freezing buffer B.

Freezing buffer B	
Freezing buffer A	700 ml
Glycerol	300 ml

Freezing buffers were stored at 4 °C.

Table A-19. 50 x TAE buffer.

50 x TAE buffer	
TRIS	242 g
Acetic acid	57.1 ml
EDTA (0.5 M, pH 8.0)	100 ml
H_2O	ad 1 l

Tris-acetate-EDTA (TAE) buffer was used as running buffer for agarose gel electrophoresis. It was stored at room temperature and diluted 1:50 with ddH_2O prior to use.

Table A-20. $MgCl_2/CaCl_2$ solution.

$MgCl_2/CaCl_2$ solution	
$MgCl_2$	8.13 g
$CaCl_2$	0.29 g
H_2O	ad 100 ml

The $MgCl_2/CaCl_2$ solution was used to make HT115 bacteria chemically competent. The solution was stored at room temperature.

Table A-21. 10 x running buffer.

10 x running buffer	
Tris	30.3 g
Glycine	144 g
SDS	10 g
H_2O	ad 1 l

Running buffer was used for SDS polyacrylamide gel electrophoresis and diluted 1:10 with ddH_2O before use. Running buffer was stored at room temperature.

Table A-22. 3x Laemmli loading dye.

3x Laemmli loading dye	
1 M Tris-HCl (pH 6.8)	2.4 ml
20% SDS (w/v)	3 ml
Glycerol	3 ml
β-mercaptoethanol	1.6 ml
Bromophenol blue	0.006 g

Laemmli loading dye was stored at –20 °C.

Table A-23. Towbin buffer.

Towbin buffer	
TRIS	3.03 g
Glycine	14.4 g
Methanol	200 ml
H_2O	ad 1 l

Towbin buffer was stored at room temperature.

Table A-24. 10x TBS buffer.

10x TBS buffer	
NaCl	8.77 g
TRIS	6.06 g
H_2O	ad 100 ml
→ pH 7.5	

Table A-25. 10x TBS-T buffer.

10x TBS-T buffer	
Tween® 20	500 µl
TBS Buffer	ad 100 ml
→ pH 7.5	

Tris buffered saline (TBS) and TBS with TWEEN (TBS-T) buffers were stored at room temperature and diluted 1:10 with ddH_2O before use.

Table A-26. Blocking buffer.

Blocking buffer	
Powdered milk	1 g
TBS-T Buffer	100 ml

Blocking buffer was prepared freshly every time.

Table A-27. ECL solution.

ECL solution	
ECL solution A	
TRIS (pH 8.5, 1M)	5 ml
p-Coumaric acid (90 mM)	110 µl
Luminol (250 mM)	250 µl
H_2O	45 ml
ECL solution B	
H_2O_2 (30%)	100 µl
H_2O	900 µl

For the detection of HRP-conjugated antibodies 1 ml of enhanced chemiluminescence (ECL) solution A was mixed with 3 µl ECL solution B. Each solution can be stored up to 3 weeks at 4 °C. The mixture was prepared freshly every time.

Table A-28. Strip buffer.

Strip buffer	
TRIS	7,51 g
SDS	20 g
DTT	15,43 g
H_2O	ad 1 l

Strip buffer was stored at room temperature. DTT was added freshly before use.

Table A-29. Lysis buffer.

Lysis buffer	
Sucrose	273.84 g
EDTA	0,29 g
TRIS-HCl	1,21 g
PMSF	45.55 g
H_2O	ad 1 l

Lysis buffer for Western blot experiments was stored 4 °C.

Table A-30. Lysis buffer II.

Lysis buffer	
TRIS-HCl	1.21 g
NaCl	0.58 g
EDTA	1.46
SDS	1g
H_2O	ad 100 ml

Lysis buffer II was used for ATP measurements and stored at 4 °C.

Table A-31. Stock solutions.

Stock solutions	Concentration	Solvent
Ampicillin*	100 mg/ml	50% ethanol
$CaCl_2$#	0.1 M	H_2O
$CaCl_2$#	1 M	H_2O
Carbenicillin*	25 mg/ml	50% ethanol
Cholesterol*	5 mg/ml	ethanol
EDTA (pH 8.0) †	0.5 M	H_2O
IPTG*	1 M	50% ethanol
IPTG*	100 mM	H_2O
Kanamycin#	25 mg/ml	H_2O
KH_2PO_4#	1 M	H_2O
KOH†	5 N	H_2O
Levamisol#	2 mM	M9 buffer
Luminol*	250 mM	DMSO
$MgSO_4$#	0.1 M	H_2O
$MgSO_4$#	1 M	H_2O
Na_2HPO_4 (pH 7.4)#	0.25 M	H_2O
NaOH†	5 N	H_2O
p-Coumaric acid*	90 mM	DMSO
SDS†	20% w/v	H_2O
Tetracyclin*	25 mg/ml	50% ethanol
TRIS (pH 8.5) †	1 M	H_2O
TRIS-HCl (pH 6.8) †	1 M	H_2O
X-gal*	40 mg/ml	DMSF

* stored at –20 °C; # stored at 4 °C; †stored at room temperature

Table A-32. Stock solutions of effectors.

Substance	Concentration	Solvent
Glucose	1 M	M9 buffer
Ascorbic acid	1 M	M9 buffer
Pyridoxamine	1 M	M9 buffer
MG132	20 mM	Ethanol:TWEEN®20 (92:8 v/v)
Quercetin	10 mM	Ethanol:TWEEN®20 (92:8 v/v)

Stock solutions of glucose were always prepared freshly. Other solutions were stored protected from light at –20 °C.

Table A-33. Stock solutions of fluorescent dyes.

Dye	Concentration	Solvent
MitoTracker® Green FM	1 mM	DMSO
MitoTracker® Red CM-XRos	100 µM	DMSO
MitoTracker® Red CM-H_2XRos	300 µM	DMSO
SYTO12	3.3 mM	DMSO
SYTOX® Green	5 mM	M9:TWEEN®20

Stock solutions were aliquoted and stored protected from light at −20 °C.

A.11 Media

Table A-34. 2x YT agar.

2x YT agar	
2x YT medium	6.2 g
Agar	3 g
H_2O	ad 200 ml
→ autoclave, chill to 60 °C	
→ *optional*	
Ampicillin (100 mg/ml)	200 µl
Tetracycline (25 mg/ml)	200 µl

2x YT agar was used for the cultivation of *E. coli* OP50 and *E. coli* HT115.

Plates were poured under sterile conditions after the agar had chilled to 55 °C and were stored at 4 °C.

Table A-35. 2x YT medium.

2x YT medium	
2x YT medium	31 g

H_2O	ad 1 l
→ pH 7.0	
→autoclave	

Liquid bacteria cultures were grown in 2 x YT medium.

2 x YT medium was obtained already mixed and consists of 16 g bacto peptone, 10 g yeast extract and 5 g NaCl per 31 g. The pH was adjusted to 7.0 with 5 N NaOH.

Table A-36. Nematode growth medium (NGM) agar.

Nematode growth medium (NGM) agar	
Agar	17 g
Peptone	2.5 g
NaCl	3 g
H_2O	947 ml
→ autoclave, chill to 60 °C	
$CaCl_2$ (0.1 M)	1 ml
Carbenicillin (25 mg / ml ethanol)	1 ml
Cholesterol (5 mg / ml ethanol)	1 ml
KH_2PO_4 (1 M, pH 6.0)	25 ml
$MgSO_4$ (0.1 M)	1 ml
Nystatin suspension	25 ml

Nematode growth medium (NGM) agar was used for *C. elegans* cultivation.

Table A-37. Liquid NGM.

Liquid NGM	
$CaCl_2$ (0.1 M)	10 µl
Cholesterol (5 mg/ml)	10 µl
KH_2PO_4 (1 M, pH 6.0)	250 µl
$MgSO_4$ (0.1 M)	10 µl
NaCl-Peptone	9.71 ml
Carbenicillin (25 mg/ml)	10 µl
→ for RNAi experiments	
Kanamycin (25 mg/ml) instead of Carbenicillin	10 µl

Liquid NGM was used for all *C. elegans* experiments and was prepared freshly every time. For RNAi experiments Carbenicillin was replaced by Kanamycin to inactivate *E. coli* HT115.

A.12 Software

Table A-38. Software.

Software	Manufacturer
Ascent Software for Fluoroskan 2.6	Thermo Labsystems (Bornheim, D)
Ascent Software for Multiskan	Thermo Labsystems (Bornheim, D)
CFX Manager Software	Bio-Rad (Hercules, USA)
GraphPad Prism 5	Graph Pad Software (San Diego, USA)
Image J 1.43	National Institute of Health (Bethesda, USA)
Motic Images Plus 2.0 ML	Beyersdörfer (Saarbrücken-Eschringen, D)

B APPENDIX: TABULAR RESULTS

B.1 Glucose Toxicity

Table B-1. Mean life span under heat stress (37 °C) of *C. elegans* TK22 (*mev-1*) and N2 (wildtype) after a 48 h treatment with various glucose concentrations.

Strain	Treatment	MLS [h]	SD [h]	n	p LogRank
TK22 (*mev-1*)	control	8.35	1.27	24	
	10 mM glucose	5.50	1.40	38	<0.001*
	25 mM glucose	5.78	1.63	37	<0.001*
	50 mM glucose	6.31	1.29	37	<0.001*
	100 mM glucose	6.27	1.47	37	<0.001*
	250 mM glucose	6.76	1.52	33	0.002*
N2 (wildtype)	control	10.05	1.23	28	
	10 mM glucose	8.83	1.05	29	<0.001*
	25 mM glucose	9.33	1.31	30	0.028*
	50 mM glucose	8.79	1.22	33	<0.001*
	100 mM glucose	8.63	8.63	20	<0.001*
	250 mM glucose	8.66	8.66	32	<0.001*

MLS: mean life span, SD: standard deviation, n: number of animals; p values show the results of the logrank test, * compared to control

Table B-2. Mean life span under heat stress (37 °C) of *C. elegans* TK22 (*mev-1*) after a 48 h treatment with glucose and ascorbic acid.

Strain	Treatment	MLS [h]	SD [h]	n	p LogRank
TK22 (*mev-1*)	control	8.09	0.97	32	
	100 µM ascorbic acid	7.96	1.53	37	0.535*
	250 µM ascorbic acid	7.97	1.46	35	0.656*
	10 mM glucose	5.90	1.65	31	<0.001*
	10 mM glucose + 100 µM ascorbic acid	6.34	1.85	32	0.196#
	10 mM glucose + 250 µM ascorbic acid	5.97	1.83	33	0.837#

MLS: mean life span, SD: standard deviation, n: number of animals; p values show the results of the logrank test, * compared to control, # compared to 10 mM glucose

B.2 Influence of Glucose on Protein Quality Control

Table B-3. Mean life span under heat stress (37 °C) of *C. elegans* TK22 (*mev-1*) after a 48 h treatment with glucose and pyridoxamine.

Strain	Treatment	MLS [h]	SD [h]	n	p LogRank
TK22 (*mev-1*)	control	8.77	1.14	56	
	10 mM glucose	7.75	1.09	50	< 0.001*
	10 mM glucose + 10 mM pyridoxamine	7.99	1.18	56	0.257#
	10 mM pyridoxamine	9.09	1.34	22	0.226*
TK22 (*mev-1*)	control	9.13	0.91	40	
	10 mM glucose	8.08	1.08	38	< 0.001*
	10 mM glucose + 50 mM pyridoxamine	9.00	1.62	37	< 0.001#
	50 mM pyridoxamine	8.84	1.54	37	0.964*

MLS: mean life span, SD: standard deviation, n: number of animals; p values show the results of the logrank test, * compared to control, # compared to 10 mM glucose

Table B-4. Effects of *hsp-6, hsp-60*, *dve-1,* or *ubl-5* RNAi on mean life span under heat stress (37 °C) of *C. elegans* TK22 (*mev-1*) after a 48 h treatment with glucose.

Strain	RNAi	Treatment	MLS [h]	SD [h]	n	p LogRank
TK22 (*mev-1*)	control	control	9.12	1.08	78	
		10 mM glucose	8.30	1.40	79	< 0.001*
	hsp-6	control	5.67	1.43	81	< 0.001*
		10 mM glucose	5.48	1.17	77	0.232#
	hsp-60	control	5.13	1.35	74	< 0.001*
		10 mM glucose	5.34	1.11	83	0.722#
	dve-1	control	7.87	1.63	73	< 0.001*
		10 mM glucose	7.68	1.59	77	0.507#
	ubl-5	control	6.34	1.32	38	< 0.001*
		10 mM glucose	6.79	1.50	36	0.349#

RNAi: RNA interference, MLS: mean life span, SD: standard deviation, n: number of animals; p values show the results of the logrank test, * compared to control RNAi, control treatment; # compared to 10 mM glucose of the corresponding RNAi

Table B-5. Effects of *abu-1*, *abu-11*, or *xbp-1* RNAi on mean life span under heat stress (37 °C) of *C. elegans* TK22 (*mev-1*) after a 48 h treatment with glucose.

Strain	RNAi	Treatment	MLS [h]	SD [h]	n	p LogRank
TK22 (*mev-1*)	control	control	9.65	1.64	50	
		10 mM glucose	8.21	1.60	58	< 0.001*
	abu-1	control	8.85	1.67	60	0.006*
		10 mM glucose	8.93	1.55	54	0.971#
	abu-11	control	8.03	1.80	59	< 0.001*
		10 mM glucose	7.95	1.47	56	0.295#
	xbp-1	control	8.77	1.39	58	0.001*
		10 mM glucose	8.48	1.30	64	0.235#

RNAi: RNA interference, MLS: mean life span, SD: standard deviation, n: number of animals; p values show the results of the logrank test, * compared to control RNAi, control treatment; # compared to 10 mM glucose of the corresponding RNAi

Table B-6. Effects of *ubq-1* or *uba-1* RNAi on mean life span under heat stress (37 °C) of *C. elegans* TK22 (*mev-1*) after a 48 h treatment with glucose.

Strain	RNAi	Treatment	MLS [h]	SD [h]	n	p LogRank
TK22 (*mev-1*)	control	control	7.79	1.78	33	
		10 mM glucose	6.74	1.78	35	0.004*
	ubq-1	control	3.63	0.78	40	< 0.001*
		10 mM glucose	3.75	0.75	40	0.539#
	uba-1	control	6.04	1.95	40	< 0.001*
		10 mM glucose	6.09	1.81	38	0.971#

RNAi: RNA interference, MLS: mean life span, SD: standard deviation, n: number of animals; p values show the results of the logrank test, * compared to control RNAi, control treatment; # compared to 10 mM glucose of the corresponding RNAi

Table B-7. Mean life span under heat stress (37 °C) of *C. elegans* TK22 (*mev-1*) after a 48 h treatment with glucose and MG132.

Strain	Treatment	MLS [h]	SD [h]	n	p LogRank
TK22 (*mev-1*)	control	9.19	0.87	39	
	10 mM glucose	7.47	1.27	40	< 0.001*
	200 µM MG132	8.29	0.87	36	< 0.001*
	10 mM glucose + 200 µM MG132	7.67	1.08	38	0.506#

RNAi: RNA interference, MLS: mean life span, SD: standard deviation, n: number of animals; p values show the results of the logrank test; * compared to control; # compared to 10 mM glucose

B.3 Glucose Induces Apoptosis

Table B-8. Effect of *ced-3* RNAi on mean life span under heat stress (37 °C) of *C. elegans* TK22 (*mev-1*) after a 48 h treatment with glucose.

Strain	RNAi	Treatment	MLS [h]	SD [h]	n	p LogRank
TK22 (*mev-1*)	control	control	9.08	0.64	30	
		10 mM glucose	8.36	0.82	39	< 0.001*
	ced-3	control	7.41	0.95	23	< 0.001*
		10 mM glucose	7.04	1.49	25	0.877#

RNAi: RNA interference, MLS: mean life span, SD: standard deviation, n: number of animals; p values show the results of the logrank test, * compared to control RNAi, control treatment; # compared to *ced-3 RNAi,* 10 mM glucose treatment

Table B-9. Effect of *ced-4* RNAi on mean life span under heat stress (37 °C) of *C. elegans* TK22 (*mev-1*) after a 48 h treatment with glucose.

Strain	RNAi	Treatment	MLS [h]	SD [h]	n	p LogRank
TK22 (*mev-1*)	control	control	8.82	0.62	36	
		10 mM glucose	7.69	0.85	40	< 0.001*
	ced-4	control	8.54	1.03	39	0.711*
		10 mM glucose	8.30	1.01	35	0.397#

RNAi: RNA interference, MLS: mean life span, SD: standard deviation, n: number of animals; p values show the results of the logrank test, * compared to control RNAi, control treatment; # compared to *ced-4* RNAi, 10 mM glucose treatment

Table B-10. Effect of *egl-1* RNAi on mean life span under heat stress (37 °C) of *C. elegans* TK22 (*mev-1*) after a 48 h treatment with glucose.

Strain	RNAi	Treatment	MLS [h]	SD [h]	n	p LogRank
TK22 (*mev-1*)	control	control	8.74	0.53	34	
		10 mM glucose	7.60	0.75	39	< 0.001*
	egl-1	control	8.42	0.62	39	0.070*
		10 mM glucose	8.21	0.71	39	0.321#

RNAi: RNA interference, MLS: mean life span, SD: standard deviation, n: number of animals; p values show the results of the logrank test, * compared to control RNAi, control treatment; # compared to *egl-1* RNAi, 10 mM glucose treatment

Table B-11. Effect of *cep-1* RNAi on mean life span under heat stress (37 °C) of *C. elegans* TK22 (*mev-1*) after a 48 h treatment with glucose.

Strain	RNAi	Treatment	MLS [h]	SD [h]	n	p LogRank
TK22 (*mev-1*)	control	control	9.24	0.75	34	
		10 mM glucose	8.36	0.82	39	< 0.001*
	cep-1	control	9.03	0.75	37	0.273*
		10 mM glucose	8.23	0.82	40	< 0.001#

RNAi: RNA interference, MLS: mean life span, SD: standard deviation; n: number of animals; p values show the results of ANOVA and Bonferroni's Multiple Comparison Test, * compared to control RNAi, control treatment, # compared to *cep-1* RNAi, 10 mM glucose treatment

B.4 Activation of Stress Response Pathways by Polyphenols

Table B-12. Mean life span under heat stress (37 °C) of *C. elegans* TK22 (*mev-1*) after a 48 h treatment with quercetin.

Strain	Treatment	MLS [h]	SD [h]	n	p LogRank
TK22 (*mev-1*)	control	8.64	0.86	37	
	1 µM quercetin	8.78	0.98	38	0.181*
TK22 (*mev-1*)	control	8.59	1.20	33	
	100 µM quercetin	8.53	1.17	19	0.593*

MLS: mean life span, SD: standard deviation, n: number of animals; p values show the results of the logrank test, * compared to control

Table B-13. Mean life span under heat stress (37 °C) of *C. elegans* TK22 (*mev-1*) after a 48 h treatment with glucose and quercetin.

Strain	Treatment	MLS [h]	SD [h]	n	p LogRank
TK22 (*mev-1*)	control	8.73	2.27	39	
	10 mM glucose	5.81	1.27	21	<0.001*
	10 mM glucose + 1µM quercetin	8.54	1.18	34	<0.001#
TK22 (*mev-1*)	control	8.88	1.15	56	
	10 mM glucose	7.11	1.86	46	<0.001*
	10 mM glucose + 100 µM quercetin	9.08	1.26	30	<0.001#

MLS: mean life span, SD: standard deviation, n: number of animals; p values show the results of the logrank test, * compared to control, # compared to 10 mM glucose

Table B-14. Effect of *sir-2.1* RNAi on mean life span under heat stress (37 °C) of *C. elegans* TK22 (*mev-1*) after a 48 h treatment with glucose and quercetin.

Strain	RNAi	Treatment	MLS [h]	SD [h]	n	p LogRank
TK22 (*mev-1*)	control	control	8.59	0.88	36	
		10 mM glucose	7.60	1.51	36	0.002*
		10 mM glucose + 1 µM quercetin	8.55	0.63	29	0.004#
	sir-2.1	control	8.35	1.46	30	0.486*
		10 mM glucose	7.69	1.15	32	<0.001†
		10 mM glucose + 1 µM quercetin	7.59	1.51	29	0.578‡

RNAi: RNA interference, MLS: mean life span, SD: standard deviation, n: number of animals; p values show the results of the logrank test, * compared to control RNAi, control treatment, # compared to control RNAi, 10 mM glucose treatment, † compared to *sir-2.1* RNAi, control treatment, ‡ compared to *sir-2.1* RNAi, 10 mM glucose treatment

Table B-15. Effects of *sir-2.2*, *sir-2.3*, or *sir-2.4* RNAi on mean life span under heat stress (37 °C) of *C. elegans* TK22 (*mev-1*) after a 48 h treatment with glucose and quercetin.

Strain	RNAi	Treatment	MLS [h]	SD [h]	n	p LogRank
TK22 (*mev-1*)	control	control	9.07	0.75	29	
		10 mM glucose	8.25	0.84	37	<0.001*
		10 mM glucose + 1 µM quercetin	9.01	1.06	37	<0.001#
	sir-2.2	control	9.69	1.04	32	0.007*
		10 mM glucose	9.00	0.99	29	0.007†
		10 mM glucose + 1 µM quercetin	9.88	1.16	37	<0.001‡
	sir-2.3	control	9.38	0.96	38	0.136*
		10 mM glucose	7.23	1.31	39	<0.001†
		10 mM glucose + 1 µM quercetin	8.88	1.08	29	<0.001‡
	sir-2.4	control	9.05	1.07	33	0.846*
		10 mM glucose	8.33	1.21	32	0.014†
		10 mM glucose + 1 µM quercetin	9.70	1.28	38	<0.001‡

RNAi: RNA interference, MLS: mean life span, SD: standard deviation, n: number of animals; p values show the results of the logrank test, * compared to control RNAi, control treatment, # compared to control RNAi, 10 mM glucose treatment, † compared to control treatment of the corresponding RNAi, ‡ compared to 10 mM glucose treatment of the corresponding RNAi

Table B-16. Effect of *aak-2* RNAi on mean life span under heat stress (37 °C) of *C. elegans* TK22 (*mev-1*) after a 48 h treatment with glucose and quercetin.

Strain	RNAi	Treatment	MLS [h]	SD [h]	n	p LogRank
TK22 (*mev-1*)	control	control	9.44	0.82	39	
		10 mM glucose	8.50	1.52	35	0.019*
		10 mM glucose + 1 µM quercetin	9.60	0.90	31	0.004#
	aak-2	control	9.82	0.83	34	0.034*
		10 mM glucose	8.98	1.27	30	0.008†
		10 mM glucose + 1 µM quercetin	9.93	0.84	37	0.001‡

RNAi: RNA interference, MLS: mean life span, SD: standard deviation, n: number of animals; p values show the results of the logrank test, * compared to control RNAi, control treatment, # compared to control RNAi, 10 mM glucose treatment, † compared to *aak-2* RNAi, control treatment, ‡ compared to *aak-2* RNAi, 10 mM glucose treatment

Table B-17. Effect of *daf-16* RNAi on mean life span under heat stress (37 °C) of *C. elegans* TK22 (*mev-1*) after a 48 h treatment with glucose and quercetin.

Strain	RNAi	Treatment	MLS [h]	SD [h]	n	p LogRank
TK22 (*mev-1*)	control	control	8.65	1.30	34	
		10 mM glucose	6.08	1.87	37	<0.001*
	daf-16	control	8.26	1.25	35	0.019*
		10 mM glucose	6.85	1.33	26	<0.001†
		10 mM glucose + 1 µM quercetin	8.27	1.02	33	<0.001‡

RNAi: RNA interference, MLS: mean life span, SD: standard deviation, n: number of animals; p values show the results of the logrank test, * compared to control RNAi, control treatment, † compared to *daf-16* RNAi, control treatment, ‡ compared to *daf-16* RNAi, 10 mM glucose treatment

Table B-18. Mean life span under heat stress (37 °C) of *C. elegans* CF1038 (*daf-16*) after a 48 h treatment with glucose and quercetin.

Strain	Treatment	MLS [h]	SD [h]	n	p LogRank
CF1038 (*daf-16*)	control	8.89	0.96	35	
	10 mM glucose	7.47	1.10	35	<0.001*
	10 mM glucose + 1 µM quercetin	8.42	0.86	36	<0.001#

MLS: mean life span, SD: standard deviation, n: number of animals; p values show the results of the logrank test, * compared to control, # compared to 10 mM glucose

Table B-19. Effects of *skn-1*, *jnk-1* or *hsf-1* knockdown or knockout on mean life span under heat stress (37 °C) of *C. elegans* after a 48 h treatment with glucose and quercetin.

Strain	RNAi	Treatment	MLS [h]	SD [h]	n	p LogRank
TK22 (*mev-1*)	control	control	9.35	1.20	39	
		10 mM glucose	8.43	1.16	40	<0.001*
		10 mM glucose + 1 µM quercetin	9.15	0.91	37	0.004#
	skn-1	control	7.18	1.31	40	<0.001*
		10 mM glucose	6.88	1.45	40	0.022†
		10 mM glucose + 1 µM quercetin	7.65	1.26	39	<0.001‡
	jnk-1	control	8.97	0.93	38	0.159*
		10 mM glucose	8.21	1.09	40	<0.001†
		10 mM glucose + 1 µM quercetin	8.54	1.01	36	0.003‡
PS3551 (*hsf-1*)		control	8.44	1.16	34	
		10 mM glucose	7.13	1.81	35	0.007*
		10 mM glucose + 1 µM quercetin	8.68	1.11	34	<0.001#

RNAi: RNA interference, MLS: mean life span, SD: standard deviation, n: number of animals; p values show the results of the logrank test, * compared to control RNAi, control treatment, # compared to control RNAi, 10 mM glucose treatment, † compared to the corresponding RNAi, control treatment, ‡ compared to the corresponding RNAi, 10 mM glucose treatment

Table B-20. Mean life span under heat stress (37 °C) of *C. elegans* AA1 (*daf-12*) and RB1716 (*nhr-49*) after a 48 h treatment with glucose and quercetin.

Strain	Treatment	MLS [h]	SD [h]	n	p LogRank
AA1 (*daf-12*)	control	10.44	1.27	33	
	10 mM glucose	6.84	1.81	35	<0.001*
	10 mM glucose + 1 µM quercetin	7.35	2.24	37	0.131#
RB1716 (*nhr-49*)	control	9.35	1.14	33	
	10 mM glucose	7.86	1.32	36	<0.001*
	10 mM glucose + 1 µM quercetin	9.15	1.13	36	<0.001#

MLS: mean life span, SD: standard deviation, n: number of animals; p values show the results of the logrank test, * compared to control, # compared to 10 mM glucose treatment

Table B-21. Effect of *daf-9* RNAi on mean life span under heat stress (37 °C) of *C. elegans* TK22 (*mev-1*) after a 48 h treatment with glucose and quercetin.

Strain	RNAi	Treatment	MLS [h]	SD [h]	n	p LogRank
TK22 (*mev-1*)	control	control	9.97	0.96	35	
		10 mM glucose	9.47	1.08	33	0.020*
		10 mM glucose + 1 µM quercetin	9.86	1.33	35	0.036#
	daf-9	control	9.63	1.07	39	0.284*
		10 mM glucose	8.36	1.16	39	< 0.001†
		10 mM glucose + 1 µM quercetin	9.46	1.27	40	< 0.001‡

RNAi: RNA interference, MLS: mean life span, SD: standard deviation, n: number of animals; p values show the results of the logrank test, * compared to control RNAi, control treatment, # compared to control RNAi, 10 mM glucose treatment, † compared to *daf-9* RNAi, control treatment, ‡ compared to *daf-9* RNAi, 10 mM glucose treatment

Table B-22. Effect of *mdt-15* RNAi on mean life span under heat stress (37 °C) of *C. elegans* TK22 (*mev-1*) after a 48 h treatment with glucose and quercetin.

Strain	RNAi	Treatment	MLS [h]	SD [h]	n	p LogRank
TK22 (*mev-1*)	control	control	8.41	1.08	39	
		10 mM glucose	7.64	1.31	36	0.016*
		10 mM glucose + 1 µM quercetin	8.43	0.85	38	0.017#
	mdt-15	control	6.90	0.87	34	< 0.001*
		10 mM glucose	5.26	1.79	37	< 0.001†
		10 mM glucose + 1 µM quercetin	4.79	1.91	34	0.243‡

RNAi: RNA interference, MLS: mean life span, SD: standard deviation, n: number of animals; p values show the results of the logrank test, * compared to control RNAi, control treatment, # compared to control RNAi, 10 mM glucose treatment, † compared to *mdt-15* RNAi, control treatment, ‡ compared to *mdt-15* RNAi, 10 mM glucose treatment

B.5 Influence of Quercetin on the Protein Quality Control System

Table B-23. Effects of *hsp-6, hsp-60*, *dve-1,* or *ubl-5* RNAi on mean life span under heat stress (37 °C) of *C. elegans* TK22 (*mev-1*) after a 48 h treatment with glucose and quercetin.

Strain	RNAi	Treatment	MLS [h]	SD [h]	n	p LogRank
TK22 (*mev-1*)	control	control	9.12	1.08	78	
		10 mM glucose	8.30	1.40	79	< 0.001*
		10 mM glucose + quercetin 1 µM	8.96	1.19	80	< 0.001#
	hsp-6	control	5.67	1.43	81	< 0.001*
		10 mM glucose	5.48	1.17	77	0.232†
		10 mM glucose + quercetin 1 µM	5.69	1.43	76	0.204‡
	hsp-60	control	5.13	1.35	74	< 0.001*
		10 mM glucose	5.34	1.11	83	0.722†
		10 mM glucose + quercetin 1 µM	5.26	1.00	82	0.450‡
	dve-1	control	7.87	1.63	73	< 0.001*
		10 mM glucose	7.68	1.59	77	0.507†
		10 mM glucose + quercetin 1 µM	7.92	1.56	78	0.391‡
	ubl-5	control	6.43	1.32	38	< 0.001*
		10 mM glucose	6.79	1.50	36	0.349†
		10 mM glucose + quercetin 1 µM	5.92	1.95	37	0.829‡

RNAi: RNA interference, MLS: mean life span, SD: standard deviation, n: number of animals; p values show the results of the logrank test, * compared to control RNAi, control treatment, # compared to control RNAi, 10 mM glucose treatment, † compared to control treatment of the corresponding RNAi, ‡ compared to 10 mM glucose treatment of the corresponding RNAi

Table B-24. Effects of *abu-1*, *abu-11*, or *xbp-1* RNAi on mean life span under heat stress (37 °C) of *C. elegans* TK22 (*mev-1*) after a 48 h treatment with glucose and quercetin.

Strain	RNAi	Treatment	MLS [h]	SD [h]	n	p LogRank
TK22 (*mev-1*)	control	control	9.65	1.64	50	
		10 mM glucose	8.21	1.60	58	< 0.001*
		10 mM glucose + 1 µM quercetin	9.36	1.60	57	< 0.001#
	abu-1	control	8.85	1.67	60	0.006*
		10 mM glucose	8.93	1.55	54	0.971†
		10 mM glucose + 1 µM quercetin	8.48	1.62	57	0.226‡
	abu-11	control	8.03	1.80	59	< 0.001*
		10 mM glucose	7.95	1.47	56	0.295†
		10 mM glucose + 1 µM quercetin	8.07	1.23	48	0.869‡
	xbp-1	control	8.77	1.39	58	0.001*
		10 mM glucose	8.48	1.30	64	0.235†
		10 mM glucose + 1 µM quercetin	8.06	1.71	57	0.364‡

RNAi: RNA interference, MLS: mean life span, SD: standard deviation, n: number of animals; p values show the results of the logrank test, * compared to control RNAi, control treatment, # compared to control RNAi, 10 mM glucose treatment, † compared to control treatment of the corresponding RNAi, ‡ compared to 10 mM glucose treatment of the corresponding RNAi

Table B-25. Effects of *ubq-1* or *uba-1* RNAi on mean life span under heat stress (37 °C) of *C. elegans* TK22 (*mev-1*) after a 48 h treatment with glucose and quercetin.

Strain	RNAi	Treatment	MLS [h]	SD [h]	n	p LogRank
TK22 (*mev-1*)	control	control	7.79	1.78	33	
		10 mM glucose	6.74	1.78	35	0.004*
		10 mM glucose + 1 µM quercetin	7.72	1.67	32	0.027#
	ubq-1	control	3.63	0.78	40	< 0.001*
		10 mM glucose	3.75	0.75	40	0.539†
		10 mM glucose + 1 µM quercetin	3.69	0.76	38	0.789‡
	uba-1	control	6.04	1.95	40	< 0.001*
		10 mM glucose	6.09	1.81	38	0.971†
		10 mM glucose + 1 µM quercetin	5.53	2.03	40	0.311‡

RNAi: RNA interference, MLS: mean life span, SD: standard deviation, n: number of animals; p values show the results of the logrank test, * compared to control RNAi, control treatment, # compared to control RNAi, 10 mM glucose treatment, † compared to control treatment of the corresponding RNAi, ‡ compared to 10 mM glucose treatment of the corresponding RNAi

Table B-26. Mean life span under heat stress (37 °C) of *C. elegans* TK22 (*mev-1*) after a 48 h treatment with glucose, MG132, and quercetin.

Strain	Treatment	MLS [h]	SD [h]	n	p LogRank
TK22 (*mev-1*)	control	9.19	0.87	39	
	10 mM glucose	7.47	1.27	40	< 0.001*
	200 µM MG132	8.29	0.87	36	< 0.001*
	10 mM glucose + 200 µM MG132	7.67	1.08	38	0.506#
	200 µM MG132 + 1 µM quercetin	8.91	1.32	39	< 0.001†
	10 mM glucose + 200 µM MG132 + 1 µM quercetin	7.84	1.05	39	0.503‡

MLS: mean life span, SD: standard deviation, n: number of animals; p values show the results of the logrank test, * compared to control, # compared to 10 mM glucose treatment, † compared to 200 µM MG132 treatment, ‡ compared to 10 mM glucose + 200 µM MG132 treatment

Table B-27. Effect of *bec-1* RNAi on mean life span under heat stress (37 °C) of *C. elegans* TK22 (*mev-1*) after a 48 h treatment with glucose and quercetin.

Strain	RNAi	Treatment	MLS [h]	SD [h]	n	p LogRank
TK22 (*mev-1*)	control	control	9.24	0.82	40	
		10 mM glucose	7.73	1.49	40	< 0.001*
		10 mM glucose + 1 µM quercetin	8.78	0.82	36	< 0.001#
	bec-1	control	9.18	0.82	39	0.718*
		10 mM glucose	9.41	1.08	38	0.091†
		10 mM glucose + 1 µM quercetin	9.41	0.89	38	0.192‡

RNAi: RNA interference, MLS: mean life span, SD: standard deviation, n: number of animals; p values show the results of the logrank test, * compared to control RNAi, control treatment, # compared to control RNAi, 10 mM glucose treatment, † compared to *bec-1* RNAi, control treatment, ‡ compared to *bec-1* RNAi, 10 mM glucose treatment

DANKSAGUNG

An dieser Stelle möchte ich mich bei allen herzlich bedanken, die durch ihre Unterstützung zum Gelingen dieser Arbeit beigetragen haben.

Zunächst möchte ich der Studienstiftung des deutschen Volkes danken, ohne deren Promotionsstipendium die Durchführung des Projekts in dieser Art nicht möglich gewesen wäre.

Mein besonderer Dank gilt Prof. Dr. Uwe Wenzel für die Überlassung des interessanten Themas und die Bereitstellung der ausgezeichneten Forschungsmöglichkeiten. Seine jederzeit konstruktive Unterstützung und kritische Auseinandersetzung mit der Thematik in zahlreichen Gesprächen und Diskussionen haben maßgeblich zum Gelingen dieser Arbeit beigetragen.

Desgleichen möchte ich mich bei Dr. Michael Boll für die konstruktiven Gespräche und wertvollen Hilfestellungen im Rahmen der experimentellen Untersuchungen bedanken. Seine Unterstützung trägt einen wertvollen Anteil am Erfolg dieser Arbeit.

Darüber hinaus geht ein großes Dankeschön an alle Kollegen des Lehrstuhls für Molekulare Ernährungsforschung für die gute Zusammenarbeit und die vielen schönen Momente. Ganz besonders danke ich Dr. Malaika Fischer für die kritische Durchsicht der Manuskripte und ihre besondere Hilfsbereitschaft, ebenso wie Charlotte Regitz und Mareike Kahl, die immer ein offenes Ohr für mich hatten.

Nicht zuletzt möchte ich meiner Familie und meinen Freunden für die moralische Unterstützung und das entgegengebrachte Verständnis danken. Ganz besonders danke ich dir, Alex, für deine unermüdliche Geduld und deine liebevolle Unterstützung.

VERSICHERUNG

Ich erkläre: Ich habe die vorgelegte Dissertation selbständig und ohne unerlaubte fremde Hilfe und nur mit den Hilfen angefertigt, die ich in der Dissertation angegeben habe. Alle Textstellen, die wörtlich oder sinngemäß aus veröffentlichten Schriften entnommen sind, und alle Angaben, die auf mündlichen Auskünften beruhen, sind als solche kenntlich gemacht. Bei den von mir durchgeführten und in der Dissertation erwähnten Untersuchungen habe ich die Grundsätze guter wissenschaftlicher Praxis, wie sie in der „Satzung der Justus-Liebig-Universität Gießen zur Sicherung guter wissenschaftlicher Praxis“ niedergelegt sind, eingehalten.

Gießen, den